MORPHOMETRIC ANALYSIS OF THE MAMMALIAN OPTIC NERVE

Dr Yohanna Yanshiyi Dangata, M.B., B.S.

Thesis presented for the degree of Doctor of Philosophy.

Edinburgh University

August 1996

ACKNOWLEDGEMENTS

First and foremost I should deeply be grateful to my principal supervisor, Professor MH Kaufman, whose unrestricted access, enthusiasm, encouragement, thorough and thoughtful supervision were sustainable throughout the period of this research. His exceptionally keen interest in my general welfare throughout the period of study was always a booster to the work.

I also thank Drs GS Findlater and B Dhillon, my other supervisors, for their invaluable discussions and advice. Dr BW Fleck kindly and patiently gave me guidance during my sessions at his clinics as part of this research.

My gratitude also goes to the Kaduna State Government, Nigeria for providing initial funding for this research, Ahmadu Bello Univerity, Zaria, and the Nigeria High Commission, London, for their support. I am also grateful for the financial support of Edinburgh University, Dr & Mrs James Sherwood, Mr Michael Farmer, Duncan Street Baptist Church, Edinburgh, The Leche Trust and Christopher Cox Memorial Fund.

I wish additionally to thank the following people:

Mr Ronnie McDougall for untiring and expert technical assistance in electron microscopy,

Staff of the Medical Faculty Animal house for good animal husbandry,

Ms June Gillam for secretarial assistance,

Rev. & Mrs Henry Telfer, Miss PJ Grierson, Mr David Rae and Mr Jim Thompson for counselling and encouragement,

I am also grateful to Dr JP Shaw, since August 1995 the Head of Department of Anatomy, and all staff of the Anatomy Department for their support and cooperation during this research.

Many friends and relations gave themselves to praying in addition to their invaluable advice and encouragement.

It would have been impossible to finish this work without the support of my family especially, Sweetie, my wife who always saw it as 'our research'.

Adieu Mum! Couldn't you just wait to see the completion of this work?

Above all, glory be to the Lord God Almighty, to whom all knowledge and wisdom belong; *'O the depth of the riches and wisdom and knowledge of God! How unsearchable are his judgements and how inscrutable his ways!'*- Rom.11[33].

DECLARATION

Except where duly acknowledged, this thesis is the result of laboratory research I carried out in the Department of Anatomy, Edinburgh University.

Dr Yohanna Yanshiyi Dangata, M.B., B.S.

August 1996

ABSTRACT

Mammalian models are increasingly playing a significant role in clinically-related research as it is often technically and ethically impossible to carry out similar research directly on humans. The mouse has been extensively used, and in many instances is the experimental animal of choice, in genetic and teratological studies. The optic nerve of the mouse is the most easily accessible component of the central nervous system and is of particular value for the investigation of the effects of mutational changes in genes and the teratogenic effects of substances on the human visual system. While adequate baseline information is a necessary prerequisite for the interpretation of findings from such studies, a comprehensive account of baseline morphometric parameters on the optic nerve of the mouse is not available.

The present study was therefore carried out to establish this baseline information; studies were carried out on the optic nerve of a variety of inbred strains and their F_1 hybrids. The postnatal development of a variety of different age groups was also analysed to provide baseline data as part of a study to determine the teratogenic effect of prenatal exposure to alcohol on the postnatal development of the optic nerve in this species. Furthermore, the optic nerve from adult heterozygous *Small eye* (*Sey*/+) mice was analysed to determine the effects of the *Sey* gene mutation on the optic nerve of the mouse. Morphometric parameters of the optic nerve were analysed by the combined use of light and electron microscopy with a Magiscan image analysis system (Applied Imaging). Parameters analysed were mean cross-sectional area (csa), mean myelinated nerve fibre count, mean myelinated nerve fibre density and myelinated nerve fibre diameter spectrum. Intra-strain and inter-strain comparisons of these parameters were carried out. Developmental events such as the onset and progression of myelinogenesis were also examined.

The findings indicated that there was neither a significant difference in any of the parameters studied between the left and the right optic nerves nor evidence of sexual dimorphism within any of the strains studied, although, a significant degree of inter-strain variation was noted. It was also observed that the mouse has a small calibre optic nerve typical of most rodents, but is in contrast to the situation observed in most primates where the optic nerve has a large calibre. In both rodents and primates, the nerve fibres in the adult optic nerve are all myelinated. These fibres are unimodally distributed (i.e. having only one peak) along the nerve fibre diameter spectrum which is also positively skewed (i.e. skewing is to the right in favour of the large diameter fibres). Furthermore, in the mouse the mean myelinated nerve fibre count is lower than that reported in all primates so far studied, and the spectrum of diameter distribution of the nerve fibres is narrower. Morphometric evidence of inbreeding vigour in the F_1 hybrids was clearly present.

During postnatal development, the optic nerve in the mouse grows rapidly during the early part of the juvenile period (first three postnatal weeks). Although, growth in the calibre of the nerve continues well into adulthood, it progressively tails off from the end of the juvenile period of life. Unlike the situation reported in man, myelinogenesis in the optic nerve of the mouse is entirely a postnatal event. Myelinogenesis begins in the larger diameter fibres and progresses to involve all fibres in decreasing order of their fibre size. The myelin lamellae are initially loosely wrapped around the axons, but as more myelin lamellae are acquired with age, they become more densely packed around the axons. The rate of progression of myelinogenesis parallels that of growth in the csa, and is completed early in adulthood. Myelinogenesis is completed in the C57BL inbred strain earlier than in its F_1 hybrids. There is a reduction in the number of myelinated nerve fibres after the completion of myelinogenesis in both the C57BL inbred strain and its F_1 hybrids.

The *Sey* gene mutation in the heterozygous state has a secondary influence on the development of the optic nerve. The nerve is small in calibre compared to that of its normal i.e. (+/+) littermates, although the nerve fibres in the adult optic nerve are fully myelinated and have a pattern of distribution along the nerve fibre diameter spectrum similar to that of other normal mouse strains. The nerve fibre density was also comparable with that of normal mouse strains. Furthermore, there was no significant difference between the left and the right optic nerve nor evidence of sexual dimorphism between males and females in the heterozygous mutant *Sey/+* mice.

Prenatal alcohol exposure significantly influences both the size of the optic nerve and the process of myelinogenesis within the nerve. The onset and progression of myelinogenesis are retarded by alcohol, however the normal sequence of events is unaffected i.e. myelinogenesis starts in the large diameter fibres and progresses to fibres in order of decreasing fibre size. Furthermore, the rate of progression of myelinogenesis is initially rapid but subsequently tails off with age. The spectrum of distribution of myelinated nerve fibres within the nerve is narrowed by alcohol, but not significantly so; it follows the same pattern as in controls in being unimodal and having a positive skew.

These morphometric findings in the optic nerve of the mouse, both in the normal state and when under either mutational or teratogenic influence, are of considerable interest in that they strongly suggest that this central tract provides a useful means of understanding some of the factors that influence the visual system. Similar work on the retina is of equal interest and is complementary to the findings presented in this thesis.

To

Sweetie and the boys - Chat and Zanang.

CONTENTS

	PAGE
CHAPTER ONE: INTRODUCTION.	1
1.1 Anatomy of the visuosensory pathway	3
1.1.1 The eyeball and retina	6
1.1.2 The optic nerve	10
1.1.3 The optic chiasma	10
1.1.4 The optic tract	11
1.1.5 The lateral geniculate body	12
1.1.6 The optic radiation	12
1.1.7 The visuosensory cortex	13
1.2 Anatomy of the optic nerve	15
1.2.1 Gross anatomy	15
1.2.2 Microscopic anatomy	18
1.2.3 Developmental anatomy	19
1.3 The mouse as a suitable model for human research	20
1.4 Some mouse strains in use as experimental models	22
1.4.1 Inbred	22
1.4.2 Hybrid	23
1.4.3 Mutant	24
1.5 Embryology and life span of the mouse	25
1.5.1 Embryology	25
1.5.2 Life span	27
1.6 Development of the optic nerve in the mouse	29
1.7 Teratology	32
1.8 The optic nerve as a model for the analysis of the central nervous system	35
1.9 The aims of the present research	35
CHAPTER TWO: MATERIALS AND METHODS.	37
2.1 Mouse stocks	40
2.1.1 General	40
2.1.2 CBA/Ca(EUMM)	40
2.1.3 C57BL/6(EUMM)	40
2.1.4 F_1 hybrid	40
2.1.5 F_2 hybrid	40
2.1.6 *Small eye (Sey)* mice	41
2.2 Induction of ovulation in female mice	41
2.3 Fixatives	42
2.3.1 Glutaraldehyde-Paraformaldehyde: primary fixative	42
2.3.2 Osmium tetroxide: secondary fixative	42
2.4 Phosphate buffer	43
2.5 General anaesthetic	43
2.6 Embedding medium	43
2.7 Surgical procedures	44
2.7.1 Anaesthesia	44
2.7.2 Perfusion	44
2.7.3 Dissection of the optic nerve	45
2.8 Tissue processing for electron microscopy	45
2.8.1 Fixation	45
2.8.1a Primary fixation	46
2.8.1b Secondary fixation	46
2.8.2 Dehydration	47

2.8.3 Embedding 47
2.9 Glass knives 47
2.10 Cutting sections from the optic nerve 48
2.10.1 Preparing blocks for cutting 48
2.10.2 Cutting semithin sections for light microscopy 48
2.10.3 Cutting ultrathin sections for electron microscopy 50
2.11 Staining semithin sections of optic nerve for light microscopy 50
2.12 Staining ultrathin sections of optic nerve for electron microscopy 51
2.12.1 Staining with lead citrate 51
2.12.2 Staining with uranyl acetate 52
2.13 Electron microscopy 52
2.14 Photographic procedures 53
2.14.1 Developing transmission electron micrographic (TEM) plates 53
2.14.2 Printing micrographs 53
2.15 Routine waste disposal 54
2.15.1 Carcasses 54
2.15.2 Surgical materials 54
2.15.3 Other hardware 54
2.15.4 Chemicals 54
2.16 Image analysis system (Magiscan) 55
2.17 Morphometric analysis 57
2.17.1 Measuring cross-sectional area (csa) of optic nerve 57
2.17.2 Sampling myelinated nerve fibre profiles in optic nerve 57
2.18 Computation of myelinated nerve fibre counts and density 62
2.18.1 Myelinated nerve fibre count 62
2.18.2 Density of myelinated nerve fibres 62
2.19 Statistical analysis 63
2.19.1 Mean 63
2.19.2 Variance 63
2.19.3 Standard deviation 63
2.19.4 Standard error of mean 64
2.20 Verification of results (Student's t-test) 64

CHAPTER THREE: MORPHOMETRIC ANALYSIS OF MYELINATED FIBRE COMPOSITION IN THE OPTIC NERVE OF ADULT C57BL AND CBA STRAIN MICE AND (C57BL X CBA) F_1 HYBRID: A COMPARISON OF INTERSTRAIN VARIATION. 65

3.1 Introduction 66
3.2 Materials and methods 68
3.3 Results 71
3.3.1 Cross-sectional areas (μm^2) 71
3.3.2 Total myelinated nerve fibre counts 74
3.3.3 Myelinated nerve fibre density (fibres $1000\mu m^{-2}$) 79
3.3.4 Myelinated nerve fibre diameter spectrum 81
3.4 Discussion 84

CHAPTER FOUR: MORPHOMETRIC STUDY OF THE OPTIC NERVE OF ADULT NORMAL MICE AND MICE HETEROZYGOUS FOR THE *SMALL EYE* MUTATION (*Sey*/+). 88

4.1 Introduction 89
4.2 Materials and Methods 90
4.3 Results 91
4.3.1 Cross-sectional areas (μm^2) 91
4.3.2 Total myelinated nerve fibre counts 95
4.3.3 Myelinated nerve fibre density (fibres $1000\mu m^{-2}$) 100
4.3.4 Myelinated nerve fibre diameter spectrum 100
4.4 Discussion 104

CHAPTER FIVE: CHANGES IN MORPHOMETRIC PARAMETERS OF THE OPTIC NERVE IN (C57BL X CBA) F_1 HYBRID MICE DURING POSTNATAL DEVELOPMENT. 110

5.1 Introduction 111
5.2 Materials and Methods 113
5.3 Results 115
5.3.1 Cross-sectional areas (μm^2) 115
5.3.2 Total myelinated nerve fibre counts 118
5.3.3 Myelinogenesis in relation to general growth of the optic nerve 122
5.3.4 Myelinated nerve fibre density (fibres $1000\mu m^{-2}$) 122
5.3.5 Myelinated nerve fibre diameter spectrum 125
5 4 Discussion 128

CHAPTER SIX: MORPHOMETRIC ANALYSIS OF THE PROCESS OF MYELINOGENESIS IN THE OPTIC NERVE OF THE (C57BL X CBA) F_1 HYBRID MOUSE. 132

6.1 Introduction 133
6.2 Materials and Methods 135
6.3 Results 136
6.3.1 Onset and progression of myelinogenesis 136
6.3.2 Myelinated nerve fibre diameter spectrum 141
6.3.3 Number of myelin lamellae per axon 146
6.4 Discussion 154

CHAPTER SEVEN: COMPARATIVE MORPHOMETRIC ANALYSIS OF THE POSTNATAL DEVELOPMENT OF THE OPTIC NERVE IN AN INBRED MOUSE STRAIN AND ITS F_1 HYBRID. 159

7.1 Introduction 160
7.2 Materials and Methods 161
7.3 Results 162
7.3.1 Cross-sectional areas (μm^2) 162
7.3.2 Total myelinated nerve fibre counts 165
7.3.3 Myelinated nerve fibre density (fibres $1000\mu m^{-2}$) 171
7.3.4 Myelinated nerve fibre diameter spectrum 171
7.4 Discussion 184

CHAPTER EIGHT: MORPHOMETRIC ANALYSIS OF THE EARLY POSTNATAL TERATOGENIC EFFECTS OF ACUTE ALCOHOL EXPOSURE TO THE PRENATAL MOUSE OPTIC NERVE. 191

8.1 Introduction 192
8.2 Materials and Methods 194
8.3 Results 196
8.3.1 Cross-sectional areas (μm^2) 196
8.3.2 Total myelinated nerve fibre counts 198
8.3.3 Myelinated nerve fibre density (fibres $1000\mu m^{-2}$) 202
8.3.4 Myelinated nerve fibre diameter spectrum 203
8.4 Discussion 207

CHAPTER NINE: GENERAL DISCUSSION. 212

9.1 Dimorphism in the mouse optic nerve 213
9.2 The normal postnatal development and growth of the mouse optic nerve 218
9.2.1 Cross-sectional area of the mouse optic nerve 218
9.2.2 Myelinogenesis in the optic nerve 220
9.3 Mutational effects on the morphometric parameters of the mouse optic nerve 223
9.4 Teratogenic effects on the morphometric parameters of the mouse optic nerve 229
9.5 Clinical implications of the present research 235

REFERENCES 239

APPENDIX 256

CHAPTER ONE

INTRODUCTION

Contents

1.1 Anatomy of the visuosensory pathway

1.1.1 The eyeball and retina

1.1.2 The optic nerve

1.1.3 The optic chiasma

1.1.4 The optic tract

1.1.5 The lateral geniculate body

1.1.6 The optic radiation

1.1.7 The visuosensory cortex

1.2 Anatomy of the optic nerve

1.2.1 Gross anatomy

1.2.2 Microscopic anatomy

1.2.3 Developmental anatomy

1.3 The mouse as a suitable model for human research

1.4 Some mouse strains in use as experimental models

1.4.1 Inbred

1.4.2 Hybrid

1.4.3 Mutant

1.5 Embryology and life span of the mouse

1.5.1 Embryology

1.5.2 Life span

1.6 Embryology of the optic nerve in the mouse

1.7 Teratology

1.8 The optic nerve as a model for the analysis of the central nervous system

1.9 The aims of the present research

1.1 ANATOMY OF THE VISUOSENSORY PATHWAY.

One of the stimuli to which nearly all living organisms respond is light, the commonest source of which is solar radiation, and this makes up part of their natural environment. However, the mechanism of response varies from one organism to the other. For example, whereas plants respond to light by photosynthetic mechanisms, animals do so by means of photochemical receptors (Williams et al., 1989) within the visible spectrum of solar radiation i.e. 400-760 nm. Depending on the level of complexity and lifestyle of the organism, the visual organs in which the photoreceptors are located may be of variable degrees of organization and complexity - from very primitive to highly specialized forms. In mammals these photoreceptors are the cones and rods which are located in the neural part of the retina of the eye. Direct communication with the external environment, enables these photoreceptors to receive light stimuli from it and transmit appropriate signals in a modified form to the brain through a network of neurons. Because the anatomy of the human visual system has been more closely studied than that of any other mammal, the account of the visual system presented in this chapter is based principally on the *human* visual system except where otherwise stated.

The general organisation of the visual system is as follows:

i) The eyeball and retina

ii) The optic nerve

iii) The optic chiasma

iv) The optic tract

v) The lateral geniculate body

vi) The optic radiation

vii) The visuosensory cortex

Figure 1.1 is a schematic presentation of the structural organization of the *human* visual pathway

7.139 A diagram of the visual pathway to show the spatial arrangement of nerve cells and their fibres in relation to the quadrants of the retinae and visual fields. The proportions at various levels are not exactly to scale and in particular the macula is exaggerated in size in the visual fields and retinae. In each quadrant of the visual field, and the parts of the visual pathway subserving it, two shades of the respective colour are used, the paler for the peripheral fields and the darker shade for the macular part of the quadrant. From the optic tract onwards these two shades are both made more saturated to denote intermixture of neurons from both retinae, the palest shade being reserved for parts of the visual pathway concerned with uniocular vision. The path of the light reflexes has also been indicated.

Figure 1.1: A schematic presentation of the structural organization of the *human* visual pathway (derived from Williams et al., 1989, with permission).

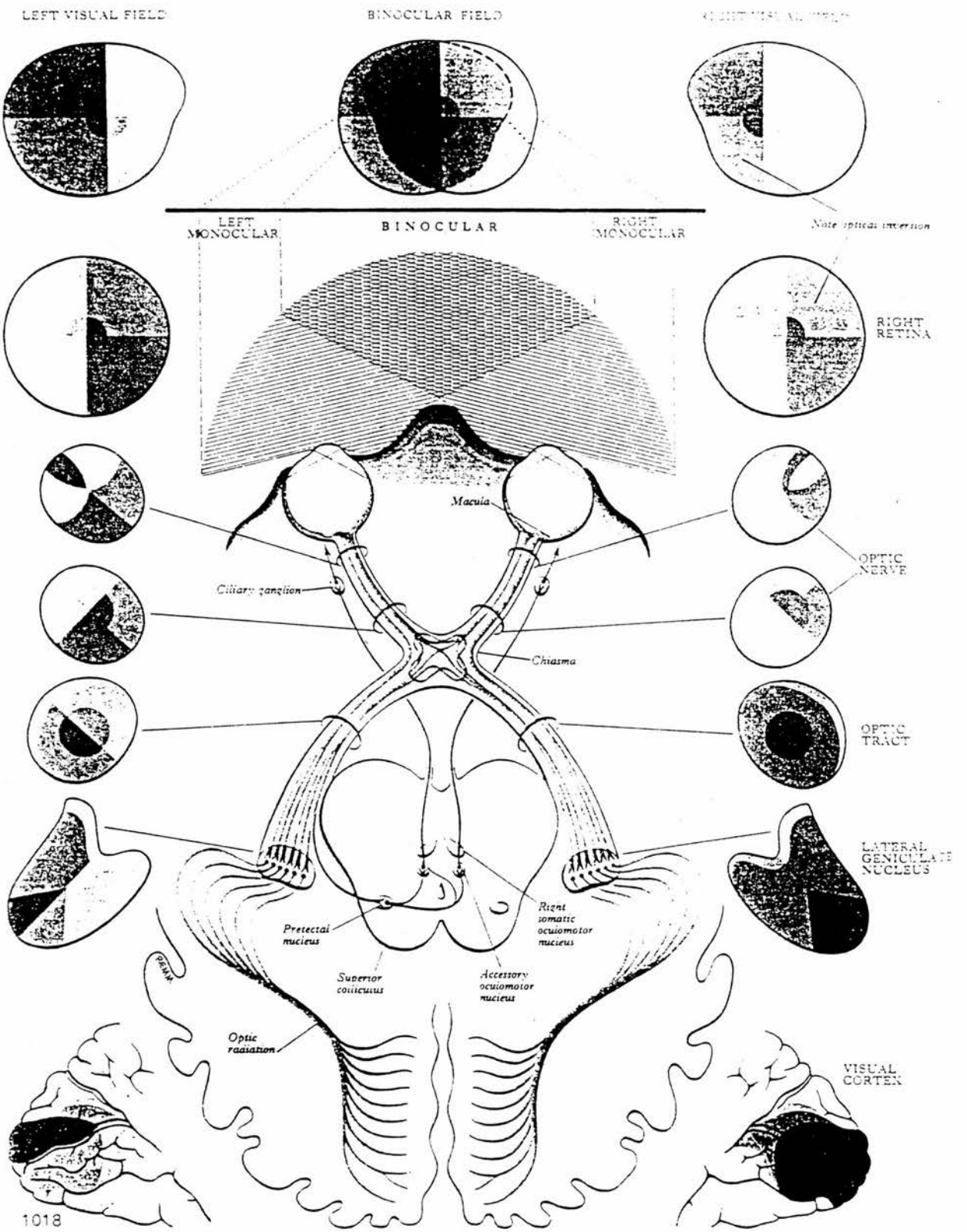
LEFT VISUAL FIELD
BINOCULAR FIELD
LEFT MONOCULAR
BINOCULAR
RIGHT MONOCULAR
Note optical inversion
RIGHT RETINA
Macula
Ciliary ganglion
OPTIC NERVE
Chiasma
OPTIC TRACT
LATERAL GENICULATE NUCLEUS
Pretectal nucleus
Right somatic oculomotor nucleus
Superior colliculus
Accessory oculomotor nucleus
Optic radiation
VISUAL CORTEX
1018

Figure 1.1

1.1.1 THE EYEBALL AND RETINA

The eyeball is the part of the visual system that is in direct contact with the external environment. It is located in the bony orbit which provides protection, rigidity and direction that are necessary prerequisites for its various functions. The eyeball is globular in shape, though not a true globe because it consists of two unequal spherical segments - a more prominent transparent anterior segment from a smaller sphere which forms about a sixth of the globe, and a larger opaque but less prominent posterior segment. The anterior segment is bounded by the cornea (anteriorly) which has an oval opening, the pupil, through which light from the exterior enters the visual system; and the lens which is suspended from the iris by suspensory ligaments more posteriorly. The iris further subdivides the anterior segment into an anterior and a posterior chamber. The larger posterior segment of the eyeball is bounded anteriorly by the posterior surfaces of the lens and the iris, and externally by the sclera. The sclera is continuous with the cornea anteriorly at the limbus and with the dural sheath of the optic nerve at the posterior pole of the eyeball. The size and shape of the eyeball are dependent on the age and sex of the individual. For example, it has been shown that all the dimensions of the eyeball in females are less than those in males (Sorsby & Sheridan, 1960). Structurally, the eyeball comprises of three tunics that enclose its contents, although the inner and intermediate tunics are deficient anteriorly. The tunics from without inwards are as follows:

a) a fibrous tunic made up of the sclera posteriorly and the cornea anteriorly. The sclera is a dense collagenous fibroelastic tissue that maintains the shape of the eyeball. It is thickest at its junction with the optic nerve posteriorly where it is continuous with the dural sheath of the nerve. The cornea is convex anteriorly, transparent and avascular but highly innervated. It is the main site for light refraction for the eye, being responsible for nearly 70% of refraction, while the lens is responsible for most of the remaining 30%.

b) a vascular pigmented tunic also called the uveal tract. This consists of the choroid posteriorly, and the ciliary body and the iris anteriorly. The choroid is a thin dark brown highly vascularised tissue. It is located between the neural retina and the sclera. The ciliary body is the direct continuation of the choroid and extends to form the iris more anteriorly. The lens is suspended by means of ligaments, by means of which accommodation is controlled. The iris is a diaphragm with a nearly centrally placed aperture, the pupil, anterior to the lens. It has a considerable number of muscle fibres within it as well as a rich neurovascular supply. The diameter of the pupil ranges from 1 to 8 mm and may be influenced by the actions of drugs. The shape and size of the pupil are altered by the iris and this in turn controls the amount of light that reaches the retina.

c) a neural tunic, the retina. It is the innermost tunic of the eyeball and is the beginning of the neural relay of light impulses to the brain. It is in close association with the inner surface of the choroid and the external surface of the hyaloid membrane of the vitreous body. It is continuous with the optic nerve at the optic disc posteriorly. The optic disc has a slightly raised margin with a central depression pierced by the vessels supplying (and draining) the retina, the central retinal vessels. In optic atrophy these vessels become attenuated and the disc diminishes and appears to consequently become pale. It is also called the 'blind spot' because it is insensitive to light reflexes, for despite the fact that nerve fibres pass through the blind spot, it is devoid of photoreceptor cells (Moore, 1985). Almost at the centre of the retina is the macula lutea, an oval area with a central depression, the fovea centralis where maximum visual resolution takes place. During embryonic development the retina differentiates from the outer component of the double layered optic cup following the invagination of the optic vesicle (Hollenberg & Spira, 1973; O'Rahilly, 1975). The outer layer differentiates into the pigment cell lamina while the inner layer gives rise to a complex multi-laminar structure that contains the rods and cones together with their first order neurons (bipolar cells), the second order neurons (ganglion cells) and interneurons (horizontal and amacrine cells), and an associated vascular system. In man, by the 8th month

of intrauterine life all the layers of the retina can be identified (Williams et al., 1989). A detailed account of the structural organization of the retina is beyond the scope of this work and has consequently only been provided schematically in figure 1.2.

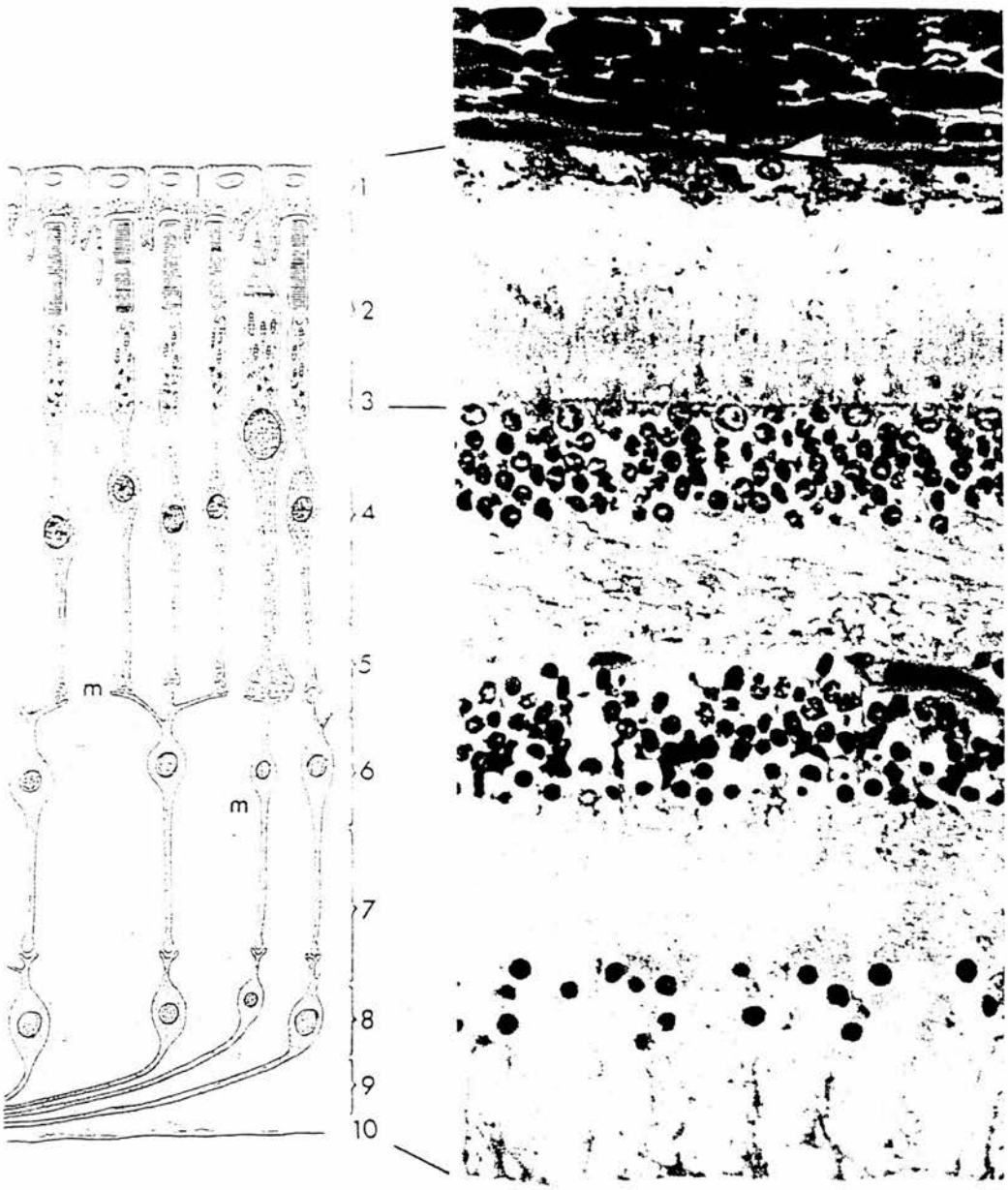

Figure 17–21. *Left:* Diagram illustrating the layers of the retina. Only photoreceptors (rods and one cone), direct conducting neurons, and the fibers of Müller are illustrated. The numbers refer to the following layers: 1, pigment epithelium; 2, layer of rods and cones; 3, external limiting membrane; 4, outer nuclear layer; 5, outer plexiform layer; 6, inner nuclear layer; 7, inner plexiform layer; 8, ganglion cell layer; 9, optic nerve fiber layer; 10, internal limiting membrane. *Right:* Photomicrograph of the same area. At top is the inner portion of the choroid with the choriocapillaris (dark, arrowhead). Cone nuclei are indicated (c). × 400.

Figure 1.2: A schematic representation of the structure of the mammalian retina (derived from Lesson et al., 1985, with permission).

1.1.2 THE OPTIC NERVE

From the retina photoreceptors, the next destination of impulses on their way to the visual cortex is the optic nerve. Since the present work has been done mainly on this central tract, a more comprehensive account of its anatomy is given in a separate section below (see section 1.2).

1.1.3 THE OPTIC CHIASMA

It is a flat and almost quadrilateral mass of nerve fibres with angles that are directed anterolaterally and posterolaterally. The anterolateral angles are in continuation with the optic nerves and the posterolateral ones with the optic tracts. It is ensheathed by the meningeal coverings of the brain and lies ventral to the diaphragma sellae, although without maintaining contact with the hypophysis and the tuber cinereum (Warwick, 1976). It forms the floor of the recess of the 3rd venticle. The anterior cerebral arteries and their anterior communicating branches cross it ventrally. The anterior perforated substance and the internal carotid artery are in contact with the lateral aspect of the chiasma. One of the most important phenomena in the visual pathway is the decussation of the nerve fibres at the optic chiasma. Fibres from the nasal half of the retina and half of those from the macula cross to the contralateral optic tract. Those from the temporal part of the retina continue to the ipsilateral tract. Chan & Guillery (1994) observed that during the development of the visual system, there is a distinct quadrant specific organization of the nerve fibres in the optic stalk immediately behind the eyeball. The result is that fibres from the nasal, dorsonasal, dorsotemporal and ventrotemporal regions of the retina are arranged sequentially along the rostrocaudal axis of the cross-section of the optic nerve. After crossing at the chiasma, the fibres begin to reorganize themselves into another distinct order again (also see Colello & Guillery, 1992 (mouse); Meissirel & Chalup, 1994 (monkey)). In the mouse the first optic axons arrive at the optic chiasma at (embryonic) day 13 post coitum (p.c.) and by day 14 p.c. they cross the midline (Silver, 1984; Colello & Guillery, 1990). The optic chiasma is richly supplied by a pial vascular plexus formed by branches mainly from the anterior cerebral and

internal carotid arteries. The plexus also receives branches from the superior hypophyseal, and the anterior and posterior communicating arteries. Venous drainage is through the basal and the anterior cerebral veins. Because of its close relationship with the hypophysis it may be compressed by tumours of the hypophysis.

1.1.4 THE OPTIC TRACT

The nerve fibres in the optic chiasma continue as the optic tracts at the posterolateral angles of the optic chiasma with most of the fibres terminating in the lateral geniculate body. Each tract represents the last part of the extracerebral portion of the visual pathway. Beyond the tract the visual fibres are found in the white matter of the brain. Each optic tract passes between the anterior perforated substance and the tuber cinereum, forming the anterolateral boundary of the interpeduncular fossa. Each tract progressively flattens as it becomes closely applied to the upper surface of the anterior border and then the lateral border of the cerebral peduncle. The posterior cerebral artery runs parallel to the tract. Each tract divides into a medial and a lateral ramus as it approaches the lateral geniculate body. The medial ramus is believed to carry supraoptic commissural fibres. The lateral ramus carries fibres from the retina and partially decussating fibres in the chiasma together with a few efferent fibres that end in the retina. Most of the fibres in the lateral ramus end in the lateral geniculate body, and are later relayed to the cerebral cortex as sensory visual fibres. Some proceed to the superior colliculus, being the fibres for general reflex response to light. Others get to the pretectal nucleus where they terminate. These are for pupillary constriction (Campos-Ortega et al., 1972; Warwick, 1976; Berman & Jones, 1977; Williams et al., 1989). In the tract, macular fibres which were central in the optic nerve become eccentric and dorsolateral, with fibres from both retinae having intermingled at the optic chiasma. Blood supply to the optic tract is from the pial network of vessels which are partly from the posterior communicating and the anterior choroidal vessels.

1.1.5 THE LATERAL GENICULATE BODY

This is a small ovoid nuclear complex that projects ventrally from the posterior thalamic area. Its anterior pole forms the thalamic termination of the fibres of the optic tract, and gives rise to the optic radiation which conveys visual impulses to the occipital lobe of the cerebral cortex. Together with the medial geniculate body they form part of the metathalamus. The lateral geniculate body is bypassed by fibres from the optic tract that reach the superior colliculus to form its brachium. The two geniculate bodies are relay nuclei, the lateral for the visual and the medial for the acoustic pathways to the cerebral cortex. The dorsal nucleus of the lateral geniculate body has six laminae of neurons all of which appear simultaneously during embryonic development (Cooper, 1945). Axons from its nucleus traverse the dorsal limb of the internal capsule to emerge as the optic radiation. The adult human lateral geniculate body has approximately one million neurons and this corresponds closely to the number of axons in the optic nerve and tract (Kupfer et al., 1967). First order neurons, i.e. axons from the retina end in the lateral geniculate body by dividing into 5-6 terminals which synapse with the same number of second order neurons i.e. neurons originating from the lateral geniculate body (Williams et al., 1989). Blood supply to the lateral geniculate body is from the posterior cerebral and the anterior choroidal vessels. There is a rich anastomosis between the two sources.

1.1.6 THE OPTIC RADIATION

The optic radiation, also sometimes known as the geniculo-calcarine pathway, is a collection of second order neurons from the lateral geniculate body to the visual cortex. The fibres spread out to form the medullary optic lamina. This is initially vertical, but subsequently becomes horizontal near the striate cortex. The ventral part of the optic radiation first plunges like a loop into the temporal pole before passing backward as an inferior longitudinal fasciculus. Because the optic radiation lies deep to the middle temporal gyrus, tumours of this part of the temporal gyrus could result in visual defects (Warwick, 1976). Although it has yet to be substantiated in man, in certain animals the optic radiation also

carries fibres from the cerebral cortex to the lateral geniculate body and superior colliculus, as well as descending fibres to the nuclei of ocular motor nerves. Fibres from the upper part of the retina which form the medial aspect of the lateral geniculate body make up the upper portion of the optic radiation and proceed to the upper lip of the calcarine fissure. Fibres from the lateral aspect of the lateral geniculate body form the lower portion of the optic radiation. As in the lateral geniculate body, macular fibres continue in the optic radiation in two separate groups representing the upper portions of the retina and those representing its lower portion. The optic radiation is supplied by perforating branches of the choroidal artery, the deep optic branch of the middle cerebral artery and the perforating cortical artery from the calcarine branch of the posterior cerebral artery. Venous drainage is through the corresponding veins.

1.1.7 THE VISUOSENSORY CORTEX.

The majority of the visual cortex is situated in the medial aspect of the occipital lobe in the posterior part of the calcarine sulcus, although it may also extend to the lateral part of this lobe where it is limited by the sulcus lunatus. It is characteristically distinguishable to the naked eye by the presence of a white line or stria (of Gennari), hence, its name the area striata or striate cortex. The latter principally constitutes area 17 and was originally believed to be the only terminal of the optic radiation. However, it has now been shown that neurons from the lateral geniculate body also radiate to areas 18 and 19 in certain animals such as cats and monkeys (Glickstein et al., 1967; Wilson & Cragg, 1967; Garey & Powell, 1968); and that there are interconnections between these three areas (Cragg, 1969; Zeki, 1969). Although the striate cortex makes up just 3% of the surface of the cerebral cortex, it receives approximately 10% of cortical neurons (Williams et al., 1989). Neurons project from all these three areas to the thalamus or brain stem or to both, and all these are also linked to other areas in both cerebral hemispheres by short and long commissural fibres. The cerebral cortex has a general laminar organization of cell bodies of its neurons and their processes which is as follows:

1) plexiform layer. This is the most external lamina. It consists of dense interweaving neurites from intrinsic cortical neurons (mostly stellate cells), pyramidal cells, dendrites and afferent fibre terminals to the cortex from other parts of the central nervous system (CNS).

2) external granular lamina. This is a collection of a large number of cell bodies of different neurons, the majority of which are stellate and pyramidal cells. The axons and processes of these neurons synapse with one another and with those of afferent fibres reaching this lamina, and also extend into adjacent laminae.

3) pyramidal lamina. This is dominated by pyramidal neurons as well as interneurons of stellate type. Processes in this lamina are arranged vertically (fusiform cells) and horizontally ('basket' cells) and extend beyond this lamina.

4) internal granular lamina. It is a thin lamina containing mainly vertically arranged stellate interneurons and a few pyramidal cells.

5) ganglionic lamina. The cells here are also stellate and pyramidal in shape. It has the highest proportion of pyramidal neurons of any cortical area. Furthermore, it also has a collection of dendrites and axons of local neurons and those in transit which extend to other cortical levels.

6) multiform lamina. This is nearest to the cerebral white matter and consists of small neurons, mainly of the pyramidal and stellate types. Also commonly found in this lamina is the Martinotti neuron, characterised by a long centrifugal axon that reaches the plexiform lamina with vertically arranged dendrites that ramify in the deeper layers of the cortex.

Whereas the typical cell type in the motor cortex is pyramidal, that of the sensory cortex is granular and is most highly developed in the striate cortex. There is a direct connection between the striate cortex and other parts of the visual cortex and with the frontal, parietal and temporal lobes by association fibres. It also connects with other areas including the superior colliculus and the oculomotor nuclei. All these interconnections help to integrate the activity of the visual cortex as a whole, in addition to providing an anatomical basis for visuotactile, visuoauditory and other associative functions including eye movements (Warwick, 1976). In the visual pathway it is only in the visual cortex that impulses originating from corresponding parts of the retinae meet. The implication of this is that a lesion at the striate cortex affects all laminae of the lateral geniculate body, indicating that impulses to its alternate layers and those arising from corresponding parts of the retinae pass to the same cortical region. The blood supply of the visual cortex is mainly from the posterior cerebral artery particularly via the calcarine artery, and the middle cerebral, the two anastomosing with each other. Venous drainage is both to cortical and basal veins.

Findings by Garey (1984) showed that in the lateral geniculate body and the visual cortex there is an increase in postsynaptic surfaces during the first postnatal months, but that this subsequently drops to the adult level by the second year. This is associated with rapid synaptogenesis which reaches a peak by the 8th postnatal month. After this there is continuous elimination of synapses until adult levels are attained at about 11 years of age.

1.2 ANATOMY OF THE OPTIC NERVE.

The optic nerve is the link between the photorecepters in the eyeball which receive light stimuli from the external environment and the rest of the visuosensory pathway. It conveys light impulses from the rods and cones of the retina to the visuosensory cortex for the mediation of the appropriate visual response.

1.2.1 GROSS ANATOMY.

The optic nerve is not a true peripheral nerve, but a central tract because its fibres, often classified as somatosensory differentiate mainly from the neuroretina which is a derivative of the embryonic forebrain. It is formed by neurons of the ganglion cells of the retina as they converge at the optic disc to leave the eyeball near its posterior pole. From here, the optic nerve runs to the anterolateral horn of the optic chiasma. As the nerve leaves the eyeball, it becomes ensheathed by extensions of the meningeal coverings of the CNS i.e. the pia, arachnoid and dura mater (from within outward) respectively. This relationship extends almost throughout the entire length of the nerve with the exception of a small portion at the chiasmatic end where both the dura and arachnoid mater are deficient. This relationship between the optic nerve and the meningeal coverings of the brain allows the subarachnoid space and subdural space of the brain to extend around the nerve. Any raised intracranial pressure affecting the brain consequently also affects the optic nerve. At its orbital end the optic nerve is pear shaped but becomes flattened as it approaches the chiasmatic end. For descriptive purposes it is often divided into 4 parts namely: intraocular, intraorbital, intracanalicular and intracranial.

i) Intraocular part: As axons of the retinal ganglion cells leave the optic disc, they pierce the outer layers of the retina, the choroid and the lamina cribrosa about 3-4 mm from the centre of the posterior pole of the eyeball. The nerve fibres which are unmyelinated, by the time they leave the retina acquire myelin and run in fascicles for the rest of the course of the optic nerve.

ii) Intraorbital part: This part of the optic nerve runs a sinuous course because it is approximately 6 mm longer than its actual course. It is the continuation of the intraocular portion of the nerve and ends at the orbital foramen of the optic canal. It is surrounded by the extraocular muscles which are separated from it more anteriorly by orbital fat. The origin of the superior and medial recti are closely adherent to the dural sheath of the nerve at its posterior portion and this relationship may give rise to orbital myositis when the muscles

are inflamed. The central retinal vessels pierce the inferomedial part of the nerve about 1 cm from the eyeball and pass through the centre of the nerve to the optic disc.

iii) Intracanalicular part: This part of the optic nerve is about 5 mm long. It begins at the orbital foramen of the canal and ends at its cranial foramen. In the optic canal the nerve is separated from the periosteum by the dural sheath. It lies superomedial to the ophthalmic artery and is separated from the sphenoidal and the posterior ethmoidal sinuses by thin osseous laminae anterior to the canal. This close relationship between the nerve and these air sinuses may result in it being affected in sinus diseases.

iv) Intracranial part: It is approximately 10 mm long. It runs posteromedially from the cranial foramen of the optic canal to the anterolateral horn of the optic chiasma. Above the nerve are the posterior part of the olfactory tract, the anterior perforated substance and the chiasmatic part of the anterior cerebral artery. The internal carotid artery is initially inferior but later becomes lateral to the optic nerve. The ophthalmic artery branches from the internal carotid artery posterior to the middle part of the nerve. Approximately half of the fibres in the optic nerve decussate at the optic chiasma, with most of them terminating in the lateral geniculate body as has already been mentioned above. Some of the fibres pass to the pretectal nucleus and the superior colliculus. A small number are efferent to the retina.

The optic nerve is supplied by the pial plexus, a rich vascular anastomotic network formed by the ophthalmic artery intracranially, the recurrent ophthalmic branches in the optic canal and the posterior ciliary arteries as well as the central retinal artery in the orbit. Various investigators have demonstrated this rich vascular anastomotic network to the optic nerve (Henkind & Levistsky, 1969; Neetens, 1977; Francois & Fryczkowski, 1978, 1982; Awai, 1985). Francois & Fryczkowski (1978), for example, observed that 85% of the anterior segment of the optic nerve was supplied by the central retinal artery which gives branches throughout its length, and that these branches anastomose with collaterals from the

ophthalmic artery (also see Isayama et al., 1983). In another study (Francois & Fryczkowski, 1982), they demonstrated three vascular networks within the optic nerve - a peripheral, a periaxial and an axial network. The peripheral and the axial networks accounted for 30% each, of the entire network. Venous drainage of the nerve is by the central retinal vein. Interference with the blood supply to the optic nerve has been reported to bear variable consequences on visual functions (King, 1979; Boke & Voigt, 1980).

1.2.2 MICROSCOPIC ANATOMY.

The adult human optic nerve contains more than a thousand bundles of myelinated nerve fibres supported by neuroglia. It carries mainly sensory fibres from the retina i.e. from the retinal ganglion cells to the brain. These fibres constitute the first order neurons of the sensory visual pathway. In addition, the optic nerve carries fibres to the tectum for pupillary reaction, the superior colliculus, some autonomic fibres and a few efferent fibres to the retina. The nerve is immediately surrounded by pia mater from which septa extend into and divide the nerve into fascicles. This is done by the septa getting into the nerve as primary septa from its periphery, then dividing and reuniting repeatedly to form a meshwork within the substance of the nerve. The vascular supply to the nerve is distributed along the septal network. The septal system ends just before the optic chiasma and is not seen for the rest of the visual pathway. The termination of the septal system also marks the point where the decussating fibres first separate from the non-decussating ones. The neuroglial elements are glial fibres and nuclei. The neuroglial cells in the developing optic nerve are predominantly oligodendrocytes but in the adult they are predominantly astrocytes.

The adult human optic nerve has approximately one million fibres all of which are myelinated. The diameter of the nerve fibres varies from about 0.7 to 10.0 μm. Over 90% of the population of the nerve fibres are less than 1.0 μm in diameter (Downer, 1967; Kupfer et al., 1967). With regard to the distribution of nerve fibres within the optic nerve, the macular fibres are lateral in the nerve at its orbital end but gradually become medial and by the time

they get to the optic chiasma they have assumed an anterior position within the nerve. Fibres from the upper and lower parts of the retina are at their respective regions of the optic nerve as it leaves the eyeball. Those from the temporal and the nasal parts of the retina are respectively lateral and medial in the nerve (Williams et al., 1989).

1.2.3 DEVELOPMENTAL ANATOMY.

During the development of the eye, the retina and the optic nerve are derived from the embryonic forebrain, the lens from the surface ectoderm and the accessory tunics from the adjacent mesoderm (Arey, 1974). By the beginning of the 4th week of gestation (day 22 p.c.) the site of the future eye is vaguely defined on either side of the future forebrain as a shallow groove. This soon becomes a shallow pit that evaginates to form the optic vesicle. Subsequently the optic vesicle becomes attached to the brain wall by a slender connection, the optic stalk. The distal end of the optic vesicle undergoes a rapid marginal growth and invagination that transforms it into a double layered structure, the optic cup. The outer layer of the optic cup differentiates into the pigmented layer of the retina and the inner layer into most of the remaining components of the retina. The optic stalk whose cavity is now in communication with that of the diencephalon (i.e. the third ventricle) subsequently differentiates into the optic nerve.

Further invagination of the optic cup and the optic stalk results in the formation of a groove which subsequently becomes the optic fissure. By the 7th week the lips of the fissure close, thus transforming the double walled cup and the stalk into a double walled tube. The continuation of the inner lumen of the optic stalk with the inner layer of the retina provides a direct path for nerve fibres from the retinal ganglion cells to grow into the optic stalk as they advance to reach the brain. By the 6th intrauterine week in man, the optic nerve fibres have reached the under-surface of the forebrain. Between the 7th and 8th weeks the optic chiasma is formed by partial decussation of the nerve fibres, and the optic tract is formed by the 10th week (Arey, 1974; Warwick, 1976). There is an initial over-production followed by

a reduction of the nerve fibres. Sturrock (1987) in a study of the optic nerve of human embryos from 8-18 weeks observed that at 8 weeks, 2.67 million unmyelinated axons were present in the optic nerve. This number dropped to 1.94 million at 10 weeks, but increased sharply to reach a peak of 5.86 million at 14 weeks. By the 18th week this peak value had dropped to 3.58 million. As is reported elsewhere (see - chapters 3 and 4; and also Dangata et al., 1994, 1995 for comparable observations in the mouse) the reduction continues until the adult value for the nerve fibres in the optic nerve has been established. The glial elements of the nerve are formed by the epithelial lining of the walls of the optic stalk. The glial cells subsequently become arranged in rows along the long axis of the nerve while the nerve fibres pass between these rows. The fibrous septa of the nerve are mesodermal in origin.

Myelinogenesis of the optic nerve begins from its cranial end and proceeds caudally to reach the lamina cribrosa just before birth. Sturrock (1987) first observed myelinogenesis in the human optic nerve at the 18th week of intrauterine life. Although myelinogenesis has reached the optic disc at birth, the process has yet to be completed within the nerve. Early in development the hyaloid artery ran in the orbital fissure and became the central retinal artery at the completion of the formation of the optic cup and stalk. This artery supplies the retina and the optic nerve. Between 15 and 18 weeks of intrauterine life, Sturrock (1987) observed fenestrated capillaries at the junction of the dura and the surrounding loose connective tissue. The vascular pattern of the optic nerve is well established by the 5th month of intra-uterine life (Arey, 1974).

1.3 THE MOUSE AS A SUITABLE MODEL FOR HUMAN RESEARCH.

The common house mouse *Mus musculus* is a member of the order Rodentia and family Muridae. This species has been a member of man's immediate family for millenia. This has made it assume different roles in man's life over the years - from being a pest to a pet, and now as a very significant experimental model for various aspects of research of great human

value. For example, European zoologists in the 19th century bred fancy mice to investigate varietal characteristics. Their findings became better interpreted with the rediscovery of Mendel's work in 1900, as this resolved problems like inbreeding, selection, decrease in fertility, appearence of abnormalities and increased susceptibility to disease (Staats, 1966). Since then, the mouse has become established as an invaluable mammalian experimental model. The result is that more information has accumulated on its genetics than that of any other vertebrate, with the exception of man.

The mouse has a number of advantages over the majority of other mammalian species as an experimental model. It is highly adaptable to experimental conditions similar to normal human environmental conditions. Its small size makes handling easy in addition to making breeding and maintenance cost effective (Dagg, 1966). By 3 weeks of age the mouse could be weaned and by 6 weeks it is already sexually mature (Theiler, 1976; Hogan et al., 1994). The gestation period of the mouse is short. Litters are large, although, there is diminishing litter size and weight of offspring with maternal age. The life span of the mouse ranges from 1.3 to 3 years, depending on the strain (Comfort, 1959), and this is long enough for most experimental procedures.

Furthermore, the mouse has many genetic variants which give a wide range of choices for various types of research. For example, in cancer research inbred strains of mice are used because of their reliability and predictability to produce specific types of tumours. Consequently, the derivation of inbred strains is one of the most important events in the history of mouse genetics. It has made a significant impact on studies in cancer research, immunology and tissue transplantation (Hogan et al., 1994). Similarly, F_1 hybrid mice combining genetic homogeneity with hybrid vigour survive longer during experimental procedures, therefore, they are generally preferred for research that does not require the production of genetically homogeneous offspring (Russell, 1966). Because the genetic constitution of the mouse is better known than that of any other mammal (excluding man) in addition to the fact that, it is subject to a number of known hereditary diseases similar to

those found in man, it is the most commonly used animal model in genetic studies (Green, 1966).

1.4 SOME MOUSE STRAINS IN USE AS EXPERIMENTAL MODELS.

Different strains in many animal species have been developed following the pioneering work of scientific animal breeding of Castle et al. (1906) who worked with *Drosophilia*, King (1911) with rats and Wright (1922) with guinea pigs. Since then hundreds of different inbred strains have been produced in the mouse alone. In the Jackson Laboratory, for example, millions of mice are raised from over 75 strains and substrains each year. This has facilitated the use of strain differences in many fields of research. For instance, strain differences with regard to life span, litter size, length of the reproductive period, adaptability to environmental and experimental conditions, and disease susceptibility are usually of considerable significance in the choice of a particular strain for any experimental procedure. Of common use in research are the inbred, hybrid and mutant-bearing mouse strains.

1.4.1 INBRED.

A mouse is regarded as belonging to an inbred strain when there has been 20 or more successive generations of brother x sister matings or more than 20 successive generations of parent x offspring matings, provided the offspring are mated to the younger parent (Staat, 1964; Lyon & Searle, 1989; Hogan et al., 1994). Mice with only a few generations of inbreeding are referred to as 'partially inbred'. The first inbred mouse strain *dbr* (which was later called dba after the three recessive genes for *dilution, brown* and *non agouti* and is presently written as DBA) was produced by Clarence Cook Little. This was a few years after Little began to study the inheritance of coat colour in mice in 1907 (Staat, 1966). Within 15 years after this initial work by Little, many other workers developed the various inbred strains commonly used in cancer research today. For example, Halsey J Bagg obtained albino mice from a dealer in Ohio in 1913 and maintained them as a closed colony which he used for behavioural experiments. Through a series of crosses between Bagg's albino and Little's DBA, Leonell C Strong produced hybrids from which he developed a

number of inbred lines e.g. C3H, CBA, C, CHI and CI2I. Of these the C3H has been the most commonly used (Staat,1964). Also of extensive used in research is another well known family of inbred strains that Little developed in 1921 while at Cold Spring Harbor. He obtained a fancy mouse and mated female 57 and male 52 to obtain progenies that segregated as black and brown. He cross bred these to obtain the C57BL and the C57BR strains.

Presently there are about 400 inbred strains of mice available (Hogan et al., 1994). As more information on inbred mouse strains becomes available, investigators have increasingly recognised their significant contribution to the field of medical research. For example, the majority of inbred mouse strains derived from the DBA to the most recently obtained lines, were developed primarily for cancer research, to provide evidence for the existence or non existence of genetic factors that influence the incidence of different types of cancer. But they are also presently extensively used for teratological studies (Randall & Taylor, 1979; Middaugh & Boggan, 1991; Becker et al., 1993; Ashwell & Zhang, 1994). Crosses between inbred strains provide F_1 hybrids for terminal experiments or as background strains for the transfer of a mutant gene from one genetic background to another. One of the commonest problems associated with inbreeding is inbreeding depression. This is the progressive loss of reproductive fitness with breeding, and this may result in reproductive failure.

1.4.2 HYBRID.

As has already been mentioned F_1 hybrids are derived by cross-breeding inbred strains. They are genetically homozygous, but for gene pairs where the parent strains differ, they are heterozygous. They are genetically more vigorous than the parent strains, and are preferred to the parent strains in some terminal experiments. Furthermore, they tend to grow faster, survive to maturity in a greater proportion and live longer than the parent strains. Chai (1959) reported a longer life span in hybrid than inbred strains and attributed this to the reduction of early mortality among hybrids, although without mentioning the mechanism by

which mortality was reduced. Reproduction starts earlier and more abundantly in hybrids than in the parent strains. Litters are usually, but not always, larger than those of either parent strains (Green, 1966). However, they are rarely used to propagate their own characteristics because genetic segregation occurs in the F_2 generations.

1.4.3 MUTANT.

The mouse has 20 pairs of chromosomes and approximately 0.5-1.0 x 10^5 genes (Hogan et al., 1994). Most named mutant genes can be maintained without attention to systematic breeding schemes because they have consistent and easily recognised effects not obscured by the normal range of environmental or genetic background variation (Green, 1966). This has made the transfer of a mutation from one genetic background to another of great significance in medical research. For example, it facilitates the comparison of the effects of a mutant and a non-mutant allele with the greatest precision possible. Such genetic transfer is done through different systems of crossing. In the backcross system, for example, mice bearing a dominant mutation of interest either as heterozygotes (D/+) or if viable, as homozygotes (D/D) are mated with an inbred strain of mice that are (+/+) at the D locus. The (D/+) progeny are then backcrossed to the (+/+) mice from the inbred strain. The same procedure is carried out if the mutation of interest is recessive. Another system for genetic transfer is the cross-intercross system. Here homozygous mice for a recessive mutation (r/r) are mated with mice of an inbred strain which are (+/+) at the r locus. The (r/+) progeny are then intercrossed to recover the homozygous (r/r) which is used to start another cycle of crossing and intercrossing. Over 300 mutant genes occupying more than 250 loci are known in the mouse (Green, 1966).

Of common use in genetic research is the *Small eye (Sey)* gene. The *Sey* mutation spontaneously arose at the Institute of Animal Genetics in Edinburgh from a line that had previously been selected for small body weight (Roberts, 1967). The *Sey* gene which is analogous to the human *aniridia* gene has since then been mapped to chromosome 2 (Hogan

et al., 1986; Jong et al., 1990; Ton et al., 1992). It has variable expressivity in the heterozygous state. The size of the eyeball could range from a few millimeters in diameter to normal. The orbit may be small and could result in asymmetry of the cranium and the brain. Sometimes the optic chiasma is absent. Other associated features include thickening of the extracellular membranes, particularly in the lens and retina of embryos older than 13 days p.c., cellular degeneration, overgrowth and invasiveness, and mutual adhesiveness of tissues. By day 10.5 p.c., homozygous embryos can be identified by the absence of the lens and nasal placodes. They have neither eyes nor nasal tissue by the end of gestation and so do not survive for more than a few hours after birth (Roberts, 1967; Hogan et al., 1986; Jong et al., 1990; Ton et al., 1992).

Also located on the same chromosome are other semidominant genes like Dickie's small eye (*Sey*^{dey} - formerly *Dey* - Theiler et al., 1978; Hogan et al., 1987) and small eye-Harwell (*Sey*^{H} - Hogan et al., 1986). The *Sey*^{dey} also arose spontaneously in the C3H/HeJ strain. It is very similar in its effects to the *Sey*^{H} in both the heterozygous and the homozygous states. The *Sey*^{H} was found among offspring of an irradiated (C3H/HeH x 101/H)F_1 female. *Sey*^{H}/+ heterozygotes which are usually small at birth, are more affected than the *Sey*/+. The eyes often have coloboma which are noticeable by day 14 p.c. The ears may be small and low set. Although both sexes are fertile, the females are poor breeders.

1.5 EMBRYOLOGY AND LIFE SPAN OF THE MOUSE.

1.5.1 EMBRYOLOGY

The development of the mouse is of interest because it is a suitable model system that sheds light on various developmental processes in man. This makes a knowledge of its own development a necessary prerequisite to such research. The early development of the mouse is much slower compared to organisms such as *Drosophila* and *Xenopus*. For example, 24 hrs following fertilization these species are almost free-living, feeding larvae and contain

thousands of cells that are already organized into many different tissue types. The mouse embryo at this stage is just at the 2-cell stage (Hogan et al., 1994).

Development of the mouse begins with the fertilization of the egg by the sperm in the ampulla of the fallopian tube (Snell & Stevens, 1966). Following fertilization the zygote undergoes cleavage (a series of successive cell divisions) up to the 64-cell stage when it implants in the uterine wall (by day 4.5 p.c.) (Ayala & Kiger, 1984; Hogan et al., 1994). At the third cleavage stage the cells are totipotential, i.e they can give rise to any cell type. After 3 or 4 cell divisions the zygote becomes known as a morula because it resembles a mulberry. It is believed that the first signal that commits sister cells to different developmental pathways occurs at the morula stage. The cells of the morula become organised into a central core of cells, the inner cell mass or embryoblast and an outer layer of cells, the trophoblast. The embryoblast subsequently gives rise to the primary germ layers of the embryo i.e. the ectoderm, mesoderm and endoderm, and the trophoblast the fetal part of the placenta. By the 64-cell stage the embryo is referred to as the blastocyst. Only a small number of the cells at this stage are totipotential.

Between days 5 and 10 p.c., the primary germ layers are established from the embryoblast as well as the basic body plan and organ primordia of the future mouse. A series of events is involved in the establishment of this body plan and organ primordia. The paraxial mesoderm on either side of the notochord is divided into pairs of somites which produce an obvious segmental pattern. The lateral plate mesoderm however remains unsegmented. The neural plate is induced to fold into the neural tube which subsequently divides to form the forebrain, midbrain, hindbrain and the spinal cord. The nasal, auditory, and lens placodes are formed from the surface of the ectoderm. The heart and the circulatory system as well as the limb buds are established. As the general development of the mouse is beyond the scope of this work, further account will now only be given on the development of the central

nervous system (CNS), in particular the optic nerve which is within the scope of the present work.

The CNS is a derivative of the neural plate which is a thickened median strip of ectoderm rostral to the primitive streak and is first distinguishable by day 7.5 p.c. It elongates by the addition of newly differentiated neuroectoderm to its caudal aspect. Following its formation, the neural plate undergoes a rapid change in shape so that its lateral edges elevate to form the neural folds. Starting from the level of the 4th to the 5th somite at about day 8.0-8.5 p.c., the neural plate fuses along the dorsal midline in both caudal and cranial directions until it has been converted into a tube, the neural tube. The cranial end of the tube (represented by the anterior neuropore in humans - see Kaufman, 1992) closes by day 9.0 p.c., while the caudal end, the posterior neuropore, does not usually close until day 10.0-10.5 p.c., although closure of the posterior neuropore was observed as early as day 9.5 p.c. by Kaufman (Kaufman, 1992; Hogan et al., 1994). Further development of the neural tube results in regional differentiation into forebrain (prosencephalon), midbrain (mesencephalon), hindbrain (rhombencephalon) and spinal cord. These subdivisions of the rostral part of the neural tube which are referred to as the primary brain vesicles are initially poorly defined. With further development, the forebrain differentiates into the telencephalon and the diencephalon. The telencephalon gives rise to the cerebral hemispheres while the optic vesicles from which the eyes develop are derived from the diencephalon. The midbrain retains its original designation. The hindbrain differentiates into the metencephalon and the myelencephalon. The metencephalon gives rise to the cerebellum and the pons and the myelencephalon to the medulla oblongata.

1.5.2 LIFE SPAN

The life span of the mouse ranges from 1.3-3 years. A summary of the vital statistics of the European House Mouse, *Mus musculus*, for example, is as follows:

number of chromosomes 40 (20 pairs)

number of genes	approximately 5×10^4
gestation	19-20 days
Age of weaning	3 weeks
Age of sexual maturity	6 weeks
Weight	1gm at birth, 8-12gm at weaning; adult: ≅ 25gm for males, 20-21gm for females.
Life span in laboratory	1.5-2.5 years
Average litter size	6-8

Total number of litters per breeding female 4-8 (Hogan et al., 1994).

The life expectancy in mice is affected by a number of factors. Body weight for example, determines the survival of mice during experimental procedures. Whereas in some experiments large mice survive longer (Chai, 1959), in others a selection of smaller mice would do better (Roberts, 1961). Roberts observed that one male in a line selected for low body weight survived 1,330 days, which possibly is one of the longest recorded life spans for the laboratory mouse. Another factor that affects the life span of mice is their genetic characteristics. For example, the F_1 crosses of a selected line often survive longer than mice of either parent strains. Studies on the effect of diet on different strains of mice by Silberberg & Silberberg (1954) and by Silberberg et al. (1961 & 1962) showed that high fat diet shortened the life span of C57BL/6J, DBA/2J and YBR strains of mice. A large study involving different strains of mice on the effect of a variety of factors gave interesting results (Russell, 1966). Females of the C57BL/6J strain were found to survive longer than females of CBA/J born on the same day. In the C57BL/6J strain, the females had a longer life span. For all strains of mice the death rate increased after 300 days of age so that, less than 20% were alive after 650 days of age. No mouse survived beyond 925 days. Virgins survived longer than their non-virgin littermate sisters, thus suggesting that life expectancy is lowered by producing and rearing offspring. Litter size and number also affects life span. Generally mice producing a large number of litters during their reproductive period live for a shorter

period than those with fewer litters. Also those that produce large litters tended to live shorter than those with smaller litters. Littermates of large litters live shorter than littermates of small litters. Litter size itself depends on other parameters such as the number of ova liberated at ovulation, prenatal mortality rate; and these are also dependent on maternal age and parity as well as environmental conditions such as stress (Hogan et al., 1994). Furthermore, infections, parasites, fighting and tumours also reduce the life span of the mouse.

1.6 DEVELOPMENT OF THE OPTIC NERVE IN THE MOUSE.

An account of the development of the optic nerve in the mouse for the purpose of the present work is best given in the context of the general development of the visual system in this species. The sequence of events given here follows closely that given in *The Atlas of Mouse Development* by Kaufman (1992).

Day 8

The development of the visual system begins on day 8 p.c. with the formation of the optic placodes on the cranial end of the primitive forebrain. From these sites the optic pits (also known as optic evaginations) which are bilateral depressions subsequently develop. The optic evaginations increase in depth resulting in the formation of the primary optic vesicles.

Day 9

By day 9 p.c. the primary optic vesicle has become prominent and is now connected to the lumen of the future forebrain by a luminal structure, the optic stalk. The lumen of the optic stalk which is originally wide is rapidly obliterated so that by day 9.5 p.c. it is significantly smaller in diameter than the lumen of the optic vesicle. By this time the walls of the optic vesicle begin to collapse to form the optic cup. The surface ectoderm overlying the optic cup is also induced to form the lens placode, which appears as a thickening of the surface ectoderm.

Day 10

Evidence of the formation of the lens vesicle is seen at this stage as the initial indentation of the lens placode to form the lens pit. Also at this stage, there is differential thickening of the two layers of the optic cup so that, the inner layer becomes 3-4 times as thick as the outer layer. It is also at this stage that the hyaloid vessels begin to develop.

Day 11

It is on day 11 p.c. that the lens pit closes to form the lens vesicle. This is followed by loss of contact between the surface ectoderm and the lens vesicle. There is a further increase in the thickness of the inner layer of the optic cup (i.e. in the future neural layer of the retina). On the ventral aspect of the optic stalk is the choroidal fissure. This is continuous with a similar indentation on the inferior aspect of the optic cup. The hyaloid vessels run in the choroid fissure and supply the optic cup and the lens vesicle. The choroid fissure later obliterates as a result of fusion of its inferior margins which extend distally. Failure of the margins of the choroid fissure to fuse results in a defect (coloboma) seen in the inferomedial part of the iris. On day 11.5 p.c. the lens vesicle is completely separated from the surface ectoderm and the hyaloid vessels become more prolific.

Day 12

By day 12 p.c. the lens vesicle is very distinct. There is also diminution of the intraretinal space.

Day 13

The layered structure of the retina and the presence of nerve fibres in its neural layer are now distinct. The nerve fibres are seen to pass from the ganglion cells towards the central region of the future optic cup, into the optic stalk to form the optic nerve.

Days 14-17

By day 14 p.c. the diameter of the optic stalk has increased considerably, its original lumen having been replaced by nerve fibres on their way to the optic chiasma. Similar findings have been reported by Colello & Guillery (1990 & 1992). They observed the first bundles of fibres reaching the optic nerve on day 12.5 p.c., and this was as a mixture of thin (< 0.5 μm) axons and thicker growth cones. Within the next two days these bundles increased in size and in number in the intra-orbital part of the optic nerve. In addition, the structure of the pathway changed significantly towards the optic chiasma. Although the optic nerve axons first arrive at the chiasma on day 13 p.c. they do not cross the midline until day 14 p.c. (also see Silver, 1984; Bovolenta & Mason, 1987). Colello & Guillery further observed that the first sign of the adult pattern of distribution of ganglion cells with uncrossed axons was located mainly in the ventrotemporal retina and seen on day 16.5 p.c. They suggested that this was an indication that the adult line of decussation is formed early in development. From 14-15 days p.c. they saw uncrossed fibres in almost all the fascicles of the optic nerve. These intermingled with the crossed axons throughout the length of the nerve. Between day 16 and day 17 p.c., although uncrossed fibres were seen to pass predominantly within the temporal part of the optic stalk, they remained intermingled with crossed axons.

These findings in the mouse are similar to those reported in the rat by Horsburgh & Sefton (1986). These workers observed the first axons to be generated by the retinal ganglion cells on day 14 p.c. and by day 14.5 p.c. fasciculi of optic axons appeared in the optic stalk which subsequently becomes the optic nerve. By day 17 p.c. the optic nerve has passed through the optic foramen and its fibres could now be seen to converge at the optic chiasma. From here the fibres progressed to the visual part of the occipital cortex via the optic tract, the lateral geniculate body and the optic radiation.

The effect of mutation on the development of the optic nerve in the mouse has also been investigated. Hero & Farjah (1992) examined the effect of the *microphthalmia* gene on the pre-natal development of the optic nerve of mice. They reported that there were no obvious morphological abnormalities in heterozygotes. The homozygous microphthalmic optic nerve/stalk was larger than that of the heterozygote and the wild-type mouse. The optic stalk persisted throughout gestation and this was attributed to a high mitotic rate, decreased cell death and failure of cell degeneration in the dorsal layer of the microphthalmic optic stalk.

1.7 TERATOLOGY

Teratology is the study of abnormal development with regard to causes, mechanisms and manifestations. Such abnormalities may be genetically, prenatally, or postnatally induced. Their expression could be in the form of lethality, malformation, developmental retardation, or functional aberration. A teratogen is an agent or factor that is potentially capable of producing abnormality during pre- or post-natal development (Koenigsberg et al., 1989; Sadler, 1990; Miller, 1992). Besides sheding light on normal development, teratological studies provide useful information for the identification of aetiological factors of malformations which is a prerequisite for the protection of future generations from such abnormalities (Miller, 1992). The susceptibility of the fetus to the teratogenic effects of a teratogen is determined by both environmental and genetic factors (Sadler, 1990; Zajac & Abel, 1992). Environmental factors include: the time of exposure, the dose and route of administration, diet, interaction with other agents e.g. infections, drugs and chemicals, radiation; while genetic factors include both maternal and embryonic genotype. These factors could act in isolation or in association with one another (Adickes, 1990). Only about 10% of congenital abnormalities result from environmental factors alone and the same percentage results from only genetic factors, the rest (i.e. 80 %) being from the interaction between environmental and genetic factors (Sadler, 1990).

The mammalian gestation period is broadly divided into three stages viz:

i) the pre-germ layer stage,

ii) embryonic stage and

iii) fetal stage.

i) The pre-germ layer stage otherwise known as the predifferentiation stage, is characterised by rapid multiplication of undifferentiated cells, and extends from fertilization to the time of the formation of the embryonic germ disc. Although there is a high rate of lethality during this period, few teratogens are known to have any effect during this period.

ii) The embryonic stage is the period of embryogenesis i.e. the period during which each of the primary germ layers gives rise to specific tissues and organs. During this stage the cells begin to show distinct morphological differences. It is also during this stage that most organs are susceptible to teratogenic insult, and gives rise to most of the congenital malformations seen at birth (Sadler, 1990). The type and degree of abnormality would, however, depend on the organ being developed. For example, reports by Nelson et al. (1952, 1955) following administration of pteroyl-glutamic acid deficient diet to rats during this period of gestation showed that CNS abnormalities were seen between 7 and 9 days p.c., urinary and cardiovascular between days 9 and 11 p.c. while skeletal abnormalities were seen between days 11 and 14 p.c.

iii) The fetal stage, also referred to as the period of fetogenesis, extends from the end of the embryonic stage to birth. It is characterised by growth and maturation of the organ systems. There is decreasing teratogenic susceptibility towards birth. The development of certain organs or parts of organs may proceed well beyond this stage into early or advanced postnatal life, for example, the optic nerve in the mouse (Dangata et al., 1996; Dangata & Kaufman, 1996).

Known environmental teratogenic factors include infections, commonest of which are viral infections such as Rubella (German measles - first suggested as a teratogen by Gregg in 1941), Cytomegalus virus and Herpes simplex. Others are Toxoplasmosis and syphilis. Radiation is also known to produce congenital malformations the nature of which is both dose and gestational age dependent. A dose-response relationship exists i.e. the response to the teratogenic effect of an agent depends on the amount of the agent administered as a single dose or spread out over time. (The teratogenic dose of an agent is one that can produce a teratogenic effect on the embryo. When the dose is insufficient to cause any teratogenic effect, it is said to be sub-threshold and when it is so high that it destroys the embryo it is said to be lethal). A single dose of an agent can be teratogenic or in fact, lethal at one stage of gestation but sub-threshold at another, depending on the stage of gestation it is given. For example, Rugh & Grupp (1960) observed that a dose of X-rays as low as 5r given at a critical period of gestation caused malformations, suggesting a low threshold dose for X-rays for the production of certain types of abnormalities for that particular stage of gestation. The time factor plays a significant role because each organ passes through a period of development during which it is particularly susceptible to teratogenicity. This is referred to as the critical period for the organ, and in most cases, it corresponds to the time of most rapid development of the organ. Occasionally an organ may be malformed by a teratogen administered prior to the appearance of its earliest rudiment. In the interplay between dose and time, an increase in the threshold dose or duration of exposure (particularly during the critical period) or both could increase the frequency and the severity of the malformations produced (Dagg, 1966).

Drugs have also been reported as teratogens. These include: alcohol, cocaine, thalidomide, aminopterin, drugs used in psychiatric practice such as anticonvulsants and antipsychotics. Hormonal therapy or imbalance during pregnancy could also produce teratogenic effects. Maternal factors such as nutritional status and hypoxia are also known to play a significant role in the aetiology of congenital abnormalities (Sadler, 1990).

Genetic factors of both mother and embryo play an important role in the aetiology of congenital malformations. Dagg (1966) stated that teratogenicity is the result of morphogenetic interactions between the genes of the embryo which confer the potential for normal or abnormal development and the embryonic environment. In chromosomal abnormalities, for example, a deviation in the normal numerical or structural chromosomal constitution could lead to abnormalities (Hirschorn & Cooper, 1961). In order to study the effect of genotype on the role of cortisone on the formation of congenital defects, Fraser & Fainstat (1951) administered an appropriate dose of cortisone to pregnant A and C57 strains of mice. They observed the spontaneous rate of oral clefting in offspring of both strains of mice to be 10% and 1%, respectively. Whereas following exposure to cortisone all offspring of strain A had a cleft lip, only 19% of the offspring of C57 had this defect. When strain C57 males were crossed with strain A females, 43% of the offspring had a cleft palate, but when strain C57 females were crossed with strain A males only 4% of the offspring had a cleft palate.

1.8 THE OPTIC NERVE AS A MODEL FOR THE ANALYSIS OF THE CENTRAL NERVOUS SYSTEM.

The optic nerve is an easily accessible central tract. Unlike the majority of central tracts, it has a well defined configuration which has been provided by the extension of the meninges of the brain over it. The definitive shape given to the tract by the meninges makes its dissection and processing relatively easy. Furthermore, its connection with the rest of the CNS can be traced with a considerable degree of precision.

1.9 AIMS OF THE PRESENT RESEARCH.

Although the study of the optic nerve could facilitate understanding of the human CNS, and in particular the visual system, the direct study of this tract in humans is only very rarely possible. The commonest sources of human specimens are from post-mortem examinations

or following enucleation of the eye as a result of pathological conditions. Even when specimens are available from such rare human sources, their normal anatomy would have been distorted by the pathological processes that took place in them. This problem has often been approached by the use of appropriate animal models. For example, human embryos are only very rarely available for the investigation of inherited human diseases as well as teratological studies. Consequently, appropriate experimental models have been developed to carry out such studies. This has shed light on how these factors control development by modifying normal development, thus giving understanding of the aetiology underlying conditions similar to specific human diseases. The mouse has been the commonest model for such genetic and teratological research because it is susceptible to a number of known hereditary diseases and malformations similar to those found in man in addition to the fact that its genetic constitution is better known and more easily manipulated than those of any other mammal other than man (Green, 1966; Hogan et al., 1994).

As has already been mentioned earlier in this chapter, the optic nerve provides invaluable access to the CNS, particularly the visual system. However, its study requires baseline morphometric data as a prerequisite, but such data are only rarely available. The principal aim of this study was to provide detailed baseline morphometric information on the optic nerve of different mouse strains during their postnatal development and growth in the belief that such information will be valuable for future research into the CNS using this central tract of this species as an experimental model. Furthermore, the effects of mutational changes and prenatal teratogenic insult on the development of the optic nerve were also investigated.

CHAPTER TWO

MATERIALS AND METHODS

Contents

2.1 Mouse stocks

2.1.1 General

2.1.2 CBA/Ca (EUMM)

2.1.3 C57BL/6 (EUMM)

2.1.4 F_1 hybrid

2.1.5 F_2 hybrid

2.1.6 *Small eye* mice

2.2 Induction of ovulation in female mice

2.3 Fixatives

2.3.1 Glutaraldehyde - primary fixative

2.3.2 Osmium tetroxide - secondary fixative

2.4 Phosphate buffer

2.5 General anaesthetic

2.6 Embedding medium

2.7 Surgical procedures

2.7.1 Anaesthesia

2.7.2 Perfusion

2.7.3 Dissection of the optic nerve

2.8 Tissue processing for electron microscopy

2.8.1 Fixation

2.8.1a Primary fixation

2.8.1b Secondary fixation

2.8.2 Dehydration

2.8.3 Embedding

2.9 Glass knives

2.10 Cutting sections from the optic nerve

2.10.1 Preparing blocks for cutting

2.10.2 Cutting semithin sections for light microscopy

2.10.3 Cutting ultrathin sections for electron microscopy

2.11 Staining semithin sections of optic nerve for light microscopy

2.12 Staining ultrathin sections of optic nerve for electron microscopy

2.12.1 Staining with lead citrate

2.12.2 Staining with uranyl acetate

2.13 Electron microscopy

2.14 Photographic procedures

2.14.1 Developing transmission electron micrographic plates

2.14.2 Printing micrographs

2.15 Routine waste disposal

2.15.1 Carcasses

2.15.2 Surgical materials

2.15.3 Other hardware

2.15.4 Chemicals

2.16 Image analysis system (Magiscan)

2.17 Morphometric analysis

2.17.1 Measuring cross-sectional area (csa) of optic nerve

2.17.2 Sampling myelinated nerve fibre diameter profiles in optic nerve

2.18 Computation of myelinated nerve fibre counts and density

2.18.1 Myelinated nerve fibre count

2.18.2 Density of myelinated nerve fibres

2.19 Statistical analysis

2.19.1 Mean

2.19.2 Variance

2.19.3 Standard deviation

2.19.4 Standard error of mean

2.20 Verification of results (Student's t-test)

2.1 MOUSE STOCKS

2.1.1 GENERAL

With the exception of the *Small eye* (*Sey*) all mouse strains were bred in the University of Edinburgh Medical Faculty Animal House. They were bred in cages under a 14 hour -10 hour light-dark cycle and maintained on a generous supply of pelleted rodent diet (S.D.S. Ltd.) and water.

2.1.2 CBA/Ca(EUMM)

These were from an original breeding stock CBA/Ca recently reclassified CBA/Ca(EUMM) (Edinburgh University Medical Microbiology). They were originally kept in barrier conditions. The original stock was obtained from Carshalton in 1970 and has undergone approximately 125 generations since that time.

2.1.3 C57BL/6(EUMM)

These were from an original stock C57BL/6 obtained from Olac in 1986 and has undergone approximately 42 generations since that time. They were kept in barrier conditions.

2.1.4 F_1 HYBRID

All F_1 hybrid mice were obtained by cross breeding female C57BL/6(EUMM) with male CBA/Ca(EUMM).

2.1.5 F_2 HYBRID

The F_2 hybrid mice were used for the alcohol studies and they were obtained by brother x sister cross breeding F_1 females with F_1 males. Pregnant F_1 females were given an intraperitoneal (i.p.) injection of ethyl alcohol (volume based on weight of female) on day 12 post coitum (p.c.). and a control group given a similar volume of 0.9% saline through the same route. Offspring from both alcohol-treated and control groups were used at the

appropriate age for alcohol studies. Those to be used after the age of 3 weeks were weaned at that age. Excess litters were killed at weaning.

2. 1.6 *SMALL EYE* (*Sey*) MICE

A breeding colony of *Small eye* (*Sey*) was obtained from Dr Ruth Clayton, formerly of the Department of Genetics, University of Edinburgh, and maintained by brother x sister matings of heterozygous male and female mice. The latter were easily distinguished from their normal siblings due to the fact that their eyes were significantly smaller than those of their genetically normal (i.e. + / +) littermates.

2.2 INDUCTION OF OVULATION IN FEMALE MICE.

At a suitable time the female mouse was induced to superovulate by giving an intraperitoneal injection of 5 international units (i.u.) of Pregnant Mares' Serum Gonadotrophin (PMSG, Intervet) on day 1. This hormone stimulates the ovarian follicles to develop and mature. Approximately 48 hours later 5 i.u. of Human Chorionic Gonadotrophin (hCG, Intervet) was given i.p. The hCG overides the mouse's Luteinising Hormone (LH) thus stimulating the mature follicles to ovulate. Ovulation occurs at about 12 hours after hCG stimulation (Edwards & Gates, 1959). Two to three hours after the hCG injection the female mouse is mated with a male. The following morning it was checked for the presence of a vaginal plug, being evidence of mating. The day on which a vaginal plug was observed was taken as 0.5 days p.c. The vaginal plug is formed from coagulation of the male's ejaculate in the female's vagina. Once a vaginal plug was observed the female was separated from the male. Offspring obtained from female mice were used as determined by each experiment. Offspring that were required after the age of three weeks were weaned at three weeks and the males separated from the females at this time. Offspring that were not required were killed at weaning.

2.3 FIXATIVES.

2.3.1 GLUTARALDEHYDE- PARAFORMALDEHYDE: PRIMARY FIXATIVE

This was constituted a day prior to use as follows:

Solution A: 8.44 gm $NaH_2PO_4.2H_2O$ in 373.5 ml of distilled water.

Solution B: 1.93 gm NaOH in 76.5ml distilled water.

Solution C: 20.0 gm Paraformaldehyde in 50 ml distilled water.

Solution D: 2.0 ml of 0.5% Calcium chloride.

Solution C was brought to 60°C in a water bath and 1M NaOH added to it drop-wise until the paraformaldehyde was completely dissolved.

Solutions A, B, C and D were mixed and titrated with lM HCl to a pH of 7.4.

10 ml of glutaraldehyde were added to the final solution. Mixing was done on a magnetic plate.

This final solution was used for transcardiac perfusion of the mice and as a primary fixative for the optic nerves following dissection. Because aldehyde solutions can cause contact dermatitis direct contact was avoided by wearing rubber gloves during the fixation procedure.

2.3.2 OSMIUM TETROXIDE: SECONDARY FIXATIVE.

This was constituted as follows:

8.3 ml 2.26% Sodium dihydrogen orthophosphate

1.7 ml 2.52% Sodium hydroxide

0.1gm Osmium tetroxide

All was carefully mixed in a clean, brown, glass-stoppered bottle in a fume cupboard a day before use. A fume cupboard was used in order to avoid any possible contact with osmium tetroxide because it is highly volatile and poisonous. Its vapour irritates the respiratory tract and may also cause severe burns to the eyes. The solution is corrosive and causes burns if in contact with the skin or any mucous membrane.

This final solution of 1% Osmium tetroxide had a pH of 7.4.

2.4 PHOSPHATE BUFFER.

Phosphate buffers are the most 'physiological' of buffers used as vehicles for fixatives in electron microscopy. This is because they mimic certain components of extracellular fluids and are non-toxic to both tissue and microscopist, thus making them suitable for fixation by perfusion, and as vehicles for slowly penetrating and reacting fixatives such as osmium tetroxide.

2.5 GENERAL ANAESTHETIC.

The general anaesthetic used was Avertin (Winthrop), made up of tribromethanol in amyl hydrate. A fresh preparation was made each time it was to be used, and this was done as follows:

0.12 ml Avertin using a lml pipette.

9.88 ml 0.9% saline using a 10ml pipette.

The saline was heated in a water bath to 50°C then the Avertin was added and mixed thoroughly until it was completely miscible. The temperature of the saline had to be raised above room temperature because Avertin is immiscible in normal saline at room temperature.

2.6 EMBEDDING MEDIUM.

Araldite was the embedding medium used. It was prepared as follows:

A. 250.0 gm Araldite (CY212) resin mixed with 250.0 gm hardener (DDSA) and left at room temperature.

B. 5.0 ml of accelerator (BDMA) mixed with 20.0 ml plasticider (Dibutyl phthalate BDH) and kept in the refrigerator at 4°C.

C. 19.0 ml of A mixed with 1.0 ml of B by continuous rotation for 12 hours at room temperature.

2.7 SURGICAL PROCEDURES.

All surgical procedures were carried out wearing disposable gloves.

2.7.1 ANAESTHESIA.

Each animal was weighed to determine the amount of anaesthetic it would receive. It was then deeply anaesthetised by an intra-peritoneal injection of 0.02 ml/g body weight of 1.2% solution of Avertin in 0.9% saline. Care was taken to avoid injecting the anaesthetic intra-vascularly or into the abdominal viscera by withdrawing the needle slightly shortly after penetrating the peritoneum (as well as drawing out the contents of the syringe to ensure there was no blood or fluid from the gut) before finally injecting the anaesthetic solution. This procedure was more difficult to perform in the immature animals. This difficulty was overcome by ensuring that the animals did not move during the injection procedure.

2.7.2 PERFUSION.

Following anaesthesia, the animal was placed supine on a board and the limbs pinned to the board. Absolute alcohol was spread on the ventral surface of the trunk as an antiseptic and to keep the hair down. The chest was opened through a subcostal and bilateral mid-axillary incision using a pair of dissecting scissors and a pair of toothed dissecting forceps. The anterior chest wall was reflected cranially to expose the heart. Using a 21G needle and a 60ml syringe, perfusion was carried out in adult mice by giving 2.0 ml/g body weight of primary fixative through the left ventricle while the heart was initially still beating. Immature mice were similarly transcardially perfused, though a 23G needle was used to avoid rupture of the left ventricle during the perfusion procedure. The surface of the liver was excoriated to avoid a build-up of fixative in the venous part of the circulation. Generalised pallor and stiffness of the whole animal by the end of perfusion were indications of adequate perfusion. Despite the use of a 23G needle to perfuse immature mice, the interventricular septum was easily ruptured before perfusion was completed. This resulted in a significant amount of fixative going through the lungs instead of into the general

circulation. The result was that the animal was poorly perfused. This was evident by the fact that the animal was not quite stiff and still significantly pink by the time the correct volume of fixative had been given. This problem was resolved by ensuring as much as possible stability of the needle once it was in the left ventricle. Also the fixative was given as slowly as possible to minimise the pressure of the fluid on the walls of the heart chambers.

2.7.3 DISSECTION OF THE OPTIC NERVE.

Each perfused animal was placed on its ventral aspect on a dissecting bench. Absolute alcohol was spread on the dorsal aspect of the head and neck in order to act as an antiseptic and keep the hair down. The skin over the head and neck was completely reflected. Through the sagittal suture an incision was made to divide the head into two hemispheres. The entire length of the optic nerve was immediately, but carefully, dissected out from each hemisphere avoiding traction on the nerve. The nerve was immediately transferred into Phosphate Buffered Saline (PBS) in a Petri dish and cleared of any surrounding tissue. A number of nerves were lost during the dissection procedure.

2.8 TISSUE PROCESSING FOR ELECTRON MICROSCOPY.

2.8.1 FIXATION.

Fixation halts post-mortem changes and stabilizes the cellular organisation of the nerves in order to preserve as much as possible of the ultrastructural relations during the more rigorous processes of dehydration, embedding, sectioning and final exposure to the electron beam (Weakley, 1981). Both glutaraldehyde and osmium tetroxide achieve this by acting as cross-linking agents i.e. by the formation of chemical bonds between molecules of cell substance which in turn produces a stable network throughout the cell (Weakley, 1981).

2.8.1a PRIMARY FIXATION.

This was actually started from the time of perfusion. Using a Pasteur pipette with a bore wide enough for the nerve to pass through and a rubber bulb, the right and the left optic nerves from each animal were transferred from the PBS into separate prelabelled bottles containing generous volumes of primary fixative and left for a total of 12 hours. The optimum time for tissue fixation is determined by the tissue type, age of animal, block size, fixative concentration and the buffer used. The primary objective is to obtain a uniform fixation of all cells in the tissue. Glutaraldehyde fixes rapidly once in contact with the tissue, while formaldehyde on the other hand penetrates rapidly but its reaction with the tissue takes a number of hours (Weakley, 1981). Glutaraldehyde and paraformaldehyde preserve the continuity of membrane systems of the tissue by reacting very rapidly with proteins through cross-linkage, and this brings about stability of structures. The calcium chloride prevents the formation of myelinic figures that could result from the interaction of glutaraldehyde with osmium tetroxide during secondary fixation. Myelinic figures are whorls of membrane resembling the myelin which covers parts of the nervous system and such figures may be seen either within cells or lying in intercellular spaces. This is caused by the partial breakdown of cellular lipoprotein membranes during aldehyde fixation (Trump & Ericsson, 1965). The lipid is then 'caught' by the osmium tetroxide used for post-fixation and fixed elsewhere. Myelin figures may also be seen at particular stages in the life history of a cell type in certain developing tissues, thus reflecting developmental phenomena rather than fixation artefact (Weakley, 1964 & 1966; Coupland & Weakley, 1968).

2.8.1b SECONDARY FIXATION.

After primary fixation the nerves were washed in buffer and transferred into a secondary fixative consisting of 1% osmium tetroxide in 0.1M phosphate buffer for another 2 hours. The specific length of time is empirically determined. The main aim is to strike a compromise between the need for complete penetration of the block containing the tissue by the fixative and the fact that protein and other substances are progressively leached out of

the tissue when immersed in osmium tetroxide (Bahr, 1955). Osmium tetroxide preserves delicate cytoplasmic processes without causing alteration to mitochondria and fat droplets, thus preventing extraction of lipid components during the subsequent processes of dehydration and embedding. This makes it suitable for the examination of fine cellular structures.

2.8.2 DEHYDRATION.

After fixation the nerves were dehydrated through a graded alcohol series to minimize damage. A direct transfer of tissue from fixative to absolute alcohol could cause mechanical damage to the tissue because of changes in surface tension and currents set up as the two fluids mix. The nerves were then cleared with propylene oxide before embedding. Propylene oxide is more miscible with Araldite and more volatile than alcohol. It replaces the alcohol and allows better penetration of the tissue by Araldite resulting in good embedding.

2.8.3 EMBEDDING.

The nerves were transferred from propylene oxide into small rectangular polythene containers filled with Araldite mixture and left at room temperature for 12-24 hours. The containers were warmed in an oven at 60°C. The Araldite was decanted and a fresh mixture added. The containers were replaced in the oven for a further 48 hours. Araldite infiltrates the tissue giving it a firm support without causing significant chemical or structural changes. This makes it firm enough to minimize damage during cutting as well as making the sections strong enough to be mounted on the grids without a supporting medium. In addition, long term storage of the specimen is enhanced.

2.9 GLASS KNIVES.

Glass knives were made from 6.6 x 25 x 400 mm Alkar glass strips. The glass strips were thoroughly washed with liquid detergent to remove grease and dust then dried with a clean hand towel. Glass knives were made from the clean strips using an LKB Knife Maker Type

7801A. Using 12 mm Aluminium tape with adhesive backing together with dental wax a trough was made on the surface close to the cutting edge of the knife for cutting ultrathin sections. For knives to be used for cutting semithin sections, a shallow trough was made by bridging the cutting surface of the glass knife that was to come in contact with the cutting edge of the block with dental wax, followed by coating the proximal part of the left and right sides to the bridge with the wax. Before use the knives were kept in a box with a tight lid to protect them from contamination. Despite this, it was frequently observed that knives that had been made a considerable period of time before use often produced a reasonably high incidence of sections with razor marks, possibly because of having been contaminated while in storage. This problem was avoided by making the knives the day they were to be used.

2.10 CUTTING SECTIONS FROM THE OPTIC NERVES.

2.10.1 PREPARING BLOCKS FOR CUTTING.

The block of Araldite with the embedded nerves was removed from its plastic container and placed on a Thermostat hotplate. After allowing it sufficient time to soften, and using a single-edge Wilkinson razor blade, it was carefully cut into smaller blocks each containing an individual nerve. Each small block and its nerve was further cut so that the nerve in it was divided into two. The Araldite was trimmed from one of the two portions of the block to produce a truncated pyramid from which sections of the nerve were to be cut. The other portion was labelled and kept in a reserve collection box. Using sealing wax the trimmed block was mounted by its base onto a dowel cut from 8.0 mm diameter wooden dowelling. The blocks were trimmed of excess sealing wax so that they could fit into the block holder.

2.10.2 CUTTING SEMITHIN SECTIONS FOR LIGHT MICROSCOPY.

Each block was clamped onto a block holder. The holder was in turn mounted onto a stage to allow for the block to be trimmed further. Final trimming was done with a new double-edged Wilkinson razor blade. This trimming was to make the cutting surface of the block into another truncated pyramid with its base and apex parallel to each other. The block was

removed from the trimming stage and clamped to a holder in a Reichert-Jung Ultracut E Microtome. A glass knife was also clamped to the stage of the microtome. The orientation of the block was adjusted so that the base of its cutting surface was parallel to the cutting edge of the knife, and would therefore be the first to hit the cutting edge during the cutting cycle. Further adjustment of the microtome was done so that semithin transverse sections were cut perpendicular to the long axis of each nerve. Both cutting edge and cutting surface were adjusted until they were just apart. The indication of this was a green-yellow reflection of light on the cutting surface as the cutting edge came close. Using a pipette with a rubber bulb the trough of the glass knife was filled with distilled water to a level that just left the cutting edge free.

Semithin sections approximately 1 μm thick were cut and these formed a ribbon that floated on the water surface in the trough. The formation of ribbons by the sections was achieved by the distal edge of one section getting attached to the proximal edge of the next section as it leaves the cutting edge to float on the water surface in the boat. Where blocks were not properly trimmed, or where the cutting edge had been defaced, it was difficult for the sections to form a ribbon and this was also an indication that the sections were likely to have razor marks. This problem was resolved by retrimming the block and changing the cutting edge. A drop of distilled water was placed on a 15 mm x 150 mm microscope slide pretreated with absolute alcohol in order to remove any contaminants on it. Using a dissecting needle only sections that were free of razor marks were lifted onto the drop of water on the slide. Blocks that were over-trimmed often produced split sections. This was corrected by cutting into the block until a considerable supporting edge of embedding material was achieved.

2.10.3 CUTTING ULTRATHIN SECTIONS FOR ELECTRON MICROSCOPY.

After cutting the semithin sections the block was further trimmed with a new blade to reduce the cutting surface. Ultrathin sections approximately 80 nm thick were cut using new knives. To minimise the effect of vibration on both block and cutting edge during cutting, they were shielded with a screen. Sections varied in colour according to their thickness, from grey (< 60nm) to blue (190-240 nm) and formed ribbons on the water surface in the trough. Grey sections are too thin to withstand the electron beam during electron microscopy and would usually break down before any analysis is done. Blue sections on the other hand are too thick to allow the electron beam to pass through to facilitate a detailed analysis of fine structures. Golden colour sections (≅100 nm) are just thick enough to allow for a detailed analysis, and these were the ones picked on the grids. To obtain golden colour sections the microtome was adjusted once ultrathin sections had started coming off until golden colour sections started to appear. They were spread out by passing a film of chloroform vapour over them. Using a pair of fine forceps the sections were picked up on the polished surface of copper grids (200) and placed on the reverse surface on a filter paper in a prelabelled and well covered Petri dish for subsequent staining.

2.11 STAINING SEMITHIN SECTIONS OF OPTIC NERVE FOR LIGHT MICROSCOPY.

The stain used was constituted as follows:

4 parts of Toluidine blue in 1% borax solution + 1 part of pyronin 'B'. Toluidine blue is a polychromatic stain while pyronin 'B' serves as a background stain.

Slides with the semithin sections were placed on a Thermostat hotplate set at 100°C until all the water evaporated. Sections were then flooded with stain for 30 seconds. After staining excess stain was removed by passing the slide through a gentle stream of tap water until all the excess stain was washed away. The slide was placed back on the hotplate to allow it to dry. The area containing the sections was demarcated on the reverse side with indelible ink. The slide was labelled and left unmounted in a clean slide rack for light microscopy.

2.12 STAINING ULTRATHIN SECTIONS OF OPTIC NERVE FOR ELECTRON MICROSCOPY.

2.12.1 STAINING WITH LEAD CITRATE.

Lead citrate was prepared according to the method described by Reynolds (1963) as follows:

1.33 gm $Pb(N0_3)_2$

1.76gm $Na_3(C_6H_5O_7).2H_2O$

30 ml distilled water is added in a 50 ml volumetric flask and shaken vigorously for 1 minute to ensure complete conversion of lead nitrate to lead citrate.

Resultant suspension is allowed to stand for 30 minutes with intermittent shaking.

8.0 ml 1 N NaOH is added after 30 minutes.

Final solution is made up to 50 ml with distilled water and mixed by inversion.

pH of final solution is 12.0±0.1.

Staining was carried out as follows: Two pellets of NaOH were placed opposite to each other on dental wax in a Conway unit. The NaOH was to absorb carbon dioxide from the surrounding air thus preventing the formation of lead carbonate precipitate upon the sections. Using a pipette with a rubber cap a drop of lead citrate for each grid was placed on the dental wax of the Conway unit. The well of the unit was filled with distilled water from a 50 ml beaker. The copper grids with the ultrathin sections were lifted in turn with a fine pair of forceps and placed with sections down to float on the drop of lead citrate for 2 minutes. The grids were then lifted with the forceps and rinsed by gentle strokes at an angle of approximately 45° in the distilled water in the well within the trough for 5 seconds, and then for a further 15 seconds in distilled water in a 50ml beaker and finally put back on the filter paper with sections up. This stain gives a clear, delicate rendering of cellular structure. The citrate acts as a chelating agent to prevent precipitation.

2.12.2 STAINING WITH URANYL ACETATE.

A fresh saturated solution of uranyl acetate was made by dissolving the powder in 50% ethanol in a tube with a plastic cap. The tube was clamped on a rotary agitator and allowed to revolve at 1 Rev/min for 1-2 hours. The mixture was centrifuged for 5 minutes and the supernatant transferred into another bottle. This was kept away from light until required.

Approximately 5.0 ml of a saturated solution of uranyl acetate was put in a small trough. The lead citrate-stained grids were immersed with their sections up in the stain one following the other at regular intervals of time and left in it for 10 minutes. The trough was covered with another trough of the same size to prevent contamination as well as fumigation of the surroundings with uranyl acetate vapour. Each grid was lifted from the stain, rinsed in 50% alcohol in another trough for 5 seconds and released from the forceps into the alcohol. The tips of the forceps were blotted using a hand towel to remove any residual stain. The grids were again lifted from the trough, rinsed in 50% alcohol in a 50ml beaker for a further 15 seconds and put back face up on the filter paper for electron microscopy.

2.13 ELECTRON MICROSCOPY.

A grid containing nerve cross-sections was mounted on a specimen holder and held in position with a stainless steel spring for viewing under the electron microscope. Selections of photomicrographs were taken from centre to periphery of each nerve using a Philips EM301 transmission electron microscope. All micrographs were exposed for 2 seconds at 60 kV on 8.3 x 10.2 cm Kodak electron microscope film 4489. For the purpose of nerve fibre sampling, micrographs were taken at a magnification of x 750 then developed and printed to a final magnification of x 3000. For other purposes other more appropriate magnifications were used. A sketch of the area of the nerve that was photographed was made for each nerve and the centre of the nerve demarcated on the sketch.

2.14 PHOTOGRAPHIC PROCEDURES.

All photographic procedures were carried out under appropriate routine safelight conditions.

2.14.1 DEVELOPING TRANSMISSION ELECTRON MICROGRAPHIC (TEM) PLATES.

Kodak Dl9 film developer was freshly prepared by adding water to a stock solution at a ratio of 2:1. The exposed plates were offloaded from the electron microscope. The films were removed from the plates and mounted on a film rack. This was fully immersed in the developer contained in a Dallan Developing Tank and left for 4 mins. The film rack was agitated for 5 seconds during each minute of development to ensure the image came out evenly on the plate. The films were removed from the developer and rinsed in a continuous flow of water from a mixing valve to remove excess developer. Following this they were immediately transferred into an already prepared fixative from a stock solution of Kodak Unifix for 5-7 minutes. While in the fixative they were also agitated for 5 seconds every minute. The films were thoroughly washed in the continuous flow of water for 30 minutes. They were then dried under atmospheric conditions. The dry films were placed in transparent plastic envelopes and appropriately labelled. The developer changes the exposed silver (latent image) to bring out a visible negative image of the subject. The chemical reaction involved is a reduction of the silver ions by the developer to metallic silver. The fixative removes the opalescence and converts all undeveloped silver to a water soluble product that is removed during washing (Weakley, 1981).

2.14.2 PRINTING MICROGRAPHS.

For printing, the developer was made fresh by adding water to a stock solution of Kodak DEKTOL liquid developer 50 I in a tray at a ratio of 9:1. Negatives were placed in a negative holder in an enlarger. The enlarger was focused and adjusted to obtain the required magnification. An appropriate filter from Kodak Polymax filter kit was used and a test strip performed to determine the appropriate period of exposure. The films were exposed on 24 x 30.5 cm Kodak POLYMAX RC F photographic paper which was subsequently developed

for $1^1/_2$-2 minutes. During development the tray was gently agitated at regular intervals of time to ensure the image was evenly brought out. The micrographs were thoroughly rinsed in a partially stoppered sink with a continuous flow of water to remove excess developer. Following this they were immediately transferred into an already prepared fixative from a stock of Kodak Unifix. They remained here for 2-3 minutes and finally were transferred into a second tray of fixative for a further 3-5 minutes in order to ensure complete removal of excess silver halide. The micrographs were removed from the fixative, thoroughly washed in a continuous stream of water and dried with a Durst RCD3200 Drier. They were then labelled. The films were replaced within their envelopes and catalogued in an album.

2.15 ROUTINE WASTE DISPOSAL.

2.15.1 CARCASSES.

At the end of each session of surgical procedures the mouse carcasses were packed in polythene bags and disposed of by incineration.

2.15.2 SURGICAL MATERIALS.

All used needles and syringes were discarded in special large plastic bottles for subsequent disposal. Surgical gloves and tissue paper were discarded in appropriate bins.

2.15.3 OTHER HARDWARE.

Blades were discarded in small mineral water cans. Glass knives and Pasteur pipettes were disposed of in large plastic bottles.

2.15.4 CHEMICALS.

Used solutions were disposed of according to manufacturers' instructions.

2.16 IMAGE ANALYSIS SYSTEM (MAGISCAN).

Magiscan image analysis system (Joyce-Loebl) was used for all morphometric analysis. This is a device with the principles of a digital computer forming the heart of its operation. Like most digital computers, the Magiscan consists of an input section, a processing section and data storage section. The inputs are images to be analysed and commands from the user to tell the Magiscan what is required to be done, and such commands are given by using a keyboard and/or a mouse for text or a light pen for images. Images get into the system from a TV camera or from other devices like electron microscopes. The processing and storage sections include three main processors: an image processing unit (IPU) for arithmetic and general tasks, a memory address processor (MAP) which works in parallel with IPU and controls access to image memory, and the host computer which is an IBM compatible Control Processor with its own programme and data memory. Output from the machine goes to three kinds of devices: a printer or display screens (monitors) or as electronic signals to other devices like images to larger computers. There are two colour monitor screens. One of the screens is primarily for displaying text, which will often be in the form of lists of options (menus) to be selected for controlling the machine. The second screen usually displays images.

The software consists of an operating system (Personal Computer Disc Operating System-PCDOS) which runs all the time once the system is switched on, to provide general management of the computer. It maintains the integrity of files on discs and gives access to them. There is a General Image Analysis Software (GENIAS) which gives access to the image processing and analysis functions of the system. A RESULT programme allows for the analysis of measurements of data obtained from GENIAS (or from the other application programmes) both statistically and graphically.

Before any analysis a task force which also includes the unit of measurement is created. Following this an image of the object to be analysed is captured by the camera and stored in

the memory of the system. The image which is grey is processed in order to improve or simplified the task of its analysis. This processing allows the grey image to undergo geometrical transformations which alter the two-dimensional layout of the image without changing its grey levels. This is important for aligning images which are at different angles or for removing distortions. The result is that objects can be detected individually in modified binary images , thus giving a simple description of the boundary of each object thereby distinguishing it from artefacts. The most important geometrical transformation is the image rotation. This involves the interpolation of grey levels between pixels to obtain a correctly rotated image without distortion.

All Magiscan's image processing and analysis operate on the concept of pointset. The pointset is a description of the geometrical shape of either part or complete image. For example, a single point can be a pointset (the simplest), whereas pointsets can also describe arbitrarily shaped lines (e.g. arc pointsets) and areas (e.g. boundary pointsets). The combine use of geometrical transformation of images and pointsets enables the system to give the most accurate measurement of the parameter being analysed in the context of its original form; thus taking account of possible errors that may be introduced by such factors as, for example, the different courses taken by the nerve fibres in a nerve trunk which make their sectioning perpendicular to their individual long axis practically impossible. The objects which are detected in images are stored compactly in memory as arc pointsets (for fibrous objects) or region pointsets (for objects with discernible thickness). Such descriptions of objects are then measured for parameters like lengths, breadths, diameters, areas, perimeters, shapes, optical densities, etc. and the final result presented in the form of graphs or tables. For the present analysis the Magiscan image analysis system used the boundary pointset for both the csa of the nerves and the nerve fibre size spectrum.

2.17 MORPHOMETRIC ANALYSIS.

2.17.1 MEASURING CROSS-SECTIONAL AREA (CSA) OF OPTIC NERVE.

The Interactive Menu of the GENIAS programme of the Magiscan image analysis system was used for measuring the cross-sectional area (csa) of each nerve. This was done as follows: A Task Force was created. A slide of the stained semithin sections of each nerve was mounted on the stage of the microscope of the Image analysis system. After obtaining a clear focus of the image at a suitable magnification, it was captured on the image screen of the image analysis system. The unit of measurement (μm^2) and the appropriate scale factor were keyed in. After obtaining an appropriate threshold for a grey image, the area of the nerve was defined by drawing round the perimeter of the nerve excluding the meningeal coverings i.e. the dura, arachnoid and pia mater. The meningeal coverings were excluded because they are devoid of any nerve fibres, whereas both the mean nerve fibre count and the mean nerve fibre density directly depend on the csa of the axon-bearing part of the optic nerve. The outlined area of the nerve was automatically measured by the system and this was read off from its second screen. From the csa of the individual nerves the mean csa of the nerve for the particular group of mice was calculated (see Figure 2.1).

2.17.2 SAMPLING NERVE FIBRE PROFILES IN OPTIC NERVE.

A task list was created for using the Execute Menu of the GENIAS programme of the Image analysis system. This was to facilitate the automatic analysis of nerve fibre profile present in sampled areas of the nerve for number and size distribution. A systematic random sampling method (Mayhew,1990) was used to determine the total number and diameter spectrum of the myelinated nerve fibres in each nerve. This was done by locating the centre of the nerve. From this point sectors of 10 degrees were drawn over different areas of the nerve (Figure 2.2). A grid of approximately 1.0 cm x 1.0 cm squares (equivalent to $7.8\mu m^2$ of nerve csa) was placed over each sector (Figure 2.3). Using the sampling method indicated above, and starting from the centre of each nerve, every 4th square in each direction (i.e. 1 in 16) was sampled for the estimation of total myelinated nerve fibre counts and fibre size distribution.

This was done by capturing the image of the area of micrograph containing the sampled square on the second screen of the image analysis system. The width of the sampled square was demarcated on the screen. The external perimeter of the myelin sheath of each myelinated nerve fibre within the square was outlined with the pen of the instrument. All marked fibres were filled with the pen and then accepted for automatic statistical and graphical morphometric analysis by the Image analyser. The objective was to sample between 150 and 200 myelinated nerve fibres in each nerve as this allows an estimate of the parameters of all fibres in the nerve to within 95% confidence limits (Mayhew, 1988, 1990). In this method only complete squares falling within each 10° sector and had myelinated nerve fibres within them were systematically sampled. Also, only myelinated nerve fibres which completely or whose centres fell within a sampled square were included in the analysis. Because nerves from immature mice contain fewer myelinated nerve fibres, sampling them took more time in order to meet the target of 150-200 sampled fibres per nerve. Although the ultrathin sections from each nerve were cut perpendicular to the long axis of the nerve, it was not practicable to cut all the nerve fibres perpendicular to their long axes because of the variable courses they run within the nerve. The Magiscan image analyser automatically resolved this limitation when measuring the diameters of such fibres. Results were pulled out of the system both in numeric and graphical forms using the Result Menu. These were used for further statistical and graphical analysis of the nerves.

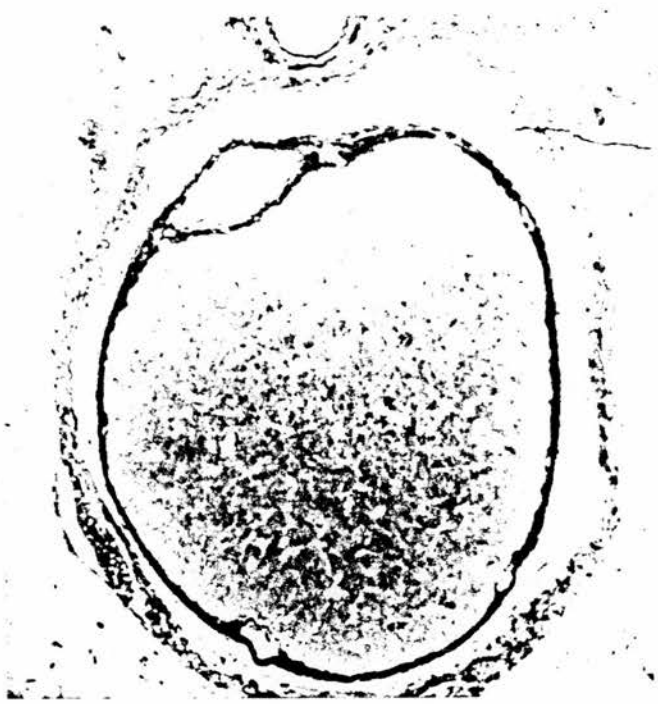

Figure 2.1: A light microscopic t.s. of the optic nerve (largest diameter of largest optic nerve from outer layer of dural sheath to outer layer of dural sheath = 370 μm) of an adult mouse showing the nerve bearing area outlined by the inner layer of the meningeal sheaths.

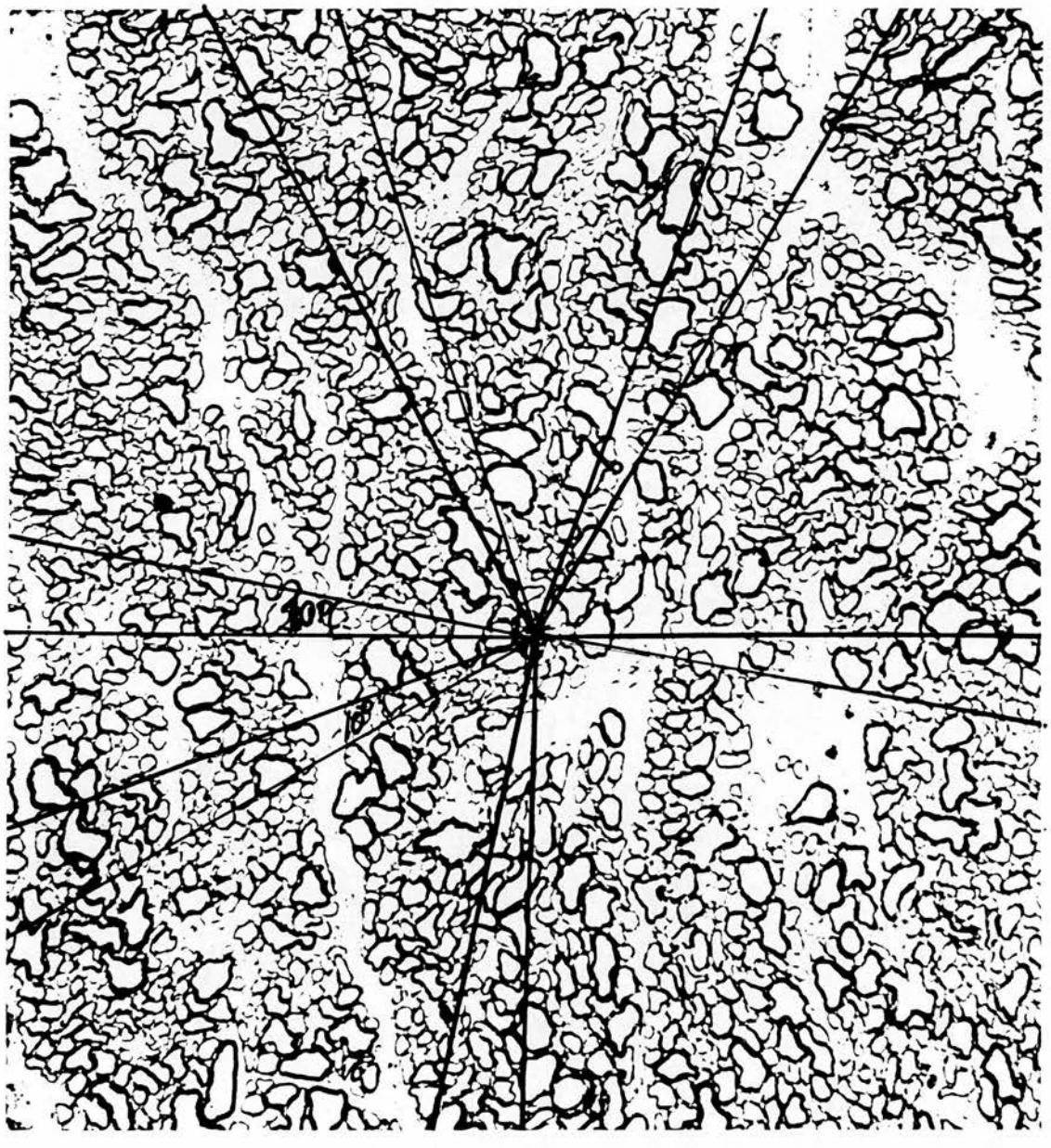

Figure 2.2: Micrograph showing outline of sectors (10°) of different areas of the optic nerve from centre to periphery for sampling myelinated fibres present in the nerve.

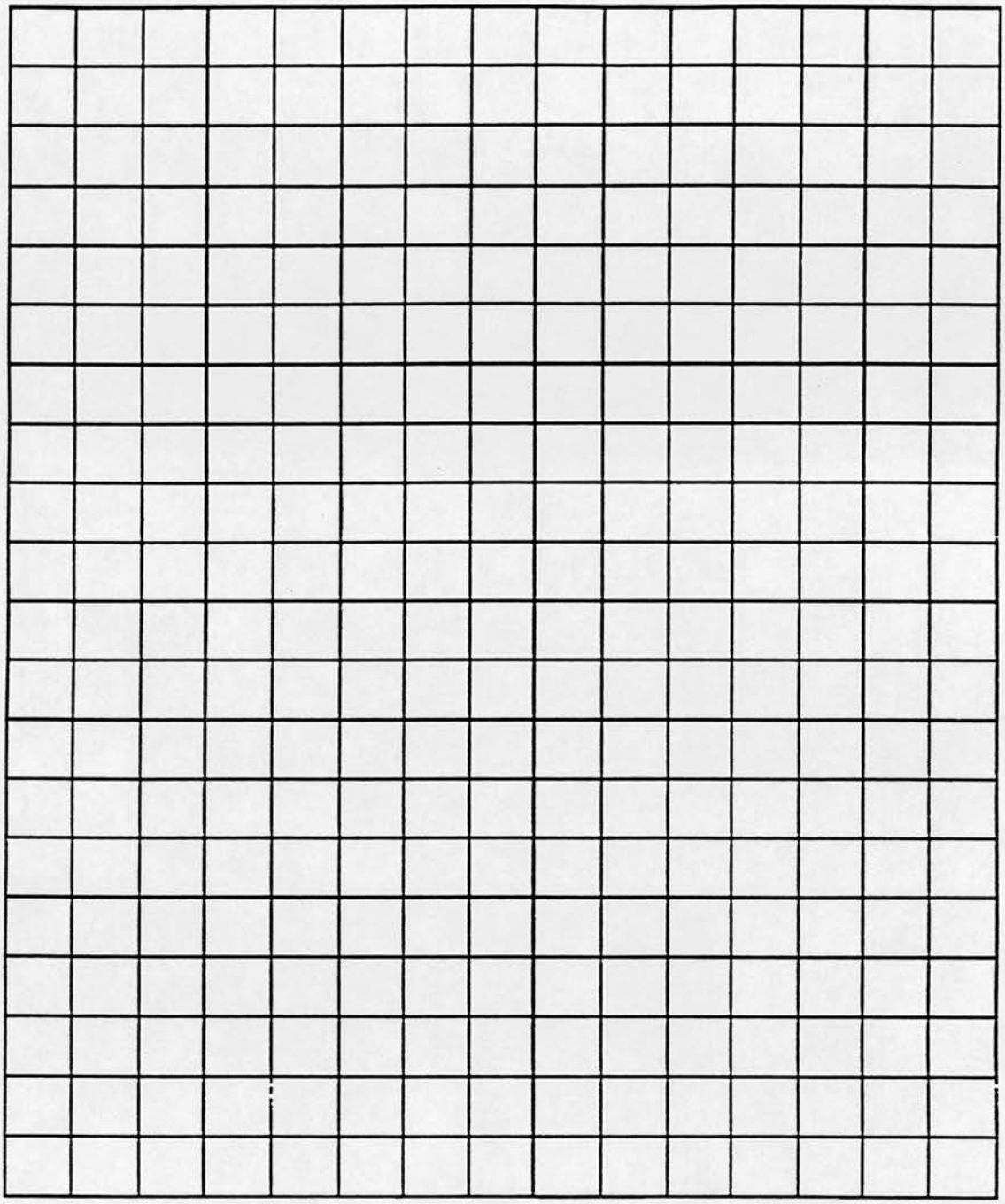

Figure 2.3: Grid used for sampling nerve fibres from micrographs of mouse optic nerve. Each 1.0 cm x 1.0 cm of grid is equivalent to 7.8 μm^2 of nerve fibre bearing area of nerve.

2.18 COMPUTATION OF MYELINATED NERVE FIBRE COUNTS AND DENSITY.

The number of myelinated nerve fibres present in each whole nerve and their numerical density i.e. myelinated nerve fibres per 1000 μm^2 were calculated using the ratio technique as follows (Matheson, 1970, Mayhew, 1988, 1990):

2.18.1.MYELINATED NERVE FIBRE COUNT.

$$\text{Number of myelinated nerve fibres in nerve} = \frac{\text{number of sampled nerve fibres from nerve}}{\text{number of sampled squares x 7.8 } \mu m^2} \times \text{csa } (\mu m^2) \text{ of nerve} \times \text{fibre bearing area}$$

2.18.2 DENSITY OF MYELINATED NERVE FIBRE (FIBRES 1000 μm^{-2}).

$$\text{Density} = \frac{\text{number of sampled nerve fibres per nerve}}{\text{number of sampled squares x 7.8 } \mu m^2} \times 1000$$

The mean myelinated nerve fibre count and fibre density of the optic nerve for each group of mice were then calculated from the results for the individual nerves in the group.

2.19 STATISTICAL ANALYSIS.

2.19.1 MEAN.

The mean is a measure of central distribution and is defined as the arithmetic average of all the observations. It is found by taking the sum of the observations and dividing by their number (Bland, 1989). This can be statistically presented thus:

$$\bar{x} = \frac{1}{n} \Sigma xi$$

x = mean, n = number of observations, Σxi = the sum of all the observations.

The mean itself alone without other measures of central distribution is a fallacy. It is usually considered along with such estimates of central distribution including the variance, standard deviation, standard error of mean.

2. 19.2 VARIANCE.

It is the estimate of variability of the observations from the mean. It is statistically defined as the average sum of the squares of all the deviations from the mean.

$$\text{Variance } (S^2) = \frac{1}{n-1} \Sigma(\bar{x}-x)^2$$

2.19.3 STANDARD DEVIATION.

This is the square root of the variance. It is presented as follows:

$$\text{Standard Deviation } (S) = \sqrt{S^2}$$

2.19.4 STANDARD ERROR OF MEAN.

The standard error of mean (s.e.m.) for a sample is an estimate of the standard deviation that would be obtained from the means of a large number of samples drawn from a population. It is statistically presented as follows:

$$\text{S.e.m.} = \frac{S}{\sqrt{n}}$$

where S = Standard Deviation. n= sample size.

2.20 VERIFICATION OF RESULTS (STUDENT'S t-TEST).

This allows for the testing of the null hypothesis i.e that no statistically significant difference exists between the mean of a sample and its population mean, nor is there any significant difference between the means of two samples. This test takes into consideration the difference between the means of the two groups as well as the variability within the data and the number of figures involved. It is statistically presented as follows:

$$t = \frac{\text{Difference between means}}{\text{Standard Deviation of the data}} \times (1/n_1 + 1/n_2)$$

$$t = \frac{\bar{x}_1 - \bar{x}_2}{\sqrt{\frac{(\Sigma \bar{x}_1^2 - n_1 x_1^2) + (\Sigma \bar{x}_2^2 - n_2 x_2^2)}{(n_1 + n_2) - 2}}} \times (1/n_1 + 1/n_2)$$

The value for t is compared with the theoretical value from a t-Distribution Table.

CHAPTER THREE

MORPHOMETRIC ANALYSIS OF MYELINATED FIBRE COMPOSITION IN THE OPTIC NERVE OF ADULT C57BL AND CBA STRAIN MICE AND (C57BL x CBA) F_1 HYBRID: A COMPARISON OF INTERSTRAIN VARIATION.

Contents

3.1 Introduction

3.2 Materials and methods

3.3 Results

3.3.1 Cross-sectional areas (μm^2)

3.3.2 Total myelinated nerve fibre counts

3.3.3 Myelinated nerve fibre density (fibres $1000\mu m^{-2}$)

3.3.4 Myelinated nerve fibre size diameter spectrum

3.4 Discussion

3.1 INTRODUCTION

The mouse is a widely used experimental model. Different strains of mice have been used for example, to study the teratogenic effects of substances like alcohol (Randall & Taylor, 1979; Chernoff, 1980; Bannigan & Burke, 1982; Uphoff et al., 1984). This is because of its small size which makes it easy to handle and economically cheap to manage (Hogan et al., 1986; Kaufman, 1992). Besides, it is easily adaptable and ancestrally close to man, thus making the correlation of findings from it to man relevant. Specific organ structures of the mouse, such as the optic nerve, have also been studied with respect to the teratogenicity of such substances, although in the absence of baseline morphometric information (Ashwell & Zhang, 1994). This makes the establishment of baseline information on, for example, the optic nerve of the mouse a basic prerequisite for human related studies involving the mouse.

Detailed morphometric studies on the myelinated fibre composition of the mouse optic nerve are few, although much work has been undertaken in a variety of other mammalian species (Bishop, 1933; Bruesch & Arey, 1942; Quilliam, 1956; Donovan, 1967; Hughes, 1977; Sanchez et al., 1986 - see Discussion). The only relevant studies in the mouse that I have so far located have been those of Gyllensten & Malmfors (1963) and Gyllensten et al. (1966) who analysed the influence of visual stimulation on myelinogenesis and fibre composition in the mouse optic nerve. These early morphometric studies on the mouse, although of interest in some respects, are incomplete in that the authors failed to establish whether there was any significant difference in myelinated fibre composition between, for example, the left and the right optic nerve, or between male and female mice of the same and different strains. Information from studies on other species have also been limited by the use of too few animals as well as the use of manual methods together with only light microscopy (Donovan 1967; Forrester & Peters, 1967).

The principal aim of the present study was to establish such baseline information which, in addition to being useful for subsequent morphometric studies of this species, would also

allow for comparison to be made with other species that have earlier been investigated by other workers. The optic nerves from adult male C57BL, CBA and (C57BL x CBA) F_1 hybrid mice, and from female CBA mice were isolated in order to undertake morphometric analyses. Both the cross-sectional areas (csa) of the optic nerves and the numbers and diameters of myelinated nerve fibres present, and nerve fibre density, were established for the various groups analysed.

3.2 MATERIALS AND METHODS.

Male C57BL (x 5) and CBA (x 10) strain mice and (C57BL x CBA) F_1 hybrid (x 5) mice, 11 weeks of age were used for this study. The mouse strains were those most commonly used for teratological studies in the Department of Anatomy. In addition, the C57BL and the (CBA x C57BL) F_1 hybrid strains were also used for developmental studies (see later). Each animal was weighed in order to determine the amount of anaesthetic and fixative it was to be given. It was then deeply anaesthetised following an intraperitoneal injection of 0.02 ml/g body weight of a 1.2 % solution of Avertin dissolved in 0.9% of saline. An intracardiac perfusion of fixative, using 2 ml/g body weight of a 2.5% solution of glutaraldehyde and 1M paraformaldehyde in 0.1 M phosphate buffer was given via a 21G needle into the left ventricle while the heart was still beating.

The optic nerves from each mouse were carefully dissected out, avoiding traction on the nerves. This was to ensure that minimal disruption with the normal anatomy of the nerve was induced during dissection. Each nerve was cut just posterior to the orbit, and anterior to the optic chiasma, immediately put into a separate bottle of fixative and left in this for a total of about l2 h. The isolated nerves were washed in buffer and then transferred into a secondary fixative consisting of 1% osmium tetroxide in 0.1M phosphate buffer for a further 2h. They were then dehydrated through a graded alcohol series, cleared in propylene oxide and finally embedded in Araldite.

Semithin transverse sections of $\cong$ 1 μm thick were cut perpendicular to the long axis of the nerve (at approximately the mid-point of the isolated section of nerve) using a Reichert-Jung Ultracut E microtome. Since the main objective was to analyse the general morphometric parameters of the optic nerve rather than the regional variation of these parameters along the nerve, it was not considered necessary to cut additional sections at other points of reference along the nerve. The semithin sections were stained with 1% Toluidine blue in 1% borax suitable for light microscopy. Ultrathin sections $\cong$ 80 nm in thickness were then cut, picked

up on copper grids (200) and subsequently stained with 0.2% lead citrate and a saturated solution of uranyl acetate (Reynolds, 1963). A selection of photomicrographs was then taken from the centre to the periphery of each nerve using a Philips EM301 transmission electron microscope. This was done to ensure that a good representation of the different nerve fibre profiles within the nerve was included for the sampling procedure. The micrographs were developed and printed at a final magnification of x 3000, sufficient to ensure that all fibres with the thinnest myelin sheaths could be unequivocally identified in counts.

The csa of the optic nerves was determined by viewing and measuring complete cross-sections of the optic nerves in a Magiscan image analysis system (Applied Imaging). Detailed morphometric analysis was performed on the electron micrographs using a systematic random sampling procedure (Mayhew, 1990) to establish the numbers and diameters of the myelinated nerve fibres by means of the image analyser. In order to determine the latter, the micrographs for each nerve were assembled and the approximate centre of the optic nerve located. From this point sectors of 10° were drawn. A grid of 1 cm x 1 cm squares (equivalent to 7.8 μm^2 of nerve csa) was placed over each sector. Starting from the centre of each nerve, and using the systematic random sampling method referred to above, every 4th square in each direction (i.e. 1 in 16) was sampled for estimating nerve fibre counts. The aim was to sample between 150 and 200 myelinated nerve fibres, and to measure as many profiles of the nerves as possible (Mayhew, 1988, 1990). In this method all nerve fibres whose centres were within a sampled square were counted and their respective sizes measured.

It was apparent that, by this sampling method, the nerve fibre profiles at the very centre of the nerve were never to be sampled. In order to establish whether this sampling procedure had any possible effect on the overall results as well as see if there was any significant regional difference in the distribution of the population of the nerve fibres within the nerve, micrographs from the CBA female series (see below) were sampled across the centre,

intermediate and periphery of the optic nerves. The results obtained were statistically tested to compare the pattern of distribution of nerve fibres within the optic nerve in the mouse at the centre, intermediate and periphery of the optic nerves. The csa of the nerve fibre-bearing area of the nerve i.e. the csa excluding the meningeal sheaths (Williams et al., 1989), was used to calculate the number of myelinated nerve fibres present in the whole nerve using the ratio technique (Matheson 1970; Mayhew, 1988, 1990). A 2-tailed Student's t test was then performed on the pooled data for each mouse strain, to establish whether there was any significant difference ($P \leq 0.05$) in csa and total nerve fibre count and size distribution between the left and right optic nerve for each of the strains studied, and to establish whether interstrain variation existed. For further verification, analysis of variance was performed. The image analyser allowed a graph to be plotted which displayed the distribution of diameters of all the nerve fibres studied from each optic nerve sampled. When all the information from the various sample groups was available, it was then possible for graphs to be plotted which displayed the overall distribution of the nerve fibre size composition for each of the mouse strains studied.

Furthermore, to establish whether evidence of sexual dimorphism was present, an additional series of 11wk-old female CBA (x 5) mice was treated as indicated above, and the findings obtained compared with those obtained previously from the analysis of the male CBA mice.

3.3 RESULTS

3.3.1 CROSS-SECIONAL AREAS (μm^2).

The optic nerve in all the mouse strains analysed had well defined meningeal sheaths as shown in Figure 3.1. Analysis of the csa of the left (L) and right (R) optic nerves of the mice studied showed that, except in the C57BL, the right optic nerve was consistently larger than the left (i.e. in the CBA strain, and in the (C57BL x CBA) F_1 hybrids). The smallest difference between the left and right optic nerves was seen in the CBA and the largest difference observed in the F_1. However the difference observed was not significant (see Table 3.4). The data from the left and right (L + R) optic nerves of each strain studied were therefore pooled. This allowed the sample size to be doubled in each case, so that in the C57BL, CBA and F_1 hybrid mice, the pooled sample size of the optic nerves studied was 10, 20 and 10 respectively, and this is presented in Table 3.1. The C57BL had the largest mean csa (72968±1876 μm^2 (s.e.m.)) and the CBA the smallest (57113±l 1513 μm^2 (s.e.m.)). Further analysis of the pooled data revealed that there was a significant difference between all the strains ($0.01 < P < 0.05$), as presented in Table 3.4.

The analysis of the csa of the 5 left and 5 right optic nerves isolated from the additional series of the 11-wk-old female CBA mice revealed that, although the right optic nerve had a higher mean csa than the left, the difference between the two sides was not significant. A comparison of the findings from this series with their CBA male littermates revealed that the males had a larger csa but this difference between the two sexes was not significant. For this reason the data for this strain were pooled as given in Tables 3.1 and 3.4.

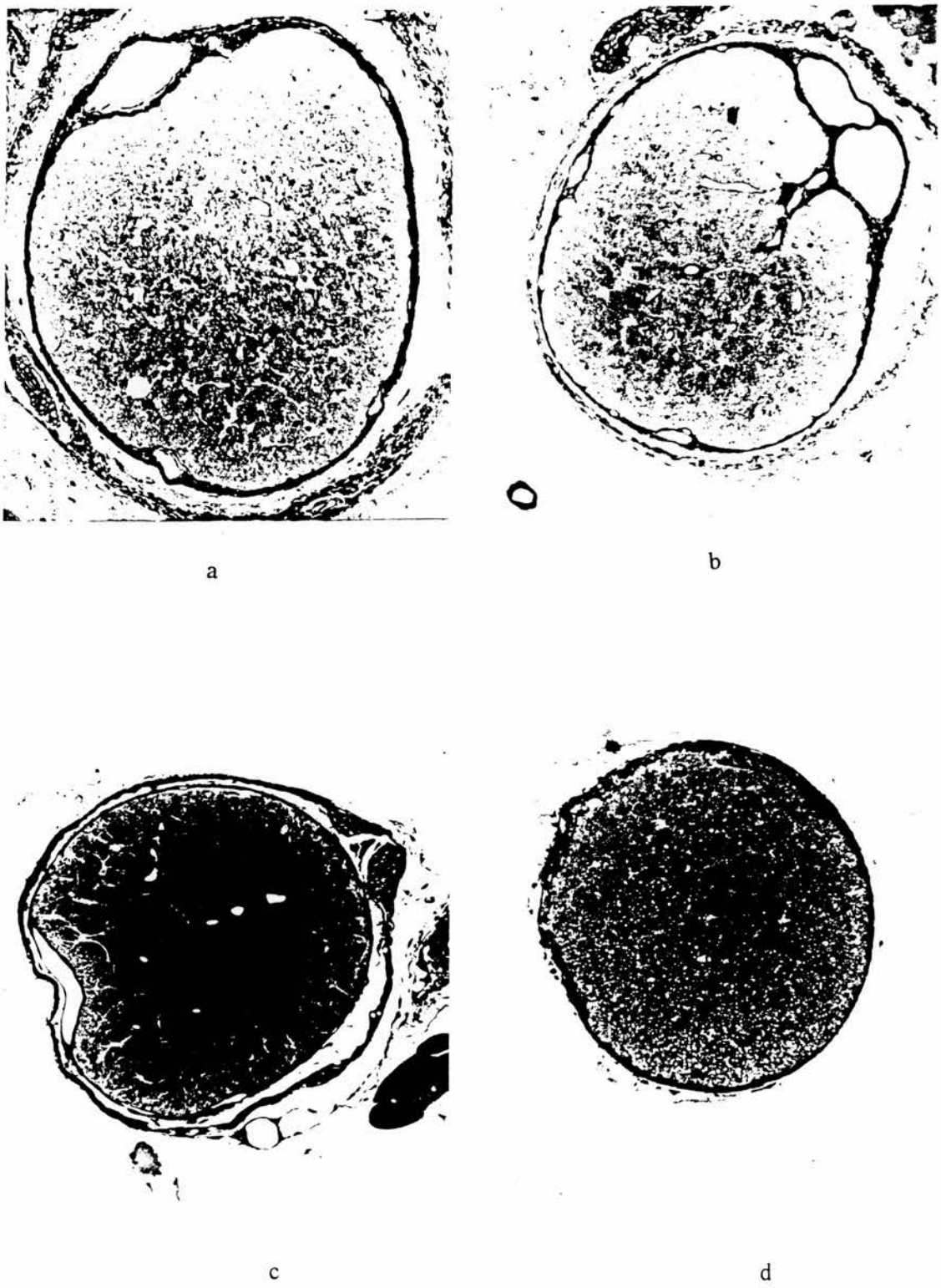

Figure 3.1: Toluidine blue stained transverse sections of optic nerve of adult C57BL, CBA and (C57BL x CBA) F_1 hybrid mice (scale factor as for Figure 2.1). The optic nerve in each mouse strain has well defined meningeal coverings. a): C57BL, b): F_1 hybrid, c): male CBA, d): female CBA.

Figure 3.2: TEM (x 3000) of ultrathin transverse sections of optic nerves of 11-week old C57BL, CBA and (C57BL x CBA) F_1 mice. Unmyelinated fibres were rarely encountered. a) male C57BL, b) male (C57BL x CBA) F_1 hybrid, c) male CBA, d) female CBA. Fibres are more concentrated at the centre of the nerve than at the periphery. The small size fibres dominate all regions of the nerve and their population density decreases from centre to periphery. Large diameter fibres are few in number and their population increases from centre to periphery.

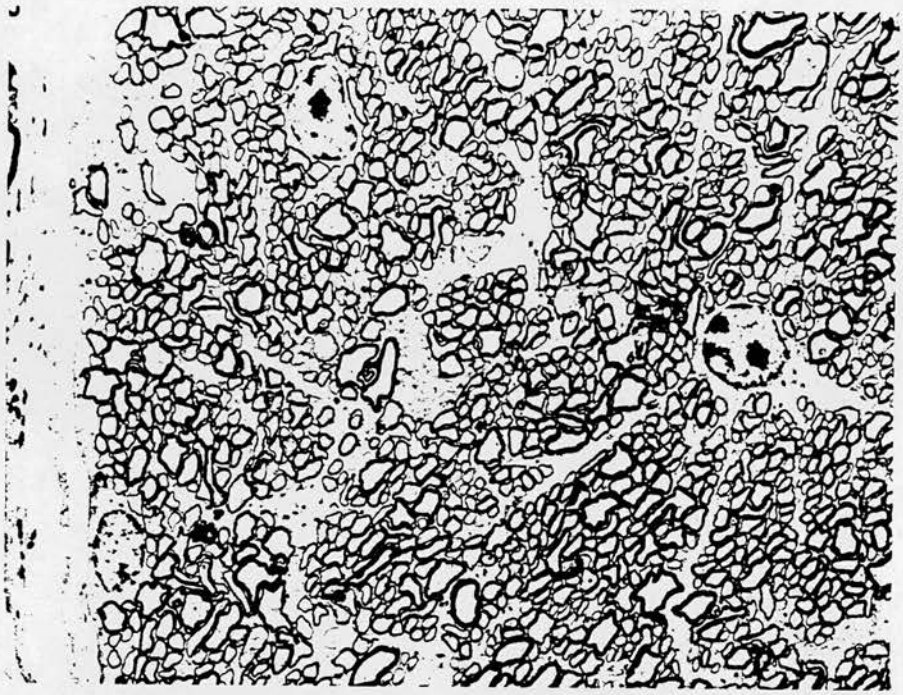

a

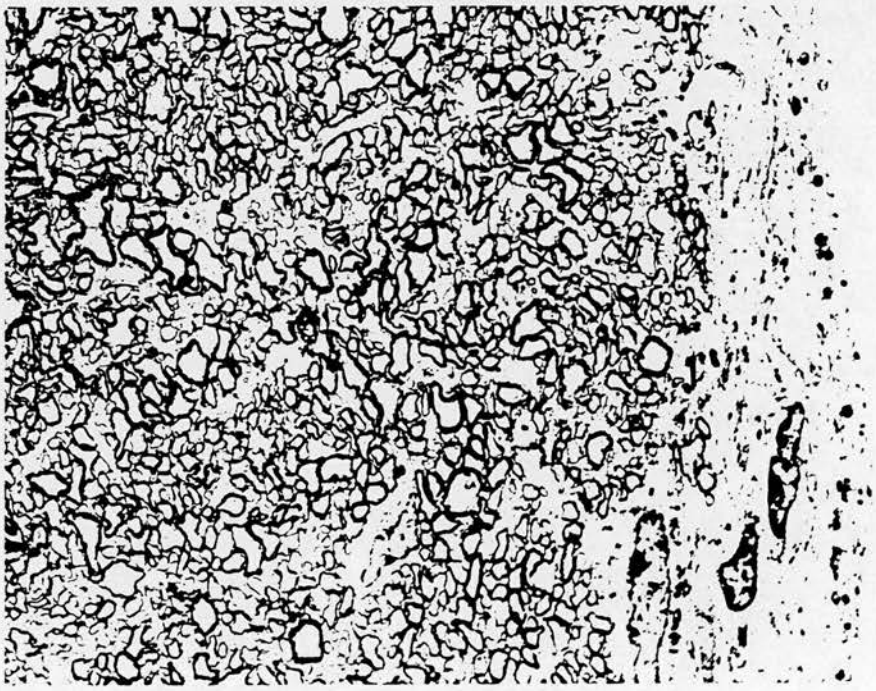

b

Figure 3.2

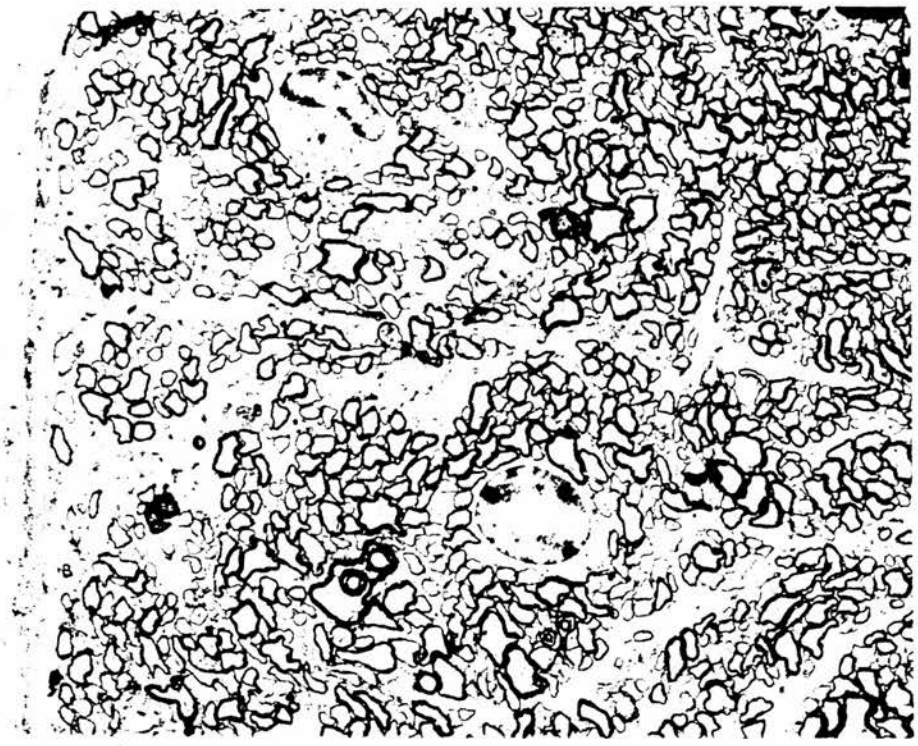

c

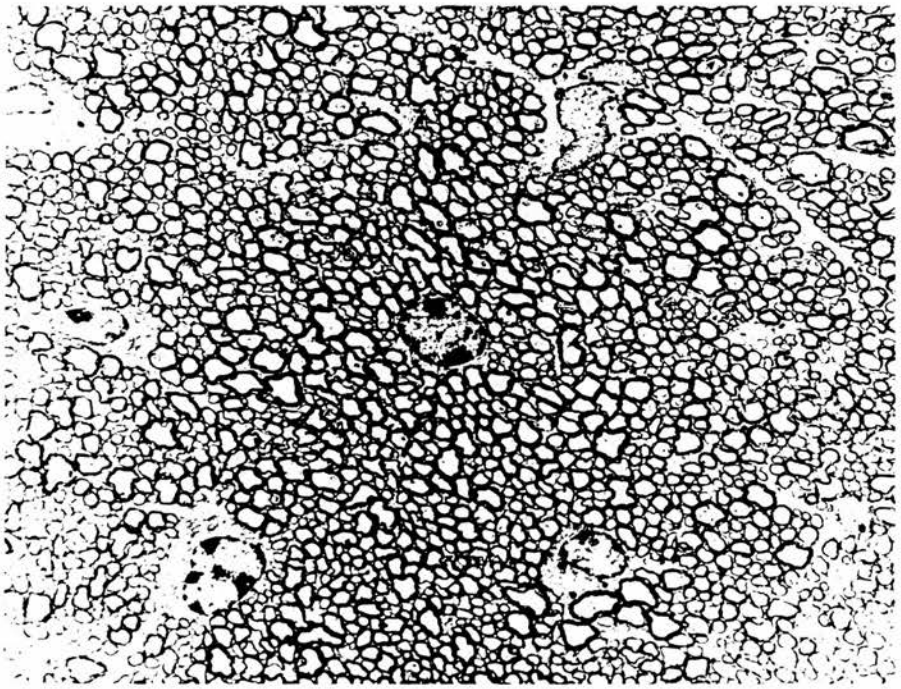

d

Strain		Mean myelinated nerve fibre count (±s.e.m.)	
		L or R	L + R
(C57BL x CBA) F_1 hybrid	L	98694±2907	
(male, n* = 9)			94086±3691
	R	90399±6017	
C57BL	L	95016±8418	
(male, n* = 10)			87398±5076
	R	79781±4005	
CBA	L	80924±4439	
(male, n* = 20)			79755±2500
	R	78586±2530	
CBA	L	80524±6400	
(Female, n* = 10)			80229±4432
	R	79934±6825	
CBA	L	80791±3517	
(male & female, n* = 30)			79913±2180
	R	79035±2696	

Table 3.2: Mean myelinated nerve fibre counts of optic nerves isolated from adult C57BL, CBA mice and (C57BL x CBA) F_1 hybrid. n* = total number of optic nerves analysed; s.e.m., standard error of mean.

3.3.3 MYELINATED NERVE FIBRE DENSITY (FIBRES 1000 μm^{-2}).

In all strains of mice, including the CBA female series, the density of myelinated nerve fibres in the right optic nerve was always lower than that observed on the left side. The difference in nerve fibre density between left and right optic nerves was, however, not significant in each of the strains studied. The pooled values showed a significant difference between the C57BL and both of the other strains ($0.01 < P < 0.05$). There was no significant difference between the F_1 and CBA. The highest mean myelinated nerve fibre density was observed in the CBA (1411±36 (s.e.m.)) and the smallest in the C57BL (1194±51 (s.e.m.)). As for csa and total myelinated fibre counts, no evidence of sexual dimorphism was seen in the CBA, so that the individual male and female findings as well as the pooled data have been included in Tables 3.3 and 3.4.

Strain		Mean myelinated nerve fibre density (fibres 1000μm^{-2}) (±s.e.m.)	
		L or R	L + R
(C57BL x CBA) F_1 hybrid (male, n* = 9)	L	1569±18	1408±61
	R	1279±48	
C57BL (male, n* = 10)	L	1258±98	1194±51
	R	1129±17	
CBA (male, n* = 20)	L	1426±80	1402±46
	R	1378±48	
CBA (Female, n* = 10)	L	1475±100	1429±60
	R	1382±69	
CBA (male & female, n* = 30)	L	1442±61	1411±36
	R	1380±38	

Table 3.3: Mean myelinated nerve fibre density of optic nerves isolated from adult C57BL, CBA and (CS7BL x CBA) F_1 hybrid mice. n* = total number of optic nerves analysed; s.e.m., standard error of mean.

Strain comparison	Variable/Level of significance		
	Mean csa (μm^2)	Mean myelinated nerve fibre count	Mean myelinated nerve fibre density (fibres $1000\mu m^{-2}$)
F_1 (L vs R, n* = 9)	n.s.	n.s.	n.s.
C57BL (L vs R, n* = 10)	n.s.	n.s.	n.s.
CBA male (L vs R, n* = 20)	n.s.	n.s.	n.s.
CBA female (L vs R, n* = 10)	n.s.	n.s.	n.s.
CBA male vs female (n* = 30)	n.s.	n.s.	n.s.
CBA male and female (L vs R, n* = 30)	n.s.	n.s.	n.s.
F_1 male vs CBA male (n* = 29)	$0.01 < P < 0.05$	$0.01 < P < 0.05$	n.s.
F_1 vs CBA male and female (n* = 39)	$0.01 < P < 0.05$	$0.01 < P < 0.05$	n.s.
F_1 male vs C57BL male (n* = 19)	$0.01 < P < 0.05$	n.s.	$0.01 < P < 0.05$
C57BL male vs CBA male (n* = 30)	$0.01 < P < 0.05$	n.s.	$0.01 < P < 0.05$
C57BL male vs CBA male and female (n* = 40)	$0.01 < P < 0.05$	n.s.	$0.01 < P < 0.05$

Table 3.4: Intrastrain and interstrain comparison for variables measured for the optic nerve of adult C57BL, CBA and (C57BL x CBA) F_1 hybrid mice. n* = Total number of optic nerves analysed; n.s., no significant difference.

3.3.4 MYELINATED NERVE FIBRE DIAMETER SPECTRUM.

The optic nerve in each strain of mice analysed was predominantly populated by small diameter fibres. Over 90 % of the nerve fibres in each strain of mice were not more than 1.04 μm in diameter. No strain of mice had fibres measuring more than 2.0 μm in diameter and this constituted only a small percentage of the total number of myelinated nerve fibres within the nerve. For example, the largest fibres analysed were seen in the C57BL and were 1.9 μm in diameter. These constituted only 0.28% of the total fibre population of that strain. The largest fibres seen in the F_1 and CBA were 1.84 μm in diameter. They constituted 0.09% and 0.04% of the total fibre population of the F_1 and CBA, respectively. The mean nerve fibre diameter was 0.62±0.02 μm (s.e.m.), 0.57±0.03 μm (s.e.m.) and 0.55±0.01 μm (s.e.m.) for the C57BL, F_1 and the CBA, respectively. In all the strains examined, the distribution of nerve fibre diameter was unimodal, with a modal value of 0.48 μm. Each strain of mice exhibited a slight skewing of the fibres in favour of those with a larger diameter. The C57BL and the CBA had similar populations of fibres (17.5% and 17.37%, respectively) with this modal diameter. The F_1 had 15.21% of its fibres with the modal diameter. Figure 3.3 shows the nerve fibre size spectrum of the myelinated nerve fibres in the optic nerve of each of the strains of mice studied. Also, from the additional female CBA series analysed for the distribution of nerve fibres within the nerve, small size fibres were more concentrated at the centre than at any other part of the nerve. The reverse phenomenon was the case with the large size fibres which were more concentrated at the periphery than in any other part of the nerve. However, in general, the population of small size fibres at any part of the nerve was more than that of the large fibres.

Figure 3.3 Graphs to show spectrum of myelinated nerve fibre diameter distribution (μm) in optic nerve of 11-week old C57BL, CBA and (C57BL x CBA) F_1 mice. All strains of mice showed a unimodal distribution of the nerve fibres with a modal diameter of 0.48 μm. There was a positive skewing of the fibres.

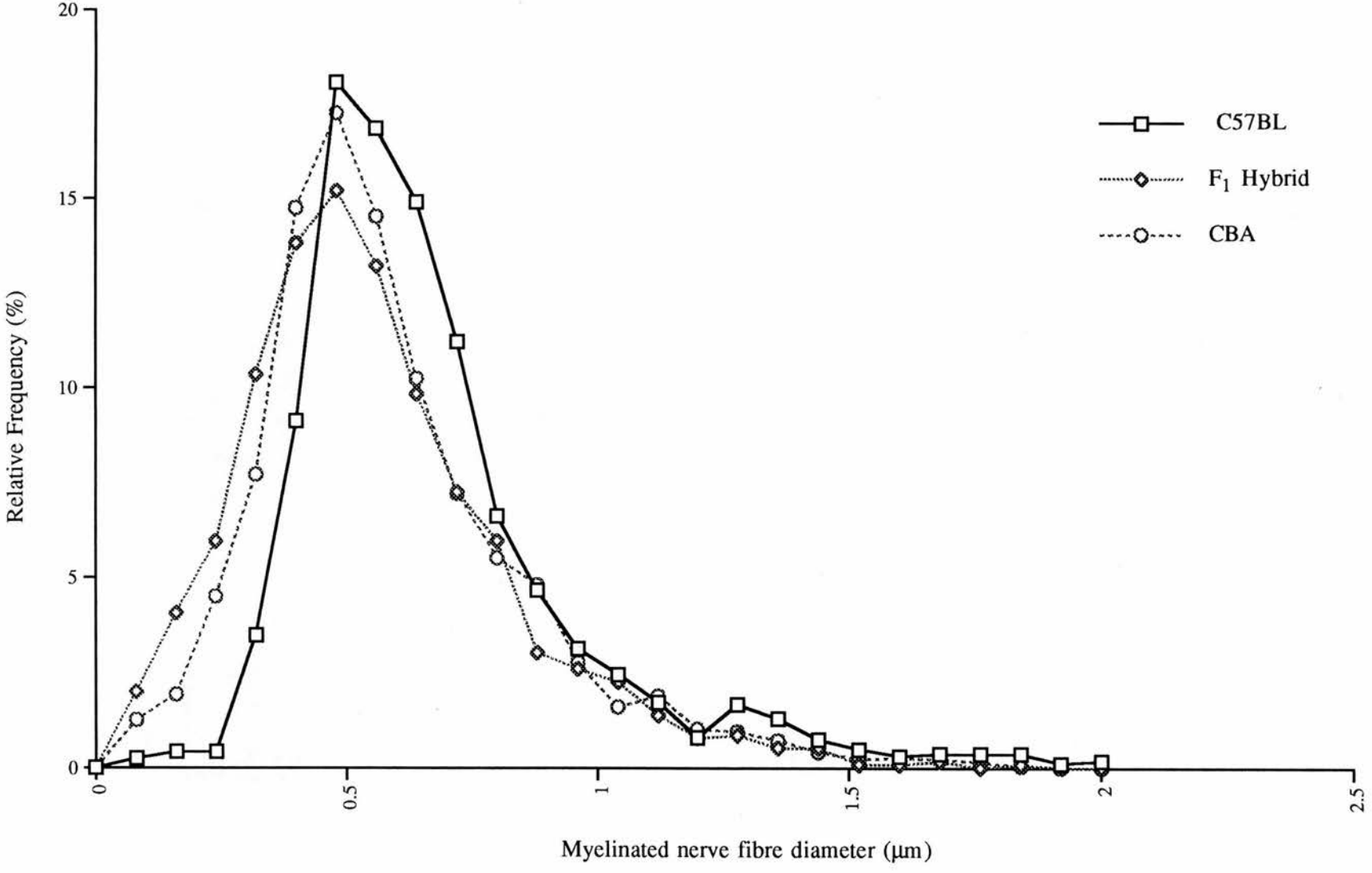
20
15
10
5
0
Relative Frequency (%)
0
0.5
1
1.5
2
2.5
Myelinated nerve fibre diameter (µm)
C57BL
F1 Hybrid
CBA

Figure 3.3

3.4 DISCUSSION.

The findings from this study indicate that of the variables analysed, the right optic nerve invariably had lower mean values than the left optic nerve except for the csa, though no significant differences were, however, observed with regard to any of these variables between the left and right optic nerves of male C57BL, CBA and (C57BL x CBA) F_1 hybrid mice. Furthermore, from the results of an additional analysis of the optic nerves isolated from a group of CBA females, no significant difference was observed in any of the variables studied between the left and right optic nerves, and between male and female mice. Interstrain differences were, however, seen between the different strains studied. Of the 3 strains of mice involved in this study, the optic nerves of the C57BL strain had the largest cross-sectional area, but they were the least densely populated with myelinated nerve fibres. Because the CBA strain has a high mean nerve fibre count and a relatively small csa, it has the highest nerve fibre density. The high density of myelinated nerve fibres in the optic nerve of this strain of mice is a reflection of the small value for its mean nerve fibre diameter and the low percentage of large fibres present in comparison with corresponding values for these parameters for the other strains of mice analysed. The relatively small difference in the variables measured between individuals of each of the strains studied, both male and female for the CBA strain mice, indicates a considerable degree of intrastrain uniformity as might be expected in inbred strains of animals. The fact that there was a significant difference in the variables measured between the various strains studied should also not be surprising, and would seem to be reasonable evidence of genetic variation induced as a result of many generations ($\geq$ 20) of brother x sister matings required in the establishment of an inbred strain of animals. The same modal value was observed in each of the strains studied for the size distribution of myelinated nerve fibres.

Since some of the variables analysed in this study have been investigated by others, this has allowed for some observations to be made on species variation particularly in the mean total myelinated nerve fibre count within the optic nerve, as this has been the area in which most

information has been published. In order to facilitate such an exercise, this information has been presented in tabular form in Table 3.5 based on the different species studied. The most obvious feature that emerges from the information presented in this Table is the very considerable difference in total number of myelinated fibres present in the primate compared with the nonprimate optic nerves. In the human optic nerve, values of 815 000-1 000 000 (Chacko, 1948) to 1 100 000-1 300 000 myelinated nerve fibres (Potts et al., 1972a, b) have been reported, while slightly higher figures were obtained from the analysis of the optic nerve of the rhesus monkey (1 400 000-1 800 000; see Ogden & Miller, 1966; Potts et al., 1972a, b), and 1 200 000 for the cynomologus monkey (Sanchez et al., 1986). A nerve fibre count of 565 000 was reported in the optic nerve of the chipmunk (Wakakuwa et al., 1987). In the rabbit, a figure of 394 000 fibres was reported (Vaney & Hughes, 1976), and in the cat, Donovan (1967) reported a nerve fibre count of 85 926. In the rodents that have been studied, the figures quoted for the total fibres present in the rat of 117 000-120 000 (Forrester & Peters, 1967; Hughes, 1977) are about 50% greater than those for mice given by Gyllensten & Malmfors (1963) and Gyllensten et al. (1966) and the values cited in the present study, with only a minimum degree of strain variation apparent in this species. The figures indicated here suggest that there might be a relationship between body size and total myelinated fibre count.

With the exception of the chipmunk (Wakakuwa et al., 1987) in which 0.9% of fibres found in the adult optic nerve were unmyelinated, there was no report of unmyelinated nerve fibres in adults of any of the other species cited above, and as indicated in this study. Most of these studies provided figures for the size range of the myelinated fibres with, in general terms, the largest fibres being seen in the primates analysed, and in the rabbit and cat. In the latter species, maximum fibre diameters of up to 10.5 μm were reported (see Donovan, 1967) compared with 1.92 μm in this study. Although the spectrum of distribution of the nerve fibres in the optic nerve in these other species was wide, there was a general preponderance of small fibres within the nerve compared to fibres of other diameter sizes. It

is obvious from the present study that the optic nerve of the mouse, besides containing a lower total myelinated nerve fibre count compared with the rat, for example, also has predominantly fibres of smaller diameter.

The difference in the total fibre counts of the C57BL strain of mice in this study and those of Gyllensten & Malmfors (1963), and Gyllensten et al. (1966) are probably most easily accounted for by differences in the methodology employed to determine this value. In contrast to the present study where transmission electron micrographs of ultrathin sections of the optic nerve were studied, these authors analysed paraffin sections of mouse optic nerves using phase-contrast microscopy. The error factor using the latter approach, both in estimating the total number of fibres present as well as determining their mean diameters, was found to be considerable. When these authors used photomicrographs obtained following transmission electron microscopy of the optic nerve, a modal diameter of 0.6-0.8 μm was reported, compared with 1.0 μm when paraffin sections were analysed. Furthermore, it is unclear why the distribution of fibre diameter should have been trimodal in Gyllensten & Malmfors (1963) and Gyllensten et al. (1966) compared with a unimodal distribution as reported in this study. Whether any clear species specificity exists between total fibre count and the lifestyle of that species has yet to be fully evaluated. Gyllensten & Malmfors (1963) suggested that this may reflect the fact that the mouse is more dependent on other senses than sight for most of its activities, and that this may be the reason why the majority of the myelinated fibres present are of small diameter.

Species	Mean nerve fibre count	Mean nerve fibre density (1000 μm^{-2})	Fibre size range (μm)	Mean fibre diameter (μm)	Modal diameter (μm)	Distribution	Reference
Man	1 100 000-1 300 000	N.P.	N.P.	N.P.	0.5	Unimodal	Potts et al., 1972a, b
Man	815 000-1 000 000	N.P.	0.70-8.00	N.P.	1.00	Bimodal	Chacko, 1948
Monkey (rhesus)	1 500 000-1 800 000	N.P.	N.P.	N.P.	0.50	Unimodal	Potts et al., 1972a, b
Monkey (rhesus)	1 400 000	N.P.	0.40-6.00	N.P.	1.20	Unimodal	Ogden & Miller, 1966
Monkey (cynomologus)	1 200 000	N.P.	0.55-1.55	0.80	N.P.	Trimodal	Sanchez et al., 1986
Cat	85 926	N.P.	1.00-10.50	N.P.	2.50	Unimodal	Donovan, 1967
Rabbit	394 000±20 000 (S.D.)	N.P.	0.25-7.00	N.P.	0.75	Unimodal	Vaney & Hughes, 1976
Rat (albino)	117 000	N.P.	N.P.	N.P.	0.90	Unimodal	Forrester & Peters, 1967
Rat (pigmented)	120 000±1600 (s.e.m.)	509000 fibres mm^{-2}	0.44-5.20	N.P.	1.00	Unimodal	Hughes, 1977
Chipmunk (*Tamias sibiricus asiaticus*)	565 000	N.P.	0.20-3.60	0.83	0.60-0.70	Unimodal	Wakakuwa et al., 1987
Mouse (C57BL	66155±10052 (S.D.)	N.P.	≤ 3.00	N.P.	0.60-0.80	Trimodal	Gyllensten & Malmfors, 1963; Gyllensten et al., 1966
Mouse (C57BL)	87398±5076 (s.e.m.)	1194±51 (s.e.m.)	≤ 2.00	0.62±0.02	0.48	Unimodal	This study
Mouse CBA)	79913±2180 (s.e.m.)	1411±36 (s.e.m.)	≤ 1.84	0.55±0.01	0.48	Unimodal	This study
Mouse (F_1)	94086±3691 (s.e.m.)	1408±61 (s.e.m.)	≤ 1.84	0.57±0.03	0.48	Unimodal	This study

Table 3.5: Comparison of variables measured in this study with other studies of the optic nerve. S.D., standard deviation; s.e.m., standard error of mean; N.P., information not provided.

CHAPTER FOUR

MORPHOMETRIC STUDY OF THE OPTIC NERVE OF ADULT NORMAL MICE AND MICE HETEROZYGOUS FOR THE *SMALL EYE* MUTATION (*Sey*/+).

Contents

4.1 Introduction

4.2 Materials and Methods

4.3 Results

4.3.1 Cross-sectional area (μm^2)

4.3.2 Total myelinated nerve fibre counts

4.3.3 Myelinated nerve fibre density (fibres $1000\mu m^{-2}$)

4.3.4 Myelinated nerve fibre diameter spectrum

4.4 Discussion

4.1 INTRODUCTION

The spontaneously occurring gene mutation in the mouse causing *Small eye* (*Sey*) was first discovered by R. C. Roberts spontaneously in Edinburgh in 1967 (Roberts, 1967). The gene is allelic to the aniridia gene in the human, and has been mapped subsequently to chromosome 2 in the mouse (Hogan et al. 1986, 1988; Jong et al. 1990; Hill et al. 1991; Ton et al. 1992). Also located on the same chromosome are other genes known to cause developmental abnormalities of the eye. These include *Ocular retardation* (or^{J}), *Dickie's small eye* (*Dey*) and *coloboma* (*Cm*) (Theiler et al. 1976, 1978, 1980; Theiler & Varnum, 1981). These are semidominant genes except the *Ocular retardation* gene which is recessive. Homozygous *Small eye* (*Sey/Sey*) embryos develop to term but do not develop either eyes or nose, and die soon after birth because of the breathing problems associated with the absence of the nose (Hogan et al., 1986). The *Sey* mutation is believed to restrict its effect to the growth and differentiation of the lens placode and nasal placode, and it is the failure of the former to develop normally that has secondary consequences on the rest of the ocular apparatus in both the homozygous in particular and, but to a considerably lesser degree, the heterozygous state.

It is the eyes that are mainly affected in the heterozygous mutant *Sey* mice (Hogan et al., 1986). Abnormalities of the eyeball associated with the presence of the mutant gene, when in the heterozygous state, include microphthalmos often associated with cataracts, partial or complete absence of the iris, absence of the lens and retinal abnormalities (Jong et al. 1990). No evidence is yet available to indicate whether the gene exercises its ocular effect on the eyeball and its contents alone, or influences, either directly or indirectly, the development of the optic nerve and other parts of the visual system; and, if the optic nerve is affected, to what extent. The aim of the present study was to establish whether the presence of the Sey gene influences the development of the optic nerve, and to attempt to quantify the extent of the influence in relation to the parameters of the optic nerve measured.

4.2 MATERIALS AND METHODS

Eleven week old normal (i.e. +/+) and heterozygous mutant *Sey* mice (i.e. *Sey*/+) of both sexes were studied. A total of 5 mice of each sex of normal, and 8 females and 5 males of heterozygous mutant *Sey* mice were used. Because of the low breeding rate of the *Sey* mice the required number of mice in each group was obtained from more than one litter. Each animal was weighed to determine the dose of anaesthetic it was to be given. The animal was then deeply anaesthetised by an intraperitoneal injection of 0.02 ml/g body weight of a 1.2 % solution of tribromoethanol (Avertin) in 0.9% saline. The heart was exposed, and using a 21G needle, intracardiac perfusion was carried out by giving 2.0ml/g body weight of a solution of 2.5 % glutaraldehyde and paraformaldehyde in 0.1 M phosphate buffer as primary fixative through the left ventricle while the heart was still beating. The whole length of the optic nerve was immediately, but carefully, dissected out avoiding traction on the nerve. The nerves from each animal were then processed for light and electron microscopy as has been described for the adult inbred mice and their F_1 hybrid (see 3.2 above). The data obtained were similarly used for the statistical analysis of the parameters of the optic nerve in the *Sey* mice.

4.3 RESULTS

4.3.1 CROSS-SECTIONAL AREA (μm^2)

The optic nerve, which had well defined meningeal coverings in both the normal (+/+) and the heterozygous mutant (*Sey*/+) mice, could be dissected from the eyeball to the optic chiasma. One nerve from the male series of each group of mice was lost during the course of dissection. The optic nerves from the *Sey* mice were generally small in size (Figure 4.1). In the male series of both normal (+/+) and heterozygous mutant (*Sey*/+) groups of mice, the left optic nerve had a higher mean csa than the right. This was also the case with the female series of the heterozygous mutant (*Sey*/+) mice, but the left optic nerve of their normal female (+/+) littermates had a lower mean csa than the right. The statistical analysis of these results showed no significant difference in the csa of the nerve between the left and the right optic nerves of either sexes of each of the two groups of mice. For this reason the sample size for each sex in each of the two groups of mice was pooled for the purpose of the statistical analysis of the mean csa for each sex (Table 4.1). The female heterozygous mutant (*Sey/+)* mice significantly differed from their male littermates with respect to their csa ($P < 0.05$). In the normal (+/+) series no significant difference was observed between the two sexes in their csa. The inter-group comparison of the csa between corresponding series revealed a significant difference between heterozygous mutant (Sey/+) males and normal (+/+) males ($0.01 < P < 0.05$). No such difference was seen between females of the two groups of mice with regard to their csa (see Tables 4.2).

Figure 4.1: Toluidine blue stained semithin transverse sections of the optic nerve of the different groups of normal (+/+) and heterozygous mutant (*Sey*/+) mice (scale factor applied as for Figure 2.1). The optic nerve shows a normal configuration with a well defined dural sheath. The nerve is, however, relatively small in calibre. The nerves from the heterozygous mutant (*Sey/+)* groups are generally smaller than their normal (+/+) littermates.
a) Normal (+/+) male.
b) Heterozygous mutant (*Sey*/+) male.
c) Normal (+/+) female.
d) Heterozygous mutant (Sey/+) female.

Figure 4.1

Group/Sex of mouse		Mean cross-sectional area (μm^2) (± s.e.m.) L or R	L+ R
Normal (+/+) Male (n* = 9)	L	49464±5335	
			49397±425
	R	49343±6932	
Female (n* = 10)	L	42154±4867	
			43996±2571
	R	45838±257	
Heterozygous Male (n* = 9) mutants (*Sey*/+)	L	34411±4968	
			33179±2778
	R	31636±1897	
Female (n* = 16)	L	41985±2420	
			40535±1685
	R	39085±2387	

Table 4.1 Optic nerve cross-sectional area for normal (+/+) and heterozygous mutant (Sey/+) adult mice. n* = number of optic nerves analysed, s.e.m. = standard error of mean.

Normal (+/+) male (n* = 9)			
n.s.	Normal (+/+) female (n*= 10)		
(0.01 < P < 0.05)	xxxxxxxx	Mutant (Sey/+) male (n* = 9)	
xxxxxxxx	n.s.	(0.01 < P < 0.05)	Mutant (Sey/+) female (n*= 16)

Table 4.2 Level of significance between nerve fibre bearing cross-sectional areas of optic nerve of normal (+/+) and heterozygous mutant (*Sey*/+) adult mice. n* = number of optic nerves analysed; n.s., no significant difference.

4.3.2 TOTAL MYELINATED NERVE FIBRE COUNTS

In all groups of adult mice studied, unmyelinated nerve fibres were very rarely encountered (Figure 4.2). The statistical analysis of the mean myelinated nerve fibre counts showed that although the population of fibres within the nerve decreases from centre to periphery, this regional difference in the distribution of nerve fibres was not significant. In the normal (+/+) groups the mean nerve fibre count for the left optic nerve of the males was higher than the right, but in their female littermates the mean nerve fibre count for the left optic nerve was lower than the right. In the heterozygous mutant groups, the right optic nerve in the males had a higher mean nerve fibre count than the left whereas, among the females, the mean nerve fibre count for the left optic nerve was higher than the right. However, there was no significant difference between the left and the right optic nerve of either males or females of the same group of mice. Because of this, all samples for each sex in each of the *Sey* groups studied were pooled together for the purpose of the statistical analysis of the mean myelinated nerve fibre count (Table 4.3). The mean nerve fibre count for the males of the normal (+/+) series was higher than that of the females whereas, in the heterozygous mutant series, the males had a lower mean nerve fibre count than the females. There was also no significant difference between males and females in each group of mice with respect to the mean myelinated nerve fibre count. The heterozygous mutant *Sey* series consistently had lower values for the mean myelinated nerve fibre count compared to their normal littermates. This difference was significant only between the heterozygous mutant *Sey* males and their normal male littermates ($0.01 < P < 0.05$ - see Table 4.4).

Figure 4.2: TEM (x3000) of ultrathin transverse sections of optic nerve of different groups of adult *Sey* mice to show myelinated nerve fibres within the nerve. Almost all nerve fibres present in each group are myelinated. The overall population of the nerve fibres decreases from centre to periphery. Also the population of small diameter fibres declines from centre to periphery while the reverse phenomenon is the case with the large diameter fibres.
a) Normal (+/+) male.
b) Heterozygous mutant (*Sey*/+) male.
c) Normal (+/+) female.
d) Heterozygous mutant (*Sey*/+) female.

a

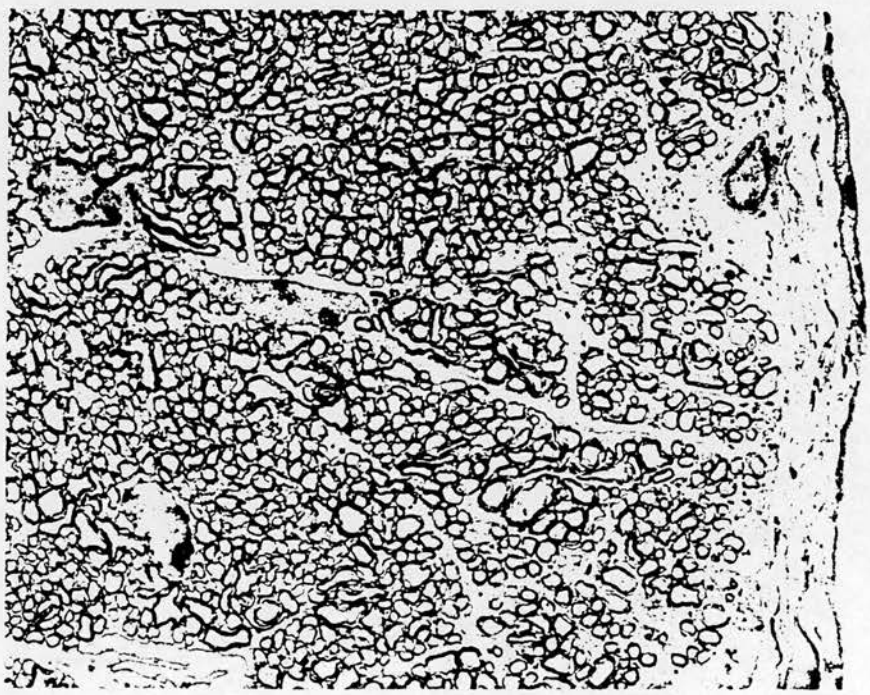

b

Figure 4.2

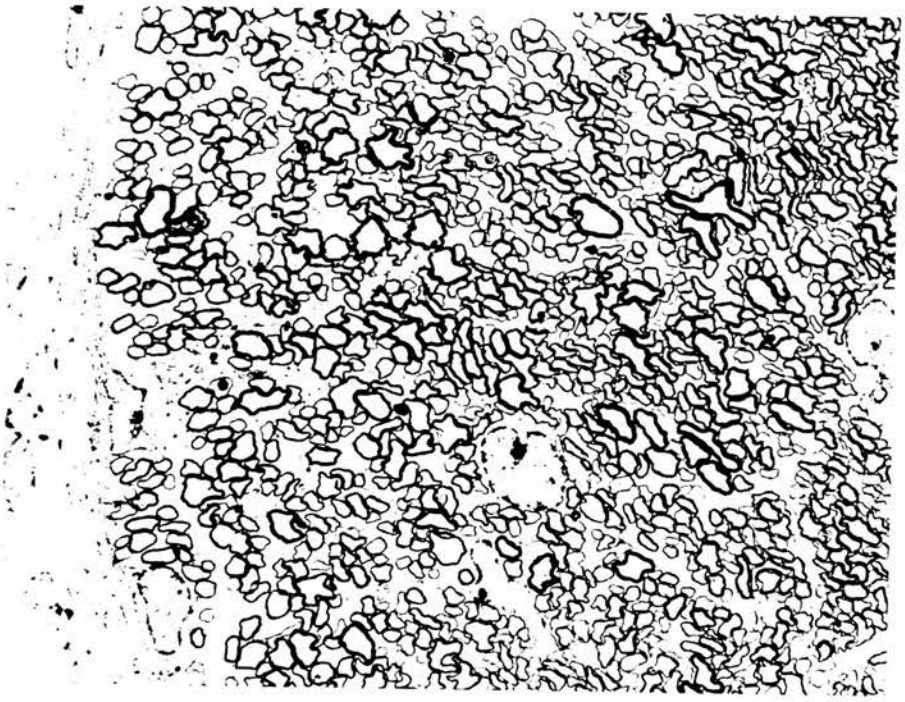

c

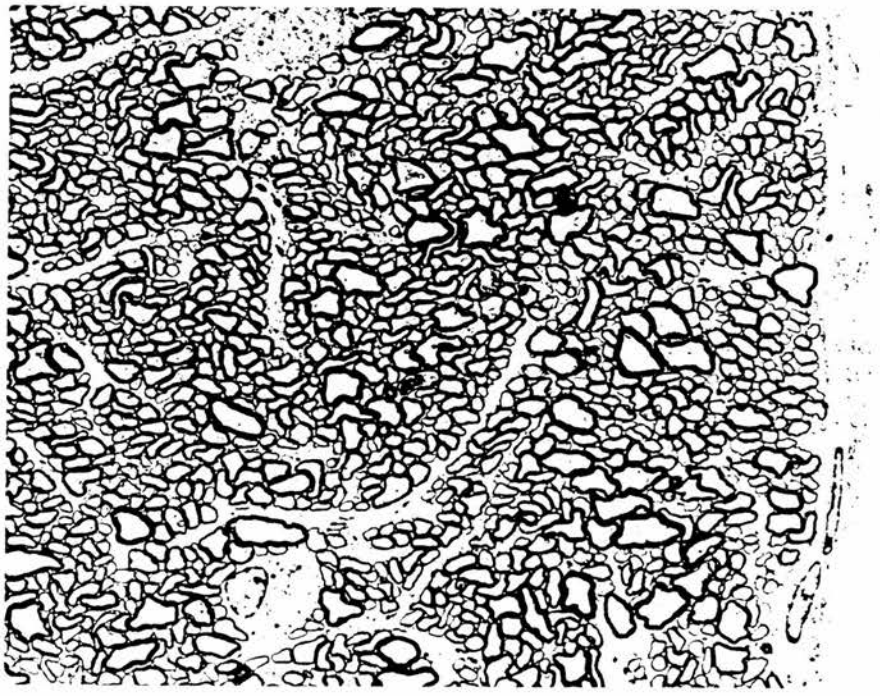

d

Group/Sex of mouse		Mean myelinated nerve fibre count (± s.e.m.) L or R	L+R
Normal (+/+) Male (n* = 9)	L	71392±3394	70021±4886
	R	68924±8836	
Female (n* = 10)	L	61241±8472	62589±4305
	R	63937±3210	
Heterozygous mutants (*Sey*/+) Male (n* = 9)	L	47584±7204	48605±4062
	R	49881±3352	
Female (n* = 16)	L	54943±4190	54558±2856
	R	54173±4161	

Table 4.3 Mean myelinated nerve fibre counts in optic nerve of normal (+/+) and heterozygous mutant (Sey/+) adult mice. n* = number of optic nerves analysed; s.e.m., standard error of mean.

Normal (+/+) male (n* = 9)			
n.s.	Normal (+/+) female (n*= 10)		
(0.01 < P < 0.05)	xxxxxxxx	Mutant (Sey/+) male (n* = 9)	
xxxxxxxx	n.s.	n.s.	Mutant (Sey/+) female (n*= 16)

Table 4.4 Level of significance of difference between mean nerve fibre count of normal (+/+) and heterozygous mutant (*Sey* /+) adult mice. n* = number of optic nerves analysed; n.s., no significant difference.

4.3.3 MYELINATED NERVE FIBRE DENSITY (FIBRES 1000μm^{-2})

The density of the nerve fibres appeared to decrease from centre to periphery, but there was no statistically significant regional difference in density observed. Values for mean myelinated nerve fibre density were generally lower in females than their male littermates. In the normal (+/+) series the left optic nerve was more densely populated than the right. The reverse was the case in the heterozygous mutant (*Sey/+)* series in which the right optic nerve in both sexes was more densely populated with nerve fibres (Table 4.5). None of these intra-group differences was significant. There was no significant inter-group difference either (see Table 4.6).

4.3.4 MYELINATED NERVE FIBRE DIAMETER SPECTRUM

More than 90 % of the myelinated nerve fibres analysed in each group of mice were less than 1.0 μm in diameter, with the largest nerve fibres measured in each group being slightly less than 2.0 μm in diameter. The population of small size fibres decreased from centre to periphery, whereas that of the large fibres increased from centre to periphery. The distribution of the fibres in both groups was unimodal, with a modal diameter of 0.48 μm. In each case, there was a positive skewing of the nerve fibres in favour of the large diameter fibres (see Figure 4.3). Representative electron micrographs which display the appearance of transverse sections through nerve fibres within the optic nerve of normal Sey (+/+) and heterozygous mutant Sey (Sey/+) mice have already been provided in Figure 4.2.

Group/Sex of mouse		Mean myelinated nerve fibre (1000 μm^{-2}) (± s.e.m.) L or R	L + R
Normal (+/+) Male (n* = 9)	L	1470±88	
			1441±75
	R	1417±123	
Female(n* = 10)	L	1437±78	
			1416±41
	R	1395±34	
Heterozygous mutants ((*Sey*/+) 9) Male (n* =	L	1373±114	
			1469±83
	R	1590±109	
Female (n* = 16)	L	1309±69	
			1349±50
	R	1389±74	

Table 4.5 Mean myelinated nerve fibre densities in the optic nerve of normal (+/+) and heterozygous mutant (*Sey*/+) adult mice. n* = number of optic nerves analysed; s.e.m., standard error of mean.

Normal (+/+) male (n* = 9)			
n.s.	Normal (+/+) female (n* = 10)		
n.s.	xxxxxxxx	Mutant (Sey/+) male (n* = 9)	
xxxxxxxx	n.s.	n.s.	Mutant (Sey/+) female (n* = 16)

Table 4.6 Level of significance between mean nerve fibre densities of normal (+/+) and heterozygous mutant (*Sey*/+) adult mice. n* = number of optic nerves analysed; n.s., no significant difference.

Figure 4.3: Graphs showing distribution of myelinated nerve fibres of different fibre diameters within the optic nerve of normal *Sey* (+/+) male and female mice, and heterozygous mutant (*Sey*/+) female and male mice. The distribution is unimodal in all the groups with a modal diameter of 0.48μm. All groups show a positive skewing. The percentage of fibres with the modal diameter is lower in the heterozygous mutant (*Sey*/+) females than in the Normal *Sey* (+/+) females. The reverse phenomenon is true with the males.

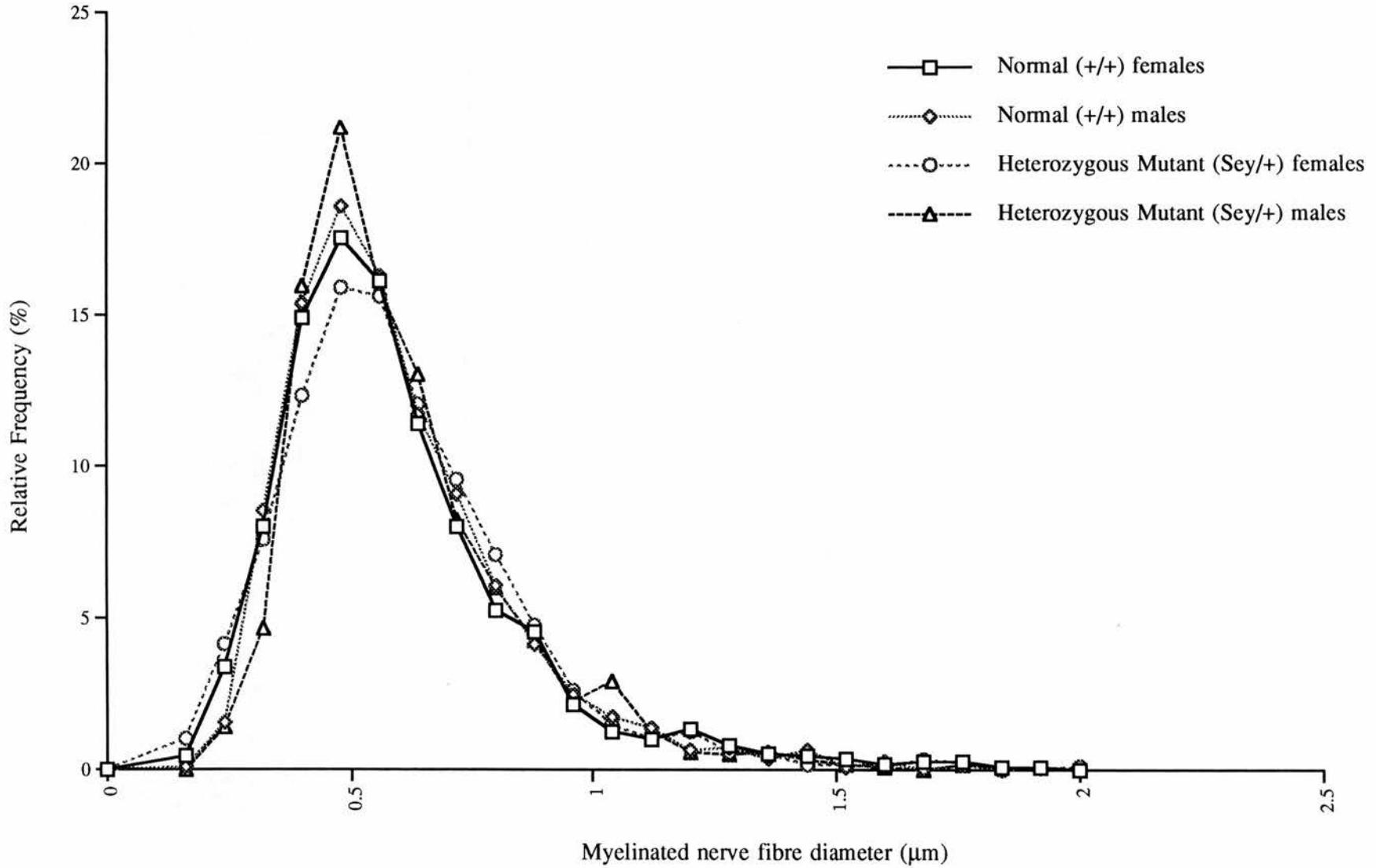
Normal (+/+) females
Normal (+/+) males
Heterozygous Mutant (Sey/+) females
Heterozygous Mutant (Sey/+) males
Relative Frequency (%)
25
20
15
10
5
0
0
0.5
1
1.5
2
2.5
Myelinated nerve fibre diameter (μm)

Figure 4.3

4.4 DISCUSSION

The findings from this study suggest that the influence of the *Sey* gene, in the heterozygous mutant mouse, is primarily on the development of the eyeball, but also extends secondarily to the optic nerve. From earlier studies, other mutant genes have been shown to have a primary effect on the development of the optic nerve in the mouse. Theiler et al. (1976) reported in the gene mutation causing *Dickie's small eye (Dey)* that, besides eyeball abnormalities, there is a direct effect on the formation of the optic stalk resulting in an abnormally folded and hypoplastic optic stalk. Robb et al. (1978) made similar findings in mice homozygous for the *Ocular retardation* gene (or^J), where they found that an aberration of the optic fissure led to the arrest of the development of the optic nerve. This resulted in aplasia of the optic nerve. By day 15 p.c. they found the fissure associated with the optic stalk had closed completely and no axons exited from the eye. The absence of an optic nerve led to the regression of the optic stalk which became a rudimentary cord of cells. In homozygotes of the *Extra-toes* mutant mouse (*Xt/Xt*), Franz & Besecke (1991) observed in some of the mutant embryos an apparent disparity between the eye and the optic nerve, so that some of the embryos showed complete atrophy of the optic nerve. By late stages of gestation, only remnants of the optic nerve were usually seen.

In the *Sey*/+ mice a well developed optic nerve was dissected from each animal, although the diameter was generally of small-calibre. This corresponded well with the small eyeballs generally observed in the heterozygous mutant *Sey*. The presence of a fully developed optic nerve suggests that the gene primarily affects some specific aspect of craniofacial morphogenesis rather than having a generalised effect on many embryonic tissues (Hogan et al., 1988), although it may also exert a secondary effect on the development of some structures such as the optic nerve. The latter appears to be both sex and strain dependent. This is highlighted by the significant difference that was observed in the mean csa and the mean myelinated nerve fibre counts between the male series of both the heterozygous mutant (*Sey*/+) and the normal (+/+) groups of mice involved in the study. Although the

difference in these two parameters between the female series of both groups of mice was not significant, values of the parameters for the heterozygous mutant (*Sey/+)* females were always considerably lower than those of their normal female littermates. The reason for the greater effect of the gene on the heterozygous mutant (*Sey/+*) male mouse compared to their female siblings is, however, not clear.

Earlier reports on the effect of the *Sey* gene on the development of the eye have been mainly concerned with the effect of the gene on the lens and contents of the orbit in the homozygous mutant during the early embryonic period. Little information is available on its effect on the development and contents of the optic nerve in the adult heterozygous mutant mouse. In the homozygous mutant, while an irregularly shaped optic vesicle initially forms, in the absence of an inductive influence from the lens vesicle, it soon degenerates, and no remnant of the optic apparatus beyond the optic chiasma is generally seen (Hogan et al. 1986, 1988). This is similar to the situation seen in the *Ocular retardation* gene (or^J), another mutant involving the eye already cited, when present in the homozygous state (see Truslove, 1962; Robb et al., 1978). Theiler et al. (1976) observed that in the adult (*or/or*) mutant, where the *or* gene was believed to be allelic but not identical to the or^J gene, small eyes are present with closed lids. This was associated with abnormalities of the retinal layers and absence of the optic nerve, the latter being replaced by a thin layer of connective tissue.

Robb et al. (1978) observed that in normal (+/+) *Ocular retardation* mice, by day 14.5 p.c. the eyeball increases in volume and the optic nerve increases in diameter as a result of the differentiation of large numbers of ganglion cells within the neural retina which send axons to the brain. This is in contrast to the situation in homozygous or^J mutant mice of about the same age, where they observed that despite the presence of a substantial retinal neuroblastic layer in which it was difficult to distinguish ganglion cells and nerve fibres, no axons exited from the eye. Furthermore, they suggested that another factor that might have induced

regression of the optic stalk was the absence of vascularisation of the optic nerve (Robb et al. 1978).

In the homozygous mouse mutant *extra-toe* (X^t /X^t), Franz & Besecke (1991) observed that the optic nerve was either completely absent or at most only partly developed. No explanation is yet available, however, for the variable phenotype observed in the (X^t /X^t) mice, nor has the developmental mechanism that leads to the ocular pathology seen in these mice yet been established. Theiler et al. (1978, 1980), in their work on *Dickie's small eye (Dey)* found that the morphogenesis of the eye in the heterozygous mutant animals was delayed compared to that observed in controls on day 12 p.c. This apparent lagging in development generally starts between day 10 and 11 p.c. though, in some instances, it was observed as early as day 7 p.c. and was invariably noted by day 12 p.c. The ocular abnormalities noted in adult (*Dey*/+) heterozygotes were small eyes with coloboma, small or absent lens, with cataract if present, abnormal folding of the retina and reduction in the pigment layers, with often absence of the anterior chamber. Homozygotes invariably die during the early postimplantation period, often at the egg cylinder stage.

The normal development of the eye in the mouse begins with the invagination of the central region of the optic placode to form the optic pit and its progressive differentiation, in association with cephalic neurulation, to form the optic vesicle. This forms from the neuroepithelium in the diencephalic region of the forebrain during day 8-9 p.c. By about day 9.5 p.c., an optic stalk is present and the optic cup has begun to indent, while between about day 9.5-11 p.c., the lens placode indents to form the lens pit and subsequently differentiates to form the lens vesicle. This then separates from the surface and progressively indents the optic cup so that it is now seen to have an inner and an outer layer which are destined, respectively, to form the neural and pigment layers of the retina (Kaufman, 1979, 1992; Rugh, 1990).

The normal process of ocular development is believed to be influenced by the process of embryonic induction by which regions of the anterior head ectoderm become progressively specified as the presumptive optic apparatus. Similar mechanisms are believed to be involved with regard to the differentiation of the nasal placode. The mechanism of embryonic induction may itself be affected by gene mutation (Jong et al., 1990). Direct contact between the neuroepithelium of the optic vesicle and the overlying surface ectoderm is believed to be a necessary prerequisite for the induction of the lens placode (Bard, 1990). Other factors that influence normal morphogenesis include programmed cell death (apoptosis) and cell resorption, the appropriate location of component tissues at the time of cell-cell interaction, and the availability of an adequate blood supply (Truslove, 1962; Silver & Hughes, 1974; Silver & Robb, 1979; Perry et al., 1983). In the optic stalk, cell death and cell resorption allow access for the ingrowing nerve fibres that exit from the neural retina with the eventual formation of the optic nerve, while the blood supply that facilitates the nutrition of this process mainly comes from the hyaloid vessels. Truslove (1962) observed that in both normal and homozygous mutant (or^J/or^J) mice the blood supply was adequate up to day 11 p.c., but from day 12 p.c. the choroid fissure in the mutant mice gradually became obliterated. A progressive reduction in the size of the eyeball was then apparent, and this was eventually followed by the resorption of the optic stalk. When an inadequate blood supply was observed in this mutant strain of mice, this was generally associated with the failure of the optic vesicle to form a proper cup. The relationship between these two events, however, is not entirely clear.

The presence of the *Sey* gene in the homozygous state is believed to interfere with the normal mechanism of embryonic induction necessary for the development of the lens vesicle (and nasal apparatus), and results in the formation of a smaller lens vesicle than normal in the heterozygous mice bearing this mutation. Although it is the lens that is primarily affected, there appears to be a consequential effect on other components of the eyeball, as well as secondary effects on the optic nerve. Had the effect of the *Sey* gene (in the

heterozygous mutants) been primarily on the development of the optic nerve, through a failure of optic vesicle and stalk formation, then it is likely that a similar effect to that seen in the or^{J} mutant would have been observed (Truslove, 1962).

It is logical that, since nerve fibres from the neural retina are directed into the optic stalk, the calibre of the optic nerve will necessarily reflect the number of nerve fibres which it contains (Ogden & Miller, 1966; Potts et al., 1972a, b; Hughes, 1977). Such a direct relationship between the calibre of the nerve and its nerve fibres has been demonstrated in this study by the csa and the mean nerve fibre count. Despite the presence of a significant difference in both mean csa and mean nerve fibre counts between the normal (+/+) male series and their heterozygous mutant (*Sey*/+) littermates, their mean nerve fibre densities, which reflect the actual relationship between calibre and the number of nerve fibres of a nerve, were not significantly different. The distribution of nerve fibres within the nerves was similar in both normal and heterozygous mutant series. This was demonstrated by the similarity of the nerve fibre diameter spectrum in both sexes of both groups of mice, with each having a modal diameter of 0.48 μm. Not surprisingly, if the overall size of the neural retina is reduced, as it is in the heterozygous mutant *Sey* mice, then the diameter of the optic nerve is also likely to be smaller than that of its normal littermates.

The similarity in myelinated nerve fibre diameter spectrum as well as the mean myelinated nerve fibre densities between the normal and the heterozygous mutant *Sey* mice is an indication of the fact that myelinogenesis is not affected by the *Sey* gene. Myelinogenesis itself does not occur in the optic nerve of the mouse before the 5th day of postnatal life (Gyellensten & Malmfors, 1963; Gyellensten et al. 1966), and this is well after the process of embryonic induction. It would seem that the primary inhibitory effect of the gene is on the induction of the lens vesicle, and this indirectly affects the size of the eyeball and the calibre of the optic nerve, but does not appear to influence to any degree retinal differentiation or myelinogenesis of the nerve fibres within the optic nerve. Mylinogenesis in the *Sey* mice

does not appear to lag behind that observed in normal strains of mice. This is evident in the density of myelinated nerve fibres in the normal and *Sey*/+ groups of mice which are also comparable with that observed in F_1, C57BL and CBA strains of mice of the same age (See 3.4 above; also see Dangata et al., 1995).

The *Sey* gene is believed to be analogous to the human aniridia gene (Glaser et al., 1990). In the mouse, the effect of the mutant gene in the homozygous state primarily causes inhibition of the inductive mechanism necessary for the formation of the lens vesicle (Harch et al., 1978). In the heterozygous state, it influences the overall size of the eyeball and its component structures such as the iris and retina, while any effect on the optic nerve is likely to be secondary to that on the eye. Optic nerve hypoplasia which is observed in about 75 % of aniridic patients is believed to be a consequence of poor macular and/or retinal development. These effects of the gene on the development of the eye in the human manifest themselves in a variety of ways. A reduction in the size of the iris leads a propensity to narrow angle glaucoma. The reduced visual acuity and nystagmus observed have been attributed to macular hypoplasia rather than being due to abnormalities of the iris (Hittner, 1989). Histological findings in the human include hypoplasia of the iris, absence of trabecular meshwork and Schlemm's canal (Hittner, 1989). From the results obtained for the myelinated nerve fibre spectrum and density for the *Sey* mouse in this study, it appears that the hypoplasia of the optic nerve observed in heterozygous mutant *Sey* mice is unlikely to have resulted from primary retinal dysgenesis. It is likely to be secondary to a smaller total number of ganglion cells present in the neural retinal resulting from an overall reduction in the size of the eyeball, which itself is a consequence of the inhibitory effect of the *Sey* gene on embryonic induction.

CHAPTER FIVE

CHANGES IN MORPHOMETRIC PARAMETERS OF THE OPTIC NERVE IN (C57BL x CBA) F_1 HYBRID MICE DURING POSTNATAL DEVELOPMENT.

Contents

5.1 Introduction

5.2 Materials and Methods

5.3 Results

5.3.1 Cross-sectional areas (μm^2)

5.3.2 Total myelinated nerve fibre counts

5.3.3 Myelinogenesis in relation to general growth of the optic nerve.

5.3.4 Myelinated nerve fibre density (fibres $1000\mu m^{-2}$)

5.3.5 Myelinated nerve fibre diameter spectrum

5.4 Discussion

5.1 INTRODUCTION.

Many studies have been carried out to analyse the postnatal development of the optic nerve in different animal species including man (Sylvester & Ari, 1961; Dolman et al., 1980; Balazsi et al., 1984; Repka & Quigley, 1989; Day, 1990), the rat (Kuwabara, 1975; Skoff et al., 1976a, 1976b; Tennekoon et al., 1977; Lam et al.,1982; Perry et al., 1983) and the guinea pig (Langford & Sefton, 1992). The majority of studies undertaken in mice have been concerned with the prenatal morphogenesis of the eye, rather than with the detailed analysis of its component parts, such as the optic nerve (Truslove, 1962; Pei & Rhodin, 1970; Robb et al., 1978; Theiler et al., 1980; Theiler & Varnum, 1981; Franz & Besecke, 1991).

Both Gyllensten & Malmfors (1963) and Gyllensten et al. (1966) studied the postnatal development of the optic nerve in C57BL mice, though these reports were not primarily concerned with the normal postnatal development of the optic nerve in this strain. Furthermore, they analysed only a few age groups of mice. In their controls, Gyllensten & Malmfors (1963) observed only unmyelinated fibres at 5 days of age, after which time myelinogenesis progressed at a slow rate until the 15th postnatal day when it progressed rapidly up to the 20th day. Little increase in myelinogenesis was then observed up to the 30th day, after which time there was no further increase in the number of myelinated nerve fibres present. The majority of myelinated fibres had a diameter of less than 1μm. No unmyelinated fibres were observed in their adult mice. In a subsequent control study, Gyllensten et al. (1966) observed a significant increase in the csa and total number of myelinated nerve fibres present between 2 and 4 months of age, followed by a slight decrease in both parameters between 4 and 7 months of age. Growth of the nerve continued well into adulthood.

The findings from other species have been quite variable. Sylvester & Ari (1961) demonstrated that the human optic nerve increases maximally in size during the first year and continues to do so, though with diminished velocity, up to the 4th year. These findings

are in general agreement with those of Todd et al. (1940). Dolman et al. (1980; see also Balazi et al., 1984) also reported a marked decrease in the rate of growth of the optic nerve between the 4th and the 12th year, with adult size being attained between the 12th and 15th years.

The principal aim of this component of the study was to establish baseline morphometric information on the postnatal developmental parameters of the optic nerve in the mouse, as relatively little information is available on this topic in the literature. Furthermore, such baseline information was necessary for subsequent teratological studies on this strain of mice. The optic nerve was carefully dissected from different age groups of both immature and adult F_1 hybrid mice under deep general anaesthesia. The cross-sectional area (csa), total myelinated nerve fibre population, their mean density and fibre size spectrum was then determined. Information from this study has allowed me to document the scenario of events with regard to the morphometric parameters of the optic nerve in the mouse during the postnatal development and to make a comparison between the optic nerve in the F_1 hybrid mouse with that of other species that have also been studied.

5.2 MATERIALS AND METHODS.

Different age groups of a range of immature and adult (C57BL x CBA) F_1 hybrid mice were studied. The objective was to ensure that as much information as possible during the early stages of postnatal development of the optic nerve in the mouse was obtained as events during this stage of postnatal development occur with such rapidity that they could be missed; the entire period of postnatal development of the optic nerve in this species was included in this study. This was to be achieved by the use of a wide age range of animals, with an age group interval that widened with advancement in postnatal development. The increasing age group interval was guided by the fact that events at later stages of development occur with less rapidity than at the early stage and are unlikely to be missed within a reasonable spacing of the age group interval.

Five mice regardless of sex (see chapters 3 & 4 as well as Dangata et al., 1994 & 1995), each at 2 weeks, 3 weeks, 5 weeks, 9 weeks, 16 weeks and 24 weeks of age were studied. Each animal was weighed and deeply anaesthetised by an intraperitoneal injection of 0.02ml/g body weight of 1.2% solution of Avertin in 0.9% saline. In the adult mice, the heart was exposed and, using a 21G needle, perfusion was carried out by giving 2.0ml/g body weight of a 2.5% solution of glutaraldehyde in 0.1M phosphate buffer through the left ventricle while the heart was still beating. Immature mice were similarly transcardially perfused, though a 23G needle was used to avoid rupture of the left ventricle during the perfusion procedure. The surface of the liver was also excoriated, to avoid a build-up of fixative in the venous part of the circulation. Despite these precautions some of the immature mice could not be adequately transfused with fixative because their interventricular septum was easily ruptured before transfusion was completed. The optic nerves from these poorly fixed mice were excluded from the analysis.

The entire length of the optic nerve was immediately, but carefully, dissected out avoiding traction on the nerve. Both optic nerves from each animal were put into the same prelabelled

bottle containing the fixative and left for a total of 12 hours. The nerves were then washed in buffer and transferred into a secondary fixative consisting of 1% osmium tetroxide in 0.1M phosphate buffer for another 2 hours. After this they were processed for light and electron microscopy and the statistical analysis of the data in the various groups of mice was carried out as has already been described in 3.2 above.

In order to determine the approximate age at which myelinogenesis in the optic nerve starts, 2 additional mice each of 9, 8, 7, 6, 5 and 4 days of age were treated as indicated above. Because of the small number of myelinated fibres present in these samples, the mean myelinated nerve fibre count for these age groups could not be estimated by the present sampling technique because a total of less than 150-200 myelinated fibres was present in the selected fields. Additional photomicrographs were taken at 22,000 magnification and printed to a final magnification of x 66,000 in the 4-, 5-, 6-, 7-, 8- and 9-day old mice in order to allow the visualization of any myelin sheaths that could not be seen at the lower magnification.

5.3 RESULTS.

5.3.1 CROSS-SECTIONAL AREAS (μm^2)

An increase in the csa of the optic nerve was noted to occur right through into adult life as shown in Table 5.1. The optic nerves from immature mice were generally characterised by the presence of thick meningeal sheaths which became relatively thinner with age as shown in Figure 5.1. The increase in the csa progressed rapidly early in life up to the 5th week with maximum rate of increase occurring between the 2nd and the 3rd weeks. From the end of the 5th week the rate of growth in the csa progressively declined with age. The csa continued to increase throughout the postnatal period examined.

Age (Weeks)	Mean cross-sectional area (μm^2) (±s.e.m.)
2	36123±2319 (10)*
3	42560±3576 (10)*
5	50085±1397 (9)*
9	62115±2322 (10)*
16	67107±1689 (9)*
24	71270±2986 (10)*

Table 5.1: Mean cross-sectional area of optic nerve of different postnatal age groups of (C57BL x CBA) F_1 hybrid mice. *total number of optic nerve analysed in parentheses.

Figure 5.1: Toluidine stained semithin transverse sections of optic nerve of different postnatal age groups of optic nerve of (CBA x C57BL) F_1 hybrid mice (scale factor applied as for Figure 2.1). Note that the optic nerves from immature mice were generally characterised by the presence of thick meningeal sheaths which became relatively thinner with age. a): 1 week old, b): 2 weeks old, c): 5 weeks old, d): 16 weeks old.

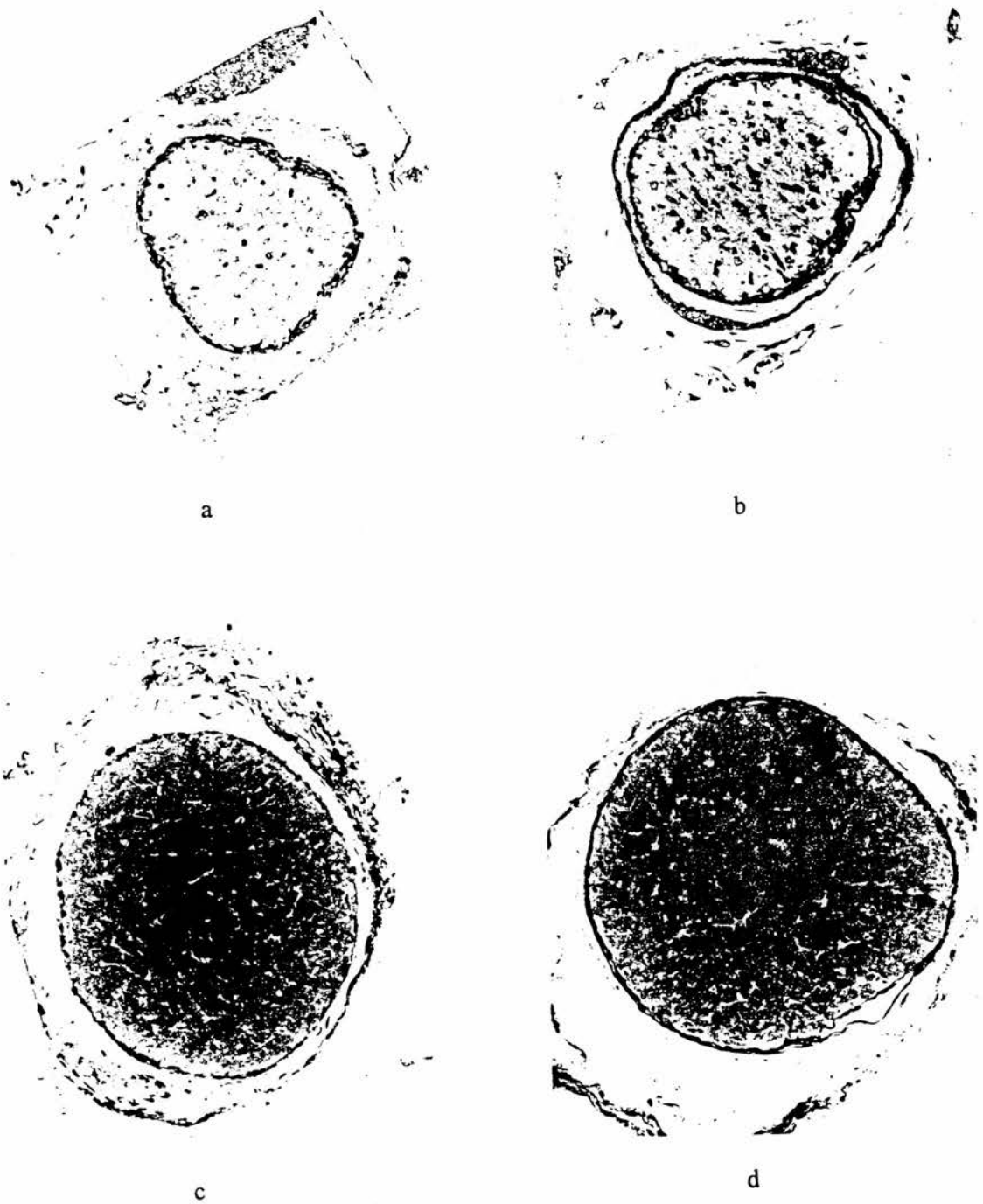

Figure 5.1

5.3.2 TOTAL MYELINATED NERVE FIBRE COUNTS.

By the 5th postnatal day (pnd), no clear evidence of myelinogenesis was observed from the x3000 TEM micrographs. Only at x66 000, was it possible to observe the presence of a few myelin sheaths wrapped around some of the largest fibres (for the purpose of this study myelinated nerve fibres were classed as small, medium and large if they were < 0.3 μm, 0.3-1.0 μm, > 1.0 μm in diameter, respectively). Increasing evidence of myelinogenesis was observed on the 6th and the 7th pnd as shown in Figure 5.2. Although myelinogenesis progressed rapidly once it started, the nerve was initially predominantly populated by unmyelinated nerve fibres up to the third week. Myelinogenesis progressed with such rapidity once it started, that by the 5th week relatively few unmyelinated nerve fibres were seen in the nerve. The peak value for the myelinated nerve fibres was seen at 16 weeks of age. Unmyelinated fibres were rarely encountered at this age. A decrease in the total number of myelinated nerve fibres counted was, however, observed afterwards as presented in Table 5.2. However the decrease which was initially rapid, but tailed off with age, was not significant.

Age (weeks)	Mean myelinated nerve fibre count (± s.e.m.)
2	19706±1474 (10)*
3	35107±3229 (10)*
5	68719±1705 (9)*
9	88087±4896 (10)*
16	94213±1799 (9)*
24	77719±4628 (10)*

Table 5.2: Mean myelinated nerve fibre counts in optic nerve of different postnatal age groups of (C57BL x CBA) F_1 hybrid mice. *total number of optic nerves analysed in parentheses.

Figure 5.2 Representative transmission electron micrographs (x66,000) (trnasverse sections) showing onset, progression and completion of myelinogenesis in the optic nerve of (C57BL x CBA) F_1 hybrid mice during their postnatal development.

a). A section through the optic nerve of an F_1 hybrid mouse isolated on the 6th pnd. Note the presence of a single layer of myelin sheath around the largest diameter axon.

b). A section through the optic nerve of an F_1 hybrid mouse isolated at the end of the 2nd week of postnatal life showing progression of myelinogenesis. The myelinated fibres are predominantly associated with the larger diameter axons. There is an increase in both the overall diameter of the myelinated nerve fibres and the number of turns of myelin sheath that wraps around them. The optic nerve is still predominantly populated by unmyelinated nerve fibres.

c). A section through the optic nerve of an F_1 hybrid mouse isolated at 5 weeks postnatal life. Myelinated nerve fibres have already dominated the nerve fibre population of the nerve and the spectrum of myelinated fibre diameter becomes broader.

d). A section through the optic nerve of an F_1 hybrid mouse isolated at 16 weeks postnatal life showing myelinated nerve fibres at peak level of myelinogenesis. Unmyelinated fibres are only exceptionally rarely seen at this stage. The myelinated nerve fibres present in the nerve at this stage show a broad fibre diameter spectrum.

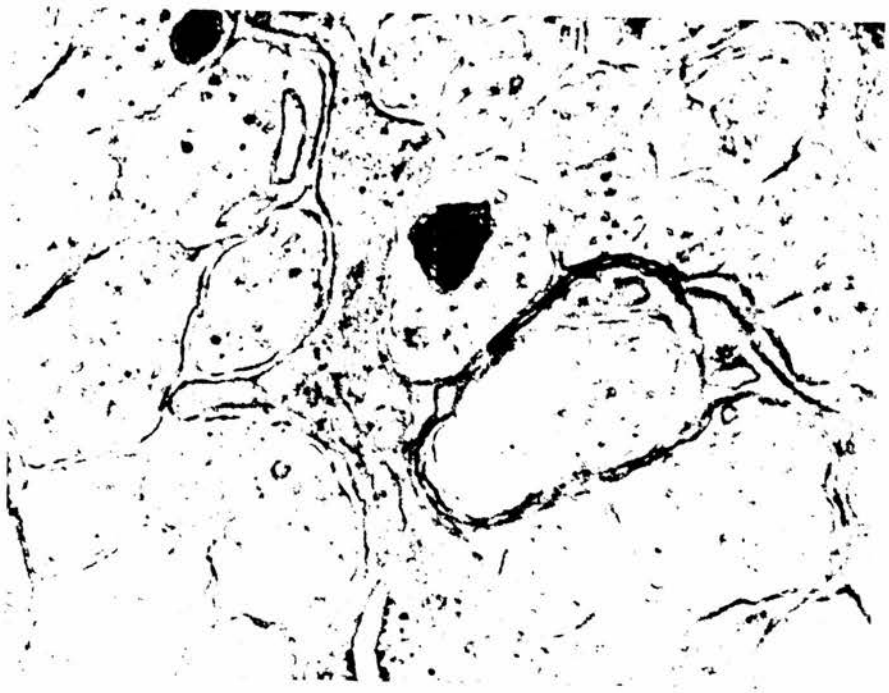

a

b

Figure 5.2

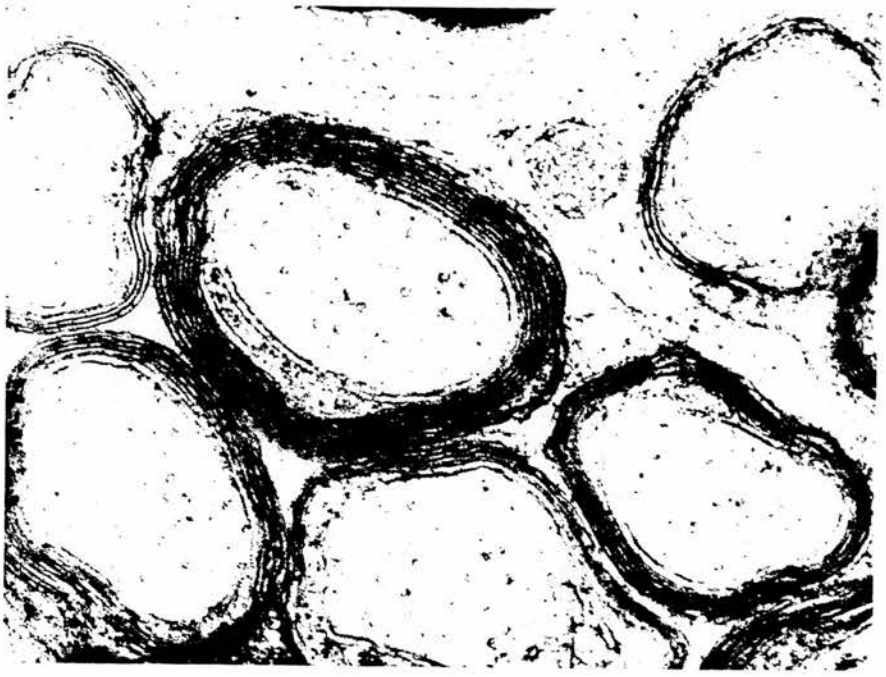

c

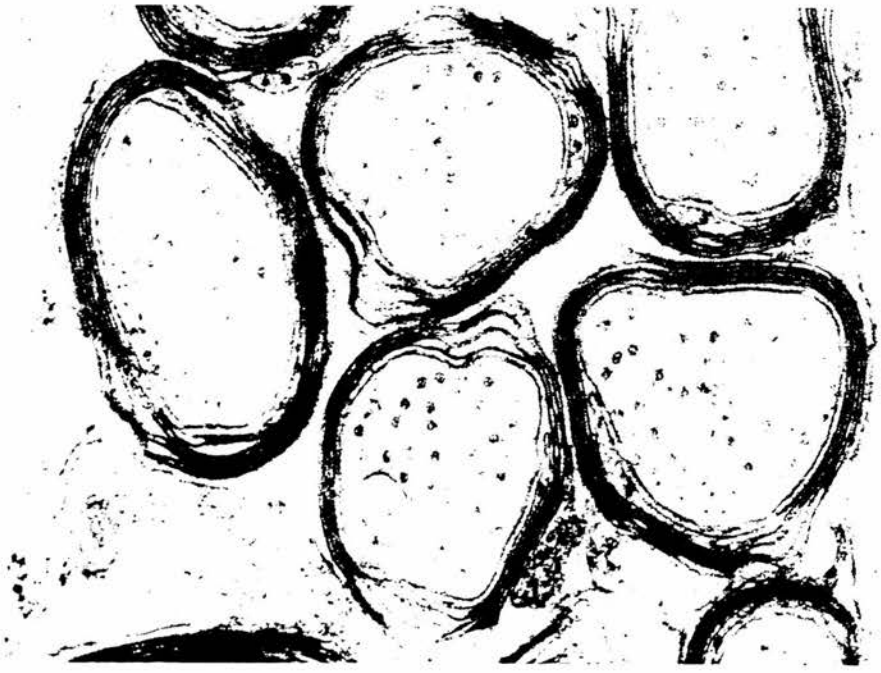

d

5.3.3 MYELINOGENESIS IN RELATION TO THE GENERAL GROWTH OF THE OPTIC NERVE.

The degree of myelinogenesis paralleled the general growth in the calibre of the optic nerve, although even after myelinogenesis was completed by the 16th week of postnatal life, the nerve continues to increase in diameter. As has already been reported both processes occur very rapidly during the early period of postnatal life with the rate of growth levelling out in each case after the 5th week of life. However, myelinogenesis proceeds at a faster rate than the general growth in the calibre of the nerve as shown in Figure 5.3.

5.3.4 MYELINATED NERVE FIBRE DENSITY (FIBRES 1000 μm^{-2}).

There was a very rapid increase in mean myelinated nerve fibre density up to the 5th week of age. This was followed by a progressive, but slower increase in density until highest density levels were achieved at an age which corresponded to the time when the maximum number of myelinated nerve fibres was observed in the nerve. A fall in the mean myelinated nerve fibre density was observed after this as presented in Table 5.3.

Age (Weeks)	Mean myelinated nerve fibre density (fibres $1000\mu m^{-2}$) (±s.e.m.)
2	546±19 (10)*
3	821±22 (10)*
5	1378±40 (9)*
9	1410±30 (10)*
16	1410±41 (9)*
24	1087±35 (10)*

Table 5.3: Mean myelinated nerve fibre density in optic nerve of different postnatal age groups of (C57BL x CBA) F_1 hybrid mice. *total number of optic nerves analysed in parentheses.

Figure 5.3: Graphs showing relationship between csa and mean myelinated nerve fibre counts in optic nerve of (CBA x C57BL) F_1 hybrid mice during postnatal development. The rate of progression of myelinogenesis almost parallels that of growth in the csa of the optic nerve during the juvenile period and early adulthood. Whereas myelinogenesis is completed early in adulthood, the optic nerve continues to grow in size well into the adult life of the mouse, although, with decreasing rapidity with age.

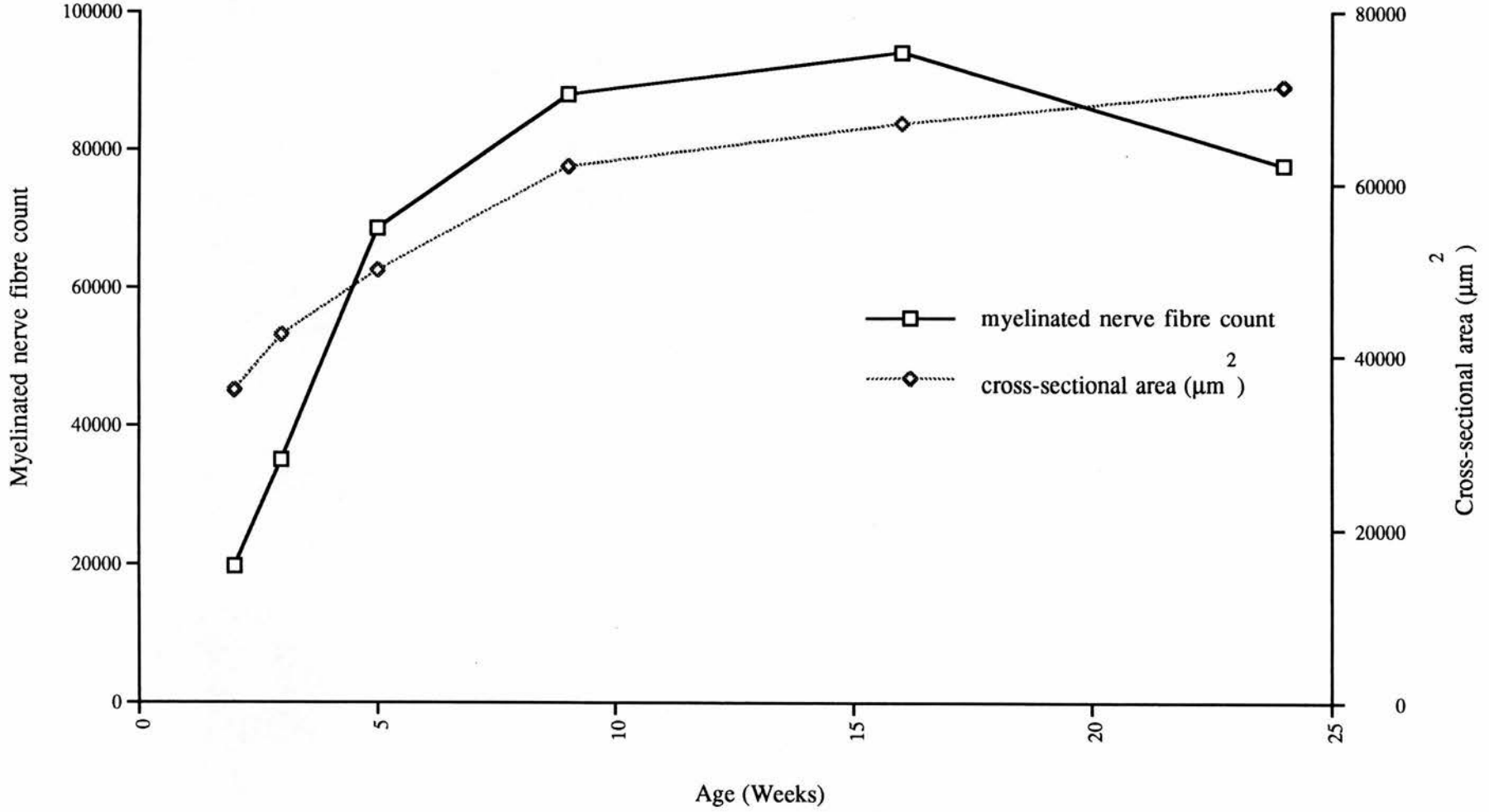
Myelinated nerve fibre count
100000
80000
60000
40000
20000
0
0
5
10
15
20
25
Age (Weeks)
Cross-sectional area (µm 2)
80000
60000
40000
20000
0
myelinated nerve fibre count
cross-sectional area (µm 2)

Figure 5.3

5.3.5 MYELINATED NERVE FIBRE DIAMETER SPECTRUM.

In all age groups no myelinated nerve fibres less than 0.16μm or greater than 1.76 μm in diameter were measured. The nerve fibre diameter spectrum was unimodal in all age groups. The highest modal diameter of 0.64μm was observed in the 2 weeks age group. This rapidly dropped to 0.40μm and was maintained at this value thereafter as presented in Figure 5.4. The largest mean myelinated nerve fibre diameter was observed in the 2 weeks old mice. This mean value dropped to its lowest level by the 5th week as shown in Table 5.4. More myelinated fibres at both extremes of the myelinated nerve fibre diameter spectrum were measured with age, and this feature was more marked in those with a larger fibre diameter. For example, the smallest fibres measured were 0.16μm in diameter, and this was after the 2nd week, with the largest fibres measured having a diameter of 1.76 μm, and this was observed in the 16 weeks age group.

Age (weeks)	Mean nerve fibre diameter (μm) (± s.e.m.)
2	0.67±0.03 (10)*
3	0.59±0.01 (10)*
5	0.55±0.01 (9)*
9	0.58±0.01 (10)*
16	0.57±0.02 (9)*
24	0.63±0.02 (10)*

Table 5.4: Mean myelinated nerve fibre diameter in optic nerve of different postnatal age groups of (C57BL x CBA) F_1 hybrid mice. *total number of optic nerves analysed in parentheses.

Figure.5.4: Graphs showing myelinated nerve fibre diameter spectrum in optic nerve of (CBA x C57BL) F_1 hybrid mice during postnatal development. Note the drop in the modal diameter to a relatively constant value that was maintained throughout after the second week. The distribution of the nerve fibres within the optic nerve in all the age groups is unimodal and is skewed in favour of the large fibres.

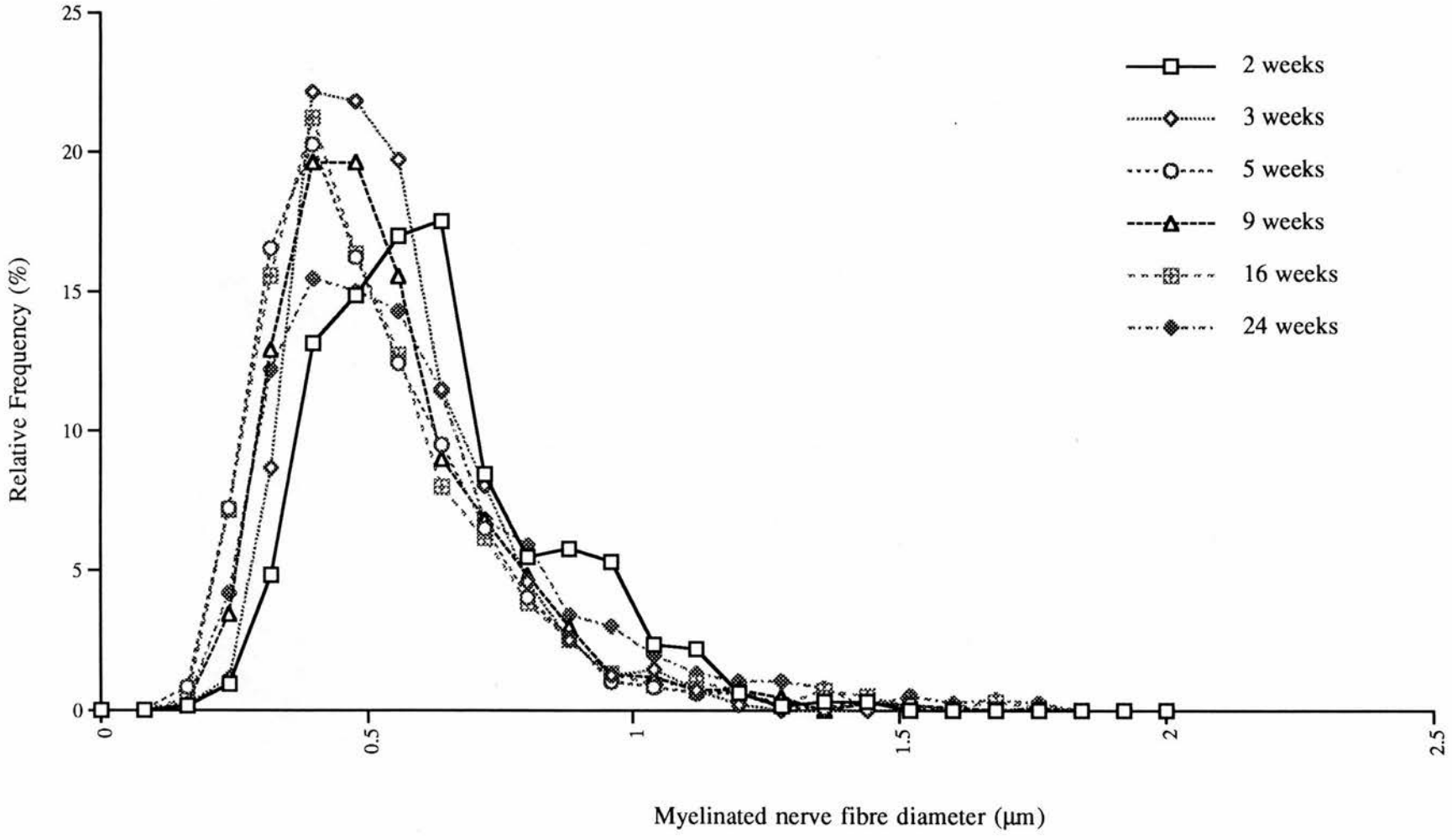
25
20
15
10
5
0
Relative Frequency (%)
0
0.5
1
1.5
2
2.5
Myelinated nerve fibre diameter (µm)
2 weeks
3 weeks
5 weeks
9 weeks
16 weeks
24 weeks

Figure 5.4

5.4 DISCUSSION.

Morphometric analysis of the optic nerve in the mouse has shown that it continues to develop from birth until well into adult life. Growth initially starts rapidly and subsequently slows down as adulthood is approached. The initial period of growth is associated with the first evidence of myelinogenesis within the nerve, and is characterised by a very rapid increase in both the cross-sectional area and the number of myelinated nerve fibres present in the nerve. This phase of growth lasts up to the end of the 5th week of postnatal life, thereafter it progressively slows down with age. During the rapid phase of growth there was over a three-fold increase in the value for mean myelinated nerve fibre count in the nerve at 5 weeks over that observed at 2 weeks. The maximum rate of growth in csa was seen between the 2nd and the 3rd weeks. These findings on the csa of the optic nerve are similar to those of Gyllensten & Malmfors (1963) with respect to their 2 and 4 month age groups, though where a gradual increase in growth after 4 months was observed in the present study, they reported a significant decrease in growth at this time. The explanation for this difference has yet to be determined.

Matheson (1970 , see also Tennekoon et al., 1977), made a similar observation in the rat to that reported here, where they also found that the period of maximum growth occurred within the first three weeks of postnatal life. A second period of growth commences during the fifth week of postnatal life, and lasts well into adult life, though the rate of change in the growth of the nerve during this second period is slower than that observed during the first period, and progressively becomes slower with age. Myelinogenesis within the optic nerve is completed during the second period of growth, though the nerve continues to grow in calibre. Hirose & Bass (1973) also reported that in the rat the period during which there is a maximum growth rate occurred between the 10th and the 20th day of postnatal life, and paralleled the period of maximum myelinogenesis within the nerve. Subsequent growth to the 50th day was slow and continued, but at an even slower rate, thereafter. The findings of these authors indicate that there are close similarities between the postnatal development of

the optic nerve in the rat and the mouse. In both of these species myelinogenesis appears to be an entirely postnatal event (myelinogenesis is first seen in the rat on the 7th postnatal day, see Vaughn, 1969).

In the human optic nerve, Scammon & Armstrong (1925) reported a slight increase in the diameter of the nerve after birth, and they noted that this principally took place during infancy. Others (e.g. Sylvester & Ari, 1961; Dolman et al., 1980) demonstrated that the human optic nerve is small at birth, but grows very rapidly within the first few years. All, however, indicate that the rate of growth of the human optic nerve slows markedly after an initial relatively rapid growth phase during early life, with the adult size being reached between 12 and 15 years of age (see also Balazi, 1984). The relatively small increase in the size of the human optic nerve after birth suggests that a considerable degree of growth takes place during the prenatal period, for the optic nerve head is almost full size at the time of birth (Day, 1990). The initial postnatal growth spurt observed in the mouse may correspond to the period of growth from birth to infancy or early childhood reported in man. Again, what appears to be a slower period of growth in man lasts only to early adolescence, while in the mouse this period extends well into adulthood.

The drop in the mean myelinated nerve fibre count observed after the completion of myelinogenesis, would seem to suggest that a progressive elimination of myelinated nerve fibres was occurring. Nerve fibres in the middle part of the nerve fibre size spectrum appeared to be maximally affected by this fall in nerve fibre count. This may have been a consequence of a greater effect of a degeneration process in relation to these myelinated nerve fibres, and might explain the rise in the proportion of myelinated nerve fibres at the two ends of the nerve fibre size spectrum, as well as a rise in the mean myelinated nerve fibre diameter. During normal development an initial over-production of non-myelinated nerve fibres is followed by a period during which degeneration of both unmyelinated and myelinated fibres occurs (Perry et al., 1983; Ng & Stone, 1982; Provis et al., 1985; Williams

et al., 1986; Langford & Sefton, 1992; Lamantia & Rakic, 1994), so that eventually the adult values are achieved. The initial period of degeneration approximately coincides with the onset of myelinogenesis. In the mouse the reduction in the number of myelinated nerve fibres observed after the period of peak myelinogenesis would suggest that by the time peak myelinogenesis occurs, the optic nerve still has more myelinated axons than is required for normal function, hence, the progression of the reduction process. It should not be surprising that the reduction in the total number of myelinated fibres in the optic nerve of the mouse proceeds after the attainment of peak myelinogenesis, since its general postnatal development proceeds well into adult life.

In the human optic nerve, an apparent over-production of axons occurs principally during the first half of intrauterine life, and this is followed by a loss of about 70% of these axons between 16 and 30 weeks of gestation (Provis et al., 1985; Repka & Quigley, 1989) in order to establish adult values. A second phase of degeneration of myelinated nerve fibres in the normal optic nerve occurs significantly later in life, but does not usually occur before the age of 60 years (Dolman et al., 1980). This second phase of degeneration, however, usually corresponds with the onset of old age, and this is in contrast to the situation in the mouse, described in this study.

In the mouse, large diameter myelinated nerve fibres characteristically dominate the nerve fibre diameter spectrum early in life. This finding would appear to be similar to that occurring in the human optic nerve at different age groups (Repka & Quigley, 1989). However, after the surge of myelinogenesis, the reverse phenomenon was observed in the mouse, where the larger diameter fibres were less frequently encountered with increasing age. The diameter spectrum was relatively narrow during the early postnatal period but broadened with age. This finding is consistent with previous observations reported here (chapters 3 and 4) and those of others, that the optic nerve of the mouse is predominantly populated by small diameter nerve fibres (Gyllensten & Malmfors, 1963; Gyllensten et al.,

1966; Dangata et al., 1994, 1995). The reduction in the mean myelinated nerve fibre diameter observed by the third week would seem to indicate that by this time myelinogenesis predominantly involves the medium size fibres, and that this is maintained until the process is completed. However, the large diameter fibres with which the process started, may continue to acquire additional lamellae of myelin sheath during this period.

Relatively few quantitative studies have been carried out on human optic nerves from different age groups. Those studies that have been undertaken may shed light on why visual function decreases with increasing age in normal individuals (Repka & Quigley, 1989). It is for this reason that appropriate animal models have been used to study both normal and abnormal development of the optic nerve, and may offer the possibility of identifying specific critical phases during its development (Miller, 1992). The mouse has previously been used to study the toxic effects of substances such as cocaine and alcohol (Isenberg et al., 1987; Cook et al., 1987). I believe that I have further shown from the present study that the mouse is also likely to provide a reasonable experimental model system to study age-related conditions of the visual system. Myelinogenesis of the human optic nerve begins at about the 7th month of intra-uterine life (Scheie & Albert, 1977; Mullaney, 1963), and this approximately corresponds to the 5th day of postnatal life in the mouse (Gyllensten & Malmfors, 1963). While the visual system in man is relatively mature and the eye ready to function within a short period after birth, and remains malleable at least for the first decade of life (Mund et al., 1972; Day, 1990), this approximately corresponds to when the surge of activity (2nd-5th weeks) in myelinogenesis during the postnatal development of the optic nerve in the mouse occurs. It is during the early part of this period that the eyelids reopen (Findlater et al., 1993). By this time, over 50% of the fibres in the optic nerve would have been myelinated. This suggests that this is likely to be the minimum number of myelinated nerve fibres required in the optic nerve to establish normal visual function in this strain of mouse.

CHAPTER SIX

MORPHOMETRIC ANALYSIS OF THE PROCESS OF MYELINOGENESIS IN THE OPTIC NERVE OF THE (C57BL x CBA) F_1 HYBRID MOUSE.

Contents

6.1 Introduction

6.2 Materials and Methods

6.3 Results

6.3.1 Onset and progression of myelinogenesis

6.3.2 Myelinated nerve fibre diameter spectrum

6.3.3 Number of myelin lamellae per axon

6.4 Discussion

6.1 INTRODUCTION

Myelinogenesis is the process by which axons become ensheathed with myelin (Williams et al., 1989). Myelin is a lipoprotein multimembrane which becomes tightly packed around an axon, and functions as an insulator to prevent the flow of ion currents across the axonal membrane, thus facilitating the conduction of nerve impulses (Asou et al., 1994, 1995; Umemori et al., 1994). Myelinogenesis in the optic nerve in the mouse and rat is entirely a postnatal process (Gyllensten & Malmfors, 1963; Gyllensten et al., 1966; Vaughn, 1969; Hirose & Bass, 1973; Skoff et al., 1976; Tennekoon et al., 1977; Lam et al., 1982; Perry et al., 1983). In man, by contrast, it starts during the 6th or 7th month of intra-uterine life (Scheie & Albert, 1977; Dolman et al., 1980; Magoon & Robb 1981). Dolman et al. (1980) observed a moderate degree of myelinogenesis in the human optic nerve at 2 months of postnatal life. By the second year the unmyelinated axons became myelinated and those that had already been myelinated acquired more lamellae of myelin which became more closely packed. By the 4th year these became thicker and remained so thereafter.

The optic nerve is the most accessible of the central tracts; this presents unique opportunities for investigators of the central nervous system and for the ophthalmologist (Cohen, 1967). Consequently, extensive studies have been carried out with regard to the analysis of myelinogenesis in this central tract of the rat (Matheson, 1970; Matheson, 1971; Hirose & Bass, 1973; Skoff et al., 1976a & b; Tennekoon et al., 1977; Black et al., 1982; Wiggins et al., 1984). These studies indicate that in this species myelinogenesis starts between the 6th and the 7th postnatal day (pnd). It begins with the large diameter fibres and with increasing age fibres in descending order of size become myelinated until the smallest fibres are myelinated (Skoff et al., 1976b; Tennekoon et al., 1977). The process is associated with the formation of glial cells such as astrocytes and oligodendroglia (Black et al., 1982; Arvanis et al., 1993; Butt & Ransom, 1993; Warrington et al., 1993; Asou et al., 1994 & 1995), the latter being responsible for the initiation and continuation of myelinogenesis at the early stage. Myelinogenesis has also been studied in other central tracts, such as those in the

dorsal funiculus of the spinal cord of the rat, and similar findings have been reported to those observed in relation to the optic nerve (Matthews & Duncan, 1971).

Although the mouse is another commonly used experimental species, few detailed reports are available on the normal events associated with the process of myelinogenesis in its optic nerve. These have mainly been concerned with the postnatal development of this tract (Goldberg & Frank, 1979; Silver & Robb, 1979; Bigbee et al., 1990; Colello & Guillery, 1992). Gyllensten & Malmfors (1963) and Gyllensten et al. (1966) reporting on the process of myelinogenesis in the optic nerve of the C57BL strain of mice in relation to visual function, observed no evidence of myelinogenesis up to the 5th pnd. The reports from these authors were limited in that the age group intervals of the animals studied as well as the method of analysis used did not allow a detailed analysis of the process of myelinogenesis to be made.

In the present study, electron microscopy and an Image Analysis system were used to undertake a detailed morphometric analysis of the normal process of myelinogenesis in the optic nerve of the mouse in order to provide useful baseline morphometric information on myelinogenesis in the optic nerve of the mouse and to compare findings with those observed in other mammalian species. In order to do this the optic nerve from mice of different postnatal ages were analysed to provide a detailed and sequential account of the events associated with myelinogenesis in this species.

6.2 MATERIALS AND METHODS.

The (C57BL x CBA) F_1 hybrid mice were used for this study. Each group of 5 mice was analysed following autopsy at 2, 3, 5, 9 and 16 postnatal weeks. The upper age limit of 16 weeks here was determined by results obtained in an earlier preliminary study in which it was seen to be the age at which the maximum number of myelinated nerve fibres in the developing optic nerve of this strain of mice was observed. In addition, mice at 5, 6 and 7 postnatal days were analysed in order to see the trend of events at the critical period of the onset of myelinogenesis. The lower age limit in this case was also determined by results of the preliminary study already cited as a guide to the age at which myelinogenesis begins in the mouse. The mice were deeply anaesthetised, the optic nerve immediately, but carefully, dissected out avoiding traction on the nerve and processed for both light and electron microscopy as previously described.

In addition, micrographs were taken at a magnification of x 22,000 and printed to a final magnification of x 66,000 in order to estimate the number of myelin lamellae present associated with each nerve fibre within the individual nerves. The number of myelin lamellae present in each nerve fibre for the different nerve fibre profiles of each nerve was determined by counting individual lamellae from these micrographs using the Magiscan. At this magnification the myelin lamellae around each nerve fibre could clearly be visualized. From the figures obtained, the mean number of myelin lamellae for the different nerve fibre profiles for each group of mice was determined, and from this the mean for the group was also determined. In order to observe myelinogenesis in detail at the onset of the process, micrographs from nerves of 5, 6 and 7 day old mice were also taken at x 22,000 and printed to a final magnification of x 66,000.

6.3 RESULTS.

6.3.1 ONSET AND PROGRESSION OF MYELINOGENESIS.

Although evidence of myelinogenesis could be seen as the selective thickening (promyelin- see Discussion) around large fibres by the 5th pnd, definite myelin sheaths were only observed by the 6th pnd, and this became even clearer by the 7th pnd as shown in Figure 6.1. Myelinogenesis starts and progresses very rapidly until the fifth postnatal week after which it progresses at a slower rate to reach a peak by the 16th postnatal week. During the rapid period of myelinogenesis the population of myelinated fibres continued to rise with increasing rapidity so that, by the 2nd week it was possible to estimate their numbers within the nerve, although, at this age unmyelinated fibres predominated. Myelinogenesis was most intense from the end of the 2nd week through to the fifth week. For example, 21%, 37% and 73% of fibres showed evidence of myelinogenesis by the 2nd, 3rd and 5th weeks, respectively as shown in Figure 6.2, indicating that by the fifth week the nerve was predominantly populated by myelinated nerve fibres. After this initial surge the rate of myelinogenesis from the end of the 5th week continued to tail off until the completion of the entire process by the 16th week. By this time unmyelinated fibres were rarely visible within the nerve. This was taken as the time when myelinogenesis was completed. The period from the end of the 5th week to the 16th week accounted for less than 30% myelinogenesis.

Figure 6.1: Representative transmission electron micrographs (x66,000) of transverse sections of the optic nerve of (C57BL x CBA) F_1 hybrid mice at the early stages of myelinogenesis.

(a): Section through the optic nerve isolated on the 6th pnd to show the onset of myelinogenesis. Note the presence of a single layer of myelin sheath around the larger diameter axons.

(b): Section through the optic nerve isolated on the 7th pnd. Both axon diameter and the number of myelin lamellae around the axons have increased, but the myelin lamellae are still loosely wrapped around the axons.

a

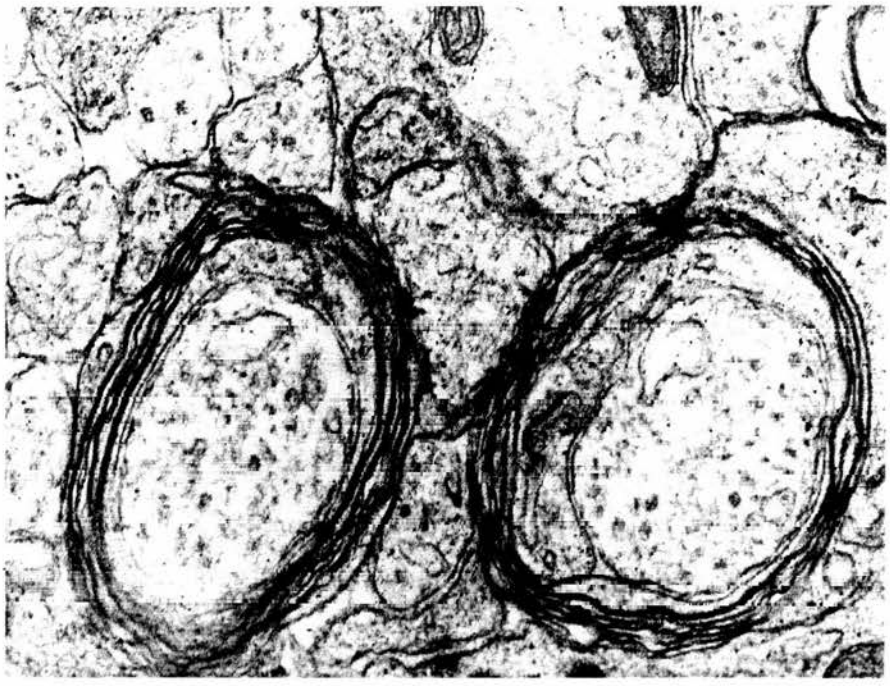

b

Figure 6.1

Figure 6.2: Graph showing progression of myelinogenesis with age in optic nerve of (CBA x C57BL) F_1 hybrid mice. Note that from a pilot study carried out during the first week only evidence of the onset of myelinogenesis was found with approximately 0% myelinogenesis (i.e. only few myelinated nerve fibres present) having taken place. Following the onset of myelinogenesis there is a rapid progression of the process within the first five weeks. Note the slowing down of the rate of myelinogenesis from the end of the 5th week up to the time the process is completed.

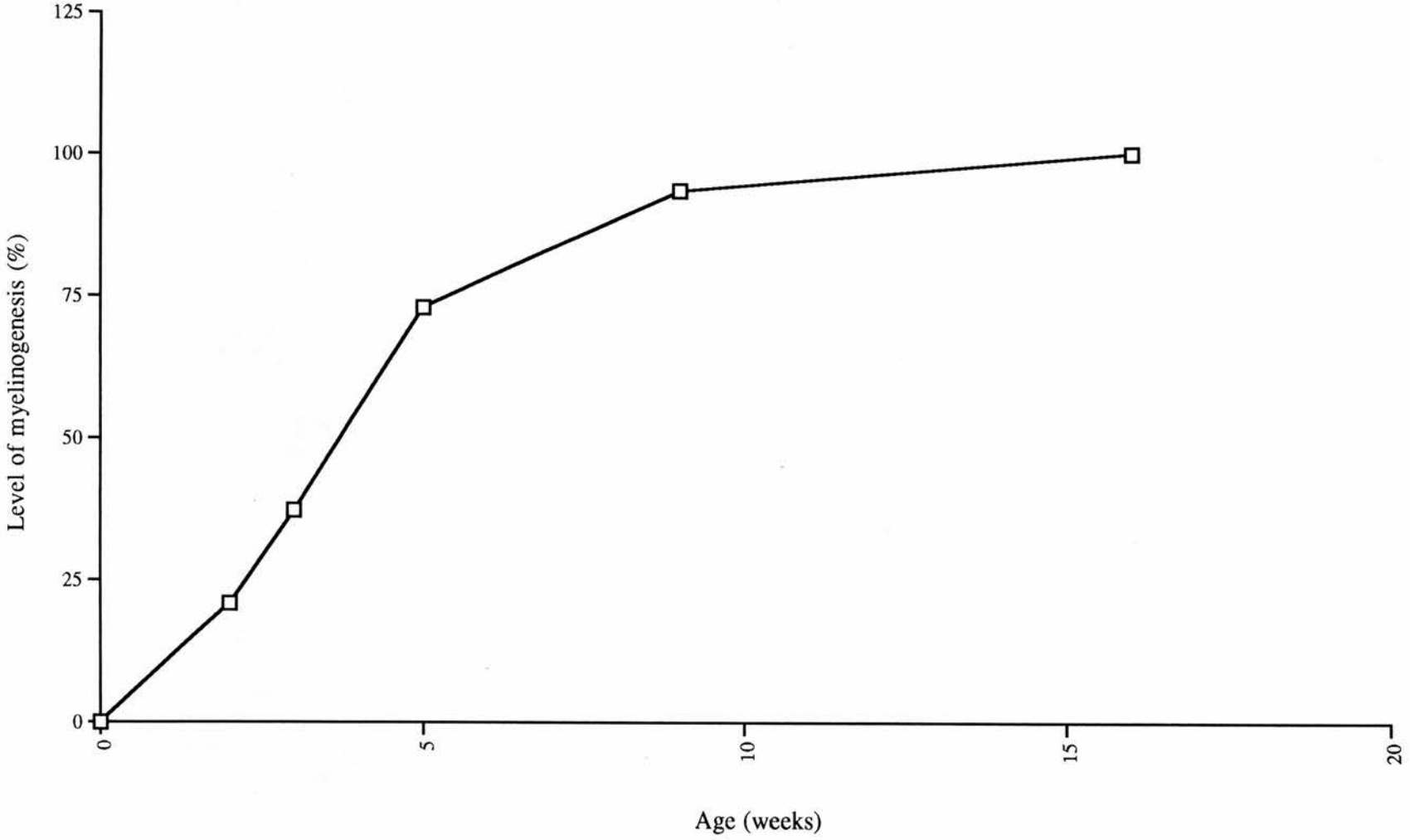
125
100
75
50
25
0
Level of myelinogenesis (%)
0
5
10
15
20
Age (weeks)

Figure 6.2

6.3.2 MYELINATED NERVE FIBRE DIAMETER SPECTRUM.

There was a selective myelinogenesis of the large fibres present in the nerve at the onset. For example, the population of fibres ≥ 1.0μm by the 2nd week was over 16% of the total myelinated fibres in the nerve, compared to < 6% for the same modality of fibres seen at 16 weeks when the process was completed. But before the end of the 5th week, more fibres within the middle part of the nerve fibre diameter spectrum were being myelinated, so that the mean nerve fibre diameter dropped from 0.67±0.03 μm seen early during the 2nd week to 0.55±0.01 μm by the end of the 5th week. From this time on, there was no significant change in this mean diameter as shown in Figure 6.3. The drop in the mean fibre diameter was associated with a corresponding drop in the modal diameter, from 0.64μm at 2 weeks to 0.40μm, and this value was maintained from then onward. All myelinated nerve fibres encountered were between 0.16μm and 1.76μm in diameter and their distribution within the nerve was unimodal for all the ages as shown in Figure 6.4. The spectrum of distribution continued to broaden with age and this was in favour of the larger fibres more than the smaller ones. For example, the smallest fibres encountered by the 2nd week were 0.24μm whereas the smallest fibres seen by the end of myelinogenesis were 0.16μm, a difference of only 0.08μm. This is in comparison with 1.36μm and 1.76μm for the large fibres at the 2nd and 16th week respectively, a difference of 0.4μm. Beyond the third week of age, more than 90% of the myelinated fibres present in the optic nerve had a diameter of less than 1.0μm.

Figure 6.3: Graph showing progression of mean myelinated nerve fibre diameter in optic nerve of (CBA x C57BL) F_1 hybrid mice with age. The mean myelinated nerve fibre diameter at the very early stages of myelinogenesis is large, indicating that, myelinogenesis starts mainly with the large fibres. There is a sudden drop in the mean diameter of the myelinated nerve fibres as more fibres within the middle part of the nerve fibre diameter spectrum become myelinated. No significant difference exists between the mean myelinated nerve fibre diameter after the rapid drop in its value and that observed at the end of myelinogenesis.

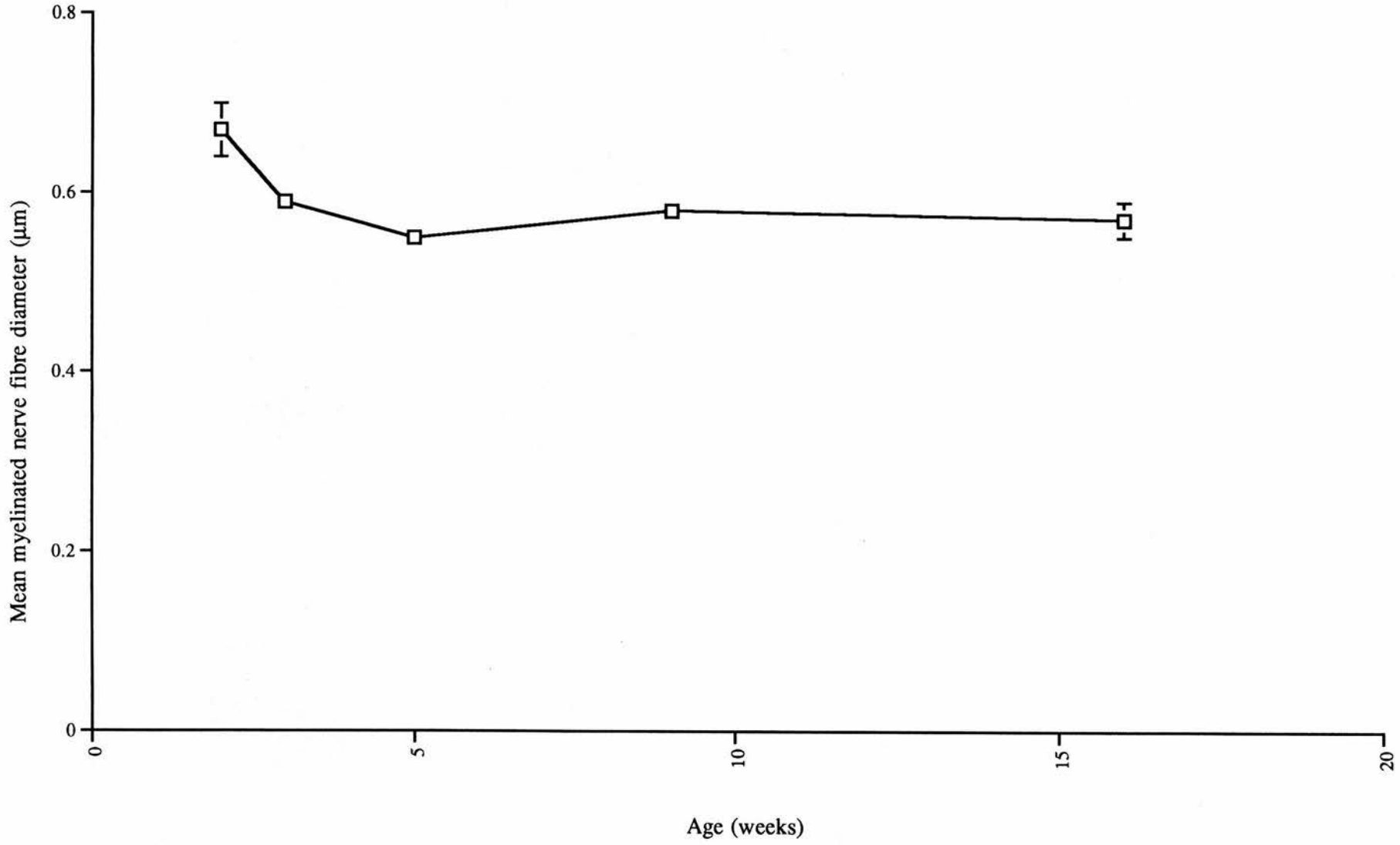
0.8
0.6
0.4
0.2
0
Mean myelinated nerve fibre diameter (µm)
0
5
10
15
20
Age (weeks)

Figure 6.3

Figure 6.4: Graphs showing myelinated nerve fibre spectrum in optic nerve of various postnatal developmental age groups of (CBA x C57BL) F_1 mice. All age groups show unimodal distribution of the myelinated nerve fibres. After the 2nd week there is a rapid drop in the modal diameter to its adult value. The distribution also shows a positive skewing in all age groups. No myelinated nerve fibre greater than 1.76 μm in diameter was seen in any age group.

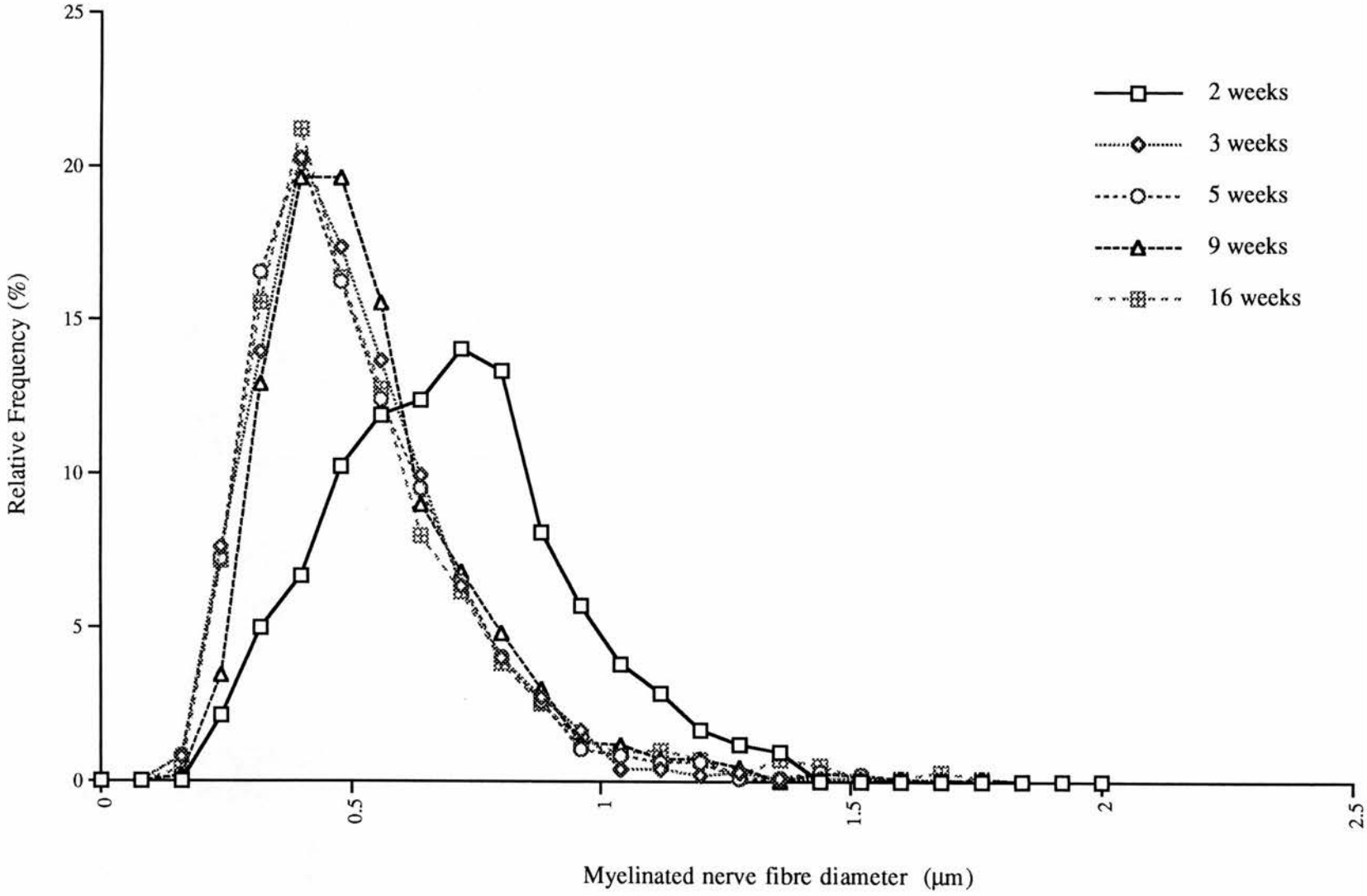
25
20
15
10
5
0
Relative Frequency (%)
0
0.5
1
1.5
2
2.5
Myelinated nerve fibre diameter (µm)
2 weeks
3 weeks
5 weeks
9 weeks
16 weeks

Figure 6.4

6.3 NUMBER OF MYELIN LAMELLAE PER AXON.

The first evidence of myelinogenesis was from micrographs of nerves of 5 pnd mice taken at x 22,000 magnification and printed to a total magnification of x 66,000; and this was seen as selective thickening around some of the large axons in the nerve. By the 6th pnd a definite ring of myelin sheath was visualised around these large axons and by the 7th pnd a small proportion of the axons had acquired a myelin lamella, with some having several lamellae. The myelin lamellae at the onset of myelinogenesis were loosely wrapped around the axons, but with increasing age, they became more compact. Figure 6.5 presents the chronological progression of myelinogenesis to completion (also see figure 6.1). By the 2nd week as many as 11 lamellae of myelin could be counted in association with some of the fibres. The spectrum of the nerve fibres at this stage was typically that of fibres at different levels of myelinogenesis, with approximately 60% of them having no more than 4 myelin lamellae around them and from the third week on, fibres with less than 2 lamellae of myelin were not encountered as shown in Table 6.1. The majority of the fibres had between 4 and 10 myelin lamellae, constituting almost 80% of the fibres in any of these age groups. The largest number of myelin lamellae seen in any fibre was 18, and this was at the end of the process. There was a simple linear relationship between fibre size and the number of myelin lamellae i.e. the bigger fibres had a greater number of myelin lamellae, while the smaller diameter fibres had fewer myelin lamellae. The mean number of myelin lamellae seen in any age group ranged from 4.2 at 2 weeks to 7.9 at 16 weeks and has been presented graphically in Figure 6.6. The increase in the mean number of myelin lamellae followed the general pattern of progression of the entire process of myelinogenesis i.e. a rapid rise from the onset of myelinogenesis through to the 5th postnatal week followed by a slow rise from then until the completion of the process.

Figure 6.5: Representative transmission electron micrographs (x 66,000) of transverse sections of the optic nerve of (C57BL x CBA) F_1 hybrid mice showing the chronological progression of myelinogenesis to its completion.

(a-c): Sections through the optic nerve showing evidence of a surge in myelinogenesis in the optic nerve from the 2nd to the 5th week of postnatal life.

The myelinated fibres are predominantly associated with the larger diameter axons. There is an increase in both the overall diameter of the myelinated nerve fibres and the number of myelin lamellae that wrap around the axons. The myelin lamellae are also becoming progressively more densely wrapped around their axons. Fibres in the middle part of the nerve fibre size spectrum show early evidence of myelinogenesis. In (a) and (b) (2nd & 3rd weeks) the optic nerve is still predominantly populated by unmyelinated nerve fibres, but in (c) (5th week) the myelinated fibres dominate the nerve fibre population of the optic nerve, although unmyelinated fibres are still numerous.

(d & e): Sections through the optic nerve of adult (9th & 16th weeks) F_1 hybrid mice showing myelinated nerve fibres during the slow period of myelinogenesis. Unmyelinated fibres are only very rarely seen during this period. The myelin lamellae are densely packed around the axons. The highest number of myelin lamellae is seen around the large diameter fibres. More myelinated nerve fibres at both extremes of the nerve fibre spectrum are present in the nerve at this stage.

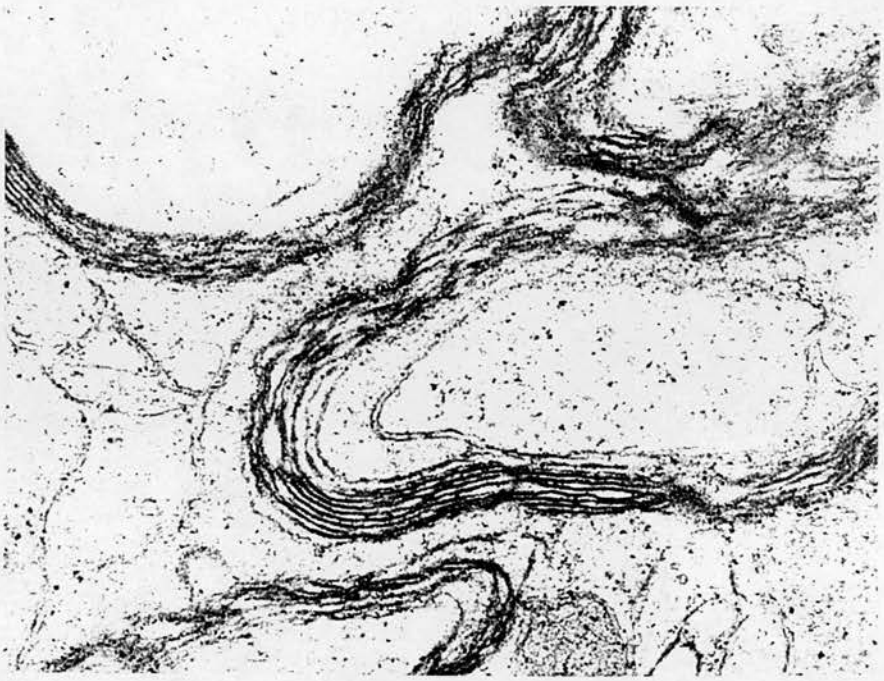

a

b

Figure 6.5

c

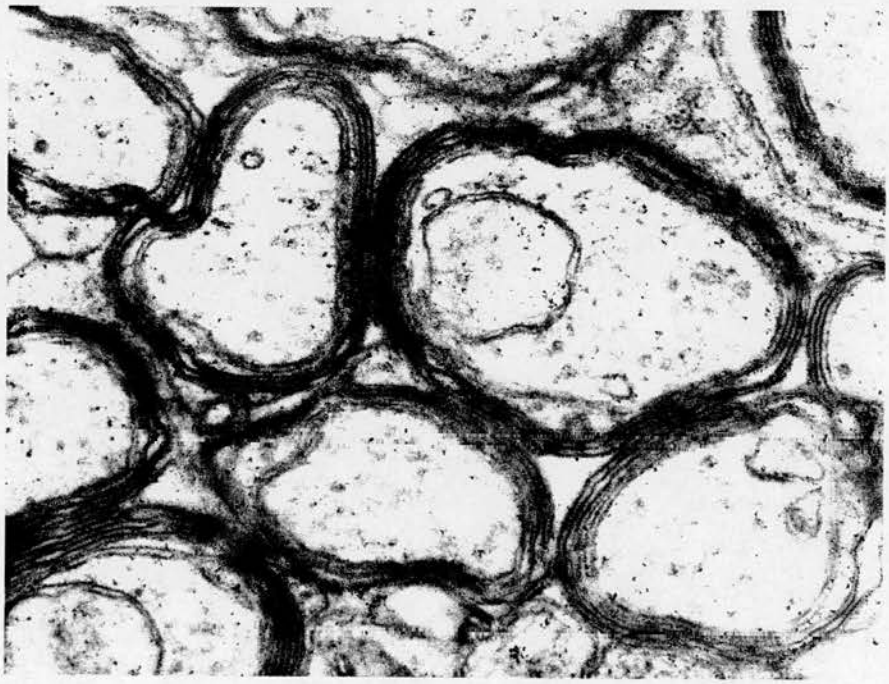

d

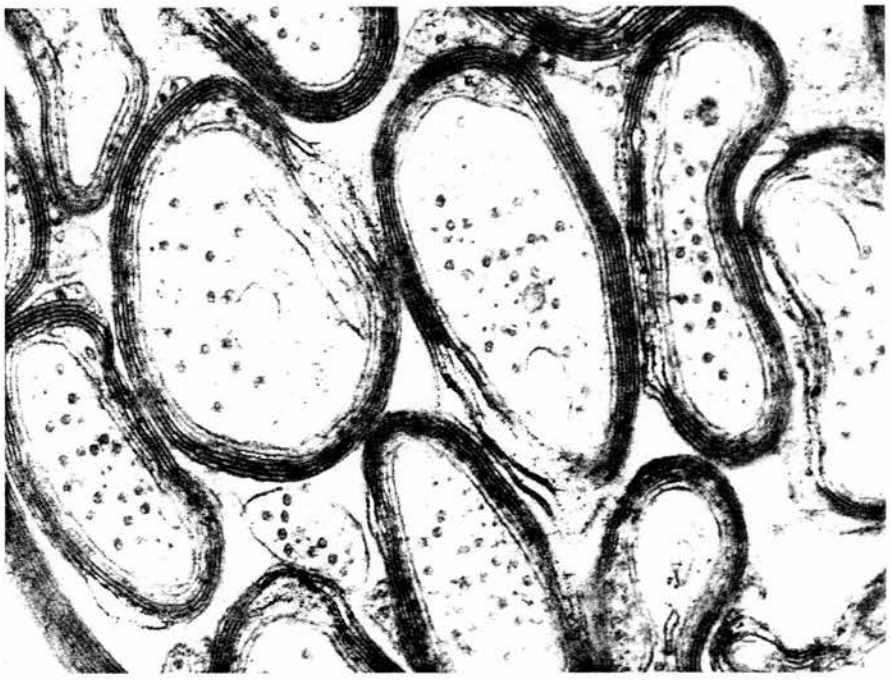

e

Number of myelin lamellae	Frequency (%) by age									
	2 weeks		3 weeks		5 weeks		9 weeks		16 weeks	
	Relative	Cumulative	Relative	Cumulative	Relative	Cumulative	Relative	Cumulative	Relative	Cumulative
1	28.21	28.21	0	0	0	0	0	0	0	0
2	7.7	35.91	1.96	1.96	0.97	0.97	0	0	0	0
3	7.7	43.61	1.96	3.92	2.91	3.88	1.16	1.16	0.88	0.88
4	15.38	58.99	9.80	13.72	7.77	11.65	11.63	12.79	7.96	8.84
5	10.26	69.25	13.73	27.45	14.56	26.21	10.47	23.26	10.62	19.46
6	5.13	74.38	19.60	47.05	18.56	44.66	12.79	36.05	19.47	38.93
7	10.26	84.64	25.49	72.54	17.48	62.14	13.95	50.00	13.27	52.20
8	5.13	89.77	9.80	82.34	8.74	70.88	9.3	59.30	12.39	64.59
9	5.13	94.90	5.88	88.22	8.74	79.62	11.63	70.93	11.50	76.09
10	2.56	97.46	3.92	92.12	5.83	85.45	9.3	80.23	6.19	82.28
11	2.56	100.02	1.96	94.08	1.94	87.39	6.98	87.21	4.42	86.70
12	0	100.02	3.92	98.00	3.88	91.27	6.98	94.19	2.65	89.35
13	0	100.02	1.96	99.96	1.94	93.21	2.33	96.52	2.65	92.00
14	0	100.02	0	99.96	1.94	95.15	1.16	97.68	1.77	93.77
15	0	100.02	0	99.96	3.88	99.03	1.16	98.84	1.77	95.54
16	0	100.02	0	99.96	0.97	100.00	0	98.84	2.65	98.19
17	0	100.02	0	99.96	0	100.00	1.16	100.00	0.88	99.07
18	0	100.02	0	99.96	0	100.00	0	100.00	0.88	99.95

Table 6.1: The chronological progression of the acquisition of myelin lamellae from the onset of myelinogenesis to its completion in optic nerve of (CBA x C57BL) F_1 hybrid mice. At the onset of myelinogenesis a large proportion of the fibres are at different stages of myelinogenesis with most of them having only a small number of myelin lamillae around them. As myelinogenesis progresses more unmyelinated fibres become myelinated and fibres in which the process has already begun acquire more myelin lamellae. After the 2nd week, the majority of fibres in any age group had 4-10 myelin lamellae and this corresponded with the group of medium size fibres. The maximum number of myelin lamellae per axon was seen at the completion of myelinogenesis.

Figure 6.6: Graph showing mean number of myelin lamellae per axon in optic nerve of different age groups of (CBA x C57BL) F_1 hybrid mice. There is a rapid rise in the mean number of myelin lamellae per axon at the onset of myelinogenesis. But after the initial rapid phase, there is a slow rise in the mean number of myelin lamellae per axon from then until the entire process is completed.

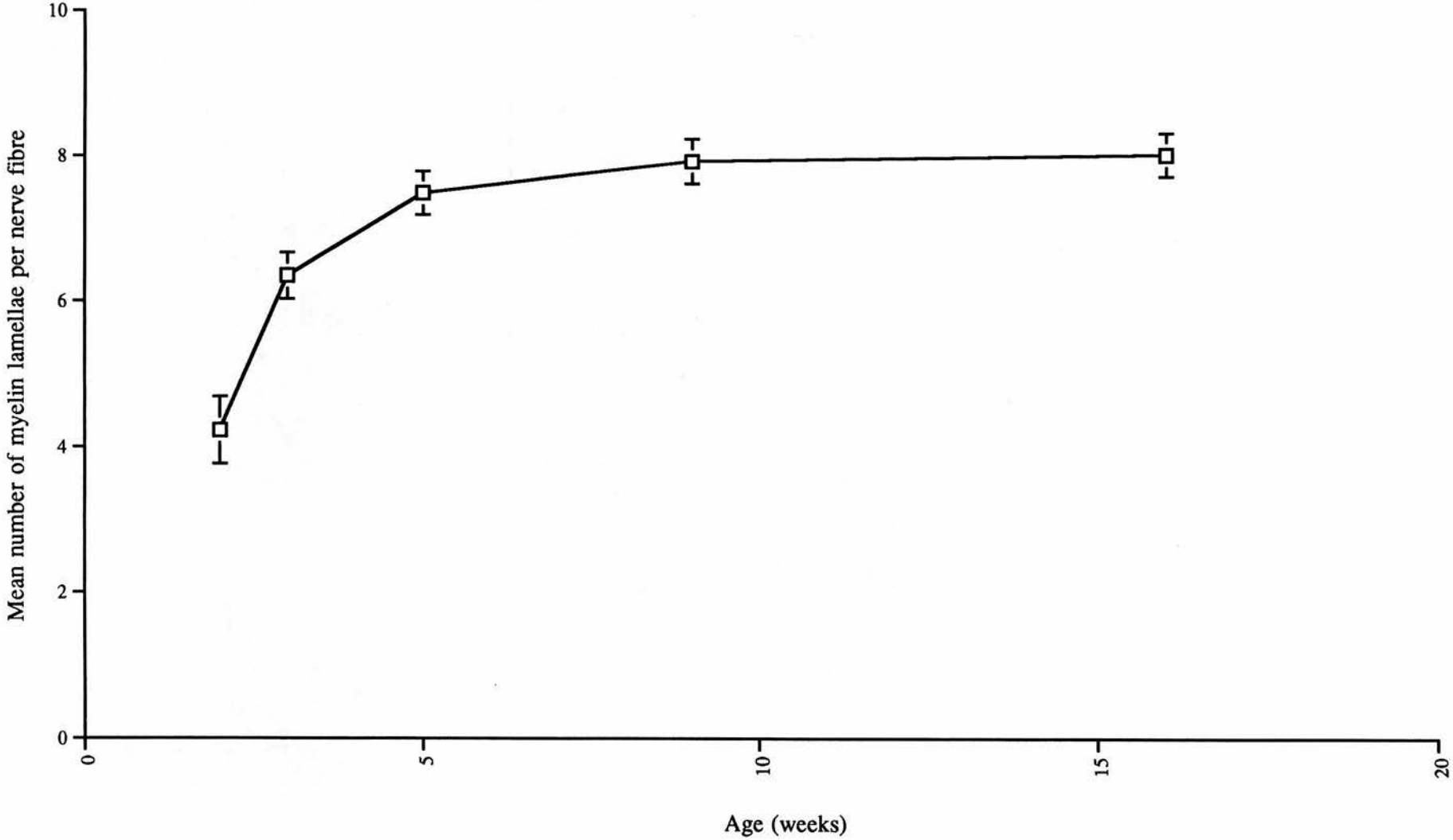
Mean number of myelin lamellae per nerve fibre
10
8
6
4
2
0
0
5
10
15
20
Age (weeks)

Figure 6.6

6.4 DISCUSSION.

Electron microscopic investigation of myelinogenesis in the optic nerve of the (C57BL x CBA) F_1 hybrid mice has shown that it starts towards the end of the first postnatal week i.e. the 5th pnd and continues into adult life i.e. the 16th postnatal week. From the onset of the process it progresses rapidly up to the end of the fifth week, with a surge between the end of the 2nd week and the 5th week. During this period there is maximum increase in both the population of the myelinated nerve fibres present, and the number of myelin lamellae acquired by them. The myelin lamellae are initially loosely wrapped around the axons, but become more densely packed as the process advances with age. From the end of the fifth week onwards, the rate of myelinogenesis gradually slows down until the process is completed by the 16th week.

The almost complete absence of unmyelinated fibres within the optic nerve of the mouse at the end of myelinogenesis suggests that the fully matured adult optic nerve of the mouse contains only myelinated fibres as already stated in chapters 3 and 4 (also see Dangata et al 1994, 1995). This is similar to findings in the adult optic nerve of many species including humans (Cohen, 1967; Magoon et al., 1981), but in contrast with the composition of the nerve fibres in species like *Xenopus laevis* in which, despite the fact that the number of myelinated nerve fibres continues to increase throughout life, the adult nerve still contains largely unmyelinated fibres (Gaze & Peter, 1961). Bruesch and Arey (1942) also reported that both myelinated and unmyelinated fibres were present in the adults of species such as the turtle, alligator, horned toad and opossum; in species such as the cat, dog, rabbit and guinea pig, they found that all the fibres in the optic nerve of the adult were myelinated.

Myelinogenesis in the mouse begins with the large fibres as is shown by the large mean diameter and the large modal diameter of the myelinated nerve fibres seen during the second week of postnatal life. The increase in myelinogenesis that occurs from the end of the 2nd week corresponds to the period when the mouse opens its eyes, which suggests that a

relationship may exist between physiological function and morphogenesis of the optic nerve of the mouse. The surge of myelinogenesis during the early postnatal period, at the end of which about 73% of the fibres show evidence of myelinogenesis, may be the minimum required to establish normal vision. Gaze and Peters (1961) reported similar findings in *Xenopus*, in which the onset of visual response corresponded with the time myelinated fibres were first observed in the optic nerve. The progressive selection of fibres for myelination in a decreasing order of fibre size also suggests that fibres myelinated early in life are probably of greater importance for establishing vision in the mouse than the smaller diameter fibres that become myelinated at a later time. In their study of the relationship between axon diameters and physiological properties of the saphenous nerve, Gasser & Grundfest (1939) found the velocity of conduction to be approximately proportional to the diameter of the myelinated axon. It may be that this relationship between axonal diameter and physiological function in peripheral nerves also exists in certain central tracts.

The rapid drop in the mean myelinated nerve fibre diameter with no further significant change after the second week would suggest that the majority of the myelinated fibres seen in myelinogenesis as large fibres were, in fact, to become medium size fibres when the fully differentiated state of the optic nerve is achieved. Relatively few of these fibres eventually become large fibres. This was further supported by the fact that there was a corresponding drop in the modal diameter without any further change thereafter. Both the mean fibre diameter and the modal diameter were within this fibre group. For all age groups the medium size fibres constituted not less than 80-90% of the total myelinated fibres present.

The adult optic nerve of the mouse is populated principally by small diameter size fibres, compared to other species such as man, the monkey, cat and rabbit (Chacko, 1948; Gyllensten & Malmfors, 1963; Ogden & Miller, 1966; Donovan, 1967; Vaney & Hughes, 1976; Ng & Stone, 1982). Fibre diameter during myelinogenesis is a reflection of both axonal growth and myelin formation (Ng & Stone, 1982). The fact that myelinogenesis is

completed last in the fibres at both extremes of the nerve fibre spectrum i.e., the largest and the smallest diameter fibres, is evident in the continuous increase in their respective populations with time. This may suggest that the smallest fibres within the nerve first undergo axonal growth to attain an optimum diameter before they are myelinated. This also suggests that a critical fibre diameter has to be attained by any nerve fibre before it is myelinated, and that the largest diameter fibres take the longest time to become completely myelinated.

The findings presented here in relation to the mouse are comparable to those previously reported in the rat. In the mouse myelin was seen to be loosely wrapped around the axons at the onset of the process, and became more densely packed with age. Tennekoon et al. (1977) observed in the optic nerve of the rat, the first lamella of myelin at the 6th pnd, with the large diameter axons (0.4μm) showing 1-3 lamellae of loosely wrapped myelin. By the 10th pnd compact myelin was already evident around some axons which became more compact thereafter. At this time 15% of the axons were in the process of myelination, rising to 30% by the beginning of the third week (15th pnd). They also reported a surge in this process which lasted from the end of the 2nd week through to the 4th week (also see Skoff et al., 1976). While the present study reported 37% and 73% of myelination, respectively, by the end of the third and the 5th week, Tennekoon et al. (1977) reported 50% and 85%, respectively, for the 3rd and the 4th week. Furthermore, the myelinated nerve fibre diameter spectrum showed a broad distribution in the rat similar to that seen in the mouse, although, the spectrum in the mouse is somewhat broader; while the largest myelinated nerve fibre observed in the mouse during this period measured 1.68μm in diameter, the comparable value was 1.3μm in the rat. A linear relationship between axon diameter and number of myelin lamellae was also reported in the rat, with the largest fibres having the highest numbers of myelin lamellae. Subsequent investigations by Black et al. (1982) on the rat gave findings similar to those observed by these earlier authors.

Matheson previously reported that, as observed in the present study, the postnatal development of the optic nerve in the rat starts and proceeds rapidly within the early postnatal period and subsequently slows down thereafter (Matheson, 1970 & 1971). He (also see Hirose & Bass, 1973) observed that in the rat myelinogenesis is not limited to the early postnatal period, but proceeded well into adulthood. Since no detailed stastistical findings were reported by these authors, it has not been possible to make a statistical comparison between the present findings and those reported in these earlier studies.

The present findings also allow a comparison to be made between results in the mouse optic nerve, and the findings of others in relation to myelinogenesis in other central tracts. Matthews and Duncan (1971) examined different parameters associated with myelinogenesis in the fibre tracts of the dorsal funiculus (i.e. fasciculus cuneatus, fasciculus gracilis and the corticospinal tract) of rats from 3-120 days of age. Myelinogenesis in these tracts in the rat was also found to be an entirely postnatal process, though with a different time of onset in each of the various systems. The fasciculus cuneatus has the largest population of large fibres and myelinogenesis was initiated in it shortly after birth, with much of this process occurring by the 20th pnd , although actual completion was achieved by the 120th pnd. The fasciculus gracilis which has a slightly lower number of large fibres, ran a similar course with the fasciculus cuneatus, so that by the 120th pnd the whole tract was almost completely myelinated. Axons in the fasciculus gracilis of adult rats were slightly smaller in diameter than those of the fasciculus cuneatus. The corticospinal tract, with predominantly small fibres (0.1-0.3μm), which are also uniform in calibre, was found to be the last to be myelinated. Myelinogenesis did not start in this tract until between the 10th and 15th pnd. It also progressed slower than in the other two tracts. In each tract myelinogenesis started by the formation of promyelin (tongues of oligodendroglial cytoplasm initially encircling axons with definitive myelin forming slightly later). During the early postnatal period, the myelinated fibres seen in each tract were at different levels of myelinogenesis. The process went through a 'wave' of activity that began with the largest fibres and then progressed to

involve fibres in descending order of size until the smallest fibre was reached. These findings would seem to suggest that myelingenesis in the dorsal funiculus of the rat is very similar to that associated with the optic nerve in both the rat and the mouse with respect to time of onset and the course it takes. The optic nerve in both the rat and the mouse is also most closely related to the fasciculus gracilis, presumably because both tracts have fibres of similar size.

CHAPTER SEVEN

COMPARATIVE MORPHOMETRIC ANALYSIS OF THE POSTNATAL DEVELOPMENT OF THE OPTIC NERVE IN AN INBRED MOUSE STRAIN AND ITS F_1 HYBRID.

Contents

7.1 Introduction

7.2 Materials and Methods

7.3 Results

7.3.1 Cross-sectional area (μm^2)

7.3.2 Total myelinated nerve fibre counts

7.3.3 Myelinated nerve fibre density (fibres $1000\mu m^{-2}$)

7.3.4 Myelinated nerve fibre diameter spectrum

7.4 Discussion

7.1 INTRODUCTION

Few studies are available on the postnatal development of the optic nerve of the mouse, although this central tract has been analysed extensively in other mammalian species including man and the rat (Kuwabara, 1975; Skoff et al., 1976a, 1976b; Tennekoon et al., 1977; Dolman et al., 1980; Lam et al.,1982; Perry et al., 1983; Balazsi et al., 1984; Repka & Quigley, 1989; Day, 1990). The few studies on the postnatal development of the optic nerve in the mouse that are available have been on individual strains of mice without any inter-strain comparison (Gyllensten & Malfors, 1963, Gyllensten et al., 1966; Goldberg & Frank, 1979).

The main object of the present study is to make a comparative morphometric analysis of the postnatal development of the optic nerve in an inbred mouse strain and its F_1 hybrid, as relatively little information is available on this topic in the literature. The optic nerve was carefully dissected from different age groups of both immature and adult C57BL and (C57BL x CBA) F_1 hybrid mice while they were under deep general anaesthesia. The cross-sectional area, total myelinated nerve fibre population, their numerical density and fibre size spectrum was then determined. Information from this study allowed a comparison to be made between the postnatal morphometric features of the optic nerve in these two groups of mice, and those of other species that have also been studied.

7.2 MATERIALS AND METHODS

The C57BL strain of mice and its (C57BL x CBA) F_1 hybrid ranging in age from birth to 24 weeks old were studied. Information for the (C57BL x CBA) F_1 hybrid had already been obtained as previously described in chapters 5 and 6. The optic nerve from corresponding age groups of the C57BL inbred strain of mice (i.e. each group of five mice taken at 2 weeks, 3 weeks, 5 weeks, 9 weeks, 16 weeks and 24 weeks of age) were processed for both light and electron microscopy, and for morphometric analysis as previously described. The results for the corresponding age groups of both strains of mice were statistically analysed as indicated in chapter 2 to establish whether there was a significant difference in the parameters measured between them.

Furthermore, in order to determine the approximate age at which myelinogenesis in the optic nerve of the C57BL inbred mouse strain starts, additional mice at 9, 8, 7, 6, 5 and 4 days of age were taken from this strain of mice and treated as indicated above for corresponding age groups of the F_1 hybrid.

7.3 RESULTS

7.3.1 CROSS-SECTIONAL AREAS (μm^2)

In both C57BL inbred and its (C57BL x CBA) F_1 hybrid mice, there was an initial rapid and progressive increase in the csa of the optic nerve noted during the early period of postnatal development i.e. up to the 5th week of postnatal life. This was later followed by a period of rather slow growth that continued through into adulthood. The rate of increase in csa during this slow period of growth progressively decreased with age. The C57BL series generally had a larger optic nerve compared to corresponding age groups of the F_1 hybrid series. This difference in the calibre of the optic nerve between corresponding age groups of either strains of immature mice was not significant. The difference between corresponding age groups of adult mice was, however, significant ($P < 0.05$) as shown in Table 7.1. In addition, the rate of growth in the calibre of the nerve in adult C57BL mice was greater than that observed in the F_1 hybrid mice as shown in Figure 7.1.

Age (weeks)	Parameter measured and level of significance		
	Mean cross-sectional area	Mean nerve fibre count	Mean nerve fibre density
2	n.s.	n.s.	n.s.
3	n.s.	n.s.	$0.01 \leq P \leq 0.05$.
5	n.s.	n.s.	$P \leq 0.05$.
9	$0.01 \leq P \leq 0.05$.	$P \leq 0.05$.	n.s.
16	$0.01 \leq P \leq 0.05$.	n.s.	$0.01 \leq P \leq 0.05$.
24	$P \leq 0.05$.	$0.01 \leq P \leq 0.05$.	n.s

Table 7.1: Level of significant difference by age of morphometric parameters of the optic nerve between C57BL and (C57BL x CBA) F_1 hybrid mice. n.s = no significant difference.

Figure 7.1: Graphs showing mean cross-sectional area of the optic nerve of postnatal developmental age groups of C57BL and (C57BL x CBA) F_1 hybrid mice. In both mouse strains growth in the calibre of the nerve continues well into adulthood. Growth in csa is rapid during the juvenile period but progressively slows down thereafter. There is no significant difference in the rate of growth in the calibre of the nerve between the two strains of mice during the juvenile period but thereafter the C57BL optic nerve grows at a significantly faster rate than that of the F_1 hybrid.

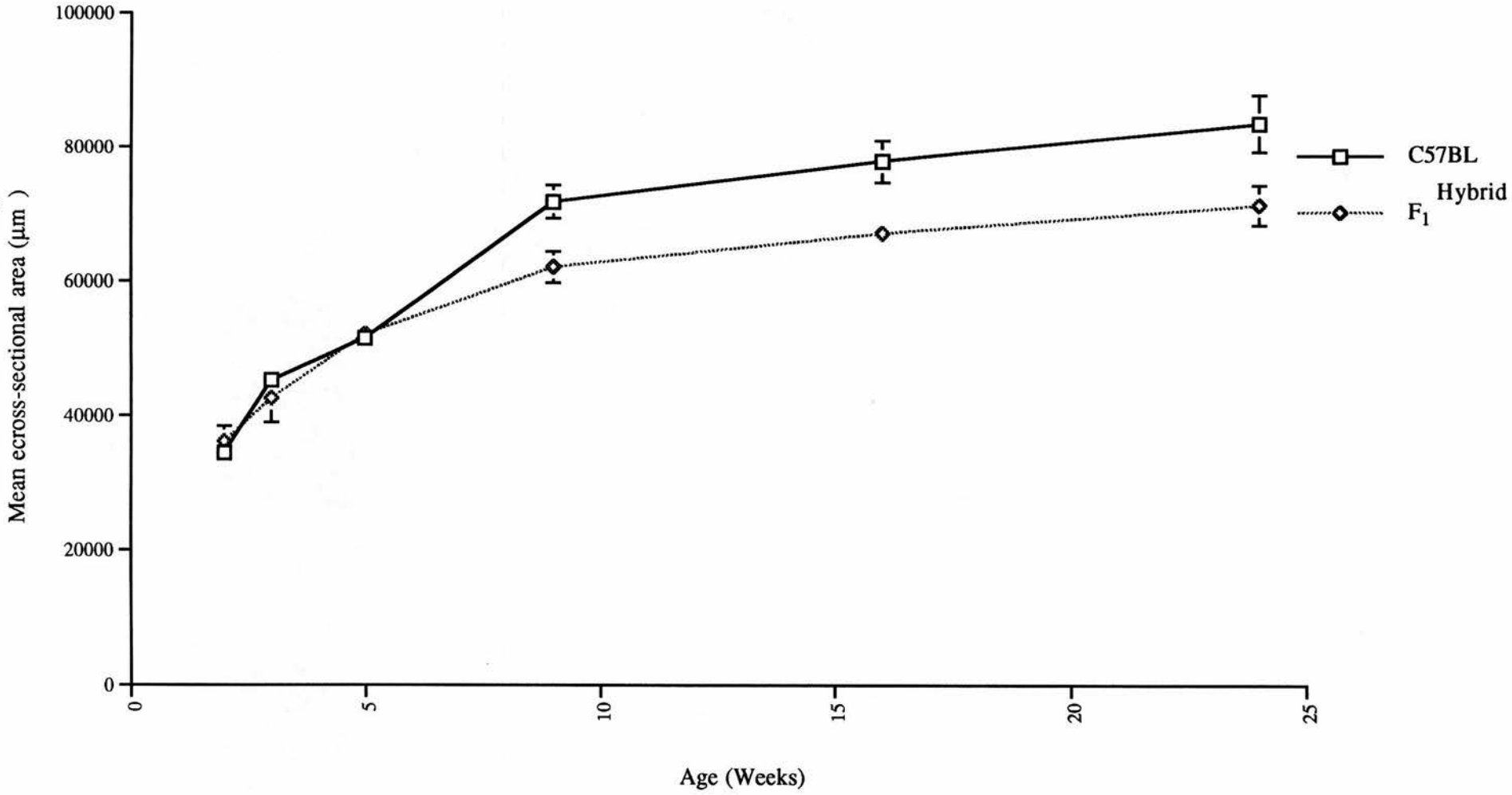
100000
80000
60000
40000
20000
0
Mean ecross-sectional area (µm 2)
0
5
10
15
20
25
Age (Weeks)
C57BL
Hybrid
F1

Figure 7.1

7.3.2 TOTAL MYELINATED NERVE FIBRE COUNTS.

No evidence of myelinogenesis was observed in either of the strains of mice studied before the 5th postnatal day (pnd). By the 5th pnd, only at x 66,000, was it possible to observe the presence of a few myelin sheaths wrapped around some of the largest fibres in both strains of mice. After its onset, the rate of myelinogenesis increased rapidly up to the end of the 5th week. As more axons became myelinated, those already myelinated acquired an increasing number of myelin lamellae which also became more densely packed around their axons. In both strains of mice the optic nerve was initially predominantly populated by unmyelinated nerve fibres, but by the end of the rapid period of myelinogenesis only a few unmyelinated fibres were seen; and by adulthood, unmyelinated fibres were only very rarely encountered (see Figure 7.2 - micrographs of optic nerves during the period of rapid rate of myelinogenesis). After the rapid phase of myelinogenesis, the process progressed at a slower rate in both the inbred and hybrid series to reach a peak by the 9th week in the C57BL and the 16th week in the F_1 hybrid. Peak values for the myelinated nerve fibres were 104832±5115 (s.e.m.) and 94213±1799 (s.e.m.) for the C57BL and F_1 hybrid, respectively. There was a progressive decrease in the total number of myelinated nerve fibres counted with increasing age after attainment of peak myelination in each of the strains (see Figure 7.3). No significant difference was observed in the mean myelinated nerve fibre counts between corresponding age groups of immature forms of both strains of mice. Corresponding age groups of adult mice with the exception of the 9 weeks age group, however, significantly differed from one other (see Table 7.1).

Figure 7.2: Representative transmission electron micrographs (x66,000) of transverse sections through the optic nerve of C57BL and (C57BL x CBA) F_1 hybrid mice during the period of surge in myelinogenesis.

a) (C57BL), b) (F_1 hybrid) 3 weeks old:
In both strains of mice, the myelinated fibres are predominantly associated with the larger diameter axons. There is an increase in both the overall diameter of the myelinated nerve fibres and the number of turns of myelin sheath that wraps around them. The optic nerve of each strain, however, is still populated by a substantial number of unmyelinated nerve fibres.

c) (C57BL), d) (F_1 hybrid) 5 weeks old: The optic nerve in both strains of mice is predominantly populated by myelinated nerve fibres. There is also a considerable increase in the population of small diameter myelinated nerve fibres.

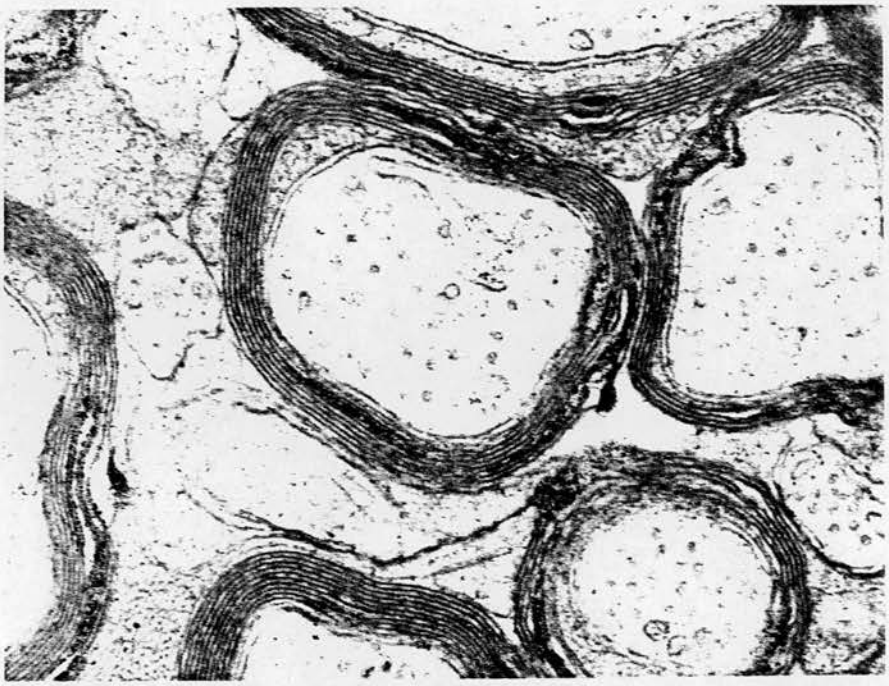

a

b

Figure 7.2

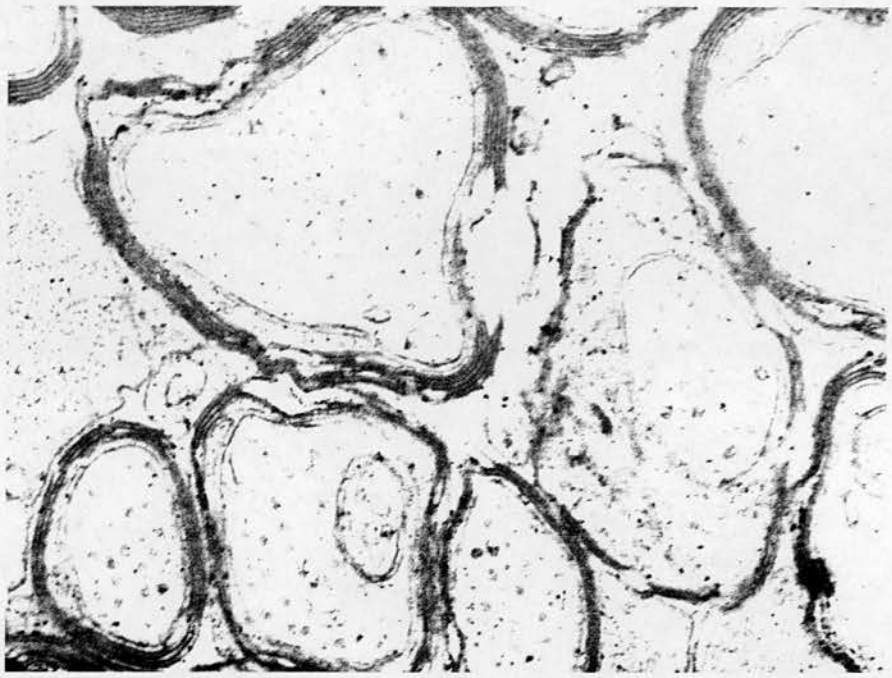

c

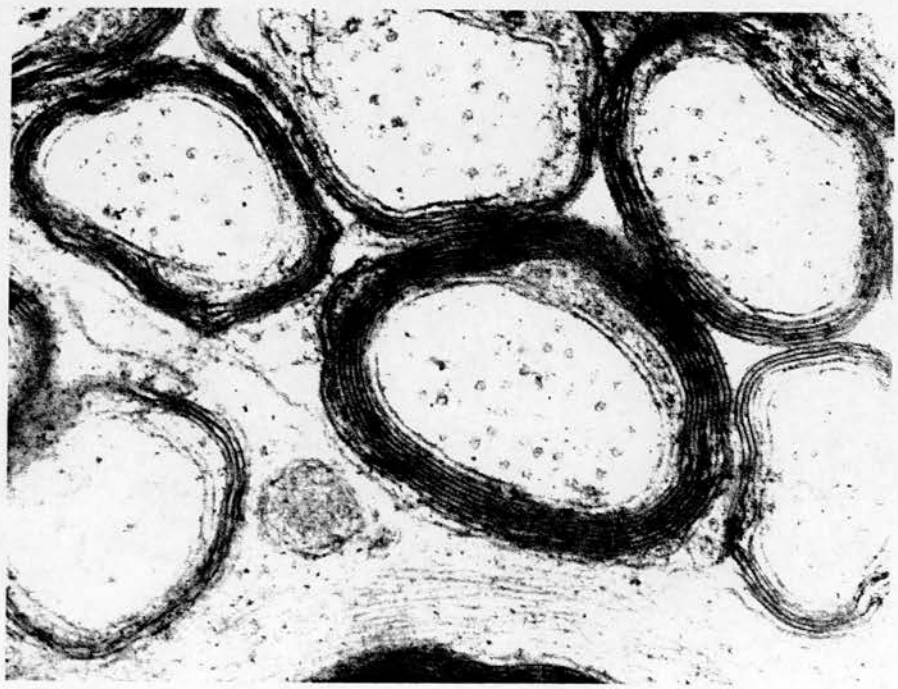

d

Figure 7.3: Graphs comparing the progression of myelinogenesis with age in C57BL and (CBA x C57BL) F_1 hybrid strains of mice. There is a rapid progression of myelinogenesis in both strains of mice during the juvenile period of life following its onset. After the juvenile period the process proceeds at a progressively slower rate until it is completed at 9 weeks and 16 weeks of postnatal life for C57BL and F_1, respectively. After the completion of myelinogenesis the population of myelinated nerve fibres in each of the mouse strains continues to drop, but at decreasing rate with age.

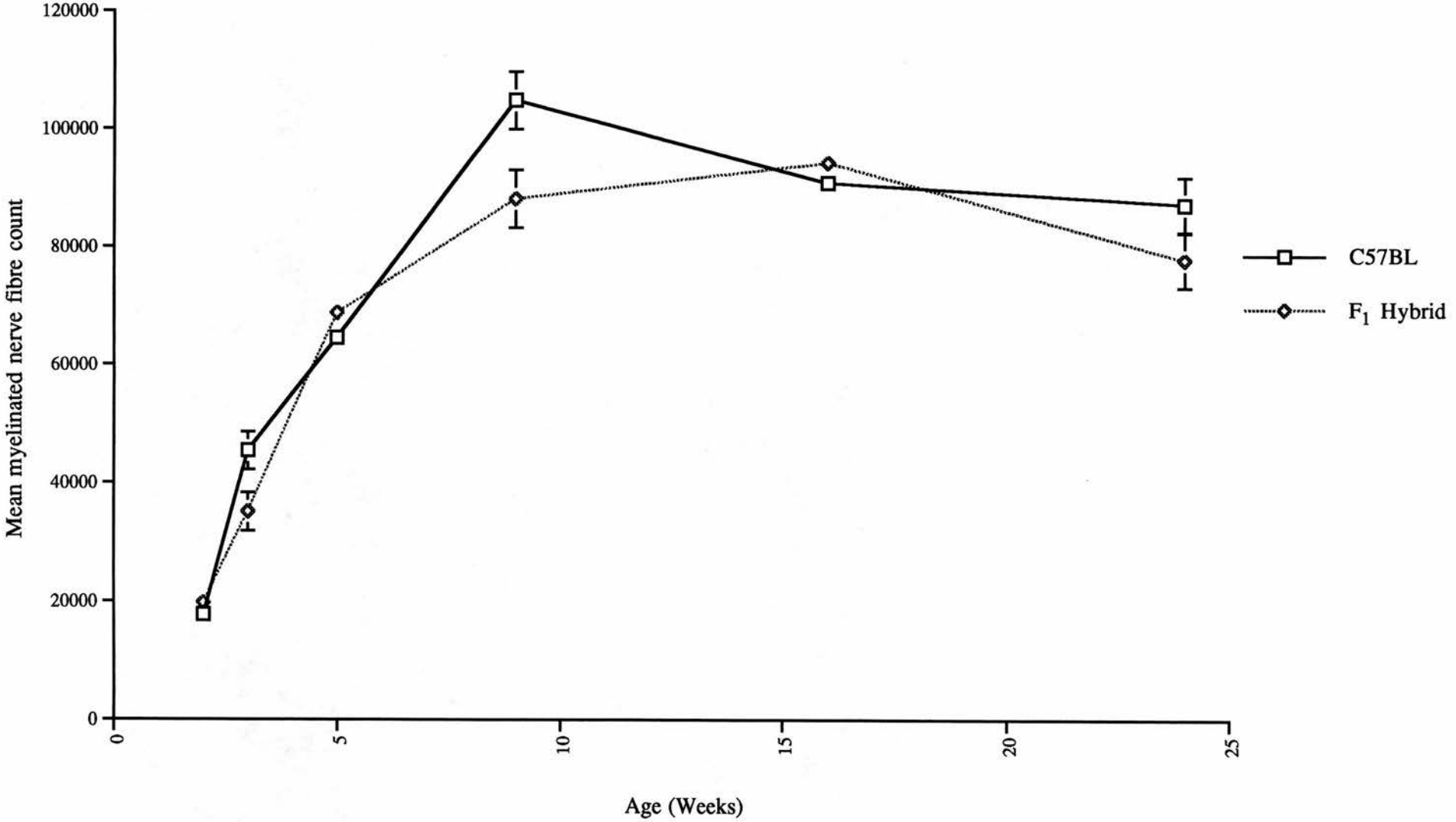
120000
100000
80000
60000
40000
20000
0
Mean myelinated nerve fibre count
0
5
10
15
20
25
Age (Weeks)
C57BL
F1 Hybrid

Figure 7.3

7.3.3 MYELINATED NERVE FIBRE DENSITY (FIBRES 1000μm^{-2}).

There was a rapid increase in numerical density of the myelinated nerve fibres in both strains of mice and this corresponded to the period of rapid myelinogenesis. This was followed by a progressively gradual increase in mean myelinated nerve fibre density until highest density levels were achieved at an age which corresponded to the time when the maximum level of myelinogenesis was achieved in each strain of mice. In the case of the C57BL, this was during the 9th week with a mean myelinated nerve fibre density of 1458±41 (s.e.m.), and the 16th week for the F_1 hybrid, with a mean myelinated nerve fibre density of 1410±41 (s.e.m.). A fall in the mean myelinated nerve fibre density was then observed with increasing age thereafter (see Figure 7.4). No significant difference in density was seen between corresponding 2, 9 and 24 weeks age groups. There was, however, a significant difference ($P < 0.05$) in density of the myelinated nerve fibres between corresponding 3, 5 and 16 weeks old mice of both strains (see Tables 1).

7.3.4 MYELINATED NERVE FIBRE DIAMETER SPECTRUM.

In all age groups of both strains of mice no myelinated nerve fibres less than 0.16 μm or greater than 2.0 μm in diameter were measured. The largest mean myelinated nerve fibre diameter was observed in the 2 weeks old mice of both strains, and this was 0.67±0.01 μm (s.e.m.) and 0.67±0.03 μm (s.e.m.) for C57BL and the F_1 hybrid, respectively. These mean values dropped to their lowest level of 0.56±0.01 μm (s.e.m.) for the C57BL and 0.55±0.01 μm (s.e.m.) for the F_1 hybrid respectively by the fifth week (see Figure 7.5). The nerve fibre diameter spectrum was unimodal in all age groups of both strains of mice (see Figure 7.6). After the second week there was a rapid drop in the modal diameter from 0.64 μm at two weeks in each series to a value that remain constant from then through to adulthood in both strains of mice, and this was 0.48 μm for the C57BL series and 0.40 μm for the F_1 hybrid series. More fibres at both extremes of the myelinated nerve fibre size spectrum were seen

with increasing age until the process of myelinogenesis was completed. This observation was more evident among the large diameter fibres than any other category of myelinated nerve fibres (see 5.3.2 for myelinated nerve fibre grouping). For example, in the C57BL series, the largest myelinated nerve fibre measured at 2 weeks of age was 1.44 μm and by 24 weeks, fibres as large as 1.92 μm were observed; with the proportion of the large fibres rising from 2.76% at 2 weeks to 8.15% at 24 weeks. At 2 weeks, the smallest myelinated fibre measured was 0.24μm in diameter and thereafter the smallest fibres measured in this series were less than 0.16μm in diameter; with the respective proportion of these fibres at 2 and 24 weeks of age being 0.59% and 1.58%. For the F_1 hybrids, the smallest fibres measured were 0.16μm in diameter, and this was at the 2nd week, with the largest fibres measured having a diameter of 1.76μm at 24 weeks. The proportion of small fibres i.e < 0.3μm in diameter for this strain rose from 1.1% at 2 weeks to 4.45 % at 24 weeks and the proportion of large diameter fibres i.e > 1.0μm rose from 5.93% at 2 weeks to 8.05% at 24 weeks, respectively. There was a significant difference in the proportion of small fibres between the corresponding age groups of both strains of mice, but no significant difference was seen in the proportion of the medium diameter fibres i.e 0.3-1.0μm between corresponding age groups of either strain of mice. After the 2nd week there was no significant difference between corresponding age groups of either strain of mice with regard to the proportion of large diameter fibres. In any age group in both strains of mice more than 90% of the myelinated fibres present in the optic nerve had a diameter of less than 1.0μm.

Figure 7.4: Graphs showing myelinated nerve fibre density in optic nerve of different age groups of C57BL and (C57BL x CBA) F_1 hybrid strains of mice during postnatal development. In both strains of mice there is an initial rapid rise in myelinated nerve fibre density during the juvenile period of life followed by a gradual rise until peak myelinogenesis has been attained. After this there is a drop in density. After the juvenile period the rate of progression of the myelinated nerve fibre density becomes more gradual in the F_1 hybrid than in the C57BL.

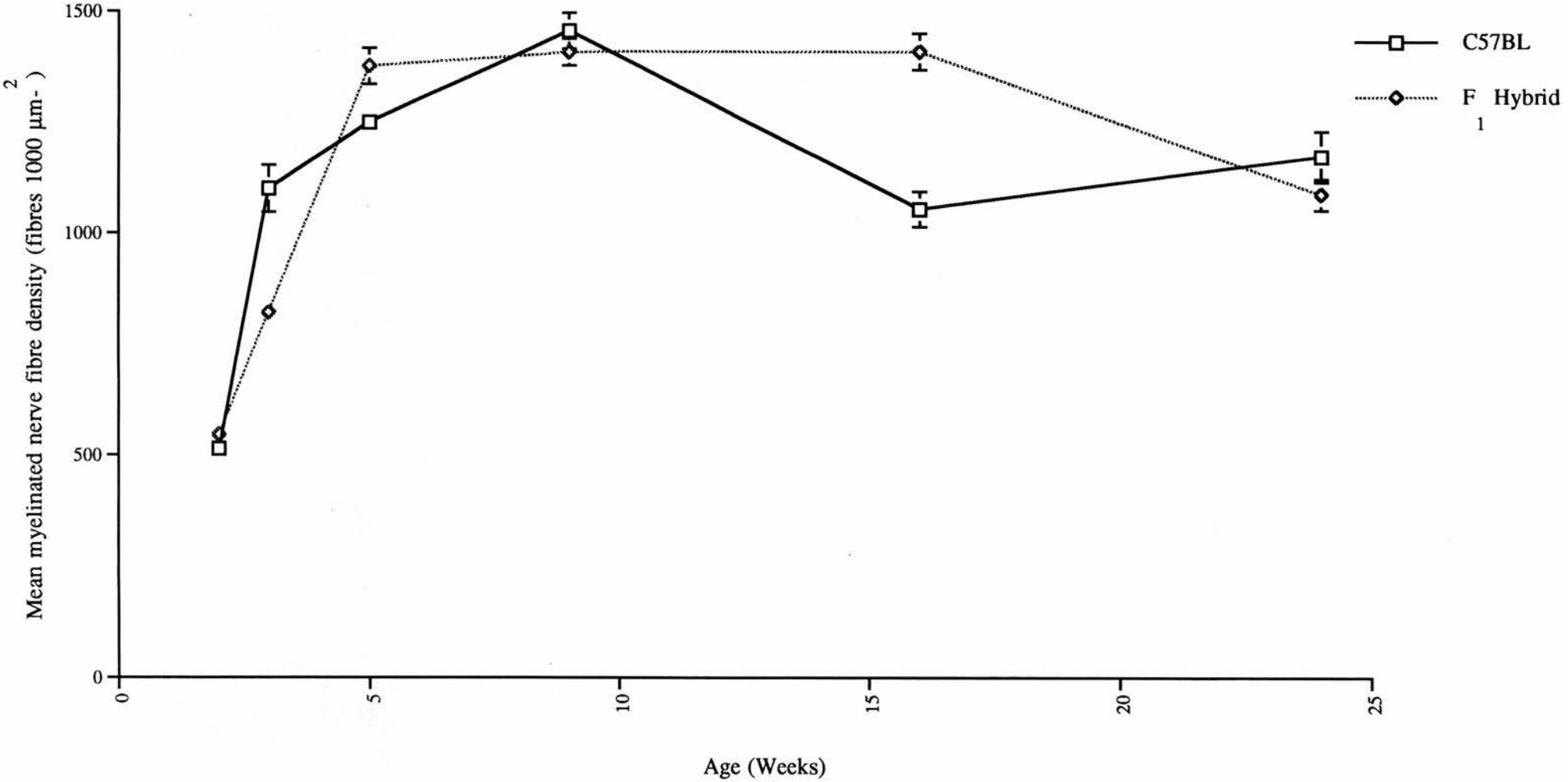
1500
1000
500
0
Mean myelinated nerve fibre density (fibres 1000 µm-2)
0
5
10
15
20
25
Age (Weeks)
C57BL
F1 Hybrid

Figure 7.4

Figure 7.5: Graphs showing mean myelinated nerve fibre diameter in optic nerve of different age groups of C57BL and (C57BL x CBA) F_1 hybrid strains of mice during postnatal development. In both strains of mice there is a sharp drop in myelinated nerve fibre diameter during the juvenile period. This is then followed by a gradual rise as myelinogenesis progresses. However, in both strains of mice, the rise is slow before attainment of peak level of myelinogenesis but becomes more rapid immediately afterwards.

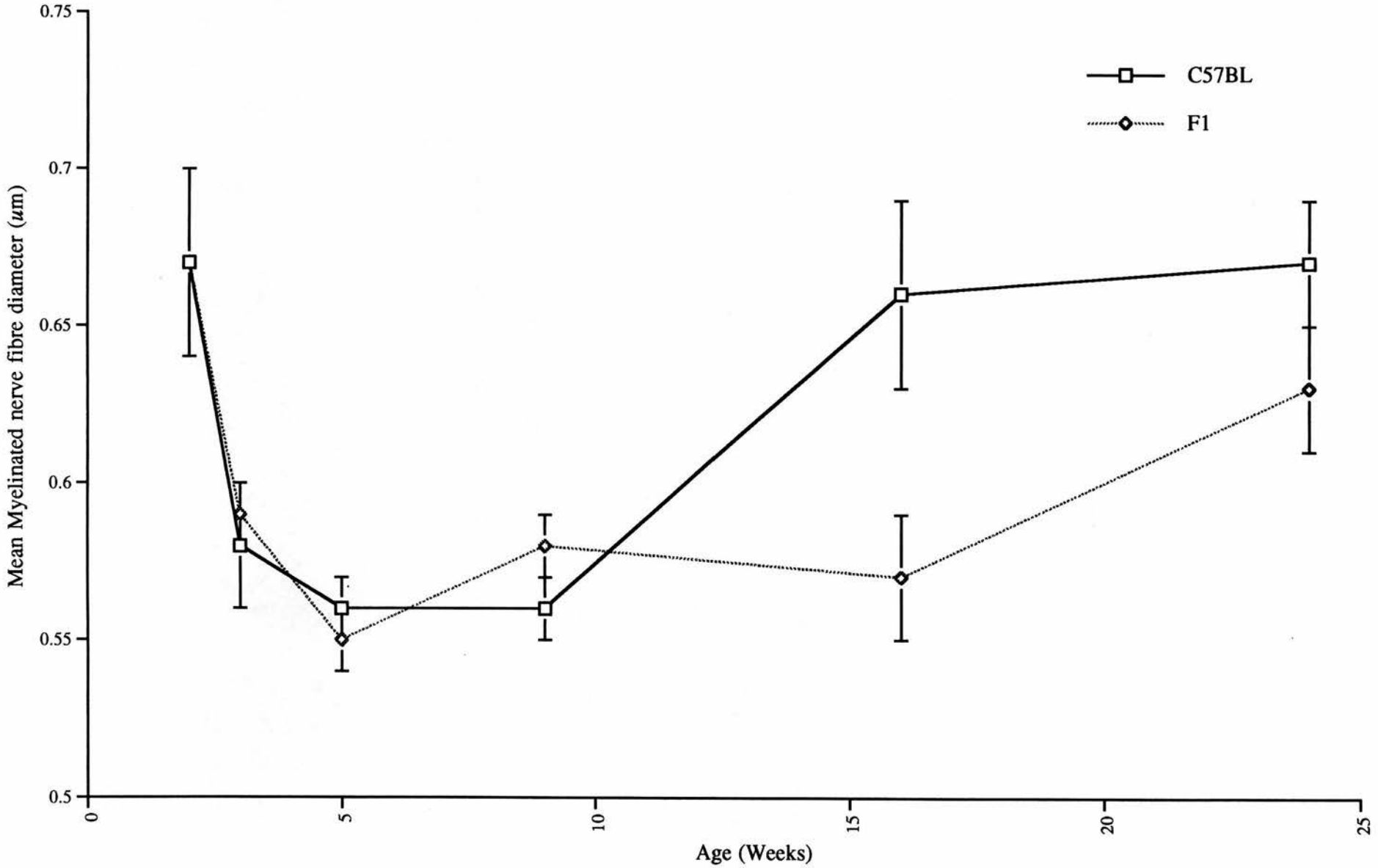
C57BL
F1
Mean Myelinated nerve fibre diameter (um)
0.75
0.7
0.65
0.6
0.55
0.5
0
5
10
15
20
25
Age (Weeks)

Figure 7.5

Figure 7.6: Graphs showing myelinated nerve fibre size spectrum in different postnatal age groups of C57BL and (C57BL x CBA) F_1 hybrid strains of mice. In all the age groups of both strains of mice the spectrum of distribution of the myelinated nerve fibres in the optic nerve is unimodal with a positive skewing. There is a rapid drop in the modal diameter to its adult value after the second week. The spectrum becomes broader with age. This was more obvious after the juvenile period. There is no significant difference in the spectrum of distribution of nerve fibres between the two groups of mice.

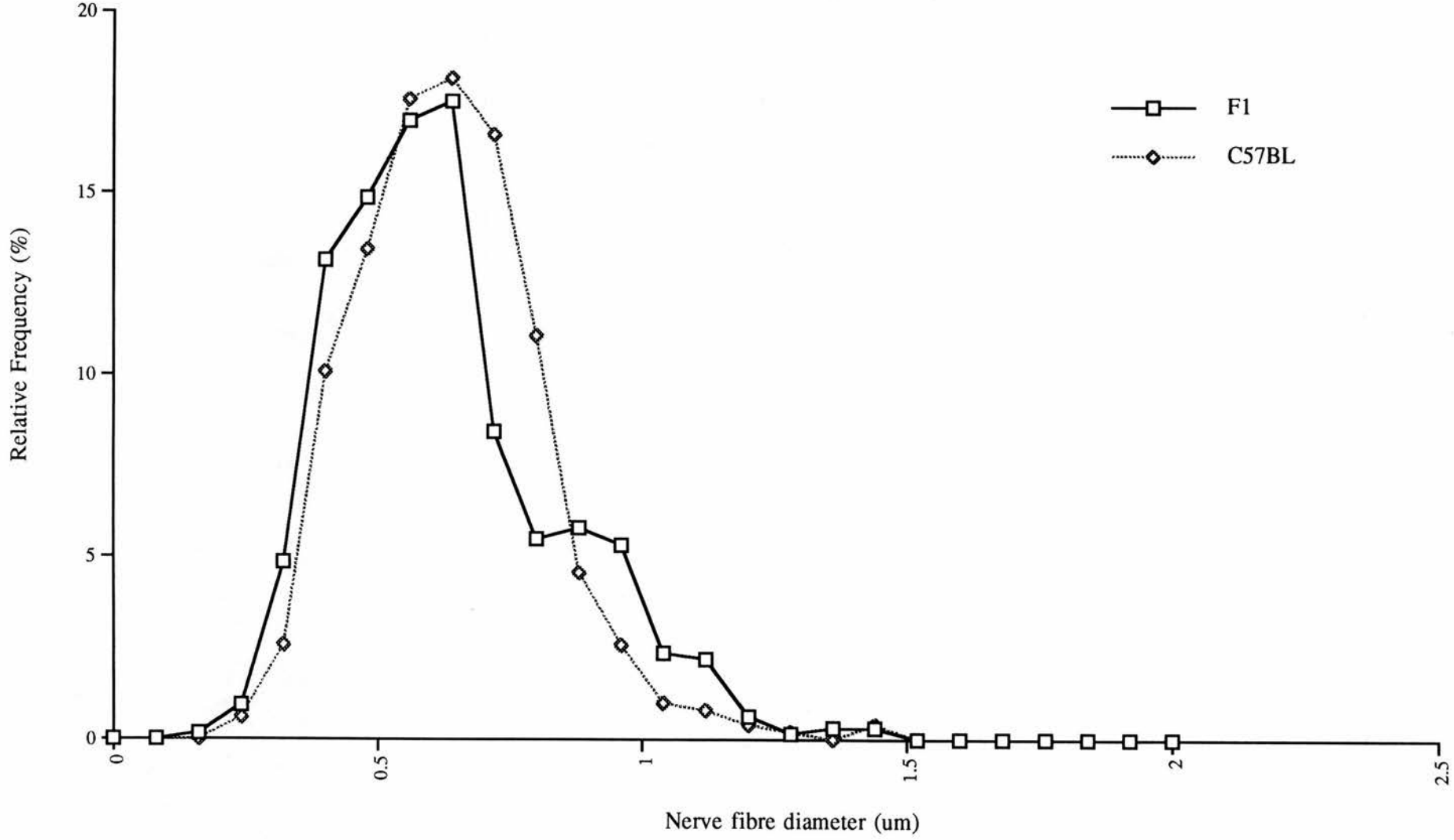
20
15
10
5
0
Relative Frequency (%)
0
0.5
1
1.5
2
2.5
Nerve fibre diameter (um)
F1
C57BL

2 weeks old

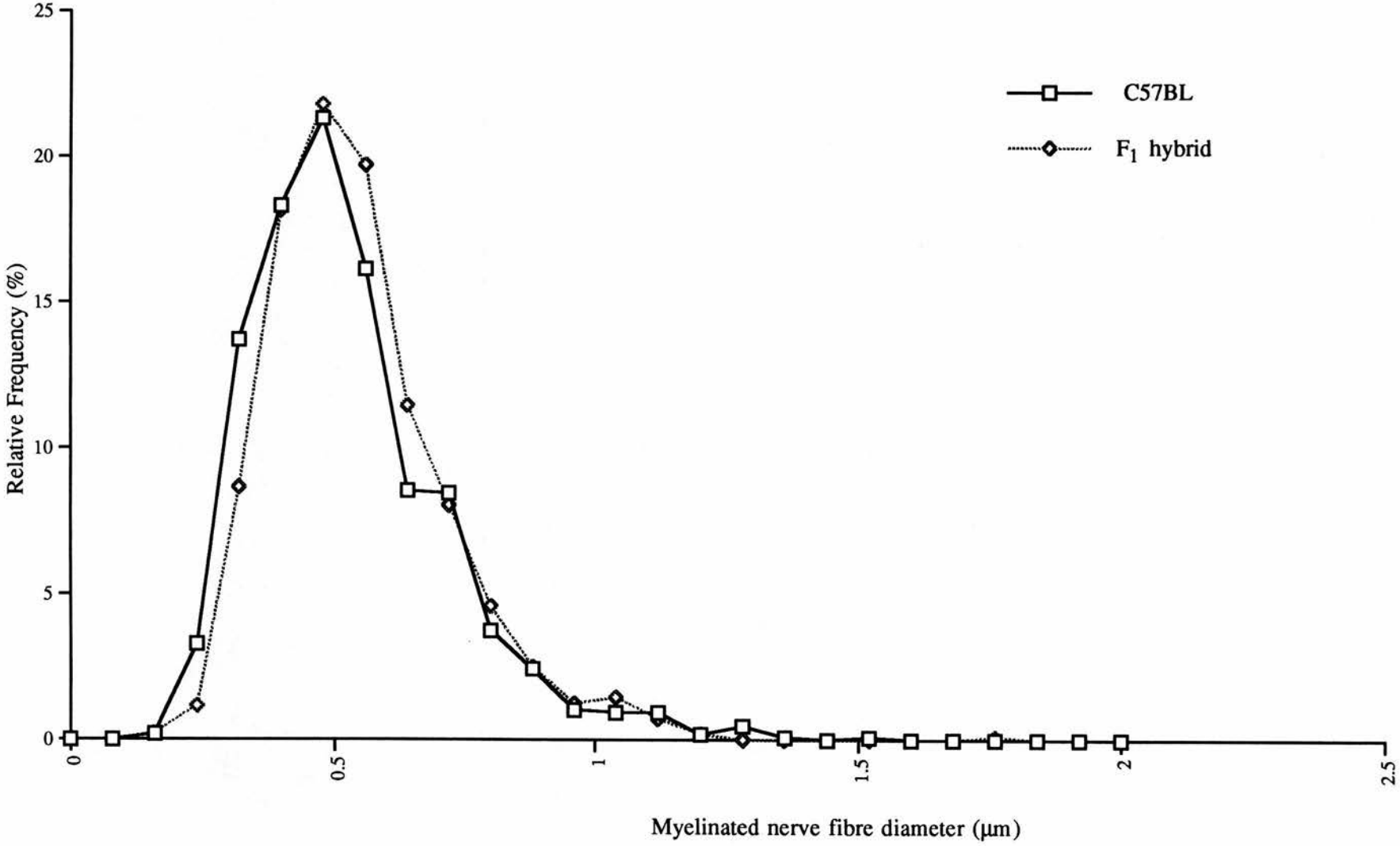
C57BL
F1 hybrid
Relative Frequency (%)
25
20
15
10
5
0
0
0.5
1
1.5
2
2.5
Myelinated nerve fibre diameter (µm)

3 Weeks old

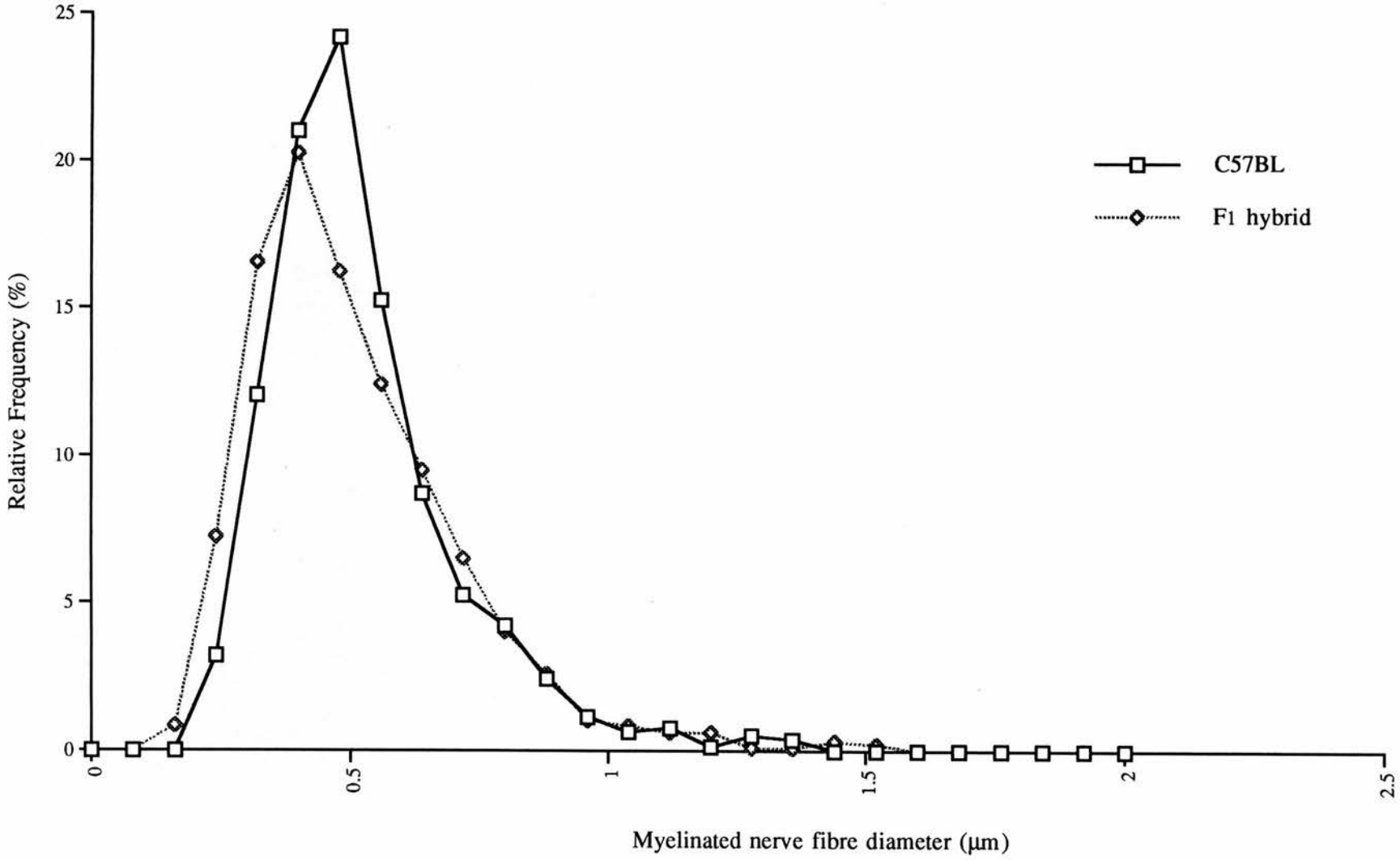
25
20
15
10
5
0
Relative Frequency (%)
0
0.5
1
1.5
2
2.5
C57BL
F1 hybrid
Myelinated nerve fibre diameter (µm)

5 Weeks old

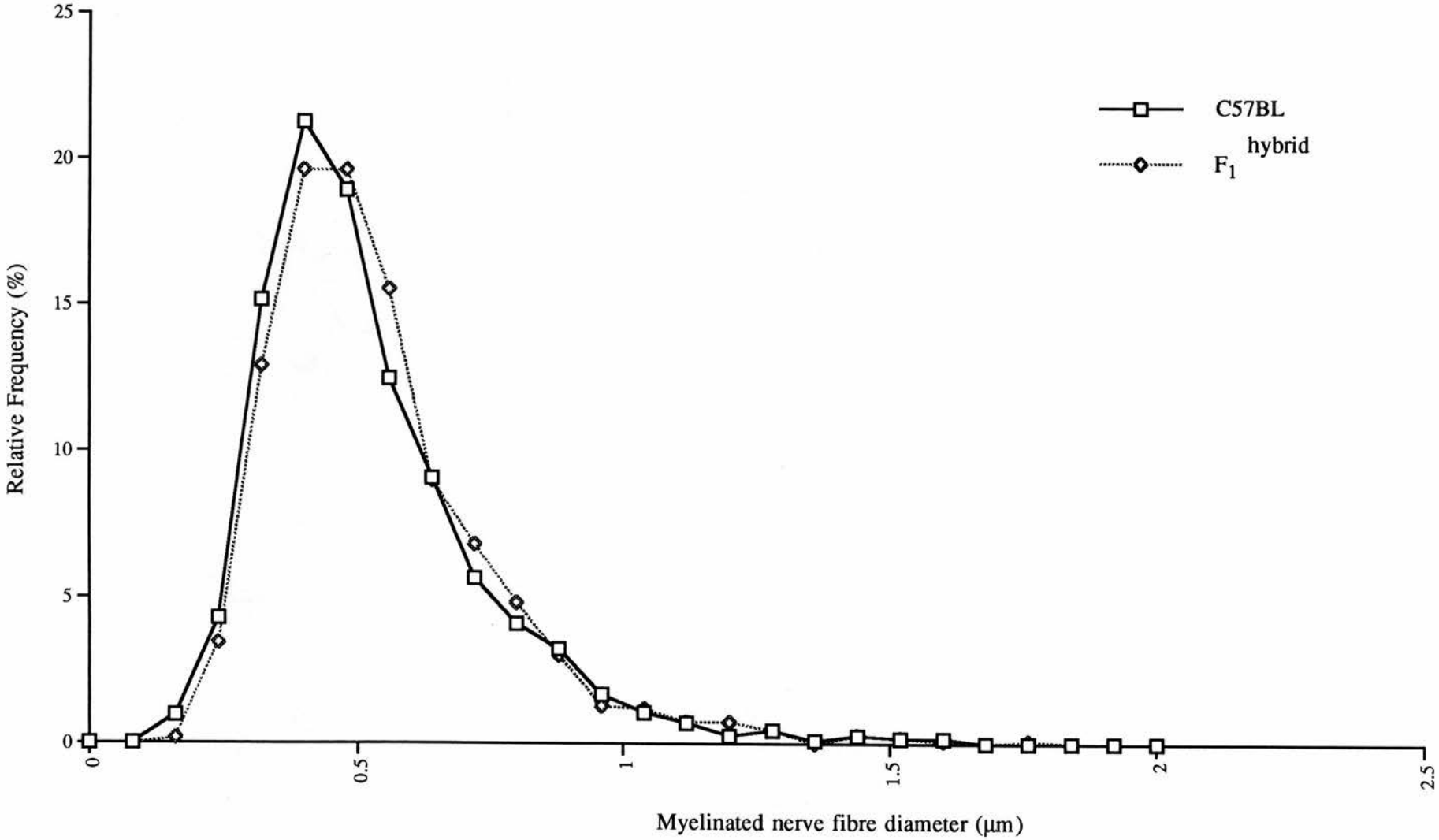
25
20
15
10
5
0
Relative Frequency (%)
0
0.5
1
1.5
2
2.5
Myelinated nerve fibre diameter (μm)
C57BL
F1 hybrid

9 Weeks old

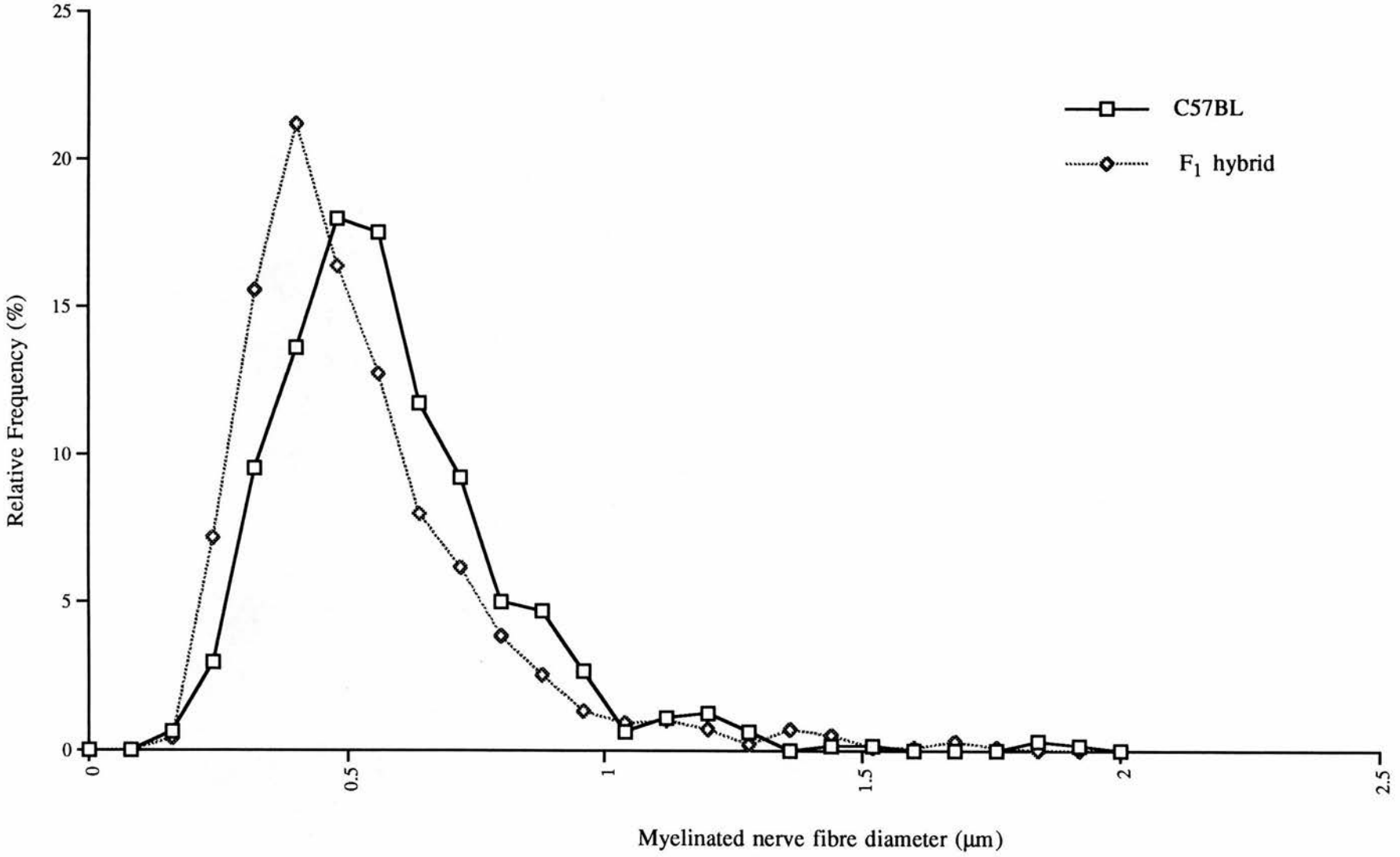
25
20
15
10
5
0
Relative Frequency (%)
0
0.5
1
1.5
2
2.5
Myelinated nerve fibre diameter (μm)
C57BL
F1 hybrid

16 Weeks old

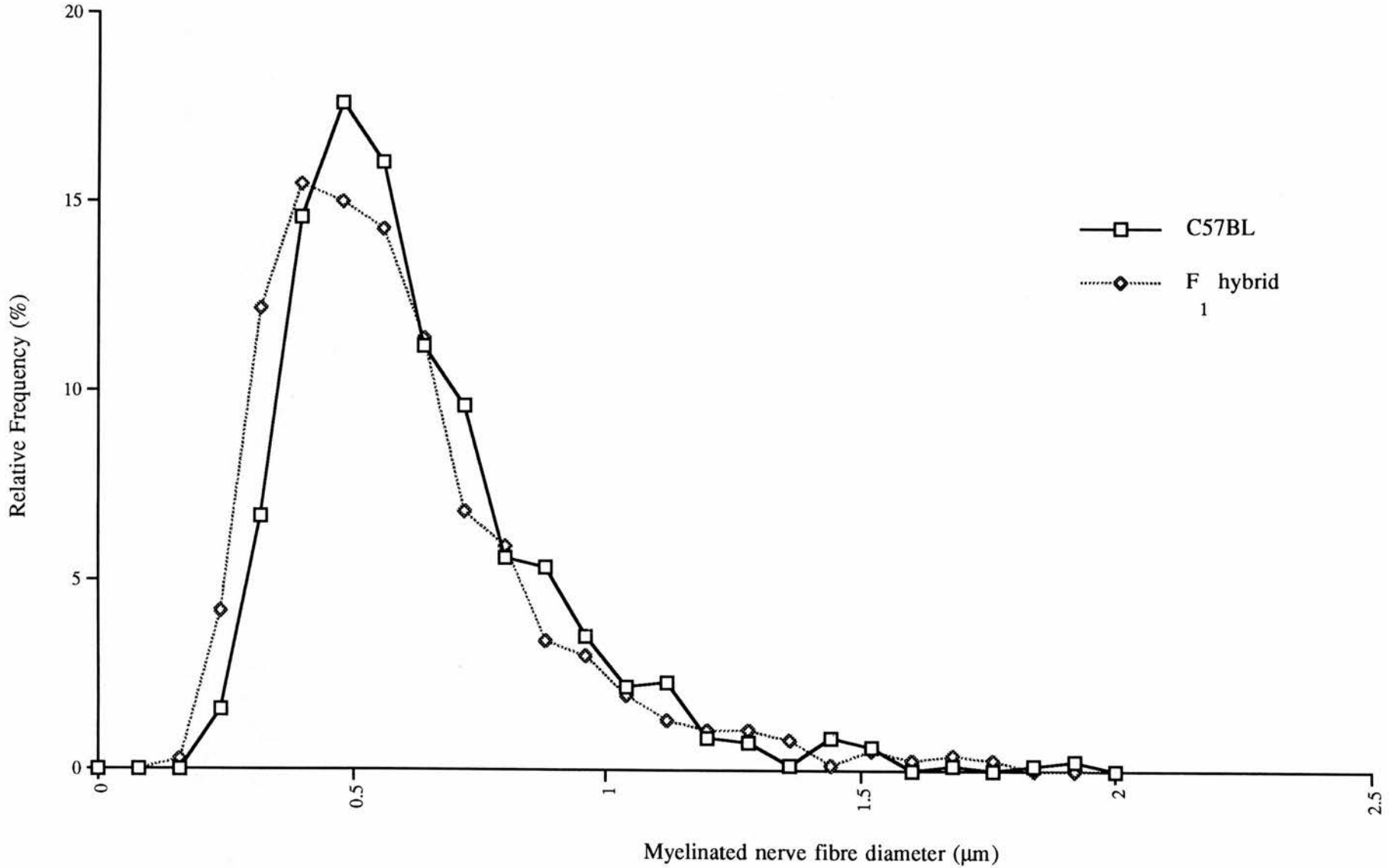
20
15
10
5
0
Relative Frequency (%)
0
0.5
1
1.5
2
2.5
Myelinated nerve fibre diameter (μm)
C57BL
F hybrid
1

24 weeks old

7.4 DISCUSSION.

The postnatal developmental morphometric findings in relation to the optic nerve of the inbred C57BL mouse strain and its (C57BL x CBA) F_1 hybrid are compared here. The sequence of events during the postnatal development of the optic nerve in both strains of mice is similar. In both strains of mice the optic nerve grows in size well into adult life while myelinogenesis which begins by the end of the first week of postnatal life is completed during early adulthood.

In both inbred and hybrid strains the optic nerve grows in calibre very rapidly during the juvenile period of postnatal development i.e. from the first week of postnatal life up to the end of the fifth week. Maximum rate of increase in size occurs during this period. Although growth in size of the nerve continues well into adulthood, after the juvenile period it proceeds at a slower rate which progressively tails off with age. In both C57BL and F_1 hybrid the optic nerve grows at a similar rate during the juvenile period of life, but after this period the optic nerve of the C57BL grows at a significantly faster rate than that of the F_1 hybrid. This finding suggests that the optic nerve in the mouse increases in size from birth well into adulthood, but that its absolute size at any time after birth may be strain dependent.

This pattern of postnatal development observed here in the optic nerve of the mouse, whereby an initial rapid growth in size is followed by a progressively slower rate of growth has also been reported to be the case in humans, although the timing of events is clearly different. Rimmer et al., (1993) observed that, in the human optic nerve, 50% of the size of the adult optic nerve is attained by the 20th week of gestation, 75% at birth while 95% of adult size is reached before the first birthday. Similar findings to those seen in the mouse were earlier reported in the rat (Matheson, 1970; Hirose & Bass, 1973; Tennekoon et al., 1977) in which the period of maximum growth occurred within the first three weeks of postnatal life, and is followed by a period of slower growth which commences during the fifth week of postnatal life, and gradually decreases with age. The picture in the cat,

however, is slightly different in that growth is steady from the embryonic period well into adulthood (Ng & Stone, 1982). For example, in the cat the csa of the optic nerve is 0.037 mm^2 at embryonic day 30, 0.29 mm^2 at birth and 2.38 mm^2 in the adult. Only 38% of the adult csa is attained at postnatal day 15 and by postnatal day 120 the csa of the nerve is just about half of its adult value. From the analysis of various mammalian species, it is evident that the pattern of growth of the optic nerve is species dependent. Whereas in both the mouse and the rat maximum growth takes place during the early postnatal period and growth in the size of the nerve continues well into adulthood, in the human maximum growth occurs from about the middle of prenatal life through to the first week of life, while in the cat growth is steady from the embryonic period to advanced adulthood.

The diameter of the optic nerve is largely controlled by the number of axons in the nerve, axon diameter, the extent of myelinogenesis of each axon and the growth of the glial component present in the nerve (Ng & Stone, 1982). The significance of the number of axons to the size of the nerve is indicated by the fact that the adult nerve 'shrinks' considerably if the axons degenerate, for example, after enucleation (Ng & Stone, 1982). The continuous growth in size of the nerve observed during the period of massive reduction in axon number indicates that factors other than the number of axons play a significant role in determining the size of the nerve at this stage of its postnatal development. Furthermore, the period of maximum rate of growth in calibre of the nerve occurs during the period of maximum rate of myelinogenesis, and this is not surprising since myelinogenesis results in an increase in both the total number of myelinated fibres present and axon diameter of individual fibres. The latter results in an increase in both the thickness of the axons and the number of large nerve fibres present. The continuous increase in size of the nerve observed after the completion of myelinogenesis would suggest that this is principally due to the growth of the glial component on the size of the nerve at this stage of development.

Findings from the present study indicate that myelinogenesis in both inbred C57BL and the F_1 hybrid commences by the end of the first postnatal week proceeding at a rate that parallels that of growth in the calibre of the nerve during the juvenile period and the early part of the adult life of the animal in both strains of mice. However, unlike the growth in size of the nerve, myelinogenesis is completed early in adulthood in both strains of mice. The time course for myelinogenesis in both strains of mice is therefore similar. During the juvenile period myelinogenesis progressed at a slightly faster rate in the F_1 hybrid than in the C57BL parent inbred (this difference, however, is not statistically significant). This was evident from the fact that the number of myelinated nerve fibres as well as the number of myelin lamellae per axon were generally higher in the F_1 hybrid than in the C57BL during this period. Furthermore, the myelin lamellae were more densely wrapped around their axons in the F_1 hybrid than in the C57BL during the same period. The significant difference in the density of the myelinated nerve fibres observed between corresponding 3 weeks and 5 weeks age groups during this period could be explained by the relative difference in rates between myelinogenesis and growth in size of the nerve. Although both events proceeded rapidly during this period, myelinogenesis was considerably faster in the F_1 hybrid than in the C57BL.

The pattern of myelinogenesis in the mouse is similar to that of the mammals already cited above, though with a species-specific and variable time course. In the cat, for example, Ng & Stone (1982) observed no myelinated nerve fibres in the oldest prenatal material taken at embryonic Day 61 (E61). At the first postnatal day, 3% of axons were myelinated, suggesting that myelinogenesis in the optic nerve of the cat starts in the last few days of gestation and involves mainly the large fibres at this stage. There was a rapid increase in the number of myelinated fibres immediately after birth, so that by 30 pnd, 90% of the fibres had been myelinated and the adult level (95%) was achieved by the 55th pnd. These findings confirmed those reported earlier in controls of this species by Moore et al. (1976). Observations made in the rat (Conradi et al., 1989) indicate that myelinogenesis in the optic

nerve follows a similar time course to that in the mouse. These workers observed no myelinated nerve fibres in the optic nerve of their 5pnd control rats, but when myelinogenesis started it progressed rapidly so that in a 12pnd rat the number of myelinated nerve fibres present in the optic nerve was 9 000, rising to 67 000 at 20 pnd and 127 000 at 30pnd (also see Black et al., 1982; Hunter & Bedi, 1986).

After the juvenile period is completed myelinogenesis proceeded at a significantly faster rate with an earlier completion in the C57BL than in the F_1 hybrid. The highest mean myelinated nerve fibre count which corresponded to the time of peak myelinogenesis in each of the two strains was observed in the C57BL. It is presently not clear why myelinogenesis initially proceeds at a slightly faster rate in the F_1 hybrid than in its parent inbred C57BL nor why it subsequently significantly lags behind after the completion of the juvenile period. It is, however, evident from the present findings that by the time myelinogenesis is completed in the optic nerve of the parent C57BL strain, approximately 6.5% of the fibres in the F_1 hybrid are still unmyelinated.

The progressive decrease in the mean myelinated nerve fibre count observed with age after the completion of myelinogenesis in both strains of mice, would seem to suggest that a progressive elimination of myelinated nerve fibres was occurring. Nerve fibres in the middle part of the nerve fibre size spectrum appeared to be maximally affected by this fall in nerve fibre count. This was evident from the observation that there was a drop in the proportion of the medium size fibres in both strains of mice after myelinogenesis was completed and this was in contrast with the rise in the respective proportions of both the small and large size fibres during the same period. The normal development of the nervous system is associated with an initial over-production of non-myelinated nerve fibres which is followed by a period during which degeneration of both unmyelinated and myelinated fibres occurs, so that eventually the adult values are achieved (Cantino & Daneo, 1972; Hughes & McLoon, 1979; Cunningham et al., 1982; Jeffery & Perry, 1982; Lam et al., 1982; Ng &

Stone, 1982; Perry et al., 1983; Cowan et al., 1984; Kirby et al., 1988; Nicoll et al., 1991). The initial period of degeneration approximately coincides with the onset of myelinogenesis. In the human optic nerve, an apparent over-production of axons occurs principally during the first half of intrauterine life, and this is followed by a loss of about 70% of these axons between 16 and 30 weeks of intrauterine life (Provis et al., 1985; Repka & Quigley, 1989). The present report confirms the earlier suggestion in chapter 5 (5.4) that in the mouse, after completion of myelinogenesis, the optic nerve still has more than the optimum number of myelinated nerve fibres needed for adequate vision in this species, and that the reduction process (which from that time involves only myelinated nerve fibres) proceeds well into adult life thereafter.

The remarkable reduction in the mean myelinated nerve fibre count which was seen soon after completion of myelinogenesis in each strain of mice suggests that the process of reduction of myelinated nerve fibres could have started earlier during the postnatal period, and proceeded even after myelinogenesis is completed, though, at a decreasing rate thereafter. The significant difference in mean myelinated nerve fibre counts noted between the corresponding 24 weeks groups of both strains of mice resulted from the fact that as the number of myelinated nerve fibres in the optic nerve of the C57BL was becoming stabilized, the reduction process in the F_1 hybrid was at its peak. Furthermore, the progressive reduction in the nerve fibre density in both strains of mice following the completion of myelinogenesis is not surprising given that, although there was no further increase in the number of myelinated nerve fibres thereafter, the nerve continued to grow in size.

All age groups of both mouse strains studied had a nerve fibre diameter spectrum that was unimodal with a positive skewing. The myelinated nerve fibre diameter spectrum was narrow during the early postnatal period but broadened with age, though fibres with a diameter greater than 2.0μm were not encountered. The myelinated fibres in the F_1 mice were generally smaller in diameter than those in the C57BL strain. Thus the modal diameter

of myelinated fibres from 3 weeks on for the F_1 mice was 0.40μm, and the largest fibre measured in this strain of mice was 1.72μm. The corresponding values for the C57BL were 0.48μm and 1.92μm, respectively. This finding is consistent with observations previously reported in adult groups of mice chapters 3 and 4 and those of other authors that, the optic nerve of the mouse is predominantly populated by small diameter nerve fibres (also see Gyllensten & Malmfors, 1963; Gyllensten et al., 1966; Dangata et al., 1994, 1995).

There was a sudden reduction in the modal diameter in both strains of mice after the second week to its adult value in each case. This value (i.e. 0.48μm in the C57BL and 0.40 μm in the F_1 hybrid) fell within the medium fibre diameter group (see 5.3.2 for fibre grouping for the purpose of this study). This suggests that, although myelinogenesis in the optic nerve of the mouse starts predominantly among fibres that were to become large fibres in the adult optic nerve, it continued mainly among the medium diameter fibre group soon afterwards. Whereas in both strains of mice the proportion of medium size fibres continued to decline with age following completion of myelinogenesis, that of the large fibres was rising. This suggests that the reduction process seen among the myelinated nerve fibres following completion of myelinogenesis affected mainly the medium size fibres. Furthermore some fibres classified as medium size fibres earlier during the process of myelinogenesis, having undergone axonal growth and acquired more lamellae of myelin, increased in size and moved from the medium fibre component into the large fibre component of the nerve fibre size spectrum.

It has been shown from the present study that the postnatal development of the F_1 hybrid mouse runs a similar course with that of its parent inbred C57BL strain, although at a relatively slower rate. Mean values for morphometric parameters for the F_1 hybrid are generally lower than those for the C57BL inbred. For example, mean csa, mean myelinated nerve fibre count at peak myelinogenesis, mean nerve fibre density at peak myelinogenesis and the modal diameter for myelinated nerve fibres are higher for the inbred C57BL than for

the F_1 hybrid. The myelinated nerve fibre diameter spectrum is broader in the inbred than the hybrid F_1. An earlier report (chapter 3) from the analysis of adults of both parental strains i.e C57BL and CBA, and their F_1 hybrid indicated that values for these morphometric parameters for the F_1, except for the mean nerve fibre count, lie between those of the parents strains, with those of the CBA strain being the lowest (also see Dangata et al., 1995;). The present findings have also shed more light as to why the mean nerve fibre counts for the F_1 hybrid mice were higher than those obtained from the analysis of the inbred C57BL in these reports. In these earlier reports the analysis of 11 weeks old mice of each strain was carried out. By this age myelinogenesis had just been completed in the C57BL while the process of reduction of myelinated nerve fibres was at its peak. The result of this was a reduction in the mean myelinated nerve fibres in this mouse strain from the mean value observed at the time of peak myelinogenesis. By contrast, in the optic nerve of the F_1 hybrid mouse at this age myelinogenesis was attaining to its peak while only minimal reduction of myelinated nerve fibres was taking place. The net effect of this was an increase in the mean myelinated nerve fibre count observed in the optic nerve of the F_1 hybrid mouse at this age. This also shows the result of genetic cross breeding between inbred strains on the postnatal development of offspring. The analysis has also allowed confirmation of the fact that the postnatal development of the optic nerve in the mouse is typical of that reported in other mammalian species.

CHAPTER EIGHT

MORPHOMETRIC ANALYSIS OF THE EARLY POSTNATAL TERATOGENIC EFFECTS OF ACUTE ALCOHOL EXPOSURE TO THE PRENATAL MOUSE OPTIC NERVE.

Contents

8.1 Introduction

8.2 Materials and Methods

8.3 Results

8.3.1 Cross-sectional area (μm^2)

8.3.2 Total myelinated nerve fibre counts

8.3.3 Myelinated nerve fibre density (fibres $1000\mu m^{-2}$)

8.3.4 Myelinated nerve fibre diameter spectrum

8.4 Discussion

8.1 INTRODUCTION.

Since the clinical entity, Fetal Alcohol Sydrome (FAS) was first described in man (Jones & Smith, 1973; Jones et al., 1973, 1974), a number of clinical and experimental studies have been carried out to investigate the pathogenesis of this condition. Reports from the use of animal models have shown that the syndrome is both species and strain dependent (Schwetz et al., 1978; Schenker et al., 1990). The mouse and the rat have been used to study FAS (Abel et al., 1981; Garro et al., 1991; Middaugh & Boggan, 1991; Kotch et al., 1992; Zajac & Abel, 1992; Pinazo-Duran et al., 1993). Considerable strain differences in sensitivity to alcohol have been reported in the mouse (Chernoff, 1977 & 1980; Cook et al., 1987; Gilliam et al., 1990). For example, using three different strains of mice, Chernoff (1980) observed that the CBA embryo was the most sensitive to the teratogenic effects of prenatal alcohol insult followed respectively, by the C3 and the C57BL strains of mice. The C57BL/6J was more sensitive to alcohol than the *long-sleep* or the *short-sleep* mouse (Gilliam et al., 1990).

The degree of susceptibility of individual organs to the teratogenic effects of alcohol varies considerably, the critical factors being: the time of exposure, the dose and frequency of alcohol given (Abel et al., 1980; Webster et al., 1983; Cook et al., 1987; Adickes, 1990; Michaelis, 1990; Kotch et al., 1992; Zajac & Abel, 1992; Ashwell & Zhang, 1994). The central nervous system (CNS) is one of the most sensitive systems to alcohol exposure. In this regard, the optic nerve has been extensively studied in experimental models to investigate the effects of alcohol on the CNS (Cohen, 1967; Ehyai & Fremon, 1983; Pinazzo-Duran et al., 1993). Although some reports are available on the morphometric analysis of the long-term effect of acute prenatal exposure of the optic nerve in the mouse to alcohol (Parson et al., 1993, 1995; Ashwell & Zhang, 1994; Parson & Sojitra, 1995), no detailed analysis of the early postnatal period is presently available.

The aim of the present study was to investigate the effect of a single prenatal exposure to alcohol on the early postnatal development of the mouse optic nerve. Brother x sister matings of mature (C57BL x CBA) F_1 hybrid mice were carried out. Pregnant female mice were divided on day 12 p.c. into a control and an experimental group. The experimental group was given a single intraperitoneal (ip) dose of 0.015ml/g body weight of 25% alcohol while the control group was given an equivalent volume of normal saline. The optic nerves were isolated from the offspring of both control and experimental groups at various postnatal ages and analysed by light and electron microscopy. It is suggested that this experimental study may shed light on the phenomenon of 'binge' drinking in pregnancy.

8.2 MATERIALS AND METHODS.

Brother x sister matings of superovulated female with male (C57BL x CBA) F_1 hybrid mice were carried out. The presence of a vaginal plug observed the next morning was considered as evidence of mating and this was taken as 0.5 p.c. Pregnant mice were maintained under a 14 hour - 10 hour light - dark cycle with food and water available ad libitum. On day 12 p.c. these were divided into an experimental and a control group. Each mouse in the experimental group was given a single intraperitoneal dose of 0.015ml /g (volume:weight) solution of 25% alcohol in distilled water. This dose has been shown to produce a peak blood alcohol level of 500-600mg/dl and this is sufficient to produce teratogenic effects (Webster et al., 1983; Ashwell & Zhang, 1993). The control group was treated with 0.9% saline in a similar way. Offspring of both experimental and control groups were used at the appropriate age for this analysis. Those that were to be used after the age of 3 weeks were weaned at this age and maintained on a diet similar to that of the parents.

Five mice from each age group of both control and experimental groups were studied at 2, 3 and 5 postnatal weeks. The 5th postnatal week has already been reported in chapter 5 as the time when the phase of rapid postnatal development of the optic nerve in the mouse is completed, with the entire period from birth to the 5th postnatal week corresponding to the juvenile period of the life of the animal (also see Dangata et al., 1996). Following anaesthesia with 0.02ml/g body weight of 1.2% solution of Avertin in 0.9% saline and perfusion with 2.0ml/g body weight of a 2.5% solution of glutaraldehyde in 0.1M phosphate buffer, the optic nerves from both control and alcohol-treated mice were isolated and processed for morphometric analysis by means of light and electron microscopy as has already been described. The results of the morphometric parameters measured in the corresponding age groups of experimental and control mice were statistically tested as decribed in chapter 2 to establish whether there was a significant difference in these parameters between the groups.

Preliminary findings showed that the optic nerves of the experimental groups were generally greater in diameter than those of the corresponding age groups of the controls, although, the difference in csa was significant only between the correseponding 2 and 3 weeks old control and experimental mice. This was in contrast to an earlier report by Ashwell & Zhang (1994) where a decrease in the csa of the optic nerve of 15 day old mice following acute prenatal exposure of C57BL/6 pregnant mothers to alcohol on day 8 p.c. They used two similar (consecutive) doses of alcohol to that used in the present study. There was an interval of 4 hours between the two doses. This interesting csa finding in the present study made me curious to want to establish if it was a true deviation from the finding observed by Ashwell & Zhang (see the Discussion section). In order to do this the optic nerves from 5 mice at 2 and 3 weeks of age from litters isolated from an additional series of alcohol-treated pregnant F_1 mothers were analysed as indicated above.

Although it has earlier been reported in chapters 5 and 6 (also see Dangata et al., 1996) that myelinogenesis in the mouse begins on the 5th pnd, the present study was undertaken to establish whether prenatal exposure to alcohol affects the time of onset of this process. In order to do this, 2 additional mice each at 8, 7, 6 and 5 postnatal days (pnd) of age were isolated from both experimental and control groups of mice and treated as indicated above. Photomicrographs of the optic nerve in these latter groups were taken at a magnification of 22,000 and printed to a final magnification of x 66,000. This was in order to allow for the visualization of any myelin sheaths that could not be seen at the lower magnification.

8.3 RESULTS.

8.3.1 CROSS-SECTIONAL AREA (μm^2).

In both alcohol- and saline-treated mice the optic nerve could be dissected from eyeball to optic chiasma. The meningeal coverings around the nerve were well defined in both groups of mice. The optic nerve grew in size rapidly in the early part of the juvenile period of life but began to decline towards the end of this period. The maximum rate of growth was seen between the second and the third week of postnatal life. The rate of growth was greater in the control group than in the experimental group. For example, in the controls the increase in csa between the 3rd and the 5th weeks was approximately 53% of the increase between the 2nd and the 3rd weeks. This was in comparison with 14% for the experimental group over the same period of time. The optic nerves of the experimental groups were, however, generally greater in diameter than those of the corresponding age groups of the controls. The difference in csa was significant between corresponding 2 and 3 weeks old mice, but by the 5th week it was no longer significant as shown in Tables 8.1 and 8.2. The csa findings (and all the other morphometric parameters analysed in the previous groups of alcohol-treated mice) from the latter groups of alcohol-treated mice were comparable with those previously analysed. Because of this, the sample size for the 2 and 3 weeks alcohol-treated mice were pooled together.

Age (Weeks)	Parameter analysed (± s.e.m.)					
	cross-sectional area (μm^{-2})		Mean myelinated nerve fibre count		Mean myelinated nerve fibre density (fibres1000μm^{-2})	
	Alcohol*	Saline*	Alcohol*	Saline*	Alcohol*	Saline*
2	41070±1813	35607±2516	18375±1599	20114±1579	444±29	563±19
3	46921±2553	41569±1201	35795±1892	40616±3338	770±22	977±74
5	48527±1706	47860±2474	55606±2364	62987±5019	1150±39	1304±57

Table 8.1 Morphometric parameters analysed in optic nerve of alcohol and saline-treated (F_1 x F_1) F_2 mice during the juvenile period of postnatal development. * = number analysed: Alcohol - 2wks = 16, 3wks = 18, 5wks = 10; Saline - 2wks = 9, 3wks = 7, 5wks = 8.

Age (weeks)	Parameter Analysed		
	Cross-sectional area	Myelinated nerve fibre count	Myelinated nerve fibre density
2	$0.01 \leq P \leq 0.05$	n.s.	$0.01 \leq P \leq 0.05$
3	$P \leq 0.01$	$P \leq 0.01$	$0.01 \leq P \leq 0.05$
5	n.s.	$P \leq 0.01$	$P \leq 0.01$

Table 8.2 Level of significant difference in morphometric parameters analysed in the optic nerve of (F_1 x F_1) F_2 mice during the juvenile period of postnatal development. n.s. = no significant difference.

8.3.2 TOTAL MYELINATED NERVE FIBRE COUNTS.

In the control group, evidence of myelinogenesis was observed in x 66,000 micrographs of optic nerves analysed on the 5th pnd as the presence of promyelin around the large fibres in the optic nerve (see chapter 6). Myelinogenesis was more obvious by the 6th pnd as it was possible at this age to distinguish between 1-2 distinct myelin lamellae loosely wrapped around some of the largest axons; by the 8th pnd up to 3-4 myelin lamellae could be counted around some of the large axons. In the experimental group, only the presence of promyelin could be observed around some of the large fibres by the 6th pnd and by the 8th pnd not more than 1-2 myelin lamellae could be seen per axon. The myelin lamellae in both control and alcohol-treated groups of mice at this stage were loosely wrapped around the axons. In both control and experimental groups, myelinogenesis progressed rapidly following the onset of this process, with the maximum rate of increase seen between the 2nd and the 3rd weeks; and by the 5th week myelinated nerve fibres dominated the optic nerve in both control and experimental groups. The myelin lamellae became more densely packed around their axons in both controls and experimental groups of mice with time (see Figure 8.1). As in the case of the csa, myelinogenesis progressed faster in controls than in the experimental group. Initially there was no significant difference between control and experimental groups, but from the 3rd week onwards the difference was significant (see Tables 8.1 and 8.2).

Figure 8.1: Micrographs of transverse sections of the optic nerve (x 66,000) from both alcohol-treated and control mice. There is a progressive increase in the number of myelinated nerve fibres in the optic nerve with age. This is associated with a corresponding decline in the population of unmyelinated nerve fibres with age so that by the 5th week the myelinated nerve fibres dominate the optic nerve in both controls and alcohol-treated mice. At any age more myelinated nerve fibres were present in the optic nerve of controls than in the corresponding age groups of the alcohol series. In each series of mice the number of myelin lamellae per axon increased and became more compact with age. a): 2 weeks control, b): 2 weeks alcohol-treated, c: 5 weeks control, 5 weeks alcohol-treated.

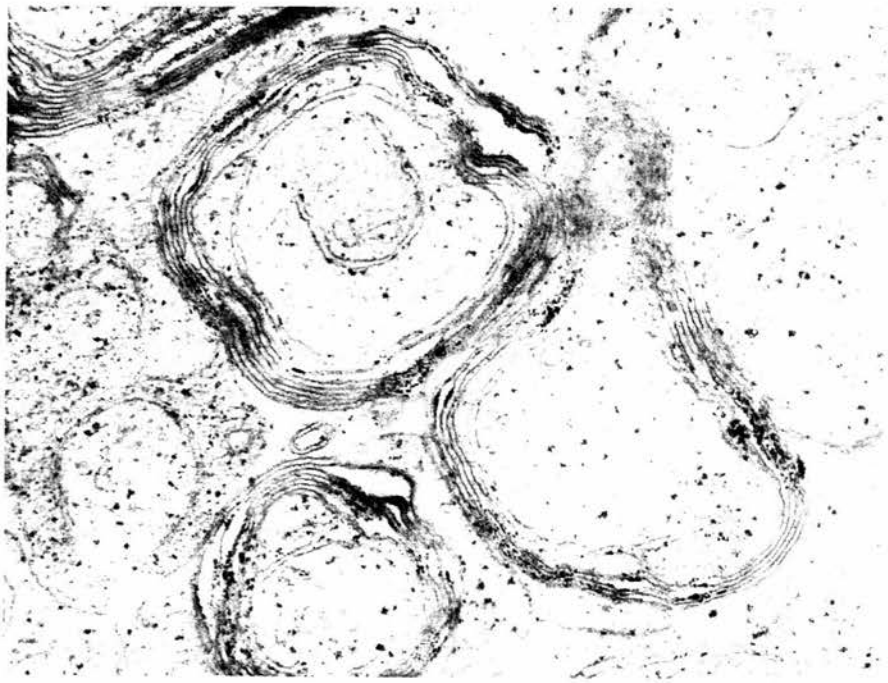

a

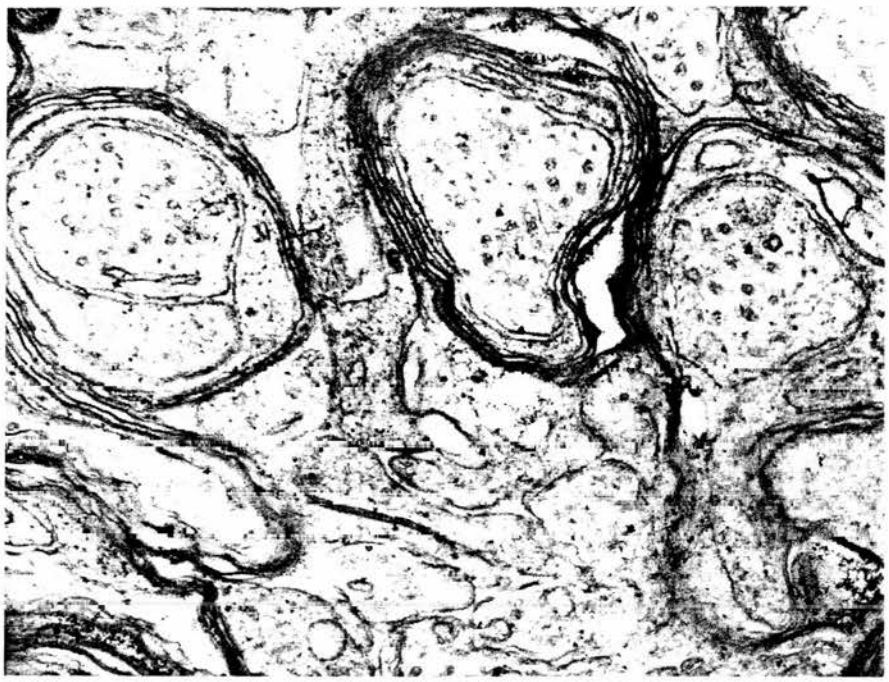

b

Figure 8.1

c

d

8.3.3 MYELINATED NERVE FIBRE DENSITY (FIBRES 1000μm^{-2}).

In both control and experimental groups of mice there was a rapid increase in the numerical density of the myelinated nerve fibres. The mean values for the myelinated nerve fibre density for controls were always higher than those of the alcohol-treated mice. The difference in density between the corresponding age groups of control and experimental animals was significant for all the age groups analysed (see Tables 8.1 and 8.2).

8.3.4 MYELINATED NERVE FIBRE DIAMETER SPECTRUM.

The smallest myelinated nerve fibres measured in any of the series were 0.16μm in diameter. The largest fibres measured were 1.60μm and 1.36μm in diameter, respectively, for the control and experimental groups and this was noted in the 5 weeks old mice. The distribution of the myelinated nerve fibres in the optic nerve was unimodal with a positive skewing for all ages in both the controls and in the experimental groups. The spectrum of distribution broadened, although, not significantly with age in favour of the large fibres more than the small. The spectrum was broader in the control series than the corresponding age groups of the experimental series. Figure 8.2 presents the spectrum of myelinated nerve fibres in optic nerve of the various age groups of each series of mice. At any age the medium diameter fibres dominated the optic nerve in each of the series. With increasing age the proportions of both small and medium size fibres increased in the experimental group compared with the controls. The reverse phenomenon was observed in the case of the large diameter fibres. These differences were, however, not statistically significant.

Figure 8.2: Graphs showing myelinated nerve fibre diameter spectrum by age in the optic nerve of alcohol-treated and control groups of mice. In both alcohol-treated and controls, the spectrum of distribution is unimodal with a positive skew, and broadens with age. The spectrum is, however, broader in controls than the corresponding age groups of alcohol-treated groups. a): 2 weeks old, c): 3 weeks old, c): 5 weeks old.

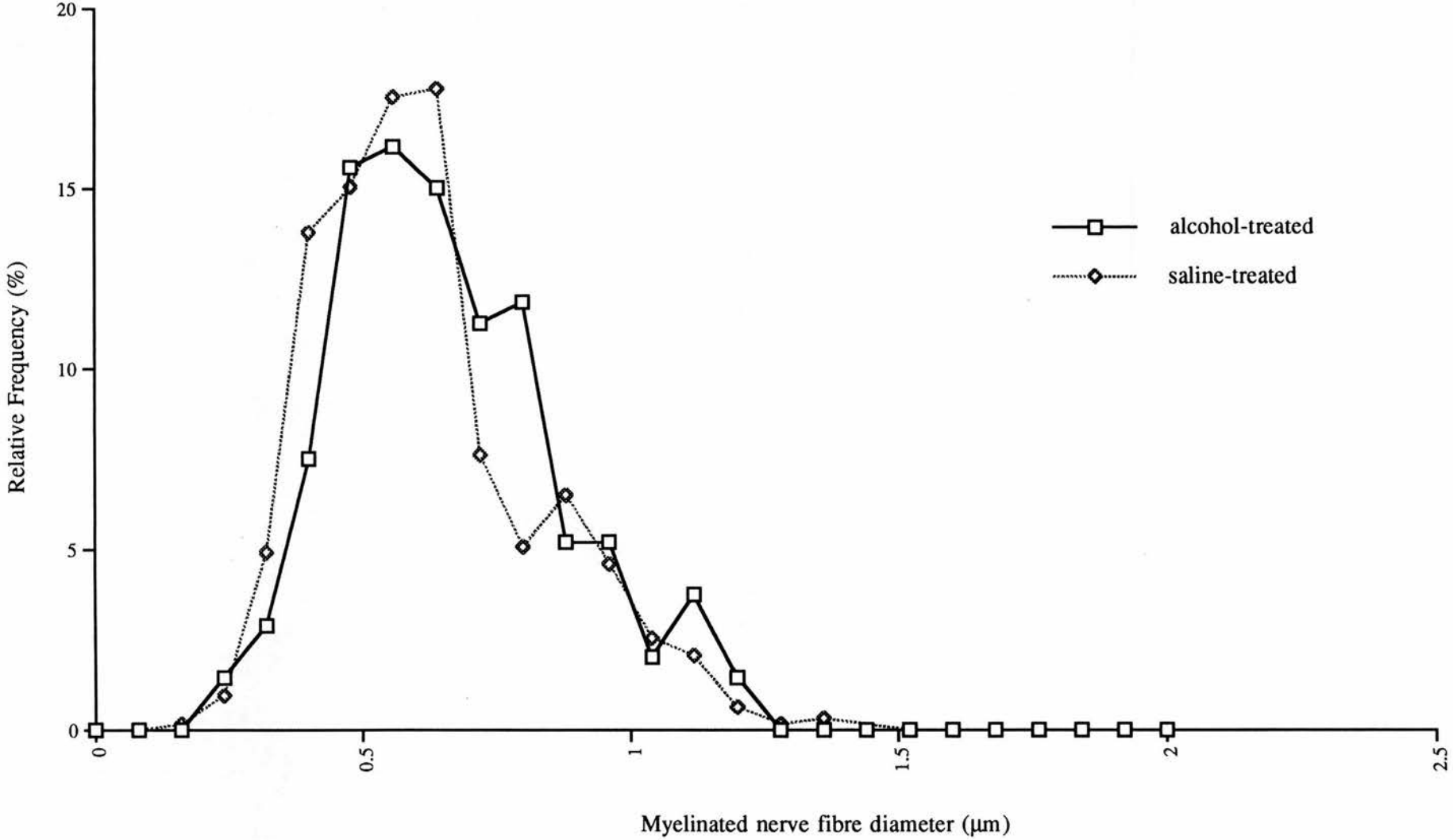
20
15
10
5
0
Relative Frequency (%)
0
0.5
1
1.5
2
2.5
Myelinated nerve fibre diameter (µm)
alcohol-treated
saline-treated

2 Weeks old

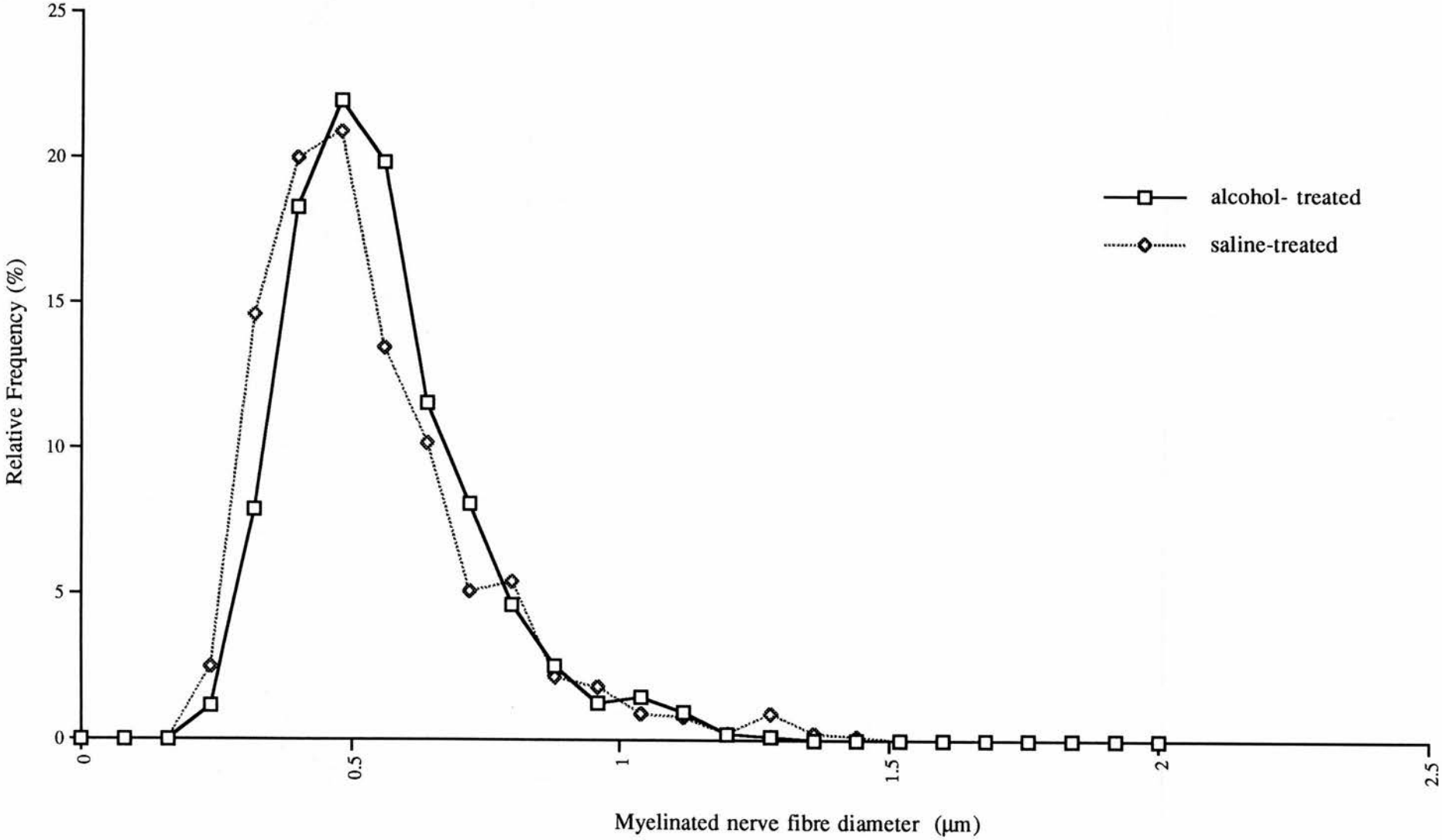
25
20
15
10
5
0
Relative Frequency (%)
0
0.5
1
1.5
2
2.5
Myelinated nerve fibre diameter (μm)
alcohol- treated
saline-treated

3 Weeks old

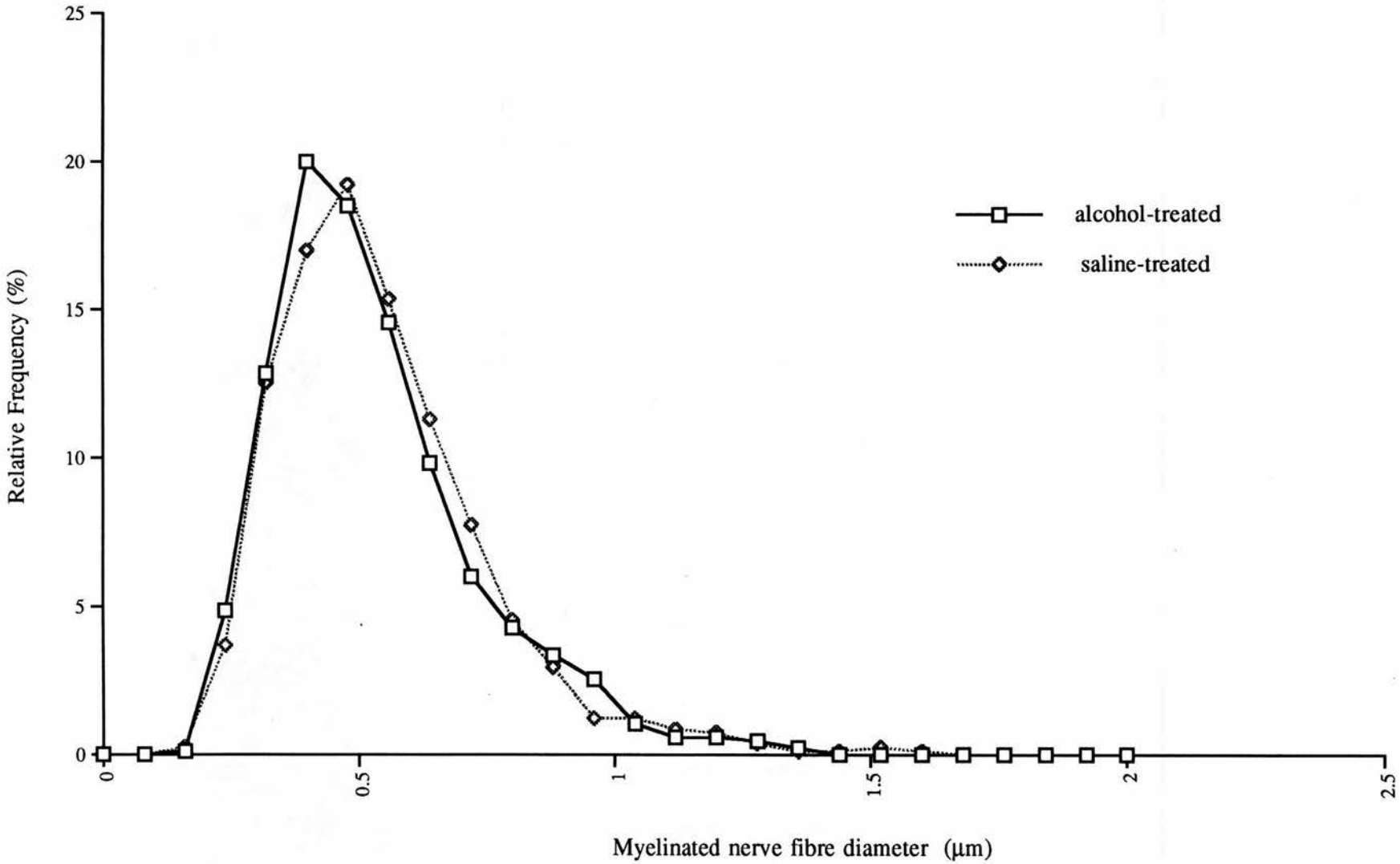
25
20
15
10
5
0
Relative Frequency (%)
alcohol-treated
saline-treated
0
0.5
1
1.5
2
2.5
Myelinated nerve fibre diameter (µm)

5 weeks old

8.4 DISCUSSION.

The optic nerves from the offspring of F_1 hybrid female mice given a single intraperitoneal dose of alcohol on day 12 of gestation and appropriate controls were analysed using light and electron microscopy and have demonstrated that there was a significant effect on morphometric parameters of the optic nerve when this is assessed at intervals during the postnatal period. It was observed that exposure to a single dose of alcohol taken at a critical period of gestation had a significant teratogenic effect. Children with features of FAS are known to have been born to mothers who had just a single dose of alcohol during pregnancy (Kronick, 1976; Hermann et al., 1980; Clarren, 1981; Padmanabhan et al., 1984).

In both controls and experimental groups of mice the optic nerve grew rapidly in calibre during the juvenile period of development. The maximum rate of growth was seen between the second and the third week of postnatal life. At any age the rate of growth in the calibre of the optic nerve was higher in controls than in the experimental groups, although, at decreasing level of significance with age. For example, up to the third week the calibre of the optic nerve of offspring of alcohol-treated mice was significantly larger than that of controls, but by the end of the juvenile period i.e. the 5th postnatal week, the difference had ceased to be significant. It has been noted in chapter 7 that the csa of the optic nerve is a function of factors such as the number of axons in the nerve, axon diameter, the extent of myelinogenesis of each axon and the growth of the glial component present in the nerve (also see - Ng & Stone, 1982; Dangata & Kaufman, 1996). The present observation in the mouse would suggest that factors other than myelinogenesis alone, which is more intense in the controls than in the alcohol series (see later), have a greater effect on the overall size of the optic nerve at this stage of postnatal development.

It is not yet clear why the size of the optic nerve in the experimental group was initially significantly larger than that of the control group, though this may reflect a degree of tissue

oedema. This finding was in contrast with the small calibre optic nerve that has earlier been reported in the rat by Pinazo-Duran et al. (1993). In their study, alcohol was administered in the diet to female rats six weeks before pregnancy and throughout the gestation period than a single acute exposure as in the present study. Findings by Ashwell and Zhang (1994) with regard to the size of the optic nerve following acute exposure of C57BL/6 pregnant mice to alcohol on day 8 p.c. were similar to those of Pinazo-Duran et al. This strongly suggests that in the study of alcohol teratogenicity the selection of an appropriate critical period is more important than the duration of administration. For example, in these two previous studies alcohol was administered before the formation of the optic stalk which determines the size of the optic nerve (Kaufman, 1979, 1992; Rugh, 1990); whereas in the present study, by the time alcohol was administered the optic stalk had already been formed.

In both experimental and control groups myelinogenesis progressed rapidly during the early part of the juvenile period, although, both its onset and the rate of its progression in the experimental group significantly lagged behind that of the controls. This was clearly shown by the presence of a significant difference between the two groups of mice in their mean myelinated nerve fibre count after the second week as well as a significant difference in their mean nerve fibre density throughout the juvenile period. Although it has been reported in chapter 5 that myelinogenesis in the optic nerve of the mouse is entirely a postnatal event (also see - Gyllensten & Malmfors, 1963; Gyllensten et al., 1966; Dangata et al., 1996), the present findings suggest a significant influence on its time of onset and progression by prenatal factors. The precursors of the myelin sheath in the central nervous system (CNS) are oligodendrocytes (Matthews & Duncan, 1971; Tennekoon et al., 1977; Dentinger et al., 1985; Asou et al., 1994; Umemori et al., 1994; Asou et al., 1995). As has already been reported in chapter 6 (also see - Asou et al., 1994; 1995), these cells develop from glial cell precursors following their cytodifferentiation. Asou et al. (1994, 1995) observed that, during the first stage of cytodifferentiation, small, round and 'glossy' cells,

the type-1 oligodendrocytes, differentiate from the glial cell precursors. These develop into type-2 oligodendrocytes which are capable of undergoing mitosis and possess cell processes. The type-3 oligodendrocytes are the mature form which arise following the differentiation of the type-2 cells. The type-3 oligodendrocytes are characterised by the presence of numerous processes and are seen shortly before the onset of myelinogenesis. These cells also synthesise myelin basic protein (also see Tennekoon et al., 1977) which constitutes 30% of the protein in the CNS and has previously been shown to be important for CNS function (Warrington et al., 1993).

In the present study the lag in the onset and the rate of progression of myelinogenesis together with the significant difference in mean myelinated nerve fibre count and density would suggest that alcohol exerts a significant teratological effect on the glial precursors of oligodendrocytes or on their cytodifferentiation, and that this could result in a reduction of both their number and their competence to synthesize myelin. On the effect of alcohol on myelinogenesis of the optic nerve in the rat, Phillips and his co-workers (Phillips, 1989; Phillips et al., 1991; Phillips & Krueger, 1992) observed a delay in oligodendroglial cell maturation and a reduction in the number of oligodendrocytes produced. This resulted in a delay in the onset of myelinogenesis. They also reported a decrease in the myelinated nerve fibre count as well as the myelin thickness per axon. The impairment in the development of myelin and consequently the myelin sheath in the optic nerve could explain some of the clinical neurological and visual dysfunctions associated with prenatal alcohol exposure.

Experimental studies involving the histological analysis of other parts of the CNS have given similar findings to those reported in the present analysis and those on the optic nerve of the rat cited above with regard to the teratogenic effect of alcohol on myelinogenesis. In a chronic prenatal exposure of pregnant rats to dietary alcohol, Miller and al-Rabial (1994) observed a

decrease in the space occupied by axons in the pyramidal tract in the alcohol-treated rats. The myelinated nerve fibres were smaller with a thinner myelin sheath. These observations confirmed an earlier report on alcohol-exposure in relation to the cerebral cortex by Miller (1993). In another report, Lancaster et al. (1982; 1984) observed a decrease in brain myelin and a delay in brain myelin synthesis following exposure of rats to acute doses of alcohol. They also reported abnormalities of the oligodendrocytes and myelin development during the rapid brain growth spurt. These findings further confirm that, given at an appropriate critical period, an acute dose of alcohol can affect CNS development.

Although a relatively higher proportion of large fibres in both controls and experimental groups was seen early in life, the medium diameter fibres dominated the optic nerve at any age. However, the spectrum of distribution of the fibres was generally broader in the controls than in the corresponding experimental age groups. During myelinogenesis myelinated nerve fibres progressively move from one part of the myelinated nerve fibre spectrum to another until they have been fully myelinated i.e. following the acquisition of the maximum number of myelin lamellae proportional to their mature size. The present findings would suggest that, in alcohol teratogenicity, in addition to a delayed onset, there is a premature arrest of the process of myelinogenesis in individual nerve fibres before they attain their final size. This is further suggested by the fact that the proportions of small and medium diameter myelinated nerve fibres in the experimental groups were greater than those of the appropriate controls, whereas the reverse phenomenon was the case with the large diameter fibres. As has been reported earlier in the present study, the size of a myelinated nerve fibre is a function of the thickness of its myelin sheath as well as the number of myelin lamellae it has acquired. However, it should be noted that myelinogenesis has yet to be completed in the optic nerve of the mouse by the end of the juvenile period.

The findings from this study indicate that prenatal exposure of the fetus to alcohol influences both the pre- and postnatal development of the optic nerve. Indirect evidence suggests that myelinogenesis, for example, is probably affected due to interference with oligodendroglial cytodifferentiation the result of which could be a delay in the onset of myelinogenesis and its subsequent progression.

CHAPTER NINE

GENERAL DISCUSSION.

Contents

9.1 Dimorphism in the mouse optic nerve

9.2 The normal postnatal development and growth of the mouse optic nerve

9.2.1 Cross-sectional area of the mouse optic nerve

9.2.2 Myelinogenesis in the mouse optic nerve

9.3 Mutational effects on the morphometric parameters of the mouse optic nerve

9.4 Teratogenic effects on the morphometric parameters of the mouse optic nerve

9.5 Clinical implications of the present research

9.1 DIMORPHISM IN THE MOUSE OPTIC NERVE.

In any species there is variable degree of heterogeneity among individual members, it therefore becomes necessary to quantify the level of variation and establish whether or not this is significant. Although some strains of mice (some of the inbred strains, for example) have been used as experimental models to study the physiological functions of the visual system (Gyllensten & Malmfors, 1963; Gyllensten et al., 1966; Drager & Hudel, 1978; Strain & Telford, 1993), this is the first comprehensive morphometric account of any part of this system in different strains of this species.

It has been possible from the present study to demonstrate some similarities and variable degrees of intra-strain and inter-strain differences in the morphometric parameters of the adult mouse optic nerve. Of the variables analysed in the optic nerve of inbred strains of C57BL and CBA male mice and their F_1 hybrid, the right optic nerve invariably had lower (except for the csa) mean values than the left optic nerve, although, this difference was not significant. An additional similar type of analysis of the optic nerve isolated from a group of CBA females, further showed that there was no significant difference in any of the variables studied between the left and right optic nerves, and between male and female mice, although, the males invariably had higher mean values for the parameters analysed than the females. The findings obtained from the analysis of the optic nerve from adult forms of the *Small eye* mutant *Sey* series i.e. the normal (+/+) and the heterozygous mutant *(Sey/+)* mice were similar in general terms to those from the normal strains of mice, except that in the *Sey* series, it was the heterozygous mutant (*Sey*/+) males that had lower mean values for the parameters analysed than the females. The insignificant difference in the variables measured between individuals of each of the strains studied, both male and female, indicates a considerable degree of inter- and intra-strain uniformity. This would suggest that the genetic constitution of the mouse i.e. either induced by inbreeding or cross-breeding on the one hand as for the inbred and their F_1 hybrid, or by

mutational changes on the other, as for the *Sey*, does not lead to a significant degree of sexual dimorphism in this species.

Significant inter-strain differences were, however, observed between the different mouse strains. It is interesting to note that when comparisons were made between the inbred strains, some significant variations were observed. The C57BL strain had a larger optic nerve with regard to the csa compared with the CBA. Although the C57BL also had a higher population of nerve fibres in their optic nerve than the CBA, the fibres were less densely packed than in the CBA. The CBA optic nerve had a lower proportion of large diameter myelinated fibres, a higher proportion of small and medium size fibres and a smaller value for the mean myelinated nerve fibre diameter than the C57BL. This could explain the fact that it had a higher packing density than the C57BL. The significant difference observed in the variables measured between the inbred strains studied should not be surprising, as this seems to be reasonable evidence of genetic variation induced as a result of many generations ($\geq$ 20) of brother x sister matings required in the establishment of an inbred strain.

Comparing adult (11 weeks old) inbred strains with their F_1 hybrid of the same age, the mean csa value for the F_1 hybrid fell between those of its parent inbred strains. Subsequent findings from the analysis of the inbred C57BL and the F_1 hybrid showed that at peak myelinogenesis and thereafter (see later), the mean myelinated nerve fibre count in the F_1 hybrid was lower than that of the C57BL. It could be extrapolated from the observations made from the age-related study and the analysis of the 11 weeks old mice that values from corresponding postnatal age groups (i.e 2-24 weeks) of the CBA would fall below those of the F_1 hybrid. The situation observed here whereby the values for the morphometric parameters for a hybrid fall between those of its parent strains demonstrates the effect of genetic cross-breeding between inbred strains on their offspring- the offspring display evidence of 'hybrid vigour'.

The optic nerves of the *Sey*/+ series were typically small in size thus conforming with the small size of their eyeball; this was exclusively evident in the heterozygous mutant (*Sey*/+) mice. Although their mean nerve fibre counts were low, the nerve fibres were more densely packed within the nerve than in the optic nerves of the normal strains of mice and their +/+ littermates. It is important to note that, despite having a low mean value for the myelinated nerve fibre population in its optic nerve, the heterozygous mutant (*Sey*/+) still achieves a degree of vision adequate for its 'normal' existence. This suggests that the optimum number of myelinated nerve fibres in the optic nerve required to achieve 'normal' vision in the mouse as a species is relatively low compared with the situation in other mammals such as man, the monkey and the rabbit (Potts et al., 1972a, b; Vaney & Hughes, 1976; Sanchez et al., 1986).

The overall amount of electrical impulses transmitted in the optic nerve is determined by such parameters as the total number of nerve fibres present and their diameter size distribution. The present findings in the mouse further suggest that in this species, of these two parameters, the nerve fibre diameter size distribution plays a greater role on the physiological function of the nerve than their absolute number. This is evident in the fact that the medium size nerve fibres dominated the nerve fibre diameter spectrum in the optic nerve of all the mouse strains analysed. For example, in the *Sey* series the low values for the total nerve fibre counts was not associated with a preponderance of small size fibres as this would have resulted in the acquisition of higher total nerve fibre counts instead; the *Sey* series recorded the lowest percentage of small fibres while having the highest percentage of the medium size fibres. The possibility exists therefore that the medium size fibres are physiologically more important than any other groups of fibres.

Furthermore, with respect to both csa and myelinated nerve fibres of the nerve among the different strains of mice, the general trend was that of an inverse relationship between csa and total myelinated nerve fibre population i.e. strains with a small calibre optic nerve tended to have the nerve fibres most densely packed. For example, the heterozygous mutant (*Sey/+)* being the strain with the smallest optic nerve, had the highest nerve fibre density. While there is no clear explanation for this phenomenon in the mouse, it is likely that mouse strains with small optic nerves tend to maximise the use of available space within the nerve to acquire the optimum number of nerve fibres necessary for adequate visual function. However, the majority of the nerve fibres in optic nerves with a small csa may not necessarily be of the smallest diameter fibre size. For example, the heterozygous mutant (*Sey/+*) optic nerve had the smallest optic nerves and these were surprisingly not associated with the highest percentage of small diameter fibres.

Another similarity encountered among all the mouse strains analysed was the fact that, unmyelinated fibres were rarely encountered in the adult optic nerve, thus suggesting that the genetic variation among member strains of this species bears very little consequence on developmental processes of the optic nerve such as myelinogenesis. This is not surprising since myelinogenesis in the optic nerve of the mouse is entirely a postnatal process as reported from the findings in the postnatal developmental age groups involved in this study (chapters 5, 6, 7 and 8; also see Gyllensten & Malmfors, 1963; Gyllensten et al., 1966; Dangata et al., 1996; Dangata & Kaufman, 1996) and this is well after the *Sey* gene, for example, might have exerted its effects on the development of the visual system. This would suggest that the optic nerve of any strain of this species could be a suitable experimental model for human related studies, for example, developmental processes such as myelinogenesis.

There have been several reports on the result of pressure effect of clinical conditions such as glaucoma on the normal morphometry of the optic nerve in primates such as man and the monkey, (Quigley et al., 1980, 1983, 1987; Quigley & Addicks, 1980, 1981). Although such morphometric reports on glaucoma in rodents (e.g. the mouse, the rabbit, the rat and the guinea pig) are only rarely available (Morrison et al., 1995), these species have been used as experimental models in the study of other aspects of this clinical condition such as the use of drugs in its treatment (Bodor et al., 1988; Camras & Podos, 1989; Huber et al., 1991; Smith et al., 1991; Wu et al., 1995), its effect on morphogenesis (Beauchamp et al., 1985; Garcia-Valenzuela et al., 1995) and pathophysiology (Mermoud et al., 1994). It is clear from these studies that experimental glaucoma can also be induced in the rodent visual system. It has already been established that although the spectrum of the nerve fibre diameter distribution in the primate optic nerve (e.g. man) is wider than that in rodents (e.g. the mouse), it follows the same pattern of distribution in being unimodal with a positive skewing of the nerve fibres. In this regard, the possibility exists that morphometric analysis of the glaucomatous rodent optic nerve may give similar results to those observed in primates. In the mouse, for example, it is possible that the optic nerve of the *Sey* mice might be particularly sensitive to the pressure effect of glaucoma since their nerve fibres are the most densely packed. Conversely, the selective degeneration of large diameter nerve fibres that is associated with glaucoma would be more severe in the C57BL than in any of the other strains.

9.2 THE NORMAL POSTNATAL GROWTH AND DEVELOPMENT OF THE OPTIC NERVE IN THE MOUSE.

The parameters of postnatal growth and development of the optic nerve analysed in the present study were the cross-sectional area of the nerve and myelinogenesis. It has been shown from the present analysis that the nerve continues to grow and develop from birth until well into adult life. The postnatal growth and development of the optic nerve in both C57BL inbred strain and its F_1 hybrid follow a similar sequence of events, and this would suggest the same trend for other strains of this species.

9.2.1 CROSS-SECTIONAL AREA OF THE OPTIC NERVE.

During the juvenile period of postnatal development i.e. from the first week of postnatal life up to the end of the fifth week the optic nerve in both inbred and hybrid strains grows in calibre rapidly, but from the end of this period onwards growth proceeds at a slower rate and this progressively tails off with age. No significant difference in growth rate of the optic nerve was found between the inbred C57BL and their F_1 hybrid during the juvenile period of life, but thereafter growth of the nerve of the C57BL proceeds significantly faster than that of the F_1 hybrid. There is strain dependence, however, for the absolute size of the optic nerve in this species during postnatal development.

In humans recent findings by Rimmer et al. (1993) suggest that most of the growth in size of the human optic nerve takes place before birth (also see chapter 7.4). The initial period of rapid postnatal growth i.e. 2nd-5th weeks observed in the mouse may correspond to the period of prenatal growth up to infancy or early childhood reported in man by Rimmer et al. (1993). Furthermore, while the slower period of growth in the mouse extends from the end of the juvenile period well into adulthood, in man it persists only into early adolescence. This

difference between the situation in the mouse and human is likely to be related to the degree of development of the two species at the time of birth - in the human, for example, the eyelids initially close at about 10-12 weeks, and reopen at about 28 weeks of gestation, in the mouse the same two events occur at about 15.5 days of gestation, and 2 weeks after birth, respectively. Thus, if a direct extrapolation is possible, then this suggests that the position in the human at 28 weeks of gestation is possibly closely equivalent to the mouse at 2 weeks after birth (see Findlater et al., 1993).

It has also been shown that the present findings in the mouse are also comparable to reports from other species. For example, reports from other rodents show that growth in the size of the optic nerve continues well into adulthood with the maximum rate seen during the early period of postnatal development. This is in comparison with the situation in the human where maximum growth occurs from about the middle of prenatal life through to the first week of life, with adult size being attained by adolescence, whereas in the cat growth is steady from the prenatal period into advanced adulthood. However, at any stage of development the overall size of the optic nerve is determined by other factors such as the total number of axons within the nerve, axon diameter, the extent of myelinogenesis of each axon and the growth of the glial component present in the nerve (Ng & Stone, 1982). The overall effect of any of these factors on the size of the nerve also depends on the stage of develoment. For example, myelinogenesis in the optic nerve of the mouse exerts a significant effect on the size of the nerve during the juvenile period of life but the effect tails off until the process is completed early in adulthood. Other factors like the volume of the glial component become prominent in their influence on the overall size of the nerve thereafter.

9.2.2 MYELINOGENESIS OF THE OPTIC NERVE.

In the mouse myelinogenesis is first evident by the end of the first postnatal week and proceeds at a rate that is analogous to that of the growth in the calibre of the nerve up to early adulthood in this species (see chapter 5 and also Dangata et al., 1996). While the optic nerve in the mouse continues to grow in size well into adult life, myelinogenesis is completed early in adulthood. Although, the time course for myelinogenesis is not strain dependent, the actual time of completion is. Following the onset of the process it progresses rapidly during the juvenile period, with a surge between the end of the 2nd week and the 5th week when there is maximum increase in both the population of the myelinated nerve fibres present, and the number of myelin lamellae acquired by individual nerve fibres. The myelin lamellae are initially loosely wrapped around the axons, but become more densely packed as the process advances with age. After the juvenile period, myelinogenesis proceeds at a rate that tails off until the process is completed early in adulthood at an age that is strain dependent. In the strains analysed in the present study, for example, it was completed by the 9th and the 16th week for the C57BL and the F_1 hybrid, respectively. Unlike growth in the size of the optic nerve, myelinogenesis progressed at a slightly faster rate during the juvenile period in the F_1 hybrid than in the C57BL inbred parent, although, this difference was not statistically significant. This was indicated by both the higher number of myelinated nerve fibres and the higher number of more densely packed myelin lamellae per axon in the F_1 hybrid than in the C57BL during this period.

These findings in relation to myelinogenesis in the mouse could be another morphological manifestation of the resultts of cross-breeding in the F_1 hybrid. A similar report was given by Bigbee et al. (1990) on the F_1 hybrid in which they observed an increase in myelinogenesis compared with its parent inbred strains. They also attributed this to inbreeding vigour. However, the findings in the present study only extended over the juvenile period after which myelinogenesis proceeded at a significantly faster rate with an earlier completion in the C57BL

than in the F_1 hybrid. It may well be that with regard to myelinogenesis of the optic nerve of the mouse, inbreeding vigour affects only the onset and the initial progression of the process in the optic nerve. In this species the highest mean myelinated nerve fibre count which corresponded to the time of peak myelinogenesis in each of the two strains was observed in the C57BL. Although, it is yet to be established why myelinogenesis subsequently significantly lags behind in the F_1 hybrid from the end of the juvenile period after proceeding at an initially faster rate than in its parent C57BL inbred strain, this finding does not contradict the earlier report from the analysis of the optic nerve of 11week old mice in which the C57BL was found to have a lower mean nerve fibre count than the F_1 hybrid mice of similar age (Chapter 3 and Dangata et al., 1995). By this stage myelinogenesis has already been completed and a significant reduction (see later) of myelinated nerve fibres has taken place in the inbred C57BL mouse strain, though myelinogenesis was still progressing with less reduction of myelinated nerve fibres occurring in the F_1 hybrid.

Myelinogenesis in the mouse selectively begins with the largest diameter fibres and progresses to fibres in order of decreasing diameter. Consequently the mean diameter and the modal diameter of the myelinated nerve fibres are initially large. As other modalities of fibres become increasingly myelinated, these values rapidly dropped to their adult ones soon afterwards. The remarkable increase in myelinogenesis from the end of the 2nd week corresponds to the period when the mouse opens its eyes, and this suggests that a relationship almost certainly exists between physiological function and morphogenesis of the optic nerve of this species. In the rabbit, for example, Tauber et al. (1980) observed that artificial opening of the eyes on day 5 of postnatal development resulted to acceleration of myelinogenesis. This progressive selection of fibres for myelination in a decreasing order of fibre size further suggests that fibres myelinated early in life are probably of greater importance for establishing vision in the mouse than the smaller diameter fibres that subsequently become myelinated.

After the completion of myelinogenesis, a progressive decrease in the mean myelinated nerve fibre count was observed with age. This could not have been an incidental (i.e. unrelated) finding as it was clearly observed in both the inbred C57BL and its F_1 hybrid. This conforms with the normal arrangement seen during CNS development i.e. an initial over-production of non-myelinated nerve fibres followed by a period of elimination of both unmyelinated and myelinated fibres aimed at eventually establishing the adult values (Cunningham et al., 1982; Kirby et al., 1988; Nicoll et al., 1991).

The myelinated nerve fibres had a characteristic unimodal distribution throughout the period of postnatal development. The spectrum of distribution was typically narrow, as no fibre greater than 2.0 μm was recorded. Both the time course of myelinogenesis and the spectrum of distribution of the myelinated nerve fibres in the optic nerve are similar to those reported in the rat and other rodents, but contrast with the reports in other mammalian species, although, the pattern of myelinogenesis is similar in all these species (human: Chacko, 1948; Scheie & Abert, 1977; Mullaney, 1982; Monkey: Ogden & Miller, 1966; cat: Donovan, 1967; Ng & Stone, 1982; Rabbit: Vaney & Hughes, 1976; rat: Tennekoon et al., 1977; Conradi et al., 1989). The nerve fibre spectrum broadened and skewed in favour of the large fibres as myelinogenesis progressed with age. However, in the mouse there is some variation with regard to the spectrum of the myelinated nerve fibres observed within the optic nerve although such variation may not be significant. For example, the myelinated fibres in the F_1 hybrid mice were generally smaller in diameter than those in the C57BL strain; thus the modal diameter in the F_1 hybrid mice was 0.40μm, and the largest fibre measured in this group was 1.72μm while the respective values for the C57BL were 0.48μm and 1.92μm. A linear relationship between axon diameter and number of myelin lamellae also exists in the mouse, with the largest fibres having the highest numbers of

myelin lamellae; and this suggests that fibre diameter during myelinogenesis is a reflection of both axonal growth and myelin formation (Ng & Stone, 1982; Dangata & Kaufman, 1996).

By birth or shortly afterward, the visual system in man is relatively mature and the eye ready to function. In the mouse this approximately corresponds to the period when the surge of myelinogenesis (2nd-5th weeks) occurs in the optic nerve resulting in the myelination of over half of the population of fibres in the optic nerve. It is also during the early part of this period that the eyelids reopen (Findlater et al.,1993; also see Fernandez et al., 1993) and this would suggest that this is likely to be the minimum number of myelinated nerve fibres required in the optic nerve to establish normal visual function in this strain of mouse.

9.3 MUTATIONAL EFFECTS ON THE MORPHOMETRIC PARAMETERS OF THE MOUSE OPTIC NERVE.

Previous reports on the effect of the *Sey* gene on the development of the eye have mainly been on the effect of the gene on the lens and olfactory placodes and contents of the orbit in the homozygous mutant during the early embryonic period (Roberts, 1967; Hogan et al., 1986, 1988; Hill et al., 1991; Ton et al., 1992), with little information available on its effect on the development and contents of the optic nerve in the adult heterozygous mutant mouse. Observations made in the present study suggest that, unlike other mutant genes that have previously been reported, the influence of the *Sey* gene in the heterozygous mutant mouse, is primarily on the development of the eyeball, but also extends secondarily to the optic nerve. In the heterozygous mutant (*Sey*/+) mice analysed in the present study a fully developed optic nerve was dissected from eyeball to optic chiasma in each animal. However, the optic nerve was generally of small calibre, and this corresponded well with the small eyeball generally observed in the heterozygous mutant *Sey*. The presence of a fully developed optic nerve (i.e. an optic nerve ensheathed by well defined meningeal coverings with its myelinated nerve fibre

density and myelinated nerve fibre diameter spectrum being comparable to those of normal mouse strains) suggests that the gene exerts a secondary effect on the development of some structures such as the optic nerve. This is in addition to its primary effect on some specific aspects of craniofacial morphogenesis, for example, rather than having a generalised effect on many embryonic tissues (Hogan et al., 1988). Such a secondary effect appears to be both sex and strain dependent, and was highlighted in the present study by the significant difference observed in the mean csa and the mean myelinated nerve fibre counts between the male series of the normal (+/+) and the heterozygous mutant (*Sey*/+) mice analysed. Although both normal (+/+) and heterozygous mutant (*Sey*/+) female mice did not significantly differ in these two parameters, values of the parameters for the heterozygous mutant (*Sey*/+) females were always lower than those of their normal (+/+) female littermates.

In the mouse the normal development of the eye starts with the invagination of the central region of the optic placode to form the optic pit and its progressive differentiation, in association with cephalic neurulation, to form the optic vesicle (Rugh, 1990; Kaufman, 1979, 1992). This is believed to be influenced by the process of embryonic induction by which regions of the anterior head ectoderm become progressively specified as the presumptive optic apparatus. The mechanism of embryonic induction may itself be affected by gene mutation (Jong et al., 1990). Other factors that influence normal morphogenesis include programmed cell death (apoptosis) and cell resorption, the appropriate location of component tissues at the time of cell-cell interaction, and the availability of an adequate blood supply (Truslove, 1962; Silver & Robb, 1979; Perry et al., 1983). Cell death and cell resorption in the optic stalk allow access for the ingrowing nerve fibres that exit from the neural retina with the eventual formation of the optic nerve, while the blood supply that facilitates the nutrition of this process mainly comes from the hyaloid vessels.

Hogan et al. (1986, 1988) reported that in the homozygous *Small eye* mouse an irregularly shaped optic vesicle initially forms without an inductive influence from the lens vesicle, but it soon degenerates leaving no remnant of the optic apparatus beyond the optic chiasma. Here the *Sey* gene in the homozygous state is believed to interfere with the normal mechanism of embryonic induction required for the development of the lens vesicle, thus resulting in the formation of a smaller lens vesicle than normal in the heterozygous mice bearing this mutation. Although it is the lens that is primarily affected, a consequential effect on other components of the eyeball, as well as secondary effects on the optic nerve exists. In the present study, a secondary effect of the *Sey* mutation in the heterozygous state on the optic nerve of the mouse was reflected in the small csa of the nerve. Although in both the normal strains of mice (i.e. the inbred C57BL and CBA strains and their F_1 hybrid) and the heterozygous mutant (*Sey*/+) optic nerves the nerve fibres were all myelinated, the mean nerve fibre counts in the heterozygous mutant (*Sey*/+) mice were generally significantly lower than those of the normal strains of mice. This is logical, since nerve fibres from the neural retina are directed into the optic stalk, the calibre of the optic nerve will necessarily reflect the number of nerve fibres which it contains as well as the overall size of the retina itself i.e.there is a direct quantitative relationship here (Ogden & Miller, 1966; Potts et al., 1972a, b; Hughes, 1977). Such a direct relationship between the overall calibre of the optic nerve and its nerve fibres has been demonstrated in this study by the csa and the mean nerve fibre count. Furthermore, the spectrum of distribution of the myelinated nerve fibres as well as the mean myelinated nerve fibre densities in the *Sey* mice was similar to that observed in the other mouse strains studied in chapter 3 (also see Dangata et al., 1995). This suggests that retinal differentiation or myelinogenesis of the nerve fibres within the optic nerve was spared by the efffect of the gene. Myelinogenesis itself does not occur in the optic nerve of the mouse before the 5th day of postnatal life (Gyllensten et al., 1966; Dangata et al., 1996), and this is well after the process of embryonic induction.

The present report on the effect of the *Sey* gene on the optic nerve of the mouse is in contrast with reports from other mutant genes which have been shown to exert a *primary* effect on the development of the optic nerve in the mouse. For example, Theiler et al. (1978, 1980) reported a direct effect of the gene mutation causing *Dickie's Small Eye* on both eyeball and the optic nerve. In this mutant, both formation of the eyeball and the optic stalk was directly affected. The morphogenesis of the eye in the heterozygous mutant animals was delayed compared to that observed in controls on 12 day p.c. This apparent lagging in development generally starts between days 10 and 11 p.c. and was invariably noted by day 12 p.c. The result was an abnormally folded and hypoplastic optic stalk in addition to eyeball abnormalities (also see Franz & Besecke, 1991). Robb et al. (1978) observed that in normal (+/+) or^J mice, by day 14.5 p.c. the eyeball increases in volume and the optic nerve increases in diameter as a result of the differentiation of large numbers of ganglion cells within the neural retina which send axons to the brain. This is in contrast to the situation in homozygous (or^J) mutant mice of about the same age, where despite the presence of a substantial retinal neuroblastic layer in which it was difficult to distinguish ganglion cells and nerve fibres, no axons exited from the eye. Furthermore, they suggested that another factor that might have induced regression of the optic stalk was the absence of vascularisation of the optic nerve.

Some mutant genes exert their effects on developmental processes of the optic nerve such as myelinogenesis. The *jimpy* mutation is an X-linked disorder that results in a variety of glial cell abnormalities during CNS myelinogenesis (Knapp et al., 1990). In mice with this mutation, for example, Meier & Bischoff (1975) observed that the number of axons in the postnatal optic nerve was not affected, but that there was a reduced number of myelinated nerve fibres compared to controls. This was associated with abnormalities of oligodendroglia, increased glial cell death in the premyelination stage, decrease in the number of maturing oligodendrocytes and a decrease in the duration of early myelinogenesis. They attributed the

low number of maturing oligodendrocytes in the premyelination stage to a disturbance in the differentiation of the oligodendroglial cell line by the *jimpy* gene. In the optic nerve of the *myelin deficient* (*md*) X-linked recessive mutant of the Wistar rat, CNS myelin fails to develop. In this mutant, Dentinger et al. (1985) reported attainment of maximum csa in the optic nerve by 16 pnd, thereafter the csa remained almost constant to 46 pnd when it was 60% of the value of littermate controls; whereas in controls, there was a rapid increase in csa up to 19 pnd followed by a steady slow increase up to 46 pnd. This arrest of growth of the csa of the optic nerve was attributed to lack of myelinogenesis since this is one of the factors that affect the csa of the optic nerve (see Ng & Stone, 1982). Abnormalities of oligodendrocytes that had consequential effect on myelinogenesis included decrease in number, immaturity and abnormal morphological appearance.

Mutational influence on the development of the optic nerve has also been reported to be exerted through factors that influence the normal process of myelinogenesis. One of such factors is myelin basic protein (MBP) which is involved in CNS myelinogenesis. Shine et al. (1992) analysed the optic nerve from neurological mutant mice i.e the *shiverer* and *myelin deficient* mice. These mice lack the functional gene for MBP, thus they have no myelin in the CNS, *shiver* have seizures and die early. The mutant homozygous for the MBP transgene have about 25% of normal MBP and mRNA. They do not shiver or have seizures and live a normal life span. Using immunochemical staining techniques, these authors observed that MBP was localised to the white matter in normal and transgenic *shiverer* mice with an intensity of staining similar to the degree of MBP gene expression. There was an increase in the percentage of myelinated axons in the optic nerve which correlated well with the increased degree of gene expression observed. In mice where lower amounts of MBP and mRNA were detected, they had axons that were loosely wrapped with oligodendrocytic processes, suggesting that the oligodendrocytes were normal and could produce sufficient MBP to initiate axon wrapping but

were not adequate to form compact myelin. As in normal strains of mice, they also observed that there was a selective myelination of nerve fibres starting from the large fibres and continuing in a decreasing order of fibre size.

In the case of proteolipid protein (PLP), an isoprotein encoded by a gene on the X-chromosome that is also known to influence CNS myelinogenesis, Boison & Stoffel (1994) observed a high degree of disorder of the ultrastructure of the multilayer myelin lamellae of all axons in the CNS of heterozygous males or homozygous females PLP deficient mice. The disruption in myelin structure was also associated with a significant reduction in the velocity of nerve impulses of the axons as well as impairement of neuromotor coordination and behavioural changes. Information on the influence of mutational changes on myelinogenesis has contributed to the development of transgenic mouse models for the study of CNS demyelination conditions such as multiple sclerosis (Yoshioka et al., 1994), and this may eventually shed light in the understanding and management of such conditions in humans.

The effect of an extra autosome on the postnatal development of the optic nerve in the mouse was also reported by Lorke & Lauer (1990). They examined gliogenesis and myelinogenesis in the optic nerves of 1-15 pnd old trisomy 19 mice. The differentiation of astrocytes and oligodendrocytes was delayed by about two days. There was also an associated delay in eye opening by about the same duration of time. The premyelinated mean axonal diameter was identical in both experimental and control groups. The myelin lamellae were of normal structure, but there was a decrease in the number of myelinated nerve fibres in the nerve.

9.4 TERATOGENIC EFFECTS ON THE MORPHOMETRIC PARAMETERS OF THE MOUSE OPTIC NERVE.

Many substances are known to exert a teratogenic effect of variable degrees during morphogenesis. One of the commonest known teratogens to affect human morphogenesis is alcohol. Its consumption is more universal than that of any other drug. Despite this, until recently its teratological effect on man remained obscured (Abel, 1984). Most recently the recognition of an alcohol-related clinical syndrome, the Fetal Alcohol Syndrome (FAS), led to many clinically designed studies that have shed much light to the clinical manifestation of the adverse effects of alcohol on human morphogenesis (Beattie et al., 1983; Chan et al., 1991). FAS is defined as the presence of prenatal and postnatal growth retardation below the tenth percentile, central nervous system involvement (neurological abnormalities, developmental delays and /or intellectual deficits), and characteristic craniofacial abnormalities including microcephaly, short palpebral fissures, poorly developed philtrum, recessed maxillary area (Sulk et al., 1981; Cook et al., 1987; Adickes, 1990; Schenker et al., 1990; Garro et al., 1991). The understanding of the pathology of specific organ involvement in FAS is essential for its management, and this is made possible by the use of suitable animal models for a comprehensive analysis. A few animal models are available for the study of the features of FAS (Sulik et al., 1981; Clarren & Bowden 1982; Lewis, 1985; see also O'Shea & Kaufman, 1979, 1981), though these are exclusively in rodents.

Because children with features of FAS are known to have been born to mothers who had just a single dose of alcohol during pregnancy (Kronick, 1976; Hermann et al., 1980; Clarren, 1981; Padmanabhan et al., 1984), the current trend in the study of FAS is to try to understand what happens to specific organ systems as a result of alcohol exposure during specific critical periods of morphogenesis. In the present study, morphometric findings in the optic nerves from the offspring of F_1 hybrid female mice exposed to a single intraperitoneal dose of alcohol on day 12

of gestation and appropriate controls assessed at intervals during the juvenile period of postnatal development demonstrated that exposure to a single dose of alcohol taken at a critical period of gestation had a significant teratogenic effect.

The optic nerve in both controls and experimental groups of alcohol-exposed mice grew rapidly in calibre during the juvenile period of life with the maximum rate of growth seen between the second and the third week of postnatal life. Although the csa of the optic nerve in alcohol-treated mice were generally larger than those of corresponding age groups of controls, the rate of growth was higher in controls than in the experimental groups, and this was seen to be at decreasing levels of significance with age. This was highlighted by the fact that up to the third week the calibre of the optic nerve of offspring of alcohol-treated mice was significantly larger than that of controls, but by the end of the 5th postnatal week, the difference was no longer significant. However, the overall mean csa in each of the experimental groups was more than that of the corresponding age groups of controls. It is not yet clear why this should have been the case, particularly since this finding was in contrast with the small calibre optic nerve that has earlier been reported in the rat by Pinazo-Duran et al. (1993) following a long term (six weeks before pregnancy and throughout pregnancy) administration of alcohol in the diet to female rat, though it may have been due to the different methodology employed in these two studies (also see Kjellstrom & Conradi, 1993; Parson & Sojitra, 1995). Report on the csa of the optic nerve following acute exposure of C57BL/6 pregnant mice to alcohol on day 8 p.c. by Ashwell and Zhang (1994) were similar to those of Pinazo-Duran et al. (1993). The present findings strongly suggest that in alcohol teratogenicity exposure at an appropriate critical period of development is more important than the duration of administration. This has been highlighted by the fact that in these two previous studies, alcohol was administered before the formation of the optic stalk which determines the size of the optic nerve (Rugh, 1990; Kaufman, 1992; Dangata et al., 1994);

whereas in the present study, by the time alcohol was administered the optic stalk had initiated its development.

Although in both controls and alcohol-treated groups myelinogenesis progressed rapidly during the early part of the juvenile period, both its onset and rate of progression in the experimental group significantly lagged behind that of the controls. This has been demonstrated by the significant difference observed between the two groups of mice in both their mean myelinated nerve fibre count and their mean nerve fibre density. The spectrum of distribution of the fibres was generally broader in controls than in the corresponding experimental age groups. These findings suggest a significant influence on the time of onset and progression of myelinogenesis by prenatal factors as has already been highlighted by others (see Tennekoon et al., 1977; Dentinger et al., 1985; Samorajski et al., 1986; Asou et al., 1994). A significant teratological influence on myelinogenesis was possibly exerted by alcohol on the glial precursors of oligidendrocytes or the process of their cytodifferentiation with this resulting in a reduction of both their number and their competence to synthesize myelin. Furthermore, in addition to a delayed onset, there was probably a premature arrest of the process of myelinogenesis in individual nerve fibres before they attained their final size. The consequences of these were therefore: a delay in the onset and a decrease in the rate of progression of myelinogenesis - as was shown by the significant difference in the mean myelinated nerve fibre count and density as well as the narrower spectrum of diameter size distribution of the myelinated nerve fibres in the experimental group compared to the control. However, it should be noted that myelinogenesis has yet to be completed in the optic nerve of the mouse by the end of the juvenile period.

Studies carried out on other animal models have also shed light on the possible mechanisms by which alcohol exerts its teratogenic effects on the development of the optic nerve. In the rat, for example, Phillips and his co-workers (Phillips, 1989; Phillips et al., 1991; Phillips &Krueger,

1992) observed a delay in oligodendroglial cell maturation and a reduction in the number of oligodendrocytes produced. This resulted in a delay in the onset of myelinogenesis. They also reported a decrease in the myelinated nerve fibre count as well as the myelin thickness per axon. Kjellstrom & Conradi (1993), however, reported a decrease in axonal calibre but not in the total fibre count. The impairment of the differentiation of myelin and consequently the development of the myelin sheath in the optic nerve could explain some of the clinical neurological and visual dysfunctions associated with prenatal alcohol exposure. The analysis of other parts of the CNS with regard to the teratogenic effect of alcohol on myelinogenesis have given similar findings to those reported in the present analysis and those on the optic nerve of the rat cited above (see Lancaster et al., 1982; 1984; Miller, 1993; Miller & al-Rabial, 1994). These findings further confirm that, given at an appropriate critical period, an acute dose of alcohol can affect CNS development. For example, the findings from this study indicate that prenatal exposure of the fetus to alcohol influences both the pre- and postnatal development of the optic nerve. Indirect evidence suggests that myelinogenesis, for example, is probably affected due to interference with oligodendroglial cytodifferentiation the result of which could be a delay in the onset of myelinogenesis and its subsequent progression.

Variable degrees of teratogenic effects of substances other than alcohol on the morphogenesis of the visual system in other experimental models have also been reported. Following a morphometric analysis of the retina and the optic nerve from neonatal rats after subcutaneous injection of a daily dose of 15mg/kg body weight of cocaine from birth to 30 pnd, Silva-Araujo et al. (1993) observed a decrease in the thickness of the ganglion cell layer of the retina, a higher proportion of small ganglion layer neurons with reduced nuclear diameters and a higher packing density compared to controls. The ganglion cell layer of some retinae showed the presence of degenerative elements, and was more severe in the retinae of the cocaine-treated animals than those of controls. These pathological changes appeared as dense shrunken figures with

condensed nuclei, enclosed by a rim of cytoplasm and were found among the normal ganglion cells. In addition, there were degenerative neurites in close association with other degenerative elements in the ganglion cell layer and the inner plexiform layer. In the optic nerve there was a significantly higher proportion of small myelinated nerve fibre profiles and a lower proportion of larger diameter fibres in concaine-treated animals compared to controls, a change that closely matched those of the retina. However, there was no significant difference in the number of myelin lamellae per axon between the optic nerves of the experimental group and controls. Their findings suggested that these changes in the retina and the optic nerve could be a general reflection of similar changes induced by prenatal cocaine exposure on other parts of the visual system.

In their analysis, Wiggins & Ruiz (1990) reported a transient but insignificant decrease in body and brain weights of offspring of cocaine-treated and pair-fed dams compared to control rats during the early period of myelinogenesis (15th pnd), although, by the time of peak myelinogenesis (20th pnd) the difference was no longer present. Brain myelin concentrations in offspring of pair-fed pups were also only slightly (1-2%) lower than those of normal controls; this was in contrast to the 10% difference observed between offspring of cocaine-treated and normal controls. It is interesting to note from their results that, despite the fact that myelinogenesis of the brain is a postnatal event, prenatal exposure to cocaine presents a greater risk to this process of brain development than postnatal exposure, and that the hypomyelinogenesis noted in the offspring of cocaine-treated rats indicated a direct toxic effect of cocaine on the developing CNS of offspring. This is in contrast to the vulnerability caused by undernutrition, suggesting that the fetus is more protected against undernutrition than the suckling pup. The characterization of such pre- and postnatal risks of drugs in offspring provide useful information for the clinical management of both the pregnant drug user and her offspring.

The effects of X-irradiation of the optic nerve of the rat during the period of oligodendrocyte proliferation was reported by Colello & Schwab (1994) to be primarily due to the prevention of myelin formation in the retinofugal pathway. An electron microscopic and histochemical analysis of the optic nerve on the 15th pnd following prenatal irradiation showed that there was virtually complete absence of oligodendrocytes and myelin. The total nerve fibre count in myelin-free nerves was 10-30% higher than that of myelinated nerves. Furthermore, they observed that fibre number along the length of myelin-free (irradiated) nerves fluctuated by about 20%, but remained constant throughout the length of myelinated nerves; thus suggesting that optic axons are able to form sprouts in the absence of myelinogenesis (also see Marciano et al., 1990). Although, Colello & Schwab (1994) did not indicate whether the sprout formation was caused by the direct effect of irradiation itself or indirectly by the absence of the myelin-forming potential of oligodendrocytes, the observations made by Marciano et al. (1990) were suggestive of the fact that the absence of the influence of oligodendrocytes on the process of myelinogenesis resulted in the formation of sprouts.

The teratogenic effects of substances such as cycloheximide on CNS myelinogenesis have been suggested to be mediated through an inhibitory mechanism on the synthesis of myelin basic protein, thus altering the ability of oligodendrocytes to incorporate membrane components into CNS myelin sheath (Cullen & Webster, 1989). This is in contrast to 5-azacytidine (5-AZ) which has been reported to exert its teratogenic effects by the alteration of gliogenesis in the rat optic nerve (Black & Waxman, 1986; Black et al., 1986). These workers observed that systemic injection of 5-AZ resulted in a severe delay in gliogenesis. By 14 pnd approximately 25% of the axons in the optic nerve of controls were myelinated and displayed an increase in axonal diameter. This was in contrast to the optic nerve of a corresponding age group of 5-AZ-treated rats where only few oligodendrocytes were present and the number of myelinated nerve fibres was markedly reduced. The axonal diameters of the few myelinated nerve fibres present in the

5-AZ-treated optic nerves were, however, comparable with those of age-matched controls. Oligodendroglia made up 17% and 40% of glial cells in the optic nerve of 5-AZ-treated and controls, respectively. Their findings suggested that 5-AZ is a potent inhibitor of oligodendrogliogenesis with a concomitant marked effect on myelinogenesis. These findings confirmed those reported by Bohn & Friedrick (1982) after giving cortisol to 7 and 18 day old rats and analysing the optic nerve at 21 and 60 pnd. At 21 pnd, the amount of myelin in cortisol-treated rats was reduced by 42% and this was accompanied by a 39% decrease in the number of myelinated axons as well as a 22% reduction in the myelin/axon ratio for myelinated axons. By 60 pnd these parameters had completely recovered to normal values. Formation of oligodrendrocytes was enhanced following cessation of treatment which suggested that the effect of cortisol on myelinogenesis could have been mediated by inhibition of formation of oligodendrocytes. Colchicine on the other hand was observed to cause demyelination similar to Wallerian degeneration in addition to a possible inhibition on myelin formation (Mathieu et al., 1981). The effect of lead on myelinogenesis of the optic nerve in the mouse was also investigated by Tennekoon et al. (1979). They analysed the optic nerves of mice given lead-containing mother's milk from 1-21 pnd and myelin basic protein MBP was biochemically assayed. The total amount of myelin produced by lead-treated mice was decreased without a concomitant alteration in the number of oligodendrocytes in the optic nerve or any alteration in the relationship between axons and myelin lamellae.

9.5 CLINICAL IMPLICATIONS OF THE PRESENT RESEARCH.

Congenital causes of visual imparement play a significant role in the general incidence of blindness in any population in the world today. Genetic and environmental factors such as infections, drugs, chemicals, radiation and nutrition play a significant role, although the trend may vary from one population to another, and even within the same population it varies with time (Foster & Gilbert, 1992). For example, in the developed societies the trend has moved

from a greater role played by infectious causes in the 1930s to the increased incidence of hereditary causes as seen today (Robinson et al., 1987; Goggin & O'Keefe, 1991); whereas in the developing societies infectious and nutritional factors continue to play a significant role having overshadowed the hereditary factors rather than an actual low level of prevalence of the latter i.e. a baseline level of hereditary causes of blindness is presumably always present, but super-added effects of nutrition, disease, etc, obsure it (Foster & Sommer, 1987; Mele et al., 1991). For example, in a clinical survey of the causes of childhood blindness in the Royal Blind School, Edinburgh, Phillips et al. (1987) reported as many as 48% of the cases of blindness to be due to hereditary factors. In a more recent follow up clinical survey in the same school which serves Scotland and the North of England, Fleck & Dangata (1994) observed that this had dropped to 32%. Of these, 15.6% were autosomal dominant with a positive family history while the majority of the rest were due to autosomal recessive conditions. In another study of congenital ocular blindness in children in British Columbia, Robinson et al. (1987) also observed that genetic factors were the most common aetiological factors throughout the period of their study. Optic nerve lesions which constituted approximately 20% of the cases appeared to be on the increase, and were largely due to congenital optic nerve hypoplasia (also see Stromland, 1987, 1990; Ashwell & Zhang, 1994). Cases of blindness due to infectious causes, for example rubella, continued to decline as a result of appropriate control measures undertaken since the identification of this virus as an important aetiological factor in congenital blindness.

Visual abnormalities impose a heavy social, health, and educational responsibility on the community, hence the need for appropriate control measures (Jay, 1987). Control strategies such as preventive and therapeutic measures for any disease condition depend on the availability of adequate information with regards to its extent and aetiology in the population (Foster & Gilbert, 1992). In childhood blindness, for example, preventive measures such as genetic counselling given at an appropriate time could play an important part in reducing the incidence

of blindness arising from genetic factors in addition to reassuring those not at risk of transmitting the disorder (Jay, 1987; Phillips et al., 1987). The establishment of appropriate animal models for the study of both genetic and environmental factors associated with clinical conditions of the visual system is a necessary prerequisite for providing the baseline information required for their management in humans.

For example, the *Sey* gene is believed to be analogous to the human *aniridia* gene (Glaser et al. 1990). As has already been stated, in the mouse the effect of the mutant gene in the homozygous state primarily causes inhibition of the inductive mechanism necessary for the formation of the lens vesicle while in the heterozygous state, it influences the overall size of the eyeball and its component structures such as the iris and retina, with any effect on the optic nerve likely to be secondary to that on the eye. In humans, however, the gene has variable effects on the morphogenesis of the visual apparatus. These manifest themselves as a variety of clinical conditions. A reduction in the size of the iris leads to narrow angle glaucoma. This reduction in size of iris has been attributed to macular hypoplasia rather than being due to abnormalities of the iris (Hittner, 1989). Histological findings in the human include hypoplasia of the iris, absence of trabecular meshwork and Schlemm's canal (Hittner, 1989). However, in humans, optic nerve hypoplasia, a congenital abnormality of one or both optic nerves associated with a diminished number of axons (Mosier et al., 1978; Zeki et al., 1992), which is observed in about 75 % of aniridic patients is believed to be a consequence of poor macular and/or retinal development. This results in poor visual acuity and nystagmus.

Furthermore, drugs are the commonest known environmental factors with teratogenic consequences and exposure to these agents at critical periods during morphogenesis is clearly of both social and clinical importance (Silva-Araujo et al., 1993). The design of clinical studies has shed light into the deleterious effects of drugs on the development of the human visual

system (Isenberg et al., 1987; Dominguez et al., 1991; Good et al., 1992), although, direct evidence of the mechanisms underlying normal development and the teratogenic effects of substances on human optic nerve morphogenesis is only rarely possible; thus emphasising the value of suitable experimental animal models. In rodents, the general development of the brain and in particular, the visual system, extends into the juvenile period (< 6 weeks) of postnatal life, which corresponds approximately to the third trimester of gestation in humans (Dobbing & Sands, 1979; West et al., 1990). The study of the development of components of the visual system in rodents during this period can shed much light on the understanding of human neuromorphogenesis of the CNS, as this is particularly vulnerable to teratogenic insult during this period of development (Bedi & Warren, 1983; Pierce & West, 1986; Silva-Araujo et al., 1991, 1993). This period of brain growth spurt is characterised by the completion of migration and maturation of neurons, formation of synaptic contacts and initiation of myelinogenesis (Dobbing & Sands, 1979; Wiggins et al., 1984; Dangata et al., 1996; Dangata & Kaufman, 1996). These developmental processes may be particularly susceptible to experimental manipulation during this period.

Since the use of human material for clinical research is only rarely possible, the findings of experimental animal and *in vitro* model research studies have been of great application to *in utero* events and processes of human gestation and development (Adickes, 1990). A model must make good biological sense. The optic nerve is a particularly suitable model for the study of the CNS, as well as the visual system. I believe that the present findings from the morphometric analysis of this central tract in the mouse provide useful baseline parameters for laboratory-based studies that could shed light to clinical conditions of the human visual system, and possibly in the long-term, on their clinical management.

REFERENCES

ABEL, E.L. (1984) Prenatal effects of alcohol. Drug & Alcohol Dependence 14, 1-10.

ABEL, E.L., DINTCHEFF, B.A. and BUSH, R. (1981) Effects of beer, wine, whisky, and ethanol on pregnant rats and their offspring. Teratology 23, 217-222.

ADICKES, E.D. (1990) Biomolecular mechanisms of ethanol teratogenicity. Alcoholism: Clinical and Experimental Research 14, 805-806.

AREY, L.B. (1974) *Developmental Anatomy: A Textbook and Laboratory Manual of Embryology*. Revised 7th ed., WB Saunders, Philadelphia.

ARVANITIS, D., POLAK, P.E. and SZUCHET, S. (1993) Electron microscopical localization of myelin/oligodendrocyte proteins in multilamellar structures by the immunogold method. Developmental Neuroscience 14, 313-327.

ASHWELL, K.W.S. and ZHANG, L-L. (1994) Optic nerve hypoplasia in an acute exposure model of the fetal alcohol syndrome. Neurotoxicology and Teratology 16, 161-167.

ASOU, H., HAMADA, K., MIYAZAKI, T., SAKOTA, T., HAYASHI, K., TAKEDA, Y., MARRET, S., DELPECH, B., ITOH, K. and UYEMURA, K. (1995) CNS myelinogenesis in vitro: Time course and pattern of rat oligodendrocyte development. Journal of Neuroscience Research 40, 519-534.

ASOU., H., HAMADA, K., UYEMURA, K., SAKOTA, T. and HAYASHI, K. (1994) How do oligodendrocytes ensheath and myelinate nerve fibers? Brain Research Bulletin 35, 359-365.

AWAI, T. (1985) Angioarchitecture of intraorbital part of human optic nerve. Japanese Journal of Ophthalmology 29, 79-98.

AYALA, F.J. and KIGER, J.A. (1984) Genetic analysis of development. In: *Modern Genetics* 2nd ed., Benjamin/Cummings, California.

BAHR, G.F. (1955) Continued studies about the fixation with osmium tetroxide. Electron stains IV. Experimental Cell Research 9, 277-285.

BALAZSI, A.G., ROOTMAN, J., DRANCE, S.M., SCHULZER, M. and DOUGLAS, G.R. (1984) The effect of age on the nerve fiber population of the human optic nerve. American Journal of Ophthalmology 97, 760-766.

BANNIGAN, J. and BURKE, P. (1982) Ethanol teratogenicity in mice: a light microscopic study. Teratology 26, 247-254.

BARD, J. (1990) Morphogenesis. In*: The Cellular and Molecular Processes of Developmental Anatomy.* Cambndge University Press: Cambridge.

BEATTIE, J.O., DAY, R.E., COCKBURN, F. and GARG, R.A. (1983) Alcohol and the fetus in the west of Scotland. British Medical Journal Clinical Research Ed. 297, 17-20.

BEAUCHAMP, G.R., LUBECK, D. and KNEPPER, P.A (1985) Glycoconjugates, cellular differentiation, and congenital glaucoma. Journal of Pediatric Ophthalmology and Strabismus 22, 149-155.

BECKER, H.C., HALE, R.L., BOGGAN, W.O. and RANDALL, C.L. (1993) Effects of prenatal ethanol exposure on later sensitivity to the low-dose stimulant actions of ethanol in mouse offspring: Possible role of catecholamines. Acoholism: Clinical and Experimental Research 17, 1325-1336.

BEDI, K.S. and WARREN, M.A. (1983) The effects of undernutrition during early life on the rat optic nerve fibre number and size-frequency distribution. Journal of Comparative Neurology 129, 125-132.

BERMAN, N. and JONES, E.G. (1977) A retino-pulvinar projection in the cat. Brain Research 134, 237-248.

BIGBEE, J.W., YU, D.S. and YU, R.K. (1990) Morphometric analysis of the developing optic nerve of the F1 heterotic mouse and its parental strains. Neuroscience Letters 119, 179-178.

BISHOP, G.H. (1933) Fibre groups in the optic nerve. American Journal of Physiology 106, 460-674.

BLACK, J.A., FOSTER, R.E. and WAXMAN, S.G. (1982) Rat optic nerve: freeze-frature studies during development of myelinated axons. Brain Research 250, 1-20.

BLACK, J.A. and WAXMAN, S.G. (1986) Molecular structure of the axolemma of developing axons following altered gliogenesis in rat optic nerve. Developmental Biology 115, 301-312.

BLACK, J.A., WAXMAN, S.G., RANSOM, B.R. and FELICIANO, M.D. (1986) A quantitative study of developing axons and glia following altered gliogenesis in rat optic nerve. Brain Research 380, 122-135.

BLAND, M. (1989) *An Introduction to Medical Statistics.* Oxford Medical Publications, Oxford.

BODOR, N., el-KOUSSI, A.A., KANO, M. and KHALIFA, M.M. (1988) Soft drugs. 7. Soft beta-blockers for systemic and ophthalmic use. Journal of medicinal Chemistry 31, 1651-1656.

BOHN, M.C. and FRIEDRICH, V.L. Jr. (1982) Recovery of myelination in rat optic nerve after developmental retardation by cortisol. Journal of Neuroscience 2, 1292-1298.

BOISON, D. and STOFFEL, W. (1994) Disruption of the compact myelin sheath of axons of the central nervous system in proteolipid protein-deficient mice. Proceedings of the National Academy of Sciences of the United State of America 91, 11709-11713.

BOKE, W. and VOIGT, G.J. (1980) Circulatory disorders of the optic nerve. Ophthalmologica 180, 88-100.

BOVOLENTA, P. and MASON, C. (1987) Growth cone morphology varies with position in the developing mouse visual pathway from retina to first targets. Journal of Neuroscience 7, 1447-1460.

BRUESCH, S.R. and AREY, L.B. (1942) The number of myelinated and unmyelinated fibres in the optic nerve of vertebrates. Journal of Comparative Neurology 77, 631-665.

BUTT, A.M. and RANSOM, B.R. (1993) Atrocytes and oligodendrocytes during development of the intact rat optic tract. Journal of Comparative Neurology 58, 342-349.

CAMPOS-ORTEGA, J.A. HAYNOW, W.R. and CLUVER, P.F. (1972) A note on the problem of retinal projections to the inferior pulvinar of primates. Brain Research 22, 126-130.

CAMRAS, C.B. and PODOS, S.M., (1989) The role of endogenous prostaglandins in clinically-used and investigational glaucoma therapy. Progress in Clinical and Biological Research 312, 459-475.

CHACHO, L.W. (1948) An analysis of fibre-size in the human optic nerve. British Journal of Ophthalmology 32, 457-461.

CHAI, C.K. (1959) Life span in inbred and hybrid mice. Journal of Heredity 50, 203-208.

CHAN, T., BOWELL, R., O'KEEFE, M. and LANIGAN, B. (1991) Ocular manifestation in fetal alcohol syndrome. British Journal of Ophthalmology 75, 524-6.

CHERNOFF, G.F. (1977) The fetal alcohol in mice: an animal model. Teratology 15, 223-230.

CHERNOFF, G.F. (1980) The fetal alcohol syndrome in mice: maternal variables. Teratology 22, 71-75.

CLARREN, S.K. (1981) Recognition of fetal alcohol syndrome. Journal of American Medical Association 245, 2436-2439.

CLARREN, S.K. and BOWDEN, D.M. (1982) Fetal alcohol syndrome: a new primate model for binge drinking and its relevance to human ethanol teratogenesis. Journal of Pediatrics 101, 819-824.

COHEN, A.I. (1967) Ultrastructural aspects of the human optic nerve. Investigative Ophthalmology 6, 294-308.

COLELLO, R.J. and GUILLERY, R.W. (1990) The early development of retinal ganglion cells with uncrossed axons in the mouse: retinal position and axonal course. Development 108, 515-523.

COLELLO, R.J. and GUILLERY, R.W. (1992) Observations of the early development of the optic nerve and tract of the mouse. Journal of Comparative Neurology 317, 357-378.

COLELLO, R.J. and SCHWAB, M.E. (1994) A role for oligodendrocytes in the stabilization of optic axon numbers. Journal of Neuroscience 14, 6446-6452.

COMFORT, A. (1959) Natural aging and the effects of radiation. Radiation Research (Supplement 1) : 216-234.

COOK, C.S., NOWOTNY, A.Z. and SULIK, K.K. (1987) Fetal alcohol syndrome: eye malformations in a mouse model. Archives of Ophthalmology 105, 1576-1581.

COOPER, E.R.A. (1945) The development of the human lateral geniculate body. Brain 68, 222-242.

COUPLAND, R.E. and WEAKLEY, B.S. (1968) Developing chromaffin tissue in the rabbit: an electron microscopic study. Journal of Anatomy 102, 425-455.

CRAGG, B.G. (1969) The topography of afferent projections in the circumstriate visual cortex of the monkey studied by the Naula method. Vision Research 9, 733-747.

CULLEN, M.J. and WEBSTER, H.D. (1989) Inhibition of protein synthesis during CNS myelination produces focal accumulation of membrane vesicles in oligodendrocytes. Journal of Neurocytology 18, 763-774.

DAGG, C.P. (1966) Teratogenesis. In: *Biology of the Laboratory Mouse* (ed., EL Green) 2nd ed., pp 329-336, McGraw-Hill, New York.

DANGATA, Y.Y., FINDLATER, G.S. and KAUFMAN, M.H. (1994) Morphometnc analysis of myelinated fibre composition in the optic nerve of adult C57BL and CBA strain mice and (C57BL x CBA) F_1 hybrids: an analysis of interstrain variation. Journal of Anatomy 184, 202.

DANGATA, Y.Y., FINDLATER, G.S., DHILLON, B. and KAUFMAN, M.H. (1994) Morphometric study of the optic nerve of adult normal mice and mice heterozygous for the Small eye mutation (Sey/+). Journal of Anatomy 185, 627-635.

DANGATA, Y.Y., FINDLATER, G.S. and KAUFMAN, M.H. (1995) Morphometric analysis of myelinated fibre composition in the optic nerve of adult C57BL and CBA strain mice and (C57BL x CBA)F_1 hybrid: a comparison of inter-strain variation. Journal of Anatomy 186, 343-348.

DANGATA, Y.Y., FINDLATER, G.S. and KAUFMAN, M.H. (1996) Postnatal development of the optic nerve in (C57BL x CBA) F_1 hybrid mice: General changes in morphometric parameters. Journal of Anatomy 189, 117-125.

DANGATA, Y.Y. and KAUFMAN, M.H. (1997) Effects of prenatal alcohol exposure on the postnatal development of the mouse optic nerve. Journal of Anatomy 191, 000-000.

DANGATA, Y.Y. and KAUFMAN, M.H. (1997) Myelinogenesis in (C57BL x CBA) F_1 hybrid mice: A morphometric analysis. European Journal of Morphology (accepted April 1996).

DAY, S. (1990) Normal and abnormal visual development. In: *Pediatric Ophthalmology*. (ed Taylor D). pp 7-20. Blackswell: Boston.

DENTINGER, M.P., BARRON, K.D. and CSIZA, C.K. (1985) Glial and axonal development in optic nerve of myelin deficient rat mutant. Brain Research 344, 255-266.

DOBBING, J. and SANDS, J. (1979) Comparative aspects of the brain growth spurt. Early Human Development 3, 79-83.

DOLMAN, C.L., MCCORMICK, A.Q. and DRACE, S.M. (1980) Aging of the optic nerve. Archives of Ophthalmology 98, 2053-2058.

DOMINGUEZ, R.D., VILA-CORO, A.A., SLOPIS, J.M. and BOHAN, T.P. (1991) Brain and ocular abnormalities in infants with in utero exposure to cocaine and other street drugs. American Journal of Diseases of Children 145, 688-695.

DONOVAN, A. (1967) The nerve fibre composition of the cat optic nerve. Journal of Anatomy 101, 1-11.

DOWNER, J de C. (1967) Quantitative histology of the optic nerve, optic tract and lateral geniculate nucleus of man. Journal of Anatomy 101, 393-402.

DRAGER, U.C. and HUBEL, D.H. (1978) Studies of visual functions and its decay in mice with hereditary retinal degeneration. Journal of Comparative Neurology 180, 85-114.

DUNCAN, D. (1934) A relation between axone diameter and myelination as determined by measurement of myelinated spinal root fibers. Journal of Comparative Neurology 60, 437-471.

EDWARDS, R.G. and GATES, A.H. (1959) Timing of the stages of maturation, divisions, ovulation, fertilisation and the first cleavage of eggs of adult mice treated with gonadotrophins. Journal of Endocrinology 18, 292-304.

EHYAI, A. and FREMON, F. (1983) Progressive optic neuropathy and senorineural hearing loss due to chronic glue sniffing. Journal of Neurology, Neurosurgery and Psychiatry 46, 349-351.

FERNANDEZ, E., CUENCA, N., CEREZO, J.R. and De JUAN, J. (1993) Visual experience during postnatal development determines the size of the optic nerve axons. Neuroreport 5, 365-367.

FINDLATER, G.S., MCDOUGALL, R.D. and KAUFMAN, M.H. (1993) Eyelid development, fusion and subsequent reopening in the mouse. Journal of Anatomy 183, 121-129.

FLECK, B.W. and DANGATA, Y.Y. (1994) Causes of visual handicap in the Royal Blind School, Edinburgh, 1991-2. British Journal of Ophthalmology 78, 421.

FORRESTER, J.F. and PETERS, S.A. (1967) Nerve fibres in optic nerve of rat. Nature 214, 245-247.

FOSTER, A. and GILBERT, C. (1992) Epidemiology of childhood blindness. Eye 6, 173-176.

FOSTER, A. and SOMMER, A. (1987) Corneal ulceration, measles, and childhood blindness in Tanzania. British Journal of Ophthalmology 71, 331-343.

FRANCOIS, J. and FRYCZKOWSKI, A. (1978) The blood supply of the optic nerve. Advances in Ophthalmology 36, 164-173.

FRANCOIS, J. and FRYCZKOWSKI, A. (1982) Functional importance of central retinal anastomoses in anterior part of the optic nerve. Ophthalmologica 185, 15-25.

FRANZ, T. and BESECKE, A. (1991) The development of the eye in homozygotes of the mouse mutant Extra-toes. Anatomy and Embryology 184, 355-361.

FRASER, F.C. and FAINSTAT, T.D. (1951) Production of congenital defects in offspring of pregnant mice treated with cortisone. Pediatrics 8, 527-533.

GARCIA-VALENZUELA, E., SHAREEF, S., WALSH, J. and SHARMA, S.C. (1995) Programme cell death of retinal ganglion cells during experimental glaucoma. Experimental Eye Research 61, 33-44.

GAREY, L.J. (1984) Structural development of the visual system of man. Human Neurobiology 3, 75-80.

GAREY, L.J. and POWELL, T.P.S. (1968) The projection of the retina in the cat. Journal of Anatomy 102, 189-222.

GARRO, A.J., McBETH, D.L., LIMA, V. and LIEBER, C.S. (1991) Ethanol consumption inhibits fetal DNA methylation in mice: Implication for the fetal alcohol syndrome. Alcoholism: Clinical and Experimental Research 15, 395-398.

GASSER, H.S. and GRUNDFEST, H. (1939) Axon diameters in relation to the spike dimensions and the conduction velocity in mammalian A fibers. The American Journal of Physiology 127, 393-414.

GAZE, R.M. and PETERS, A. (1961) The development, structure and composition of the optic nerve of Xenopus laevis (Daudin). Quarterly Journal of Experimental Neurology 46, 299-309.

GHOORAY, G.T. and MARTIN, G.F. (1993) The development of myelin in the spinal cord of the North American opossum and its possible role in loss of rubrospinal plasticity: a study using myelin basic protein and galactocerebroside immuno-histochemistry. Developmental Brain Research 72, 67-74.

GILLIAM, D.M., KOTCH, L.E., DUDEK, B.C. and RILEY, E.P. (1990) Ethanol teratogenesis in selectively bred long-sleep and short-sleep mice: a comparison to inbred C57BL/6J mice. Alcoholism: Clinical and Experimental Research 13, 667-672.

GLASER, T., LANE, J. and HOUSMAN, D. (1990) A mouse model of the Aniridia-Wilms tumor. Science 250, 823-827.

GLICKSTEIN, M., KING, R.A., MILLER, J. and BERKLEY, M. (1967) Cortical projections from the dorsal lateral geniculate nucleus of cats. Journal of Comparative Neurology 130, 55-76.

GOLDBERG, S. and FRANK, B. (1979) The guidance of optic axons in the developing and adult mouse retina. Anatomical Record 193, 763-774.

GOOD, W.V., FERRIERO, D.M., GOLABI, M. and KOBORI, J.A. (1992) Abnormalities of the visual system in infants exposed to cocaine. Ophthalmology 99, 341-346.

GREEN, E.L. (1966) Breeding systems. In: *Biology of the Laboratory Mouse* (ed. E.L. Green) 2nd ed, pp 11-22, McGraw-Hill, New York.

GREEN, M.C. (1966) Genes and development. In: *Biology of the Laboratory Mouse* (ed., E.L. Green) 2nd ed., pp 329-336, McGraw-Hill, New York.

GREEN, M.C. (1966) Mutant genes and linkages. In: *Biology of the Laboratory Mouse* (ed., E.L. Green) 2nd ed., pp 87-135, McGraw-Hill, New York.

GYELLENSTEN, L. and MALMFORS, T. (1963) Myelinization of the optic nerve and its dependence on visual function - a quantitative investigation in mice. Journal of Embryology and Experimental Morphology 11, 255-266.

GYELLENSTEN, L., MALMFORS, T. and NORRLIN-GRETTVE, M-L. (1966) Developmental and functional alterations in the fibre composition of the optic nerve in visually deprived mice. Journal of Comparative Neurology 128, 413-418.

HARCH, C., CHASE, H.B. and GONSALVES, N. (1978) Studies on an anophthalmic strain of mice. VI. Lens and cup interaction. Developmental Biology 63, 352-357.

HENKIND, P. and LEVITSKY, M. (1969) Angiarchitecture of the optic nerve. I. American Journal of Ophthalmology 68, 979-986.

HERMANN, J., PALLISTER, P.D. and OPITZ, J.M. (1980) Tetraectrodactyly and other skeletal manifestations in the fetal alchol syndrome. European Journal of Pediatrics 133, 221-226.

HERO, I., FARJAH, M. and SCHOLTZ, C.L. (1992) The effect of the microphthalma gene on pre-natal optic nerve development in the mouse. Experimental Eye Research 54, 161-171.

HILL, R.E., FAVOR, J., HOGAN, B.L.M., TON, C.C.T., SAUNDERS, G.F., HANSON, I.M., PROSSER, J., JORDAN, T., HASTIE, N.D. and HEYNINGEN, V.V. (1991) Mouse small eye results from mutation in a paired-like homeobox-containing gene. Nature 354, 522-525.

HIROSE, G. and BASS, N.H. (1973) Maturation of oligodendroglia and myelinogenesis in rat optic nerve: a quantitative histochemical study. Journal of Comparative Neurology 152, 201-210.

HIRSCHORN, K. and COOPER, M.L. (1961) Chromosomal aberations in human disease. American Journal of Medicine 31, 442-470.

HITTNER, H.M. (1989) Aniridia. In: *The Glaucomas*, vol. 2, 869-884, C. V. Mosby, Toronto.

HOGAN, B., BEDDINGTON, R., COSTANTINI, F. and LACY, E. (1994) Developmental genetics and embryology of the mouse: Past, present, and future, 1. In: *Manipulating the Mouse Embryo. A Laboratory Manual.* 2nd ed. pp 1-20, Cold Spring Harbor Laboratory Press, New York.

HOGAN, B.L.M., HIRST, E.M.A., HORSBURGH, G. and HETHERINGTON, C.M. (1988) Small eye (Sey): a mouse model for the genetic analysis of craniofacial abnormalities. Development 103 (Suppl.), 115-119.

HOGAN, B.L.M., HORSBURGH, G., COHEN, J., HETHERINGTON, C.M., FISHER, G. and LYON, M.F. (1986) *Small eyes (Sey)*: a homozygous lethal mutation on chromosome 2 which affects the differentiation of both lens and nasal placodes in the mouse. Journal of Embryology and Experimental Morphology 97, 95-110.

HOLLENBERG, M.J. and SPIRA, A.W. (1973) Human retinal development. American Journal of Anatomy 157, 357-386.

HORSBURGH, G.S. and SEFTON, A.J. (1986) The early development of the optic nerve and chiasma in embryonic rat. Journal of Comparative Neurology 243, 547-560.

HUBER, D. EHRHARDT, J.D.,DECKER, N., HIMBER, J., ANDERMANN, G. and LECLERC, G. (1991) Synthesis and ocular antihypertensive activity of new imidazoldine derivatives containing a beta-blocking side chain. Journal of Medicinal Chemistry 34, 3197-3204.

HUGHES, A. (1977) The pigmented-rat optic nerve: fiber count and fiber diameter spectrum. Journal of Comparative Neurology 176, 263-268.

ISAYAMA, Y., HIRAMATSU, K., ASAKURA, S. and TAKAHASHI, T. (1983) Posterior ischaemic optic neuropathy. I. Blood supply of the optic nerve. Ophthalmologica 186, 197-203.

ISENBERG, S.J., SPIERER, A. and INKELIS, S.H. (1987) Ocular signs of cocaine intoxication in neonates. American Journal of Ophthalmology 103, 211-214.

JAY, B. (1987) Causes of blindness in schoolchildren. British Medical Journal 294, 1183-1184.

JONES, K.L. and SMITH, D.W. (1973) Recognition of the fetal alcohol syndrome in early pregnancy. Lancet 2, 999-1001.

JONES, K.L., SMITH, D.W., STREISSGUTH, A.P. and MYRIANTHOPOULOS, N.C. (1974) Outcome in offspring of chronic alcoholic women. Lancet 1, 1076-1078.

JONES, K.L., SMITH, D.W., ULLELAND, C.N. and STREISSGUTH, A.P. (1973) Pattern of malformation in offspring of chronic alcoholic mothers. Lancet 1, 1267-1271.

JONGS, R.V.D.M-D, DICKSON, M.E., WOYCHIK, R.P., STUBBS, L. and HETERINGTON, C. (1990) Location of the gene involved in the small eye mutation on mouse chromosome 2 suggests homology with human aniridia 2 (AN2). Genomics 7, 270-275.

KAUFMAN, M.H. (1979) Cephalic neurulation and optic vesicle formation in the early mouse embryo. American Journal of Anatomy 155, 425-444.

KAUFMAN, M.H. (1992) *The Atlas of mouse development.* Academic Press: London.

KING, J. (1979) Ischemic optic neuropathy. Clinical and Experimental Neurology 16, 205-216.

KJELLSTROM, C. and CONRADI, N.G. (1993) Decreased axonal calibres without axonal loss in optic nerve following chronic alcohol feeding in adult rats: a morphometric study. Acta Neurologica 85, 117-121.

KNAPP, P.E., DUTTA, A. and SKOFF, R.P. (1990) Differences in levels of neuroglial cell death in jimpy male mice and carrier females. Developmental Neuroscience 12, 145-152.

KOENIGSBERG, R. (1989) *Illustrated Churchill's Medical Dictionary.* (ed: R. Koenigsberg), Churchill Livingstone, New york.

KOTCH, L.E., DEHART, D.B., ALLES, A.J., CHERNOFF, N. and SULIK, K.K. (1992) Pathogenesis of ethanol-induced limb reduction defects in mice. Teratology 46, 323-332.

KOTKOSKIE, L.A. and NORTON, S. (1988) Prenatal brain malformations following acute ethanol exposure in the rat. Alcoholism: Clinical and Experimental Research 12, 831-836.

KRONICK, J.B. (1976) Teratogenic effects of ethyl alcohol administered to pregnant mice. American Journal of Obstetrics and Gynecology 124, 676-680.

KUPFER, C., CHUMBLAY, L. and DOWNER, J. de C. (1967) Quantitative histology of the optic nerve, optic tract and lateral geniculate nucleus of man. Journal of Anatomy 101, 392-402.

LAM, K., SEFTON, A.J. and BENNETT, M.R. (1982) Loss of axons from the optic nerve of the rat during early postnatal development. Developmental Brain Research 3, 487-491.

LAMANTIA, A.S. and RAKIC P (1994) Axon over production and elimination in the anterior commissure of the developing rhesus monkey. Journal of comparative Neurology 340, 328-336.

LANCASTER, F.E., MAYUR, B.K., PATSALOS, P.N., SAMORAJSKI, T. and WIGGINS, R.C. (1982) The synthesis of myelin and brain subcellar membrane proteins in the offspring of rats fed ethanol during pregnancy. Brain Research 235, 105-113.

LANCASTER, F.E., PHILIPS, S., PATSALOS, P.N. and WIGGINS, R.C. (1984) Brain myelin in the offspring of ethanol treated rats: in utero versus lactational exposure by crossfostering offspring of control, pairfed and alcohol treated dams. Brain Research 309, 209-216.

LANGFORD, C. and SEFTON, J. (1992) The relative time course of axonal loss from the optic nerve of the developing guinea pig is consistent with that of other mammals. Visual Neuroscience 9, 555-564.

LESSON, C.R., LESSON, T.S. and PAPARO, A.A. (1985) *Textbook of Histology*. 5th ed. W.B. Sauder, Tokyo.

LEWIS, P.D. (1985) Neuropathological effects of alcohol on the developing nervous system. Alcohol and Alcoholism 20, 195-200.

LORKE, D.E. and LAUER, M. (1990) Gliogenesis and myelination in the optic nerve of trisomy 19 mice. A quantitative electron microscopic study. Acta Anatomica 137, 222-233.

LYON, M.F. (1989) Rules for nomenclature of inbred strains. In: *Genetic Variants and Strains of the Laboratory Mouse* (ed. LYON, M.F. and SEARLE, A.G.) 2nd ed. pp 632-635. Oxford University Press, New York.

MAGOON, E.H. and ROBB, R.M. (1981) Development of myelin in human optic nerve and tract. A light and electron microscopic study. Archives of Ophthalmology 99, 655-659.

MARCIANO, T.F., GOCHT, A., DENTINGER, M.P., HOF, L., CSIZA, C.K. and BARRON, K.D. (1990) Axonal regrowth in the amyelinated optic nerve of the myelin-deficient rat: ultrastructural observations and effects of ganglioside administration. Journal of Comparative Neurology 295, 219-234.

MATHESON, D.F. (1970) Some quantitative aspects of myelination of the optic nerve in rat. Brain Research 24, 257-269.

MATHESON, D.F. (1971) Evidence in support of centripedal gradient in myelination in the rat optic nerve. Experimental Neurology 32, 195-205.

MATHIEU, J.M., MOTTET, S., KRAUS-RUPPERT, R., COHEN, S.R. and WEBSTER, H.D. (1981) Effects of colchicine on myelination of rabbit optic nerve: a biochemical study. Neurotoxicology 2, 451-461.

MATTHEWS, M.A. (1968) An electron microscopic study of the relationship between axon diameter and the initiation of myelin production in the peripheral nervous system. Anatomical Record 161, 337-352.

MATTHEWS, M.A. and DUNCAN, D. (1971) A quantitative study of morphological changes accompanying the initiation and progress of myelin production in the dorsal funiculus of the rat spinal cord. Journal of Comparative Neurology142, 1-22.

MAYHEW, T.M. (1988) An efficient sampling scheme for estimating fibre number from nerve cross sections: the fractionator. Journal of Anatomy 157, 127-134.

MAYHEW, T.M. (1990) An efficient and unbiased sampling of nerve fibres for estimating fibre number and size. In: *Methods in Neuroscience*, vol. 3, pp. 172-187, Academic Press, New York.

MAYHEW, T.M. and SHARMA, A.K. (1984a) Sampling schemes for estimating nerve fibre size. 1. Methods for nerve trunks of mixed fascicularity. Journal of Anatomy 139, 45-58.

MAYHEW, T.M. and SHARMA, A.K. (1984b) Sampling schemes for estimating nerve fibre size. 11. Methods for unifascicular nerve trunks. Journal of Anatomy 139, 59-66.

MEIER, C. and BISCHOFF, A. (1975) Oligodendroglial cell in jimpy mice and controls. An electron-microscopic study in the optic nerve. Journal of Neurological Science 26, 517-528.

MEISSIREL, C. and CHALUPA, L.M. (1994) Organisation of pioneer retinal axons within the optic tract of the rhesus monkey. Proceedings of the National Academy of Sciences of the United States of America 91, 3906-3910.

MELE, L., WEST, K.P., KUSDIONO, Jr., PANDJI, A., NENDRAWATI, H., TILDEN, R.L., TARWOTJO, I. and THE ACEH STUDY GROUP (1991) Nutritional and household risk factors for xerophthalmia in Aceh, Indonesia: a case-control study. American Journal of Clinical Nutrition 53, 1460-1465.

MERMOUD, A., BAERVELDT, G., MICKLER, D.S., WU, G.S. and RAO, N.A., (1994) Animal model for uveitic glaucoma. Graefes Archive for Clinical and Experimental Ophthalmology 232, 553-560.

MICHAELIS, E.K. (1990) Fetal alcohol exposure: Cellular toxicity and molecular events involved in toxicity. Alcoholism: Clinical and Experimental Research 14, 819-826.

MIDDAUGH, L.D. and BOGGAN, W.O. (1991) Postnatal growth deficit in prenatal ethanol-exposed mice: Characteristics and critical periods. Alcoholism: Clinical and Experimental Research 15, 919-926.

MILLER, M.T. (1992) Ocular teratology observations, speculations, questions, principles reaffirmed. Eye 6, 177-180.

MILLER, W.M. (1993) Migration of cortical neurons is altered by gestational exposure to ethanol. Alcoholism: Clinical and Experimental Research 17, 1275-1280.

MILLER, W.M. and Al-RABIAI, S. (1994) Effects of prenatal exposure to ethanol on the number of axons in the pyramidal tract of the rat. Alcoholism: Clinical and Experimental Research 18, 346-364.

MOORE, K.L. (1985) The head. In: *Clinically Oriented Anatomy* 2nd ed., pp 794-982. Williams & Wilkins, Baltimore.

MORRISON, J., FARRELL, S., JOHNSON, E., DEPPACEIER, L., MOORE, C.G. and GROSSMANN, E. (1995) Structure and composition of the rodent lamina cribrosa. Experimental Eye Research 60, 127-135.

MOSIER, M.A., LIEBERMAN, M.F., GREEN, W.R. and KNOX, D.L. (1978) Hypoplasia of the optic nerve. Archives of Ophthalmology 96, 1437-1442.

MULLANEY, J. (1982) Normal development and developmental anomalies of the eye. In: *Pathobiology of Ocular Diseases: A Dynamic Approach. Part A*, (ed. Garner, A. & Klintworth, G.K.) pp 443-521, Marcel Dekker, New York.

MUND, M.L., RODRIGUES, M.M. and FINE B.S. (1972) Light and electron microscopic observations on the pigmented layers of the developing human eye. American Journal of Ophthalmology 73, 167-182.

NEETENS, A. (1977) Autoregulation of the blood supply to the anterior optic nerve and lamina cribrosa. Transactions of the Ophthalmological Societies of the United Kingdom 97, 168-176.

NELSON, M.M., ASLING, C.V. and EVANS, H.M. (1952) Production of multiple congenital malformations in young by maternal pteroyl-glutamic acid deficiency during gestation in rats. Journal of Nutrition 48, 61-80.

NELSON, M.M., WRIGHT, H.V., ASLING, C.V. and EVANS, H.M. (1955) Multiple congenital abnormalities resulting from transitory deficiency of pteroyl-glutamic acid during gestation in rats. Journal of Nutrition 56, 349-370.

NG, A.Y. and STONE, J. (1982) The optic nerve of the cat: appearance and loss of axons during normal developemt. Brain Research 281, 263-271.

NICOLL, A., BEDI, K.S. and WIGMORE, P.M. (1991) The effect of neonatal monocular enucleation on the optic nerves of the rat. Journal of Anatomy 174, 27-35.

OGDEN, T.E. and MILLER, R.F. (1966) Studies of the optic nerve of the rhesus monkey: nerve fiber spectrum and physiological properties. Vision Research 6, 485-506.

O' RAHILLY, R. (1975) The prenatal development of the human eye. Experimental Eye Research 21, 92-112.

O'SHEA, K. S. and KAUFMAN, M. H. (1979) The teratogenic effect of acetaldehyde: implications for the study of the fetal alcohol syndrome. Journal of Anatomy 128, 65-78.

O'SHEA, K. S. and KAUFMAN, M. H. (1981) Effect of acetaldehyde on the neuroepithelium of early mouse embryos. Journal of Anatomy 132, 107-118.

PADMANABHAN, R., HAMEED, M.S. and SUGATHAN, T.N. (1984) Effects of acute dose of alcohol on pre- and postnatal development in the mouse. Drug and Alcohol Dependence 14, 197-208.

PARSON, S.H., DHILLON, B., FINDLATER, G.S. and KAUFMAN, M.H. (1995) Optic nerve hypoplasia in the fetal alcohol syndrome: a mouse model. Journal of Anatomy 186, 313-320.

PARSON, S.H., FINDLATER, G.S., KAUFMAN, M.H and DHILLON, B. (1993) Morphometric analysis of optic nerve hypoplasia in the fetal alcohol syndrome: a mouse model. Journal of Anatomy 184, 212.

PARSON, S.H. and SOJITRA, N.M. (1995) Loss of myelinated axons is specific to the central nervous system in a mouse model of the fetal alcohol syndrome. Journal of Anatomy 187, 739-748.

PEI, Y.F. and RHODIN, J.A.G. (1970) The prenatal development of the mouse eye. Anatomical Record 168, 105-125.

PERRY, V.H., HENDERSON, Z. and LINDEN, R. (1983) Postnatal changes in retinal ganglion cell and optic axon populations in the pigmented rat. Journal of Comparative Neurology 219, 356-368.

PHILLIPS, C.I., LEVY, A.M., NEWTON, M. and STOKOE, N.L. (1987) Blindness in schoolchildren: importance of heredity, congenital cataract, and prematurity. British Journal of Ophthalmology 71, 578-584.

PHILLIPS, D.E. (1989) Effects of limited postnatal alcohol exposure on the development of myelin and nerve fibers in rat optic nerve. Experimental Neurology 103, 90-100.

PHILLIPS, D.E. and KRUEGER, S.K. (1992) Effects of combined pre- and postnatal ethanol exposure (three trimester equivalency) on glial cell development in rat optic nerve. International Journal of Developmental Neuroscience 10, 197-206.

PHILLIPS, D.E., KRUEGER, S.K. and RYDQUIST, J.E. (1991) Short- and long-term effects of combined pre- and postnatal ethanol exposure (three trimester equivalency) on the development of myelin and axons in rat optic nerve. International Journal of Developmental Neuroscience 9, 631-647.

PINAZO-DURAN, M.D., RENAU-PIQUERAS, J. and GUERRI, C. (1993) Developmental changes in the optic nerve related to ethanol consumption in pregnant rats: Analysis of the ethanol-exposed optic nerve. Teratology 48, 305-322.

POTTS, A.M., HODGES, D., SHELMAN, C.B., FRITZ, K.J., LEVY, N.S. and MANGNALL, Y. (1972a) Morphology of the primate optic nerve. 1. Method and total fiber count. Investigative Ophthalmology 11, 980-988.

POTTS, A.M., HODGES, D., SHELMAN, C.B., FRITZ, K.J., LEVY, N.S. and MANGNALL, Y. (1972b) Morphology of the primate optic nerve. 11. Total fiber size distribution and fiber density distribution. Investigative Ophthalmology 11, 989-1003.

PROVIS, J.M., VAN DRIEL, D., BILLSON, F.A. and RUSSELL, P. (1985) Human fetal optic nerve: overproduction and elimination of retinal axons during development. The Journal of Comparative Neurology 238, 92-100.

QUIGLEY, H.A. and ADDICKS, E.M. (1980) Chronic experimental glaucoma in primates II. Effect of extended intraocular pressure elevation on the optic nerve head and axonal transport. Investigative Ophthalmology and Visual Science 19, 137-153.

QUIGLEY, H.A. and ADDICKS, E.M. (1981) Regional differences in the structure of the lamina cribosa and their relation to glaucomatous optic nerve damage. Archives of Ophthalmology 99, 137-143.

QUIGLEY, H.A., ADDICKS, E.M. and GREEN, W.R. (1982) Optic nerve damage in human glaucoma III. Quantitative correlation of nerve fiber loss and visual field defect in glaucoma, ischemic neuropathy, papilledema, and toxic neuropathy. Archives of Ophthalmology 100, 135-146.

QUIGLEY, H.A., FLOWER, R.W., ADDICKS, E.M. and McLEOD, D.S. (1980) The mechanism of optic nerve damage in experimental acute intraocular pressure elevation. Investigative Ophthalmology and Visual Science 19, 505-517.

QUIGLEY, H.A., HOHMAN, R.M., ADDICKS, E.M., MASSOF, R.W. and GREEN, W.R. (1983) Morphologic changes in the lamina cribrosa correlated with neural loss in open-angle glaucoma. American Journal of Ophthalmology 95, 673-691.

QUIGLEY, H.A., SANCHEZ, R.M., DUNKELBERGER, G.R., L'HERNAULT, N.L. and BAGINSKI, T.A. (1987) Chronic angle glaucoma selectively damages large optic nerve fibers. Investigative Opthalmology and Visual Science 28, 913-920.

QUILLAM, T.A. (1956) Some characteristics of myelinated fibre populations. Journal of Anatomy 90, 172-187.

RANDALL, C.L. and TAYLOR, W.J. (1979) Prenatal ethanol exposure in mice: Teratogenic effects. Teratology 19, 305-312.

REPKA, M.X. and QUIGLEY, H.A. (1989) The effect of age on normal human optic nerve fiber number and diameter. Ophthalmology 96, 26-32.

REYNOLDS, E.S. (1963) The use of lead citrate at high pH as an electron-opaque stain in electron microscopy. Journal of Cell Biology 17, 208-212.

RIMMER, S., KEATING, C., CHOU, T., FARB, M.D., CHRISTENSON, P.D., FOOS, R.Y. and BATEMAN, J.B. (1993) Growth of the human optic nerve disk and nerve during gestation, childhood, and early adulthood. American Journal of Ophthalmology 116, 748-753.

ROBB, R.M., SILVER, J. and SULLIVAN, R.T. (1978) Ocular retardation (or) in the mouse. Investigative Ophthalmology and Visual Science 17, 468-473.

ROBERTS, R.C. (1961) The lifetime growth and reproduction of selected strains of mice. Heredity 16, 369-381.

ROBERTS, R.C. (1967) Small eyes - a new dominant eye mutant in the mouse. Genetical Research 9, 121-122.

ROBINSON, G.C., JAN, J.E. and KINNIS, C. (1987) Congenital ocular blindness in children, 1945 to 1984. American Journal of Diseases of Children 141, 1321-1324.

ROMANES, G.J. (1986) *Cunningham's Manual of Practical Anatomy*. 5th ed., Vol. III, Oxford University Press, New York.

RUGH, R. (1990) *The Mouse: Its Reproduction and Development*. Oxford Science Publications, Oxford.

RUGH, R. and GRUPP, E. (1960) Congenital defects following low level of X-irradiation. Anatomical Record 138, 380-381.

RUSELL, E.S. (1966) Lifespan and aging pattern. In: *Biology of the Laboratory Mouse* (ed. E.L. Green) 2nd ed, pp11-22, McGraw-Hill, New York.

SADLER, T.W. (1990) *Langman Medical Embryology*. 6th ed., William and Wilkinson, Baltimore.

SAMORAJSKI, T., LANCASTER, F. and WIGGINS, R.C. (1986) Fetal ethanol exposure: a morphometric analysis of myelination in the optic nerve. International Journal of Development and Neuroscience 4, 369-374.

SANCHEZ, R.M., DUNKELBERGER, G.R. and QUIGLEY, H.A. (1986) The number and diameter distribution of axons in the monkey optic nerve. Investigative Ophthalmology and Visual Science 27, 1342-1350.

SCAMMON, R.E. and ARMSTRONG, E.L. (1925) On the growth of the human eyeball and optic nerve. Journal of Comparative Neurology 38, 165-219.

SCHEIE, H.G. and ALBERT, D.M. (1977) Embryology of the human eye. In: *Textbook of Ophthalmology*, 9th ed, pp.79-92. WB Saunders, Philadelphia.

SCHENKER, S., BECKER, H.C., RANDALL, C.L., PHILIPS, D.K., BASKIN, G.S. and HENDENSON, G.I. (1990) Fetal alcohol syndrome: Current status of pathogenesis. Alcohol: Clinical and Experimental Research 14, 635-647.

SCHWETZ, B.A., SMITH, F.A. and STAPLES, R.E. (1978) Teratogenic potential of ethanol in mice, rats and rabbits. Teratology 18, 385-392.

SHINE, H.D. and READHEAD, C. (1992) Morphometric analysis of normal, mutant, and transgenic CNS: correlation of myelin basic protein expression to myelinogenesis. Journal of Neurochemistry 58, 342-349.

SILBERBERG, M. and SILBERBERG, R. (1954) Factors modifying the lifespan of mice. American Journal of Physiology 177, 23-26.

SILBERBERG, R., JARRETT, S.R. and SILBERBERG, M. (1961) Life span of mice fed enriched or restricted diets during growth. American Journal of Physiology 200, 332-334.

SILVA-ARAUJO, A., SALGADO-BORGES,J., CARDOSO, V., SILVA, M.C., CASTRO-CORREIA, J. and TAVARES, M.A. (1993) Changes in the retinal ganglion cell layer and optic nerve of rats exposed neonatally to cocaine. Experimental Eye Research 56, 199-206.

SILVA-ARAUJO, A., SALGADO-BORGES, J., and TAVARES, M.A. (1991) Morphological changes in the optic nerve after chronic exposure of neonatal rats to cocaine and amphetamine. Ophthalmic Research 23, 295-302.

SILVER, J. (1984) Studies on factors that govern directionality of axonal growth in the embryonic optic nerve and at the chiasm of mice. Journal of Comparative Neurology 223, 238-251.

SILVER. J. and HUGHES, A.F.W. (1974) The relationship between morphogenetic cell death and the development of congenital anophthalmia. Journal of Comparative Neurology 157, 281-302.

SILVER, J. and ROBB, R.M. (1979) Studies on the development of the eye cup and optic nerve in normal mice and in mutants with congenital optic nerve aplasia. Developmental Biology 68, 175-190.

SKOFF, R.P., PRICE, D.L. and STOCKS, A. (1976a) Electron microscopic autoradiographic studies of gliogenesis in rat optic nerve. I. Cell proliferation. Journal of Comparative Neurology 169, 291-312.

SKOFF, R.P., PRICE, D.L. and STOCKS, A. (1976b) Electron microscopic autoradiographic studies of gliogenesis in rat optic nerve. II. Time of origin. Journal of Comparative Neurology 169, 313-334.

SMITH, D.L., SKUTA, G.L., KINCAID, M.C., RABBANI, R., CRUESS, D.F. and KAO, S.F. (1991) The effects of glaucoma medication on Tenon's capsule and conjunctiva in the rabbit. Ophthalmic Surgery 22, 336-340.

SNELL, G.D. and STEVENS, L.C. (1966) Early embryology. In: *Biology of the Laboratory Mouse* (ed. E.L. Green) 2nd ed, pp11-22, McGraw-Hill, New York.

SORSBY, A. and SHERIDAN, M. (1960) The eye at birth: measurements of the principal diameters in forty-eight cadavers. Journal of Anatomy 94, 192-197.

STAAT, J. (1964) Standardized nomenclature for inbred strains of mice, Third listing. Cancer Research 24, 147-168.

STAATS, J. (1966) The laboratory mouse. In: *Biology of the Laboratory Mouse* (ed. E.L. Green), 2nd ed., pp 1-9, McGraw-Hill, New York.

STRAIN, G.M. and TELFORD, B.L. (1993) Flash and pattern reversal visual evoked potentials in C57BL/6J and B6CBAF1/J mice. Brain Research Bulletin 32, 57-63.

STURROCK, R.R. (1987) Development of the meninges of the human embryonic optic nerve. Journal fur Hirnforshung 28, 603-613.

STURROCK, R.R. (1987) Changes in the number of axons in the human embryonic optic nerve from 8 to 18 weeks of gestation. Journal fur Hirnforshung 28, 649-652.

STURROCK, R.R. (1987) Vascularization of the human embryonic optic nerve. Journal fur Hirnforshung 28, 615-624.

SULIK, K.K., JOHNSTON, M.C. and WEBB, M.A. (1981) Fetal alcohol syndrome: embryogenesis in a mouse model. Science 214, 936-938.

SYLVESTER, P.E. and ARI K (1961) The size and growth of the human optic nerve. Journal of Neurology, Neurosurgery and Psychiatry 24, 45-49.

TAUBER, H., WASHNELDT, T.V. and NEUHOFF, V. (1980) Myelination in the rabbit optic nerves is accelerated by artificial eye opening. Neuroscience Letters 16, 235-238.

TENNEKOON, G., AITCHISON, C.S., FRANGIA, J., PRICE, D.L. and GOLDBERG, A.M. (1979) Chronic lead intoxication: effects on developing optic nerve. Annals of Neurology 5, 558-564.

TENNEKOON, G.I., COHEN, S.R., PRICE, D.L. and MCKHANN, G.M. (1977) Myelinogenesis in optic nerve. A morphological, autoradiographic, and biochemical Analysis. The Journal of Cell Biology 72, 604-616.

THEILER, K. (1976) *The House Mouse: Development and Normal Stages from Fertilization to 4 weeks of Age*. Springer-erlag, Berlin.

THEILER, K. and VARNUM, D.S. (1981) Development of coloboma (Cm/+), a mutation with anterior lens adhesion. Anatomy and Embryology 162. 121-126.

THEILER, K., VARNUM, D.S., NADEAU, J.H., STEVENS, L.C. and CAGIANUT, B. (1976) A new allele of ocular retardation: early development and morphogenetic cell death. Anatomy and Embryology 150, 85-97.

THEILER, K., VARNUM, D.S. and STEVENS, L.C. (1978) Development of Dickie's small eye, a mutation in the house mouse. Anatomy and Embryology 155, 81-86.

THEILER, K., VARNUM, D.S. and STEVENS, L.C. (1980) Development of Dickie's small eye: an early lethal mutation in the house mouse. Anatomy and Embryology 161, 115-120.

TODD, T.W., BEECHER, H., WILLIAMS, G.H. and TODD, A.W. (1940) The weight and growth of the human eyeball. Human Biology 12, 1-20.

TON, C.C.T, MIWA, H. and SAUNDERS, G.F. (1992) Small eye (Sey): cloning and characterization of the murine homolog of the human aniridia gene. Genomics 13, 251-256.

TRUSLOVE, G.M. (1962) A gene causing ocular retardation in the mouse. Journal of Embryology and Experimental Morphology 10, 652-660.

TRUMP, B.F. and ERICSSON, J.L.E. (1965) The effect of the fixative solution on the ultrastructure of cells and tissues. Laboratory Investigation 14, 1245-1323.

UMEMORI, H., SATO, S., YAGI, T., AIZAWA, S. and YAMAMOTO T (1994) Initial events of myelination involve fyn tyrosine kinase signalling. Nature 367, 572-576.

UPHOFF, C., NYQUIST-BATTIE, C. and TOTH, R. (1984) Cardiac muscle development in mice exposed to ethanol in utero. Teratology 30, 119-129.

VANEY, D.I. and HUGHES A. (1976) The rabbit optic nerve: fibre diameter spectrum, fibre count, and comparison with a retinal ganglion cell count. Journal of Comparative Neurology 170, 241-252.

VAUGHN, J.E. (1969) An electron microscopic analysis of gliogenesis in rat optic nerves. Zeitschrift fur Zellforschung und Mikroskopische Anatomie 94, 293-324.

WAKAKUWA, K., WATANABE, M., SUGIMOTO, T., WASHIDA, A. and FUKUDA, Y. (1987) An electron microscopic analysis of the optic nerve of the eastern chipmunk (Tamias sibiricus asiaticus): Fiber count and retinotopic organisation. Vision Research 11, 1891-1901.

WARRINGTON, A.E., BARBARESE, E. and PFEIFFER, S.E. (1993) Differential myelinogenic capacity of specific developmental stages of the oligodendrocyte lineage upon transplantation into hypomyelinating hosts. Journal of Neuroscience Research 34, 1-13.

WARWICK, R. (1976) *Eugene Wolff's Anatomy of the Eye and Orbit*. 7th ed. Lewis, London.

WEAKLEY, B.S. (1964) Ultrastructure of the fetal thymus in the golden hamster. Journal of Morphology 115, 319-354.

WEAKLEY, B.S. (1966) Electron microscopy of the oocyte and granulosa cells in the developing ovarian follicles of the golden hamster. Journal of Anatomy 100, 503-534.

WEAKLEY,B.S. (1981) *A beginner's Handbook in Biological Transmission Electron Microscopy* 2nd ed., Churchill Livingstone, New York.

WEBSTER, W.S., WALSH, D.A., McEwen, S.E. and LIPSON, A.H. (1983) Some teratogenic properties of ethanol and acetaldehyde in C57BL/6J mice: Implication for the study of the fetal alcohol sydrome. Teratology 27, 231-243.

WEST, J.R., GOODLETT, C.R., BONTHIUS, D.J., HAMRE, K.M., MARCUSSEN, B.L. (1990) Population depletion associated with fetal alcohol damage: Mechanisms of BAC-dependent cell loss. Alcoholism: Experimental and Clinical Research 14, 813-818.

WIGGINS, R.C., FULLER, G.N., BRIZZEE, L., BISSEL, A.C. and SAMORAJSKI, T. (1984) Myelination of the rat optic nerve during postnatal undernourishment and recovery: a morphometric analysis. Brain Research 308, 263-272.

WILLIAMS, P.L., WARWICK, R., DYSON, M. and BANNISTER, L.H. (1989) *Gray's Anatomy*, Longman, Edinburgh.

WILLIAMS, R.W., BASTANI, M.J., LIA, B. and CHALUPA, L.M. (1986) Growth cones, dying axons, and developmental fluctuations in the fiber population of the cat's optic nerve. Journal of Comparative Neurology 246, 32-69.

WILSON, M.E. and CRAGG, B.G. (1967) Projections from the lateral geniculate nucleus in the cat and monkey. Journal of Anatomy 101, 677-692.

WU, B.N., HONG, S.J., SHEU, M.M., CHEN, I.J., LIU, S. and CHIOU, G.C. (1995) Vaninolol: a novel compound for the treatment of glaucoma and ischemic retinopathy. Journal of Ocular Pharmacology and Therapeutics 11, 213-220.

YOSHIOKA, T., FEIGENBAUM, L. and JAY, G. (1991) Transgenic mouse model for central nervous system demyelination. Molecular and Cellular Biology 11, 5479-5486.

ZAJAC, C.S. and ABEL, E.L. (1992) Animal models of prenatal alcohol exposure. International Journal of Epidemiology 21, S24-S32.

ZEKI, S.M. (1969) Representation of central visual fields in prestriate cortex of monkey. Brain Research 14, 271-291.

ZEKI, S.M., HOLLMAN, A.S. and DUTTON, G.N. (1992) Neuroradiological features of patients with optic nerve hypoplasia. Journal of Pediatric Ophthalmology and Strabismus 29, 107-112.

APPENDIX

PUBLICATIONS:

DANGATA, Y.Y., FINDLATER, G.S. and KAUFMAN, M.H. (1994) Morphometnc analysis of myelinated fibre composition in the optic nerve of adult C57BL and CBA strain mice and (C57BL x CBA) Fl hybrids: an analysis of interstrain variation. Journal of Anatomy 184, 202.

DANGATA, Y.Y., FINDLATER, G.S., DHILLON, B. and KAUFMAN, M.H. (1994) Morphometric study of the optic nerve of adult normal mice and mice heterozygous for the Small eye mutation (Sey/+). Journal of Anatomy 185, 627-635.

DANGATA, Y.Y., FINDLATER, G.S. and KAUFMAN, M.H. (1995) Morphometric analysis of myelinated fibre composition in the optic nerve of adult C57BL and CBA strain mice and (C57BL x CBA)F1 hybrid: a comparison of inter-strain variation. Journal of Anatomy 186, 343-348.

DANGATA, Y.Y., FINDLATER, G.S. and KAUFMAN, M.H. (1996) Postnatal development of the optic nerve in (C57BL x CBA) F1 hybrid mice: General changes in morphometric parameters. Journal of Anatomy 189, 117-125.

DANGATA, Y.Y. and KAUFMAN, M.H. (1997) Effects of prenatal alcohol exposure on the postnatal development of the mouse optic nerve. Journal of Anatomy 191, 000-000

DANGATA, Y.Y. and KAUFMAN, M.H. (1997) Myelinogenesis in (C57BL x CBA) F_1 hybrid mice: A morphometric analysis. European Journal of Morphology (accepted April 1996).

FLECK, B.W. and DANGATA, Y.Y. (1994) Causes of visual handicap in the Royal Blind School, Edinburgh, 1991-2. British Journal of Ophthalmology 78, 421.

J. Anat. (1996) 189, pp. 117–125, with 4 figures Printed in Great Britain

Postnatal development of the optic nerve in (C57BL × CBA)F1 hybrid mice: general changes in morphometric parameters

Y. Y. DANGATA, G. S. FINDLATER AND M. H. KAUFMAN

Department of Anatomy, University of Edinburgh, UK

(*Accepted 5 March 1996*)

ABSTRACT

A morphometric analysis of the optic nerve in different age groups of (C57BL × CBA)F1 hybrid mice was carried out. Morphometric parameters examined were mean nerve cross-sectional area (*csa*), mean myelinated nerve fibre count, mean myelinated nerve fibre density and myelinated nerve fibre size distribution. The findings revealed that the optic nerve continues to develop well into adult life. Growth in calibre was very rapid during the early stage of postnatal life, but progressively slowed with age thereafter. No myelinated nerve fibres were observed before the 5th day of postnatal life. Similarly, once myelination was initiated, it progressed very rapidly during the early stage of postnatal development and, as for the *csa*, it slowed thereafter. Peak level of myelination within the optic nerve, which corresponded with the age when the maximum number of myelinated nerve fibres, i.e. 94213 ± 1799 (S.E.M.) was measured, occurred at the 16th week of postnatal life. The earliest myelinated nerve fibres seen were predominantly large in diameter, but with increasing age, fibres of smaller diameter dominated the myelinated nerve fibre spectrum in the nerve. The highest mean myelinated nerve fibre density was observed in mice at the age of peak myelination.

Key words: Growth; myelination.

INTRODUCTION

Many studies have been carried out to analyse the postnatal development of the optic nerve both in man (Sylvester & Ari, 1961; Dolman et al. 1980; Balazsi et al. 1984; Repka & Quigley, 1989; Day, 1990), and in the rat (Skoff et al. 1976*a*, *b*; Tennekoon et al. 1977; Lam et al. 1982; Perry et al. 1983). The majority of studies undertaken with mice have been concerned with the prenatal morphogenesis of the eye, rather than with the detailed analysis of its component parts, such as the optic nerve (Truslove, 1962; Pei & Rhodin, 1970; Robb et al. 1978; Theiler et al. 1980; Theiler & Varnum, 1981; Franz & Besecke, 1991).

Both Gyllensten & Malmfors (1963) and Gyllensten et al. (1966) studied the postnatal development of the optic nerve in C57BL mice, although these reports were not primarily concerned with the normal postnatal development of the optic nerve in this strain. Furthermore, they analysed only a few age groups of mice. In their controls, Gyllensten & Malmfors (1963) observed only unmyelinated fibres at day (d) 5, after which time myelination progressed at a slow rate until d 15, when it progressed rapidly up to d 20. Little increase in myelination was then observed up to d 30, after which time there was no further increase in the number of myelinated nerve fibres present. The majority of myelinated fibres had a diameter of less than 1 μm. No unmyelinated fibres were observed in their adult mice. In a subsequent control study, Gyllensten et al. (1966) observed a significant increase in the *csa* and total number of myelinated nerve fibres present between 2 and 4 mo of age, followed by a slight decrease in both parameters between 4 and 7 mo. Growth of the nerve continued well into adulthood.

The findings from other species have been quite variable. Sylvester & Ari (1961) demonstrated that the

Correspondence to Prof. M. H. Kaufman. Department of Anatomy, University Medical School, Teviot Place, Edinburgh EH8 9AG, UK.

human optic nerve increases maximally in size during the 1st year and continues to do so, though with diminished velocity, up to the 4th year. These findings are in general agreement with those of Todd et al. (1940). Dolman et al. (1980; see also Balazsi et al. 1984) also reported a marked decrease in the rate of growth of the optic nerve between the 4th and the 12th year, with adult size being attained between the 12th and 15th years.

This report is one of a series of studies on the morphometric analysis of the optic nerve in different strains of mice. It was also undertaken to establish baseline morphometric information necessary for future teratological studies on this strain of mice. Unlike the previous studies (see Dangata et al. 1994, 1995) it has concentrated on the postnatal developmental parameters of the optic nerve in the mouse, as relatively little information is available on this topic in the literature. The optic nerve was obtained from different age groups of both immature and adult F1 hybrid mice and the cross-sectional area (*csa*), total myelinated nerve fibre population, numerical density and fibre size spectrum determined. Information from this study has allowed a comparison to be made between the postnatal features of the optic nerve in the F1 hybrid mouse, and those of other species that have also been studied.

MATERIALS AND METHODS

Different age groups of a range of immature and adult male (C57BL × CBA)F1 hybrid mice were studied. Five mice each at 2, 3, 5, 9, 16 and 24 wk of age were studied. Each animal was weighed and deeply anaesthetised by an intraperitoneal injection of 0.02 ml/g body weight of 1.2% solution of tribromoethanol (Avertin) in 0.9% saline. In the adult mice, the heart was exposed and, using a 21 G needle, perfusion was carried out by giving 2.0 ml/g body weight of a 2.5% solution of glutaraldehyde in 0.1 M phosphate buffer through the left ventricle while the heart was still beating. Immature mice were similarly perfused transcardially, although a 23 G needle was used to avoid rupture of the left ventricle during the perfusion procedure. The surface of the liver was excoriated, to avoid a build-up of fixative in the venous part of the circulation.

The entire length of the optic nerve was immediately and carefully dissected out, avoiding traction on the nerve. Because in 2 earlier studies (Dangata et al. 1994, 1995) no significant difference was observed in any of the parameters to be analysed in the present study between the right and the left optic nerves in either male or female mice, both optic nerves from each animal were put into the same prelabelled bottle containing the fixative and left for a total of 12 h. The nerves were then washed in buffer and transferred into a secondary fixative consisting of 1% osmium tetroxide in 0.1 M phosphate buffer for another 2 h. After this they were dehydrated through a graded alcohol series and finally embedded in Araldite.

Semithin transverse sections (~ 1 μm) were cut perpendicular to the long axis of each nerve using a Reichert-Jung Ultracut E Microtome. Sections were stained with 1% toluidine blue in 1% borax for light microscopy. For electron microscopy ultrathin sections (~ 80 nm thickness) were cut. These were picked up on 200 mesh copper grids and subsequently stained with 0.2% lead citrate and a saturated solution of uranyl acetate (Reynolds, 1963). A selection of photomicrographs was taken from the centre to the periphery of each nerve using a Philips EM301 transmission electron microscope. This was done by locating the centre of the nerve (already marked on a sketch for each nerve during photography) and moving in one direction, photomicrographs were randomly taken from the centre, intermediate zone and periphery of the nerve making sure there was no overlap between the fields photographed. The micrographs were developed and printed to a final magnification of × 3000.

Using the semithin sections, the cross-sectional area (*csa*) of each optic nerve excluding its meningeal coverings was measured in a Magiscan image analysis system (Applied Imaging). We have used meningeal coverings to describe the extensions of the meningeal sheath that encloses the nerve as described in Gray's Anatomy, namely the dura mater, arachnoid mater and pia mater (Warwick et al. 1989). These were excluded in order to avoid errors that they would introduce to such parameters as the mean nerve fibre count and mean nerve fibre density, since the area occupied by them was devoid of any nerve fibres and the computation of the parameters was directly dependent on the *csa* of the axon-bearing part of the optic nerve. From the *csa* of the individual nerves the mean *csa* of the nerve for each age group of mice was calculated. Other detailed morphometric measurements of the nerves were also carried out on the photomicrographs of the ultrathin sections using the image analyser.

A systematic random sampling method (Mayhew & Sharma, 1984; Mayhew, 1988, 1990) was used to determine the total number and diameter spectrum of the myelinated nerve fibres in each nerve. This was done by locating the centre of the nerve and from this

point sectors of 10° were drawn over different areas of the nerve. A grid of approximately 1 cm × 1 cm squares (equivalent to 7.8 μm² of nerve *csa*) was placed over each sector. Using the sampling method indicated above, and starting from the centre of each nerve, every 4th square in each direction (i.e. 1 in 16) was sampled for the estimation of total myelinated nerve fibre counts and fibre diameter (i.e. axon plus myelin sheath) distribution. The objective was to sample between 150 and 200 myelinated nerve fibres, as this enables an estimate of within 95% of the actual number of nerve fibres present in the whole nerve to be obtained. It has been shown that it is not necessary to sample more than 200 nerve fibres for the estimation of the nerve fibre population in the nerve as this would give results that are comparable with those obtained by counting all the individual nerve fibres in the nerve which is uneconomical in terms of time and labour (Mayhew & Sharma, 1984; Mayhew, 1988, 1990). In this method only complete squares falling within each 10° sector were systematically sampled. Also, only myelinated nerve fibres which completely fell within or whose centres fell within a sampled square were included in the analysis. Although the ultrathin sections from each nerve were cut perpendicular to the long axis of the nerve, it was not practicable to cut all the nerve fibres perpendicular to their long axes because of the variable courses they run within the nerve. The external diameter of each sampled nerve fibre (i.e. axon and myelin sheath) was highlighted with the calibrating pen of the image analyser which then automatically measured the shortest diameter which is the true diameter of the highlighted nerve fibre. This resolved the limitation brought about by the variable courses of those fibres not cut along their long axes. The Magiscan image analyser provided a histogram of the sampled nerve fibres in each nerve. From the histograms of the individual nerves in each age group, a summary histogram was plotted for the age group. The number of myelinated nerve fibres present in each whole nerve and their numerical density, i.e. myelinated nerve fibres per 1000 μm² was calculated using the ratio technique (Matheson, 1970; Mayhew, 1988, 1990). The mean myelinated nerve fibre count and fibre density of the optic nerve for each age group of mice was also calculated.

In order to determine the approximate age at which myelination in the optic nerve starts, 2 additional mice each at age 9, 8, 7, 6 and 5 d were treated as indicated above. Because of the small number of myelinated fibres present in these samples, the mean myelinated nerve fibre count for these age groups could not be estimated by the present sampling technique because a total of less than 200 myelinated fibres were present in the selected fields. Additional photomicrographs were therefore taken at a higher magnification and printed to a final magnification of × 66000 in the 5, 6 and 7 d mice in order to allow the visualisation of any myelin sheaths that could not be seen at the lower magnification.

RESULTS

Cross-sectional areas (μm²)

Growth in the *csa* of the optic nerve was noted to occur from the earliest stage that could be studied using the image analysis system (i.e. age 2 wk) right through into adult life. The increase in the *csa* progressed rapidly early in life up to wk 5 with maximum rate of increase occurring between wk 2 and wk 3. From the end of wk 5 the rate of growth in the *csa* progressively declined with age. The *csa* continued to show an increase even after myelination was completed (see Table 1).

Total myelinated nerve fibre counts

By the postnatal d 5, no clear evidence of myelination was observed from the × 3000 TEM micrographs, but at × 66000 it was possible to detect the presence of a few myelin sheaths around some of the largest axons. Increasing evidence of myelination was observed on d 6 and 7 (Fig. 1). Although myelination progressed rapidly once it started, the optic nerve was initially predominantly populated by unmyelinated axons up to wk 2 (Fig. 2). Myelination progressed with such rapidity once it started, that after 5 wk relatively few unmyelinated axons were seen in the nerve. The peak value for the myelinated nerve fibres was seen at 16 wk of age (Fig. 3). Unmyelinated axons were rarely

Table 1. *Mean cross-sectional area of optic nerve of different postnatal age groups of (C57BL × CBA)F1 hybrids*

Age (wk)	Mean cross-sectional area (μm²) (±S.E.M.)*
2	36123 ± 2319 (10)
3	42560 ± 3576 (10)
5	50085 ± 1397 (9)
9	62115 ± 2322 (10)
16	67107 ± 1689 (9)
24	71270 ± 2986 (10)

* Total analysed in parentheses.

encountered at this age. A decrease in the total number of myelinated nerve fibres counted was, however, observed afterwards (see Table 2).

Numerical density of myelinated nerve fibres (fibres per 1000 μm²)

There was a very rapid increase in numerical density up to wk 5. This was followed by a progressive, but slower increase in mean myelinated nerve fibre density until highest density levels were achieved at an age which corresponded to the time when the maximum number of myelinated nerve fibres was observed in the nerve. A fall in the mean myelinated nerve fibre density was observed after this (see Table 3).

Myelinated nerve fibre diameter spectrum

In all age groups no myelinated nerve fibres less than 0.16 μm or greater than 2.0 μm in diameter were measured. The nerve fibre diameter spectrum was unimodal in all age groups. The highest modal diameter of 0.64 μm was observed in the 2 wk age group. There was a general and rapid drop in the modal diameter to 0.40 μm thereafter. The largest mean myelinated nerve fibre diameter, i.e. 0.67 ± 0.03 μm was observed in the 2 wk old mice. This mean value dropped to its lowest level, i.e. 0.55 ± 0.01 μm by wk 5. More myelinated fibres at both extremes of the myelinated nerve fibre diameter spectrum were measured with age, and this feature was more marked in those with a larger fibre diameter. For example, the smallest fibres measured were 0.16 μm in diameter, and this was after wk 2, with the largest fibres measured having a diameter of 1.76 μm, and this was observed in the 16 wk age group (see Fig. 4). Beyond wk 3, more than 90% of the myelinated fibres present in the optic nerve had a diameter of less than 1.0 μm (see Table 4).

DISCUSSION

Morphometric analysis of the optic nerve in the mouse has shown that it continues to develop from birth until well into adult life. Two periods of growth were observed. The initial period of growth was associated with the first evidence of myelination within the nerve, and was characterised by a very rapid increase both in the cross-sectional area and the number of myelinated nerve fibres present in the nerve. This phase of growth lasted up to the end of postnatal wk 5 and was then followed by a second, but progressively slower phase of growth. During the rapid phase of growth there was approximately a 3-fold increase in the value for mean myelinated nerve fibre count in the nerve at 5 wk over that observed at 2 wk. The maximum rate of growth in *csa* was seen between wk 2 and 3. Our findings on the *csa* of the optic nerve are similar to those of Gyllensten & Malmfors (1963) with respect to their 2 and 4 mo age groups, although where we observed a gradual increase in growth after 4 mo, they reported a significant decrease in growth at this time. The explanation for this difference has yet to be determined.

The observations in the present study are similar to those earlier reported by Matheson (1970; see also Tennekoon et al. 1977) in the rat, where they also found that the period of maximum growth occurred within the 1st 3 wk of postnatal life. A 2nd period of growth commenced during wk 5 of postnatal life, and lasted well into adult life, although the rate of change in the growth of the nerve during this second period was slower than that observed during the 1st period, and progressively became slower with age. Myelination within the optic nerve was completed during the 2nd period of growth, although the nerve continued to grow in calibre. Hirose & Bass (1973) also reported that in the rat the period during which there is a maximum growth rate occurred between d 10 and d 20 of postnatal life, and paralleled the period of maximum myelination within the nerve. Growth subsequent to d 50 was slow and continued, but at an even slower rate, thereafter. The findings of these authors indicate that there are close similarities between the postnatal development of the optic nerve in the rat and the mouse. In both of these species myelination appears to be an entirely postnatal event (myelination is first seen in the rat on the postnatal d 7; see Vaughn, 1969).

In the human optic nerve, Scammon & Armstrong (1925) reported a slight increase in the diameter of the nerve after birth, and they noted that this principally took place during infancy. Others (e.g. Sylvester & Ari, 1961; Dolman et al. 1980) demonstrated that the human optic nerve is small at birth, but grows very rapidly within the first few years. All, however, indicate that the rate of growth of the human optic nerve slows markedly after an initial relatively rapid growth phase during early life, with the adult size being reached between 12 and 15 y of age (see also Balazsi et al. 1984). The relatively small increase in the size of the human optic nerve after birth suggests that a degree of growth takes place during the prenatal period, for the optic nerve head is almost full size at the time of birth (Day, 1990). The initial postnatal growth

Table 2. *Mean myelinated nerve fibre counts in optic nerve of different postnatal age groups of (C57BL × CBA)F1 hybrids*

Age (wk)	Mean myelinated nerve fibre count (±S.E.M.)*
2	19706±1474 (10)
3	35107±3229 (10)
5	68719±1705 (9)
9	88087±4896 (10)
16	94213±1799 (9)
24	77719±4628 (10)

* Total analysed in parentheses.

spurt observed in the mouse may correspond to the period of growth from birth to infancy or early childhood reported in man. Again, what appears to be a 2nd and slower period of growth in man lasts only to early adolescence, while in the mouse this 2nd period of growth extends well into adulthood.

The drop in the mean myelinated nerve fibre count observed after the completion of myelination, would seem to suggest that a progressive elimination of myelinated nerve fibres was occurring. Nerve fibres in the middle part of the nerve fibre size spectrum appeared to be maximally affected by this fall in nerve fibre count. This may have been a consequence of a degenerative process in relation to these myelinated nerve fibres, and might explain the rise in the proportion of myelinated nerve fibres at the 2 ends of the nerve size spectrum, as well as a rise in the mean myelinated nerve fibre diameter. This decrease in mean myelinated nerve fibre count with age after the attainment of peak myelination within the optic nerve has also been observed in the C57BL strain of mice (Dangata et al. unpublished results). During normal development an initial over-production of nerve fibres is followed by a period during which degeneration of nerve fibres occurs, so that eventually the adult values are achieved (Potts et al. 1982; Lam et al. 1982; Perry et al. 1983; Crespo et al. 1985; Provis et al. 1985; Repka & Quigley, 1989). The initial period of degeneration coincides approximately with the onset of myelination. In the mouse the reduction in the number of myelinated nerve fibres observed after the period of peak myelination would suggest that by the time peak myelination occurs, the optic nerve still has more myelinated nerve fibres than is required for normal function. This is further explained by the sudden onset of the reduction in number of myelinated nerve fibres after peak myelination. It should not be surprising that the reduction in the total number of myelinated fibres in the optic nerve of the mouse proceeds after the attainment of peak myelination, since its general postnatal development proceeds well into adult life.

In the human optic nerve, an apparent over-production of axons occurs principally during the first half of intrauterine life, and this is followed by a loss of about 70% of these axons between 16 and 30 wk of gestation (Provis et al. 1985; Repka & Quigley, 1989) in order to establish adult values. A second phase of degeneration of myelinated nerve fibres in the normal optic nerve occurs significantly later in life, but does not usually occur before the age of 60 y (Dolman et al. 1980). This 2nd phase of degeneration usually corresponds with the onset of old age, and this is in contrast to the situation in the mouse, described in this study. In the mouse, large diameter myelinated nerve fibres characteristically dominate the nerve fibre diameter spectrum early in life. For example, the largest mean myelinated nerve fibre diameter and the largest modal diameter were observed in the 2-wk-old mice. This suggests the presence of a relatively higher proportion of large diameter fibres early in life than is seen during the latter stages of postnatal development. This finding would appear to be similar to that occurring in the human optic nerve at different age groups (Repka & Quigley, 1989). However, after the surge of activities, the reverse phenomenon was observed in the mouse, where the larger diameter fibres were less frequently encountered with increasing age. The diameter spectrum was relatively narrow during the early postnatal period but broadened with age, although fibres with a diameter greater than 2.0 μm were not encountered.

This finding is consistent with our previous observations and those of others, that the optic nerve of the mouse is predominantly populated by small diameter nerve fibres (Gyllensten & Malmfors, 1963; Gyllensten et al. 1966; Dangata et al. 1994, 1995). The reduction in the mean myelinated nerve fibre diameter observed by the 3rd postnatal week would seem to indicate that by this time myelination predominantly involves the medium size fibres, and that this is maintained until the process is completed. However, the large diameter fibres with which the process started, may continue to acquire additional lamellae of myelin sheath during this period.

Relatively few quantitative studies have been carried out on human optic nerves from different age groups. Those studies that have been undertaken may shed light on why visual function decreases with increasing age in normal individuals (Repka & Quigley, 1989). It is for this reason that appropriate animal models have been used to study both normal and abnormal development of the optic nerve, and

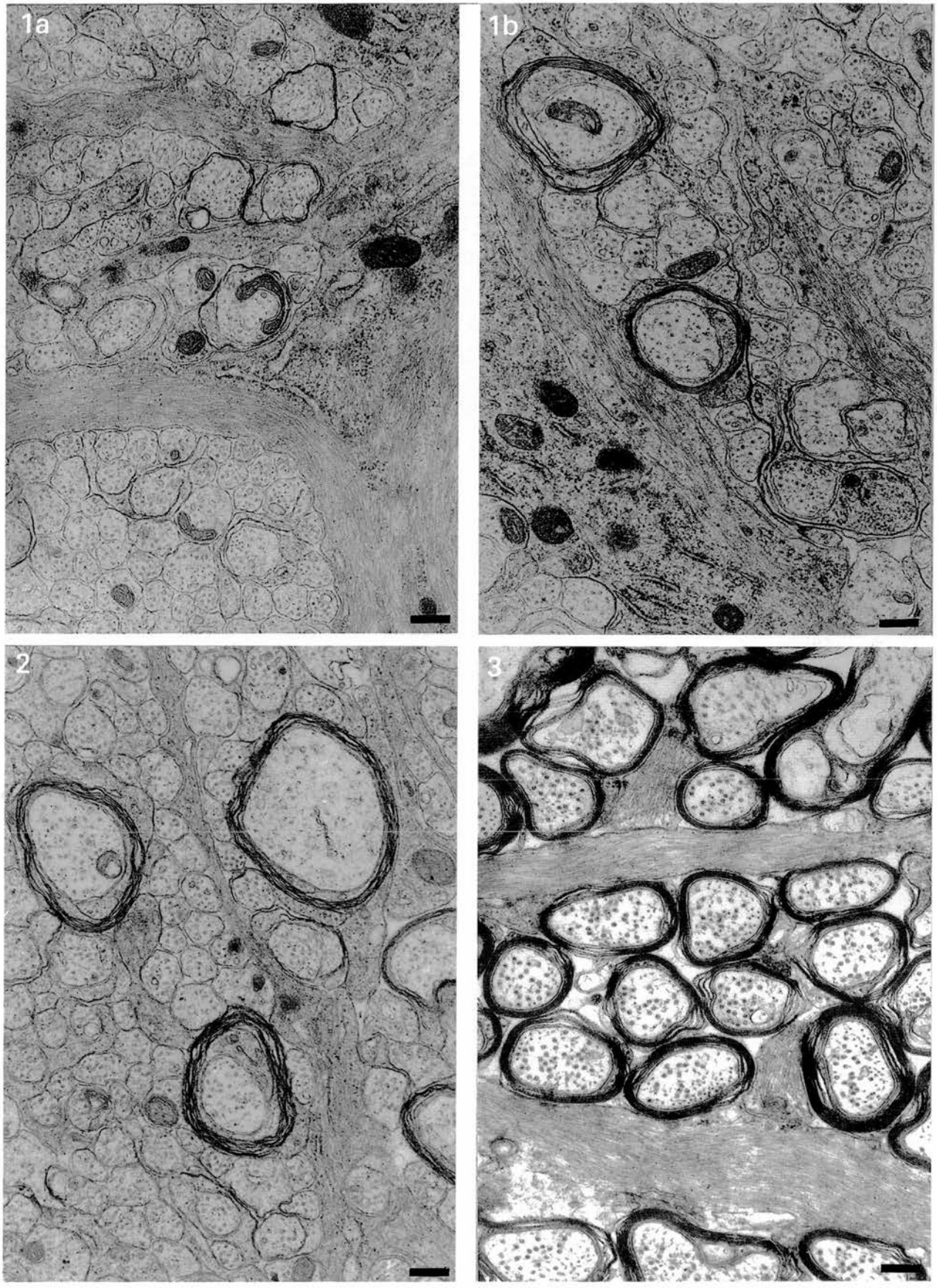

Fig. 1. Representative transmission electron micrographs (× 66000) showing onset of myelination in the optic nerve of (C57BL × CBA)F1 hybrid mice during their early postnatal development. (*a*) Section through the optic nerve of a d 6 F1 hybrid mouse. A few turns of myelin

Table 3. *Mean myelinated nerve fibre density in optic nerve of different postnatal age groups of (C57BL × CBA)F1 hybrids*

Age (wk)	Mean myelinated nerve fibre density (fibres/1000 μm²) (S.E.M.)*
2	546±19 (10)
3	821±22 (10)
5	1378±40 (9)
9	1410±30 (10)
16	1410±41 (9)
24	1087±35 (10)

* Total analysed in parentheses.

Table 4. *Mean myelinated nerve fibre diameter in optic nerve of different postnatal age groups of (C57BL × CBA)F1 hybrids*

Age (wk)	Mean nerve fibre diameter (μm) (±S.E.M.)*
2	0.67±0.03 (10)
3	0.59±0.01 (10)
5	0.55±0.01 (9)
9	0.58±0.01 (10)
16	0.57±0.02 (9)
24	0.63±0.02 (10)

* Total analysed in parentheses.

may offer the possibility of identifying specific critical phases during its development (Miller, 1992). The mouse has previously been used to study the toxic effects of substances such as cocaine and alcohol (Cook et al. 1987; Isenberg et al. 1987). We believe that the mouse is also likely to be a reasonable experimental model to study age-related conditions of

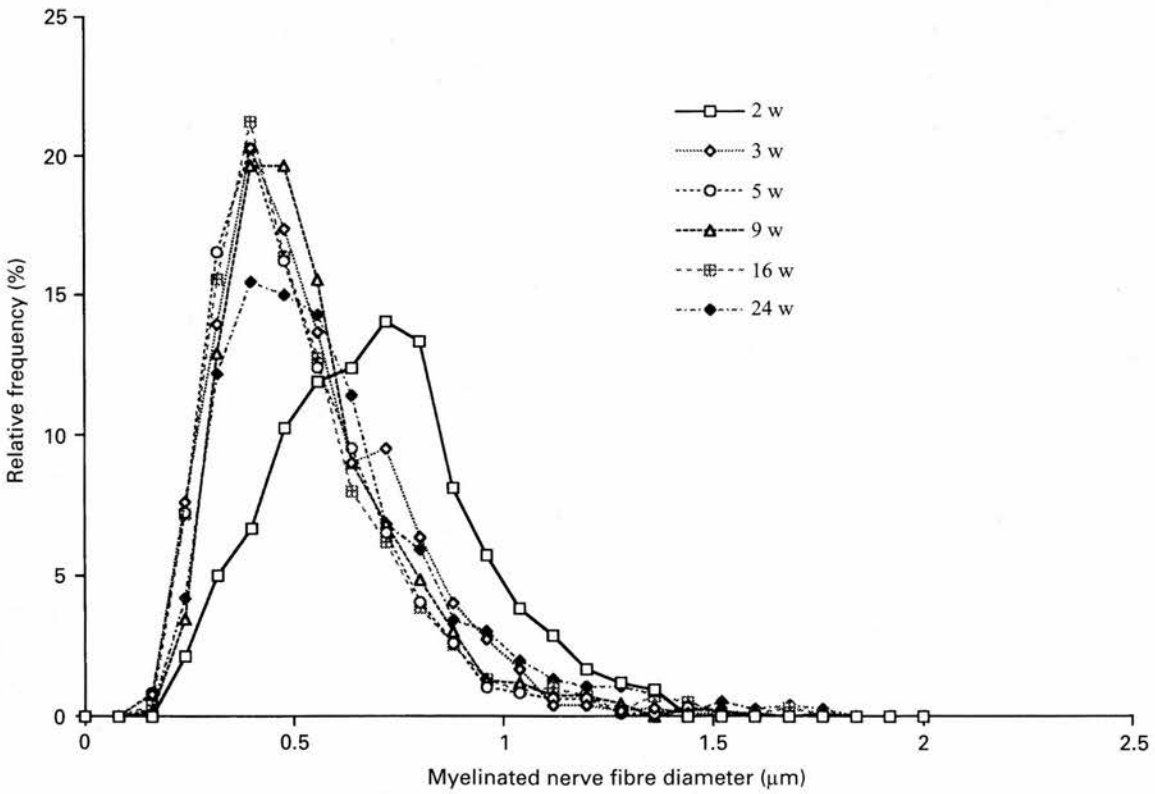

Fig. 4. Histograms showing nerve fibre diameter spectrum in the optic nerve for different postnatal age groups of (C57BL × CBA)F1 hybrid mice. Note the rapid drop in the modal diameter after the 2nd postnatal week to its adult value. The fibre spectrum is unimodal for all age groups and broadens with age. There is a positive skewing of the nerve fibre diameters.

are present around the larger diameter axons. (*b*) Section through the optic nerve of a d 7 F1 hybrid mouse. While the majority of the axons are still unmyelinated, a few of the larger diameter axons are surrounded by several layers of myelin. Bar, 0.1 μm.

Fig. 2. Representative transmission electron micrograph (×66000) showing evidence of progressive myelination in the optic nerve of (C57BL × CBA)F1 hybrids by wk 2 of postnatal life. It is mainly the larger axons that have become myelinated. At this stage there is an increase both in the overall diameter of the myelinated nerve fibres and in the number of turns of myelin. Fibres in the middle part of the nerve fibre size spectrum show evidence of early myelination. The optic nerve is still predominantly populated by unmyelinated nerve fibres. Bar, 0.1 μm. See also Figure 4.

Fig. 3. Representative transmission electron micrograph (×66000) of the optic nerve of an adult (C57BL × CBA)F1 hybrid showing myelinated nerve fibres at the peak level of myelination. Unmyelinated axons are exceptionally rare at this stage. The myelinated nerve fibres present show a broad diameter spectrum. Bar, 0.1 μm. See also Figure 4.

the visual system. Myelination of the human optic nerve begins at about mo 7 of intrauterine life (Scheie & Albert, 1977; Mullaney, 1962), and this approximately corresponds to d 5 of postnatal life in the mouse (Gyllensten & Malmfors, 1963). While the visual system in man is relatively mature and the eye ready to function within a short period after birth, and remains malleable at least for the 1st decade of life (Mund et al. 1972; Day, 1990), this corresponds approximately to when the surge of myelination activity (wk 2–5) in the postnatal development of the optic nerve in the mouse occurs. It is during the early part of this period that the eyelids reopen (Findlater et al. 1993). By this time, over 50% of the fibres in the optic nerve would have been myelinated. This suggests that this is likely to be the minimum number of myelinated nerve fibres required in the optic nerve to establish normal visual function in the mouse.

ACKNOWLEDGEMENTS

We are grateful to the staff of the Microbiology Animal House for animal care and Mr R. D. McDougall for excellent electron microscopy technical assistance. This work was supported by a grant from the Scottish Office, Home and Health Department (K/MRS/50/C1875).

REFERENCES

Balazsi AG, Rootman J, Drance SM, Schulzer M, Douglas GR (1984) The effect of age on the nerve fiber population of the human optic nerve. *American Journal of Ophthalmology* **97**, 760–766.

Crespo D, O'Leary DDM, Cowan WM (1985) Changes in the numbers of the optic nerve fibres during late prenatal and postnatal development in the albino rat. *Developmental Brain Research* **19**, 129–134.

Cook CS, Nowotny AZ, Sulik KK (1987) Fetal alcohol syndrome eye malformations in a mouse model. *Archives of Ophthalmology* **105**, 1576–1581.

Dangata YY, Findlater GS, Dhillon B, Kaufman MH (1994) Morphometric study of the optic nerve of adult normal mice and mice heterozygous for the *Small eye* mutation (*Sey*/+). *Journal of Anatomy* **185**, 627–635.

Dangata YY, Findlater GS, Kaufman MH (1995) Morphometric analysis of myelinated fibre composition in the optic nerve of adult C57BL and CBA strain mice and (C57BL × CBA)F1 hybrid: a comparison of inter-strain variation. *Journal of Anatomy* **186**, 343–348.

Day S (1990) Normal and abnormal visual development. In *Pediatric Ophthalmology*. (ed. Taylor D). pp. 7–20. Oxford: Blackwell.

Dolman CL, McCormick AQ, Drance SM (1980) Aging of the optic nerve. *Archives of Ophthalmology* **98**, 2053–2058.

Findlater GS, McDougall RD, Kaufman MH (1993) Eyelid development, fusion and subsequent reopening in the mouse. *Journal of Anatomy* **183**, 121–129.

Franz T, Besecke A (1991) The development of the eye in homozygotes of the mouse mutant extra-toes. *Anatomy and Embryology* **184**, 355–361.

Gyllensten L, Malmfors T (1963) Myelinization of the optic nerve and its dependence on visual function – a quantitative investigation in mice. *Journal of Embryology and Experimental Morphology* **11**, 255–266.

Gyllensten L, Malmfors T, Norrlin-Grettve M-L (1966) Developmental and functional alterations in the fiber composition of the optic nerve in visually deprived mice. *Journal of Comparative Neurology* **128**, 413–418.

Hirose G, Bass NH (1973) Maturation of oligodendroglia and myelinogenesis in rat optic nerve: a quantitative histochemical study. *Journal of Comparative Neurology* **152**, 201–210.

Isenberg SJ, Spierer A, Inkelis SH (1987) Ocular signs of cocaine intoxication in neonates. *American Journal of Ophthalmology* **103**, 211–214.

Lam K, Sefton AJ, Bennett MR (1982) Loss of axons from the optic nerve of the rat during early postnatal development. *Developmental Brain Research* **3**, 487–491.

Matheson DF (1970) Some quantitative aspects of myelination of the optic nerve in rat. *Brain Research* **24**, 257–269.

Mayhew TM (1988) An efficient sampling scheme for estimating fibre number from nerve cross sections: the fractionator. *Journal of Anatomy* **157**, 127–134.

Mayhew TM (1990) An efficient and unbiased sampling of nerve fibres for estimating fibre number and size. In *Methods in Neuroscience*, vol. 3, *Quantitative and Qualitative Microscopy* (ed. Conn PM), pp. 172–187. New York: Academic Press.

Mayhew TM, Sharma AK (1984) Sampling schemes for estimating nerve fibre size. I. Methods for nerve trunks of mixed fascicularity. *Journal of Anatomy* **139**, 45–58.

Miller MT (1992) Ocular teratology observations, speculations, questions, principles reaffirmed. *Eye* **6**, 177–180.

Mullaney J (1982) Normal development and developmental anomalies of the eye. In *Pathobiology of Ocular Diseases: A Dynamic Approach*, Part A (ed. Garner A, Klintworth GK), pp. 443–521. New York: Marcel Dekker.

Mund ML, Rodrigues MM, Fine BS (1972) Light and electron microscopic observations on the pigmented layers of the developing human eye. *American Journal of Ophthalmology* **73**, 167–182.

Pei YF, Rhodin JAG (1970) The prenatal development of the mouse eye. *Anatomical Record* **168**, 105–125.

Perry VH, Henderson Z, Linden R (1983) Postnatal changes in retinal ganglion cell and optic axon populations in the pigmented rat. *Journal of Comparative Neurology* **219**, 356–368.

Potts RA, Dreher B, Bennett MR (1982) The loss of ganglion cells in the developing retina of the rat. *Developmental Brain Research* **3**, 481–486.

Provis JM, Van Driel D, Billson FA, Russell P (1985) Human fetal optic nerve: overproduction and elimination of retinal axons during development. *Journal of Comparative Neurology* **238**, 92–100.

Repka MX, Quigley HA (1989) The effect of age on normal human optic nerve fiber number and diameter. *Ophthalmology* **96**, 26–32.

Reynolds ES (1963) The use of lead citrate at high pH as an electron-opaque stain in electron microscopy. *Journal of Cell Biology* **17**, 208–212.

Robb RM, Silver J, Sullivan RT (1978) Ocular retardation (or) in the mouse. *Investigative Ophthalmology and Visual Science* **17**, 468–473.

Scammon RE, Armstrong EL (1925) On the growth of the human eyeball and optic nerve. *Journal of Comparative Neurology* **38**, 165–219.

Scheie HG, Albert DM (1977) *Textbook of Ophthalmology* 9th edn, pp. 79–92. Philadelphia: W. B. Saunders.

Skoff RP, Price DL, Stocks A (1976*a*) Electron microscopic autoradiographic studies of gliogenesis in rat optic nerve. I. Cell proliferation. *Journal of Comparative Neurology* **169**, 291–312.

Skoff RP, Price DL, Stocks A (1976*b*) Electron microscopic

autoradiographic studies of gliogenesis in rat optic nerve. II. Time of origin. *Journal of Comparative Neurology* **169**, 313–334.

SYLVESTER PE, ARI K (1961) The size and growth of the human optic nerve. *Journal of Neurology, Neurosurgery and Psychiatry* **24**, 45–49.

TENNEKOON GI, COHEN SR, PRICE DL, MCKHANN GM (1977) Myelinogenesis in optic nerve. A morphological, autoradiographic, and biochemical Analysis. *Journal of Cell Biology* **72**, 604–616.

THEILER K, VARNUM DS, STEVENS LC (1980) Development of Dickie's Small Eye: an early lethal mutation in the house mouse. *Anatomy and Embryology* **161**, 115–120.

THEILER K, VARNUM DS (1981) Development of coloboma (Cm/+), a mutation with anterior lens adhesion. *Anatomy and Embryology* **162**, 121–126.

TODD TW, BEECHER H, WILLIAMS GH, TODD AW (1940) The weight and growth of the human eyeball. *Human Biology* **12**, 1–20.

TRUSLOVE GM (1962) A gene causing ocular retardation in the mouse. *Journal of Embryology and Experimental Morphology* **10**, 652–660.

VAUGHN JE (1969) An electron microscopic analysis of gliogenesis in rat optic nerves. *Zeitschrift für Zellforschung und mikroskopische Anatomie* **94**, 293–324.

WARWICK R, WILLIAMS PL, DYSON M, BANNISTER LH (1989) *Gray's Anatomy*. Edinburgh: Longman.

J. Anat. (1997) **191**, pp. 000–000, with 1 figure Printed in Great Britain

Morphometric analysis of the postnatal mouse optic nerve following prenatal exposure to alcohol

Y. Y. DANGATA AND M. H. KAUFMAN

Department of Anatomy, University Medical School, Edinburgh, UK

(*Accepted 11 February 1997*)

ABSTRACT

Pregnant female mice were divided on day 12 post coitum into a control and an experimental group. The experimental group was given a single intraperitoneal dose of 0.015 ml/g body weight of 25% solution of alcohol in distilled water while the control group was exposed to a similar weight related dose of normal saline. The optic nerves were isolated from the offspring of both control and experimental groups at wks 2, 3 and 5 (i.e. during the juvenile period of postnatal development) and analysed by light and electron microscopy. Although in both groups the optic nerve grew in size rapidly during the period studied, the rate of growth in the experimental groups lagged behind that of the controls. The difference was initially significant but tailed off, so that by wk 5 it was no longer significant. The time of initial onset and progression of myelinogenesis in the optic nerve of alcohol exposed mice also lagged behind that of controls. In both groups the size distribution of the myelinated nerve fibres in the optic nerve was unimodal with a positive skewing for all ages. The spectrum of size distribution of the nerve fibres was, however, broader in controls than in the corresponding experimental groups. With increasing age the proportion of small and medium size fibres was greater in the experimental group than in the controls, while for the large diameter fibres the reverse was observed. It is suggested that this study may shed light on the teratogenic effect of 'binge' drinking during pregnancy and that it is the critical period when exposure occurs that is more important than the duration of administration.

Key words: Morphometry; optic neuropathy; myelinogenesis; fetal alcohol syndrome.

INTRODUCTION

Since the clinical entity, the fetal alcohol sydrome, was first described in man (Jones & Smith, 1973; Jones et al. 1973, 1974), a number of clinical and experimental studies have been carried out to investigate its pathogenesis. This syndrome appears to be both species and strain dependent (Schwetz et al. 1978; Schenker et al. 1990; Zajac & Abel, 1992), with rodents being used in the majority of these studies (Abel et al. 1981; Garro et al. 1991; Middaugh & Boggan, 1991; Kotch et al. 1992; Pinazo-Duran et al. 1993). Considerable strain differences in sensitivity to alcohol have been reported in the mouse (Chernoff, 1977, 1980; Cook et al. 1987; Gilliam et al. 1990). For example, using 3 different strains of mice Chernoff (1980) observed that the CBA embryo was the most sensitive to prenatal alcohol exposure followed respectively, by the C3 and the C57BL strains of mice, while the C57BL/6J strain was more sensitive than the *long-sleep* or the *short-sleep* mouse (Gilliam et al. 1990).

The degree of sensitivity of individual organs to the teratogenic effects of alcohol varies considerably, the critical factors being the time of exposure during the prenatal period and the dose and frequency of exposure (Abel et al. 1981; Webster et al. 1983; Cook et al. 1987; Adickes, 1990; Michaelis, 1990; Kotch et al. 1992; Zajac & Abel, 1992; Ashwell & Zhang, 1994). The central nervous system (CNS) is particularly sensitive and the optic nerve in particular has been extensively studied to determine the effects of alcohol on this system (Cohen, 1967; Ehyai & Freemon, 1983; Pinazo-Duran et al. 1993). Although some morphometric studies have been carried out on the long-term effect of acute prenatal exposure to

Correspondence to Prof. M. H. Kaufman, Department of Anatomy, University Medical School, Teviot Place, Edinburgh EH8 9AG, UK.

alcohol on the optic nerve in the mouse (Ashwell & Zhang, 1994; Parson et al. 1995), no detailed analysis of the findings during the early postnatal period is presently available. The aim of the present study was to investigate the effect of exposure to a single prenatal dose of alcohol on the early postnatal development of the mouse optic nerve.

MATERIALS AND METHODS

Brother × sister matings of superovulated (C57BL × CBA) F_1 hybrid mice were carried out. The presence of a vaginal plug observed the next morning was considered as evidence of mating and this was designated as day (d) 0.5 post coitum (pc). Pregnant mice were maintained under a 14 h–10 h light–dark cycle with food and water available ad libitum. On d 12 pc the pregnant females were divided into an experimental and a control group. Each mouse in the experimental group was given a single intraperitoneal (i.p.) dose of 0.015 ml/g (volume:weight) 25% solution of alcohol in distilled water. This dose has been shown to produce a peak blood alcohol level of 500–600 mg/100 ml 4–4.5 h after injection (Webster et al. 1983; Ashwell & Zhang, 1994). The control group was treated with 0.9% saline in a similar way. Offspring of both experimental and control groups were used in this study. Those that were to be used after the age of 3 wk were weaned at this age and maintained on a diet similar to that of the parents.

Five mice from each age group of both control and experimental animals were studied at wk 2, 3 and 5 postnatally. The 5th postnatal week was selected because we have already demonstrated that this is the time when the phase of rapid postnatal development of the optic nerve in the mouse is completed, with the period from birth to the end of the 5th postnatal week corresponding to the juvenile period of life in this species (Hogan et al. 1994; Dangata et al. 1996). Each animal was deeply anaesthetised following an i.p. injection of 0.02 ml/g body weight of a 1.2% solution of tribromoethanol (Avertin) in 0.9% saline. The heart was then exposed and, using a 23G needle, intracardiac perfusion of fixative was carried out by giving 2.0 ml/g body weight of a 2.5% solution of glutaraldehyde in 0.1 M phosphate buffer through the left ventricle while the heart was still beating.

The optic nerve was immediately, but carefully, dissected out avoiding traction on the nerve. Both nerves from each animal were put in the same prelabelled bottle containing 2.5% glutaraldehyde and 1 M paraformaldehyde fixative in 0.1 M phosphate buffer and left for a total of 12 h. The nerves were then washed in 0.1 M phosphate buffer and transferred into a secondary fixative consisting of 1% osmium tetroxide in 0.1 M phosphate buffer for a further 2 h. After this they were dehydrated in a graded alcohol series and then embedded in Araldite.

From each nerve, semithin sections ($\sim$ 1 μm) were cut perpendicular to the long axis of the nerve using a Reichert-Jung Ultracut E microtome. Sections were stained with 1% toluidine blue in 1 % borax for light microscopy. Ultrathin sections ($\sim$ 80 ηm) thickness were then cut for electron microscopy. These were picked up on copper grids (200) and subsequently stained with 0.2 % lead citrate solution and a saturated solution of uranyl acetate (Reynolds, 1963).

From the ultrathin sections, a selection of photomicrographs was taken at an initial magnification of × 750 from centre to periphery of each nerve using a Philips EM301 transmission electron microscope. The objective here was to include as many representative profiles of each nerve as possible for the sampling procedure without having an overlap of the sampled fields. The micrographs were developed and printed to a final magnification of × 3000 in order to estimate the total number of myelinated nerve fibres present in each nerve. Additional micrographs were taken at a magnification of × 20000 as it was possible to clearly visualise distinct myelin lamellae present associated with each nerve fibre within the individual nerves.

Using the semithin sections, the cross-sectional area (csa) of each nerve, excluding its meningeal coverings (Williams et al. 1989) was measured in a Magiscan image analysis system (Applied Imaging). Other detailed morphometric measurements of the nerves were also carried out on the photomicrographs of the ultrathin sections using the image analyser. A systematic random sampling method (Mayhew, 1990) was used to determine the number and diameter spectrum of the myelinated nerve fibres present in each nerve. This was done by locating the centre of the nerve from which point sectors of 10° were drawn over different areas of the nerve. A grid of approximately 1 cm × 1 cm squares (equivalent to 7.8 μm^2 of nerve csa) was placed over each sector. Using the sampling method indicated above, and starting from the centre of each nerve, every 4th square falling completely within each sector in each direction (i.e. 1 in 16) was sampled for the estimation of nerve fibre counts and fibre size distribution. Only myelinated nerve fibres whose centres fell within a sample square were included in the analysis. Mayhew (1988, 1990) and Mayhew & Sharma (1984*a*, *b*) have shown that it is only necessary to count in the region of 150–200 nerve fibres to obtain an estimate of within 95% of

the actual number of nerve fibres present in the whole nerve (also see Dangata et al. 1994, 1995, 1996; Dangata & Kaufman, 1997; Parson et al. 1995). The Magiscan allowed a histogram of the diameter profile of the sampled nerve fibres of each nerve studied to be plotted. From this a summary histogram of the nerve fibre diameter profile for each age group of mice was also plotted. The number of myelinated nerve fibres present in each whole nerve was calculated using the ratio technique (Matheson, 1970; Mayhew, 1988, 1990). From the figures obtained the mean myelinated nerve fibre count of the optic nerve for each group of mice was then calculated.

A Student's 2-tailed t test was performed on the results of the morphometric parameters measured in the corresponding age groups of experimental and control mice to establish whether there was a significant difference in these parameters between the groups. Level of significance was taken as $P \leqslant 0.05$ (also see Dangata et al. 1994, 1995; Parson et al. 1995).

Our preliminary findings showed that the optic nerves of the experimental groups were generally greater in diameter than those of the corresponding age groups of the controls, although the difference in csa was significant between only the corresponding 2 and 3 wk old groups of both control and experimental mice. This finding, however, was in contrast to an earlier report by Ashwell & Zhang (1994) who noted a decrease in the csa of the optic nerve of 15 d old C57BL/6 mice following acute prenatal exposure of pregnant mothers to alcohol on d 8 pc. They used 2 similar (consecutive) doses of alcohol to the single dose used in the present study. There was an interval of 4 h between the 2 doses. This difference in the csa finding between that observed in the present study and that reported by Ashwell & Zhang made us curious to investigate whether our finding was a true deviation from that previously observed by them (see Discussion). In order to investigate this in detail the optic nerves from each group of 5 mice isolated at 2 and 3 wk of age from an additional series of alcohol-treated pregnant F_1 mothers were analysed as indicated above.

Although it has been reported (Dangata et al. 1996) that myelinogenesis in the mouse begins during the 5th postnatal day (pnd), the present study was undertaken to establish whether prenatal exposure to alcohol affects the time of onset of this process. In order to do this, 2 additional mice each at 8, 7, 6 and 5 pnd were isolated from both experimental and control groups of mice and their optic nerves processed for electron microscopy as indicated above. Photomicrographs of the optic nerve in these latter groups were taken at a magnification of $\times 20000$ and printed to a final magnification of $\times 40000$. This was undertaken principally in order to ensure visualisation of any myelin sheaths at this critical period of postnatal development that would not otherwise have been seen at the lower magnification.

RESULTS

Cross-sectional area (μm^2)

In both alcohol and saline-treated mice the optic nerve could, with little difficulty, be dissected from eyeball to optic chiasma. The meningeal coverings around the nerve were well defined in both groups of mice. The csa of the optic nerve grew rapidly during the early part of the juvenile period but began to decline towards the end of this period. The maximum rate of growth was observed between the 2nd and 3rd weeks of postnatal life, though this was invariably greater in the control than in the experimental group. Thus in the controls the increase in csa between the 3rd and the 5th wk was approximately 53% of the increase between the 2nd and the 3rd wk. This was in comparison with 14% for the experimental group over the same period of time. The optic nerves of the experimental groups were, however, generally greater in diameter than those of the corresponding age groups of the controls. The difference in csa between the corresponding age groups of 2 and 3 wk old control and experimental groups of mice was significant, but by the 5th wk it was no longer significant (see Table). The csa findings of the optic nerves from the additional series of 2 and 3 wk old alcohol-treated mice were comparable with those previously analysed. Therefore the 2 groups of 2 wk alcohol-treated mice were pooled together; similarly, both groups of 3 wk alcohol-treated mice were pooled.

Myelinated nerve fibre counts

In the control group, the first evidence of myelinogenesis was observed in $\times 40000$ micrographs of optic nerves analysed on the 5th pnd due to the presence of promyelin around the largest diameter fibres. Myelinogenesis was more obvious by the 6th pnd as it was possible at this age to distinguish up to 2 distinct myelin lamellae loosely wrapped around some of the largest axons; by the 8th pnd up to 3–4 myelin lamellae could be counted around some of the largest diameter axons. In the experimental group, only the presence of promyelin could be observed around some

Table. ~~PCFI~~ Morphometric parameters analysed in optic nerve of alcohol and saline-treated mice during the juvenile period of postnatal development

Age (wk)	Mean cross-sectional area (μm^2)			Mean myelinated nerve fibre count			Mean myelinated nerve fibre density (fibres per 1000 μm^2)		
	Alcohol*	Saline*	Student's *t* test	Alcohol*	Saline*	Student's *t* test	Alcohol*	Saline*	Student's *t* test
2	41070 ± 1813	35607 ± 2516	$0.01 \leqslant P \leqslant 0.05$	18375 ± 1599	20114 ± 1579	n.s.	444 ± 29	563 ± 19	$0.01 \leqslant P \leqslant 0.05$
3	46921 ± 2553	41569 ± 1201	$P \leqslant 0.01$	35795 ± 1892	40616 ± 3338	$P \leqslant 0.01$	770 ± 22	977 ± 74	$0.01 \leqslant P \leqslant 0.05$
5	48527 ± 1706	47860 ± 2474	n.s.	55606 ± 2364	62987 ± 5019	$P \leqslant 0.01$	1150 ± 39	1304 ± 57	$P \leqslant 0.01$

* Number of optic nerves analysed: alcohol-treated: 2 wk = 16, 3 wk = 18, 5 wk = 10; saline-treated: 2 wk = 9, 3 wk = 7, 5 wk = 8; n..s., no significant difference.

of the largest diameter fibres by the 6th pnd and by the 8th pnd not more than 1–2 myelin lamellae could be seen per axon. The myelin lamellae in both groups of mice at this stage were loosely wrapped around the axons. Similarly, in both groups, myelinogenesis progressed rapidly following the onset of this process, with the maximum rate of increase seen between the 2nd and the 3rd wk; by the 5th wk myelinated nerve fibres dominated the optic nerve in both groups. The myelin lamellae became more densely packed around their axons in both groups of mice with time, although, after the 2nd wk there was no significant change in the packing density of the myelin lamellae around the axons (see Fig.). As for the csa (see above), myelinogenesis progressed faster in controls than in the experimental group. Initially there was no significant difference between control and experimental groups, but from the 3rd wk onwards the difference was significant (see Table).

Numerical density of myelinated nerve fibres (fibres per 1000 μm^2)

In both groups of mice there was a rapid increase in the numerical density of the myelinated nerve fibres with age. The mean values for the myelinated nerve fibre density for controls were always higher than those of the alcohol-treated mice. The difference in density between the corresponding age groups of control and experimental animals was significant for all the age groups analysed (see Table).

Myelinated nerve fibre diameter spectrum

The smallest myelinated nerve fibres in any of the series measured 0.16 μm in diameter. The largest fibres measured were 1.60 μm and 1.36 μm in diameter, respectively, for the control and experimental groups, and these values were noted in the 5 wk old mice. The distribution of the myelinated nerve fibre diameters in the optic nerve was unimodal with a positive skewing for all ages in both groups. By the 5th wk a shift in the spectrum of distribution of the myelinated nerve fibres to the right, i.e. in favour of the large diameter fibres could be observed. This shift was more obvious in the control series than the corresponding age groups of the experimental series. At each of the ages studied, the medium diameter fibres dominated the myelinated nerve fibre spectrum of the optic nerve in both control and experimental groups. With increasing age the proportions of both small and medium size fibres increased in the experimental group compared with the controls. The reverse phenomenon was observed in the case of the large diameter fibres. These differences were not, however, statistically significant.

DISCUSSION

The optic nerves of the offspring of F_1 hybrid mice given a single intraperitoneal injection of 25% (v:w) solution of 0.015 ml/g body weight of alcohol in distilled water on d 12 of gestation and appropriate saline-injected controls were analysed using light and electron microscopy. A significant effect on various morphometric parameters of the optic nerve was observed when these were assessed at 2, 3 and 5 wk after birth. It was observed that in this experimental system, exposure to a single dose of alcohol taken at a critical period of gestation had a significant teratogenic effect. Children with the characteristic features of the fetal alcohol syndrome (FAS) are known to have been born to mothers who had taken only a single dose of alcohol during pregnancy

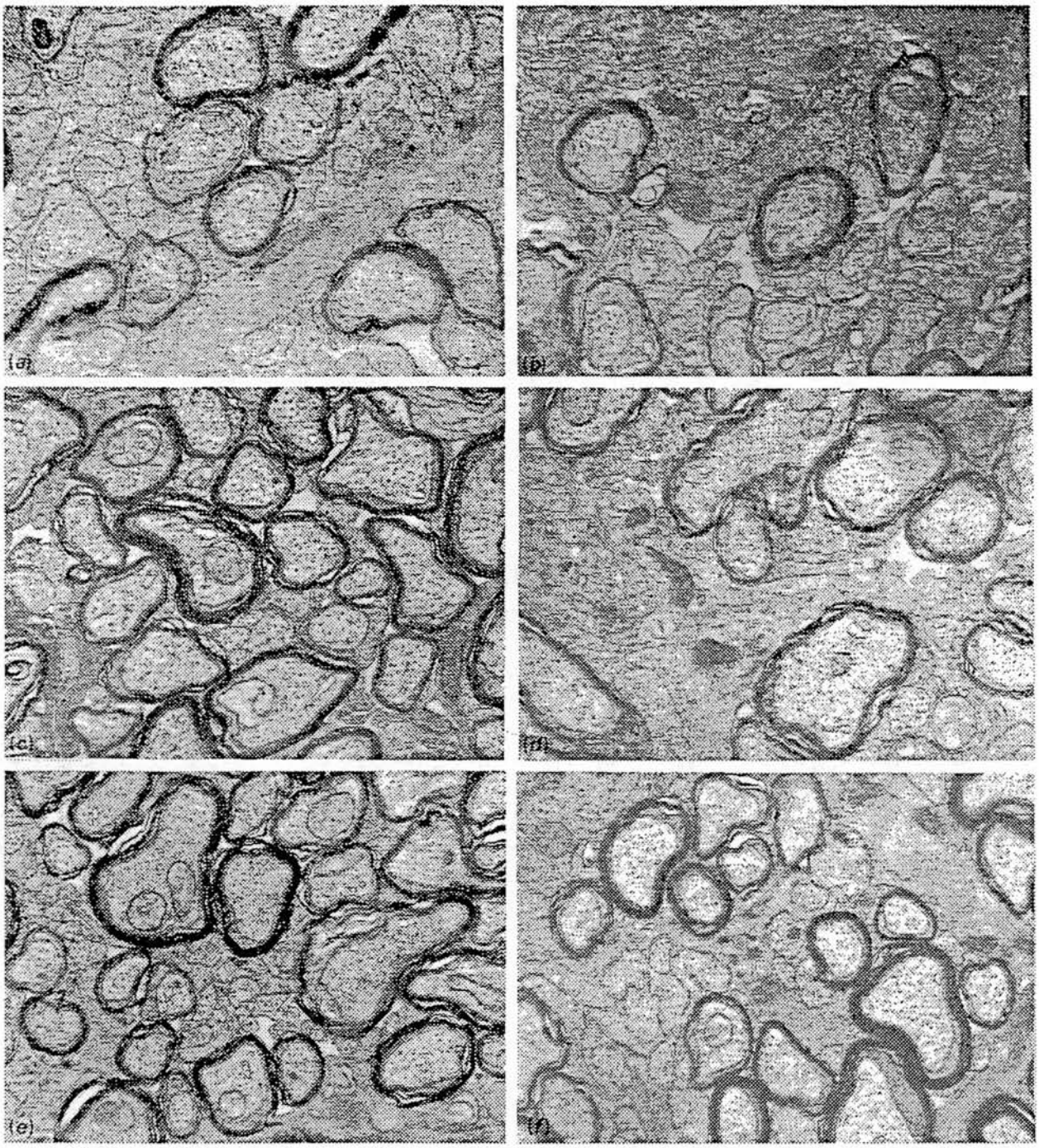

Fig. (*a–f*) Electron micrographs of transverse sections of the optic nerve from both alcohol-treated and control mice to show the progression of myelinogenesis during the juvenile period of postnatal development (*a*, *b*: 2 wk old control and alcohol-treated mice, respectively; *c*, *d*: 3 wk old control and alcohol-treated mice, respectively; *e*, *f*: 5 wk old control and alcohol-treated mice, respectively). A progressive increase in the number of myelinated nerve fibres was observed in the optic nerve with age. This was associated with a corresponding decline in the population of unmyelinated nerve fibres, so that by the 5th wk myelinated nerve fibres dominated the optic nerve in both controls and alcohol-treated mice. At each of the age groups studied, more myelinated nerve fibres were present in the optic nerve of controls than in the corresponding age groups of the alcohol-treated series. The myelin lamellae were distinct in all age groups of both control and experimental groups of mice. In each series of mice the number of myelin lamellae per axon increased and became more compact with age. Although the myelin lamellae became more compact around the axon with age, there was no significant difference in their degree of compaction with age. There was a linear relationship between axon size and the number of myelin lamellae in both control and experimental groups, i.e. the number of myelin lamellae around an axon is proportional to axon diameter. (All micrographs × 20 000)

(Kronick, 1976; Herrmann et al. 1980; Clarren, 1981; Padmanabhan et al. 1984).

In both controls and experimental groups of mice in this study the optic nerve grew rapidly in calibre during the juvenile period of development. The maximum rate of growth was seen between the 2nd

and the 3rd wk of postnatal life. At all of the age groups studied, the rate of growth in the calibre of the optic nerve was greater in controls than in the experimental groups, although at decreasing level of significance with age; up to the 3rd wk the calibre of the optic nerve of the offspring of alcohol-treated mice was significantly larger than that of controls, but by the end of the 5th postnatal week, the difference had ceased to be significant. Ng & Stone (1982) noted that the csa of the optic nerve reflected a number of factors, such as the total number of axons in the nerve, axon diameter, the extent of myelinogenesis of each axon and the volume of the glial component present in the nerve. The present observations suggest that factors other than myelinogenesis alone, which is more intense in the controls than in the alcohol-treated series (see later), had a greater effect on the overall csa of the optic nerve during the juvenile period of postnatal development.

It is not clear why the csa of the optic nerve in the experimental group was initially significantly larger than that of the matched control group, although this may reflect a degree of tissue oedema. This finding contrasts with the small calibre optic nerve observed in the rat at this time by Pinazo-Duran et al. (1993). In their study, alcohol was administered in the diet to female rats 6 wk before pregnancy and throughout the gestation period, rather than as a single acute (or 'binge') exposure as in the present study. Similar findings to those reported by Pinazo-Duran et al. with regard to the size of the optic nerve were also reported by Ashwell & Zhang (1994) following acute exposure of C57BL/6 pregnant mice to alcohol on d 8 pc. This finding strongly suggests that in the study of alcohol teratogenicity the exact timing of exposure during pregnancy is probably more important than the duration of administration. For example, in these 2 previous studies alcohol was administered *before* rather than *after* the formation of the optic stalk (as in the present study); the optic stalk is the precursor of the optic nerve (Kaufman, 1979, 1992; Rugh, 1990; Dangata et al. 1994) and may play a role in determining its eventual size.

In both experimental and control groups, myelinogenesis progressed rapidly during the early part of the juvenile period, although both its onset and the rate of its progression in the experimental group significantly lagged behind that of the controls. This was clearly shown by the presence of a significant difference between the 2 groups of mice in their mean myelinated nerve fibre count after the 2nd wk as well as a significant difference in their mean nerve fibre density throughout the juvenile period. Although it has previously been reported that myelinogenesis in the optic nerve of the mouse is entirely a postnatal event (Gyllensten & Malmfors, 1963; Gyllensten et al. 1966; Dangata et al. 1996), the present findings suggest that prenatal factors (such as exposure to alcohol) may have a significant influence on its time of onset and progression. Oligodendrocytes play a critical role in the formation of the myelin sheath in the central nervous system (CNS) (Matthews & Duncan, 1971; Tennekoon et al. 1977; Dentinger et al. 1985; Asou et al. 1994, 1995; Umemori et al. 1994). These cells develop from glial cell precursors following their cytodifferentiation. The mature forms, i.e. the type-3 oligodendrocytes, are characterised by the presence of numerous processes and are first seen to be present shortly before the onset of myelinogenesis (Asou et al. 1994, 1995). These cells also synthesise myelin basic protein (see also Tennekoon et al. 1977) which constitutes approximately 30% of the protein in the CNS and is important for CNS function (Warrington et al. 1993).

In the present study the delay in the onset and the rate of progression of myelinogenesis, together with the reduction in mean myelinated nerve fibre count and density suggests that alcohol probably exerts a significant teratogenic effect either on the glial precursors of oligodendrocytes or on their cyto-differentiation, and that this could result in both a reduction in their number and/or their competence to synthesise myelin. It is worthy of note that Phillips and his coworkers (Phillips, 1989; Phillips et al. 1991; Phillips & Krueger, 1992) observed a delay in oligodendroglial cell maturation as well as a reduction in the number of oligodendrocytes produced in the optic nerve of the rat following exposure to alcohol. This resulted in a delay in the onset of myelinogenesis. They also reported a decrease in the myelinated nerve fibre count as well as the overall myelin thickness per axon. The impairment in the development of myelin and consequently the formation of the myelin sheath around the axons in the optic nerve could explain some of the neurological signs and severe visual dysfunction commonly associated with prenatal alcohol exposure in infants diagnosed as having the FAS (Phillips et al. 1991; Phillips & Krueger, 1992).

Experimental studies involving the histological analysis of other regions of the CNS have given similar findings to those here, and in comparable studies on the rat optic nerve cited above with regard to the teratogenic effect of alcohol on myelinogenesis. Following chronic prenatal exposure of pregnant rats to dietary alcohol, Miller & al-Rabiai (1994) observed a decrease in the space occupied by axons in the

pyramidal tract in the alcohol-treated compared with that in control rats. The individual diameters of the myelinated nerve fibres were smaller and each had a proportionately thinner myelin sheath. These observations confirmed an earlier finding on alcohol-exposure in relation to the histological features of the cerebral cortex (Miller, 1993). In 2 earlier reports, Lancaster et al. (1982, 1984) observed a decrease in brain myelin and a delay in brain myelin synthesis following exposure of rats to acute doses of alcohol. These findings further confirm that, given at an appropriate critical period, an acute dose of alcohol can significantly affect CNS development.

Although a relatively higher proportion of large diameter fibres in both controls and experimental groups was seen early in life, in the 2 wk old mice, the medium diameter fibres dominated the optic nerve fibre spectrum at any age. As myelinogenesis progressed, those fibres in which it had already started continued to acquire additional myelin lamellae until they had attained the maximum number proportionate to their mature size. The result of this phenomenon was the progressive shift of myelinated nerve fibres from one part of the myelinated nerve fibre spectrum to another and this may account for the shift in the spectrum to the right. The present findings clearly indicate that, in alcohol teratogenicity, there is a delayed onset of myelinogenesis. It should be noted that, as in the rat, myelinogenesis has yet to be completed in the optic nerve of the mouse by the end of the juvenile period (Black et al. 1982; Lancaster et al. 1984; Dentinger et al. 1985; Dangata et al. 1996; Dangata & Kaufman, 1997).

The findings from this study indicate that prenatal exposure of the conceptus to alcohol has a significant influence on the postnatal development of the optic nerve. We have no direct evidence from the present study that there is an effect on the prenatal development of the optic nerve. Indirect evidence, however, suggests that myelinogenesis is probably affected due to interference with oligodendroglial cytodifferentiation, the net result of which is likely to be a delay in the onset of myelinogenesis and its subsequent progression.

ACKNOWLEDGEMENTS

We thank Dr S. H. Parson for providing alcohol-treated mice and Mr W. Adams for verification of statistical analyses. We thank also Mr R. D. McDougall for excellent electron microscopy technical assistance and the staff of the Microbiology Animal House for animal care.

REFERENCES

Abel EL, Dintcheff BA, Bush R (1981) Effects of beer, wine, whisky, and ethanol on pregnant rats and their offspring. *Teratology* **23**, 217–222.

Adickes ED (1990) Biomolecular mechanisms of ethanol teratogenicity. *Alcoholism: Clinical and Experimental Research* **14**, 805–806.

Ashwell KWS, Zhang LL (1994) Optic nerve hypoplasia in an acute exposure model of the fetal alcohol syndrome. *Neurotoxicology and Teratology* **16**, 161–167.

Asou H, Hamada K, Uyemura K, Sakota T, Hayashi K (1994) How do oligodendrocytes ensheath and myelinate nerve fibers? *Brain Research Bulletin* **35**, 359–365.

Asou H, Hamada K, Miyazaki T, Sakota T, Hayashi K, Yakeda Y et al. (1995) CNS myelinogenesis in vitro: Time course and pattern of rat oligodendrocyte development. *Journal of Neuroscience Research* **40**, 519–534.

Black JA, Foster RE, Waxman, SG (1982) Rat optic nerve: freeze-fracture studies during development of myelinated axons. *Brain Research* **250**, 1–20.

Chernoff GF (1977) The fetal alcohol syndrome in mice: an animal model. *Teratology* **15**, 223–230.

Chernoff GF (1980) The fetal alcohol syndrome in mice: maternal variables. *Teratology* **22**, 71–75.

Clarren SK (1981) Recognition of fetal alcohol syndrome. *Journal of American Medical Association* **245**, 2436–2439.

Cohen AI (1967) Ultrastructural aspects of the human optic nerve. *Investigative Ophthalmology* **6**, 294–308.

Cook CS, Nowotny AZ, Sulik KK (1987) Fetal alcohol syndrome. Eye malformations in a mouse model. *Archives of Ophthalmology* **105**, 1576–1581.

Dangata YY, Findlater GS, Dhillon B, Kaufman MH (1994) Morphometric study of the optic nerve of adult normal mice and mice heterozygous for the *Small eye* mutation (*Sey*/+). *Journal of Anatomy* **185**, 627–635.

Dangata YY, Findlater GS, Dhillon B, Kaufman MH (1995) Morphometric analysis of myelinated fibre composition in optic nerve of adult C57BL and CBA strain mice and (C57BL × CBA) F_1 hybrid: comparison of inter-strain variation. *Journal of Anatomy* **186**, 343–348.

Dangata YY, Findlater GS, Kaufman MH (1996) Postnatal development of the optic nerve in (C57BL × CBA) F_1 hybrid mice: general changes in morphometric parameters. *Journal of Anatomy* **189**, 117–125.

Dangata YY, Kaufman MH (1997) Myelinogenesis in the optic nerve of (C57BL × CBA) F_1 hybrid mice: a morphometric analysis. *European Journal of Morphology*, in press.

Dentinger MP, Barron KD, Csiza CK (1985) Glial and axonal development in optic nerve of myelin deficient rat mutant. *Brain Research* **344**, 255–266.

Ehyai A, Freemon FR (1983) Progressive optic neuropathy and sensorineural hearing loss due to chronic glue sniffing. *Journal of Neurology, Neurosurgery and Psychiatry* **46**, 349–351.

Garro AJ, McBeth DL, Lima V, Lieber CS (1991) Ethanol consumption inhibits fetal DNA methylation in mice: implications for the fetal alcohol sydrome. *Alcoholism: Clinical and Experimental Research* **15**, 395–398.

Gilliam DM, Kotch LE, Dudek BC, Riley EP (1990) Ethanol teratogenesis in selectively bred long-sleep and short-sleep mice: a comparison to inbred C57BL/6J mice. *Alcoholism: Clinical and Experimental Research* **13**, 667–672.

Gyllensten L, Malmfors T (1963) Myelinization of the optic nerve and its dependence on visual function – a quantitative investigation in mice. *Journal of Embryology and Experimental Morphology* **11**, 255–266.

Gyllensten L, Malmfors T, Norrlin-Grettve M-L (1966) Developmental and functional alterations in the fiber com-

position of the optic nerve in visually deprived mice. *Journal of Comparative Neurology* **128**, 413–418.

HERRMANN J, PALLISTER PD, OPITZ JM (1980) Tetraectrodactyly and other skeletal manifestations in the fetal alcohol syndrome. *European Journal of Pediatrics* **133**, 221–226.

HOGAN B, BEDDINGTON R, CONSTANTINI F, LACY E (1994) Summary of mouse development. In *Manipulating the Mouse Embryo. A Laboratory Manual*. 2nd edn. pp. 19–114. New York: Cold Spring Harbor Laboratory Press.

JONES KL, SMITH DW (1973) Recognition of the fetal alcohol syndrome in early pregnancy. *Lancet* **2**, 999–1001.

JONES KL, SMITH DW, ULLELAND CN, STREISSGUTH AP (1973) Pattern of malformation in offspring of chronic alcoholic mothers. *Lancet* **1**, 1267–1271.

JONES KL, SMITH DW, STREISSGUTH AP, MYRIANTHOPOULOS NC (1974) Outcome in offspring of chronic alcoholic women. *Lancet* **1**, 1076–1078.

KAUFMAN MH (1979) Cephalic neurulation and optic vesicle formation in the early mouse embryo. *American Journal of Anatomy* **155**, 425–444.

KAUFMAN MH (1992) *The Atlas of Mouse Development*. London: Academic Press.

KOTCH LE, DEHART DB, ALLES AJ, CHERNOFF N, SULIK KK (1992) Pathogenesis of ethanol-induced limb reduction defects in mice. *Teratology* **46**, 323–332.

KRONICK JB (1976) Teratogenic effects of ethyl alcohol administered to pregnant mice. *American Journal of Obstetrics and Gynecology* **124**, 676–680.

LANCASTER FE, MAYUR BK, PATSALOS PN, SAMORAJSKI T, WIGGINS RC (1982) The synthesis of myelin and brain subcellular membrane proteins in the offspring of rats fed ethanol during pregnancy. *Brain Research* **235**, 105–113.

LANCASTER FE, PHILIPS S, PATSALOS PN, WIGGINS RC (1984) Brain myelin in the offspring of ethanol treated rats: in utero versus lactational exposure by crossfostering offspring of control, pairfed and alcohol treated dams. *Brain Research* **309**, 209–216.

MATHESON DF (1970) Some quantitative aspects of myelination of the optic nerve in rat. *Brain Research* **24**, 257–269.

MATTHEWS MA, DUNCAN D (1971) A quantitative study of morphological changes accompanying the initiation and progress of myelin production in the dorsal funiculus of the rat spinal cord. *Journal of Comparative Neurology* **142**, 1–22.

MAYHEW TM (1988) An efficient sampling scheme for estimating fibre number from nerve cross sections: the fractionator. *Journal of Anatomy* **157**, 127–134.

MAYHEW TM (1990) Efficient and unbiased sampling of nerve fibres for estimating fiber number and size. In *Methods in Neuroscience*, vol. 3, *Quantitative and Qualitative Microscopy* (ed. Conn PM), pp. 172–187. New York: Academic Press.

MAYHEW TM, SHARMA AK (1984*a*) Sampling schemes for estimating nerve fibre size. I. Methods for nerve trunks of mixed fascicularity. *Journal of Anatomy* **139**, 45–58.

MAYHEW TM, SHARMA AK (1984*b*) Sampling schemes for estimating nerve fibre size. II. Methods for unifascicular nerve trunks. *Journal of Anatomy* **139**, 59–66.

MICHAELIS EK (1990) Fetal alchohol exposure: cellular toxicity and molecular events involved in toxicity. *Alcoholism: Clinical and Experimental Research* **14**, 819–826.

MIDDAUGH LD, BOGGAN WO (1991) Postnatal growth defects in prenatal ethanol-exposed mice: Characteristics and critical periods. *Alcoholism: Clinical and Experimental Research* **15**, 919–926.

MILLER MW (1993) Migration of cortical neurons is altered by gestational exposure to ethanol. *Alcoholism: Clinical and Experimental Research* **17**, 304–314.

MILLER MW, AL-RABIAI S (1994) Effects of prenatal exposure to ethanol on the number of the axons in the pyramidal tract of the rat. *Alcoholism: Clinical and Experimental Research* **18**, 346–354.

NG AY, STONE J (1984) The optic nerve of the cat: appearance and loss of axons during normal development. *Brain Research* **281**, 263–271.

PADMANABHAN R, HAMEED MS, SUGATHAN TN (1984) Effects of acute dose of alcohol on pre- and postnatal development in the mouse. *Drug and Alcohol Dependence* **14**, 197–208.

PARSON SH, DHILLON B, FINDLATER GS, KAUFMAN MH (1995) Optic nerve hypoplasia in the fetal alcohol syndrome: a mouse model. *Journal of Anatomy* **186**, 313–320.

PHILLIPS DE (1989) Effects of limited postnatal alcohol exposure on the development of myelin and nerve fibers in rat optic nerve. *Experimental Neurology* **103**, 90–100.

PHILLIPS DE, KRUEGER SK, RYDQUIST JE (1991) Short- and long-term effects of combined pre- and postnatal ethanol exposure (three trimester equivalency) on the development of myelin and axons in rat optic nerve. *International Journal of Developmental Neuroscience* **9**, 631–647.

PHILLIPS DE, KRUEGER SK (1992) Effects of combined pre- and postnatal ethanol exposure (three trimester equivalency) on glial cell development in rat optic nerve. *International Journal of Developmental Neuroscience* **10**, 197–206.

PINAZO-DURAN MD, RENAU-PIQUERAS J, GUERRI C (1993) Developmental changes in the optic nerve related to ethanol consumption in pregnant rats: analysis of the ethanol-exposed optic nerve. *Teratology* **48**, 305–322.

REYNOLDS ES (1963) The use of lead citrate at high pH as an electron-opaque stain in electron microscopy. *Journal of Cell Biology* **17**, 208–212.

RUGH R (1990) *The Mouse: Its Reproduction and Development*. Oxford: Oxford Science Publications.

SCHENKER S, BECKER HC, RANDALL CL, PHILIPS DK, BASKIN GS, HENDENSON GI (1990) Fetal alcohol syndrome: current status of pathogenesis. *Alcoholism: Clinical and Experimental Research* **14**, 635–647.

SCHWETZ BA, SMITH FA, STAPLES RE (1978) Teratogenic potential of ethanol in mice, rats and rabbits. *Teratology* **18**, 385–392.

TENNEKOON GI, COHEN SR, PRICE DL, MCKHANN GM (1977) Myelinogenesis in optic nerve. A morphological, autoradiographic, and biochemical analysis. *Journal of Cell Biology* **72**, 604–616.

UMEMORI H, SATO S, YAGI T, AIZAWA S, YAMAMOTO T (1994) Initial events of myelination involve fyn tyrosine kinase signalling. *Nature* **367**, 572–576.

WARRINGTON AE, BARBARESE E, PFEIFFER SE (1993) Differential myelinogenic capacity of specific developmental stages of the oligodendrocyte lineage upon transplantation into hypomyelinating hosts. *Journal of Neuroscience Research* **34**, 1–13.

WEBSTER WS, WALSH DA, MCEWEN SE, LIPSON AH (1983) Some teratogenic properties of ethanol and acetaldehyde in C57BL/6J mice: Implication for the study of the fetal alcohol sydrome. *Teratology* **27**, 231–243.

WILLIAMS PL, WARWICK R, DYSON M, BANNISTER LH (1989) *Gray's Anatomy*. Edinburgh: Longman.

ZAJAC CS, ABEL EL (1992) Animal models of prenatal alcohol exposure. *International Journal of Epidemiology* **21**, S24-S32.

J. Anat. (1995) 186, pp. 343–348, with 1 figure Printed in Great Britain

Morphometric analysis of myelinated fibre composition in the optic nerve of adult C57BL and CBA strain mice and (C57BL × CBA) F1 hybrid: a comparison of interstrain variation

Y. Y. DANGATA, G. S. FINDLATER AND M. H. KAUFMAN

Department of Anatomy, University Medical School, Edinburgh, UK

(*Accepted 17 October 1994*)

ABSTRACT

In a study involving 50 optic nerves isolated from 3 different strains of adult male mice, C57BL, CBA and (C57BL × CBA) F1 hybrids, and from adult female CBA strain mice, we observed that the mouse had a lower mean total myelinated nerve fibre count than other mammals such as the rat, cat, rabbit, monkey and man where similar information was available from the literature. The nerve fibre spectrum, however, which mostly consisted of small diameter fibres, was similar to the distribution seen in these other species. The largest myelinated nerve fibres observed in any of the strains of mice investigated had a diameter of not more than 1.92 μm. The C57BL optic nerve had the largest population of large diameter fibres, while the F1 had the largest population of small diameter fibres. In all the strains of mice investigated, the distribution of nerve fibres was unimodal, with a modal diameter of 0.48 μm. The mean nerve fibre diameter was 0.62 ± 0.02 μm (S.E.M.), 0.57 ± 0.03 μm and 0.55 ± 0.01 μm for C57BL, F1 and CBA, respectively. The F1 had the lowest population of fibres around the modal diameter. The myelinated nerve fibres were most densely packed in the CBA strain of mice, whereas the C57BL was the least densely populated. There was a significant interstrain difference in the parameters measured between the 3 strains of mice studied, whereas there was no significant intrastrain difference.

INTRODUCTION

Few detailed studies are available on the myelinated fibre composition of the mouse optic nerve, although much work has been undertaken in a variety of other mammalian species (see Discussion). The only relevant studies in the mouse that we have so far located have been those of Gyllensten & Malmfors (1963) and Gyllensten et al. (1966) who analysed the influence of visual stimulation on myelination and fibre composition in the mouse optic nerve. These early morphometric studies, although of interest in some respects, are incomplete in that the authors failed to establish whether there was any significant difference in myelinated fibre composition between, for example, the left and the right optic nerve, or between male and female mice of the same and different strains.

The principal aim of the present study was to establish baseline information which would be useful for subsequent teratological studies. The optic nerves from adult male C57BL, CBA and (C57BL × CBA) F1 hybrid mice, and from female CBA mice were isolated in order to undertake morphometric analyses. Both the cross-sectional areas of the optic nerves and the numbers and diameters of myelinated nerve fibres present, and nerve fibre density, were established for the various groups analysed. This information has allowed a comparison to be made between our findings in the mouse and comparable findings from a wide range of other mammalian species including man.

MATERIALS AND METHODS

Three different strains of 11-wk-old male mice were used in this study. C57BL (× 5) and CBA (× 10) strain mice and (C57BL × CBA) F1 hybrid (× 5) mice were deeply anaesthetised following an intraperitoneal injection of 0.02 ml/g body weight of a 1.2% solution

Correspondence to Professor M. H. Kaufman, Department of Anatomy, University Medical School, Teviot Place, Edinburgh EH8 9AG, UK.

of Avertin dissolved in 0.9% saline. An intracardiac perfusion of fixative, using 2 ml/g body weight of a 2.5% solution of glutaraldehyde in 0.1 M phosphate buffer was given via a 20 G needle into the left ventricle while the heart was still beating.

The optic nerves from each mouse were carefully dissected out, avoiding traction on the nerves. Each nerve was cut just posterior to the orbit, and anterior to the optic chiasma, immediately put into a separate bottle of fixative and left in this for a total of about 12 h. The isolated nerves were washed in buffer and then transferred into a secondary fixative consisting of 1% osmium tetroxide in 0.1 M phosphate buffer for a further 2 h. They were then dehydrated through a graded alcohol series and finally embedded in Araldite.

Semithin transverse sections of ~ 1 μm thick were cut perpendicular to the long axis of the nerve using a Reichert-Jung Ultracut E microtome and stained with 1% toluidine blue in 1% borax suitable for light microscopy. Thin sections 80 nm in thickness were then cut, put onto copper grids (200) and subsequently stained with 0.2% lead citrate and a saturated solution of uranyl acetate (Reynolds, 1963). A selection of photomicrographs was then taken from the centre to the periphery of each nerve using a Philips EM301 transmission electron microscope. The micrographs were developed and printed at a final magnification of × 3000, sufficient to ensure that all fibres with the thinnest myelin sheaths could be unequivocally identified in counts.

The cross-sectional areas (*csa*) of the optic nerves were determined by viewing and measuring complete cross-sections of the optic nerves in a Magiscan image analysis system (Applied Imaging). Detailed morphometric analysis was performed on the electron micrographs using a systematic random sampling procedure (Mayhew, 1990) to establish the numbers and diameters of the myelinated nerve fibres by means of the image analyser. In order to determine the latter, the approximate centre of each optic nerve was located, and from this point sectors of 10° were drawn 120° apart which produced 3 sectors/nerve. A grid of 1 cm × 1 cm squares (equivalent to 7.8 μm^2 of nerve cross-sectional area) was placed over each sector. Starting from the centre of each nerve, and using the systematic random sampling method referred to above, every 4th square in each direction (i.e. 1 in 16) was sampled for estimating nerve fibre counts. The aim was to sample between 150 and 200 myelinated nerve fibres, and to measure as many profiles of the nerves as possible. In this method all nerve fibres whose centres were within a sampled square were counted and their transverse diameter measured. The image analyser allowed a histogram to be plotted which displayed the distribution of diameters of all the nerve fibres studied from each optic nerve sample. When all the information from the various sample groups was available, it was then possible for histograms to be plotted which displayed the overall distribution of the nerve fibre diameter composition for each of the mouse strains studied.

An estimate of the number of myelinated nerve fibres present in the entire nerve and their density was calculated using a ratio technique (Matheson, 1970; Mayhew, 1988, 1990). A 2-tailed Student's t test was then performed on the pooled data for each strain of mouse, to establish whether there was any significant difference ($P \leqslant 0.05$) in cross-sectional area and total nerve fibre count and size distribution between the left and right optic nerve for each of the strains studied, and to establish whether interstrain variation existed. Furthermore, to establish whether evidence of sexual dimorphism was present, an additional series of 11-wk-old female CBA (× 5) mice was treated as indicated above, and the findings obtained compared with those obtained previously from the analysis of the male CBA mice.

RESULTS

Cross-sectional areas (csa)

Analysis of the *csa* of the left and right optic nerves of the male mice studied showed that, except in the C57BL, the right optic nerve was consistently larger than the left (i.e. in the CBA strain, and in the (C57BL × CBA) F1 hybrids). The smallest difference between the left and right optic nerves was seen in the CBA and the largest difference observed in the F1. However the difference observed was not significant. The data from the left and right optic nerves of each strain studied were therefore pooled. This allowed the sample size to be doubled in each case, so that in the C57BL, CBA and F1 hybrid mice, the pooled sample size of the optic nerves studied was 10, 20 and 10 respectively. The C57BL had the largest mean *csa* (72968 ± 1876 μm^2 (S.E.M.)) and the CBA the smallest (57113 ± 1513 μm^2) (S.E.M.). Further analysis of the pooled data has revealed that there was a significant difference between all the strains ($0.01 < P < 0.05$) (see Tables 1, 2).

In an additional series, a total of 5 left and 5 right optic nerves were isolated from 11-wk-old female CBA mice. Analysis of the *csa* of this group revealed that there was no significant difference between the two sides. A comparison of the findings from this

Table 1. *Mean cross-sectional area, myelinated nerve fibre count and nerve fibre density of optic nerves isolated from (C57BL × CBA) F1 hybrid, C57BL and CBA strains of adult mice*

Strain	Mean cross-sectional area ± S.E.M. (μm^2)			Mean nerve fibre count ± S.E.M.			Mean nerve fibre density per 1000 μm^2 (L + R) ± S.E.M.		
	Left (L)	Right (R)	L + R	Left (L)	Right (R)	L + R	Left (L)	Right (R)	L + R
(C57BL × CBA) F1 hybrid (male, n = 9)	62925 ± 1849	70452 ± 1384	67107 ± 1603	98694 ± 2907	90399 ± 6017	94086 ± 3691	1569 ± 18	1279 ± 48	1408 ± 61
C57BL (male, n = 10)	75264 ± 1219	70667 ± 3410	72968 ± 1876	95016 ± 8418	79781 ± 4005	87398 ± 5076	1258 ± 98	1129 ± 17	1194 ± 51
CBA (male, n = 20)	57200 ± 2040	57308 ± 1788	57254 ± 1320	80924 ± 4439	78586 ± 2530	79755 ± 2500	1426 ± 80	1378 ± 48	1402 ± 46
CBA (female, n = 10)	54654 ± 2809	59005 ± 7483	56830 ± 3847	80524 ± 6400	79934 ± 6825	80229 ± 4432	1475 ± 100	1382 ± 69	1429 ± 60
CBA (male & female, n = 30)	56351 ± 1625	57874 ± 2603	57113 ± 1513	80791 ± 3517	79035 ± 2696	79913 ± 2180	1442 ± 61	1380 ± 38	1411 ± 36

Table 2. *Intrastrain and interstrain comparison for variables measured for the optic nerve of adult F1, C57BL and CBA strains of mice*

Strain comparison	Variable/level of significance*		
	Mean cross sectional area (μm^2)	Mean myelinated nerve fibre count	Mean myelinated nerve fibre density (per 1000 μm^2)
F1 (L vs R, n = 9)	n.s.	n.s.	n.s.
C57BL (L vs R, n = 10)	n.s.	n.s.	n.s.
CBA male (L vs R, n = 20)	n.s.	n.s.	n.s.
CBA female (L vs R, n = 10)	n.s.	n.s.	n.s.
CBA male vs CBA female (n = 30)	n.s.	n.s.	n.s.
CBA male and female (L vs R, n = 30)	n.s.	n.s.	n.s.
F1 male vs CBA male (n = 29)	$0.01 < P < 0.05$	$0.01 < P < 0.05$	n.s.
F1 male vs CBA male and female (n = 29)	$0.01 < P < 0.05$	$0.01 < P < 0.05$	n.s.
F1 male vs C57BL male (n = 19)	$0.01 < P < 0.05$	n.s.	$0.01 < P < 0.05$
C57BL male vs CBA male (n = 30)	$0.01 < P < 0.05$	n.s.	$0.01 < P < 0.05$
C57BL male vs CBA male and female (n = 40)	$0.01 < P < 0.05$	n.s.	$0.01 < P < 0.05$

* Student's t test; n.s., not significant.

series with their CBA male littermates revealed no significant difference between the two sexes. For this reason the pooled data for this strain have been given in Table 1.

Total myelinated nerve fibre counts

Although the *csa* of the optic nerve of the right eye, except for the C57BL, was consistently greater than that of the left, the opposite finding was observed with respect to the mean myelinated nerve fibre counts, where the left optic nerve consistently showed a higher myelinated nerve fibre count than the right in all groups of mice studied. This difference between the left and right optic nerve, however, was not significant. As in the *csa* analysis indicated above, this has allowed the sample size in each strain to be doubled. The total myelinated nerve fibre count varied between 79913 ± 2180 (S.E.M.) (CBA) and 94086 ± 3691 (S.E.M.) (F1). Further analysis of the pooled data has revealed that the F1 differ significantly from the CBA ($0.01 < P < 0.05$). There was no significant difference, however, between the C57BL and either of the other strains. As for *csa* the CBA findings provided no evidence of sexual dimorphism, so that the individual male and female findings, as well as the pooled data have been provided in Tables 1 and 2.

Myelinated nerve fibre density per 1000 μm^2

No significant difference was observed in the mean myelinated nerve fibre density between the left and

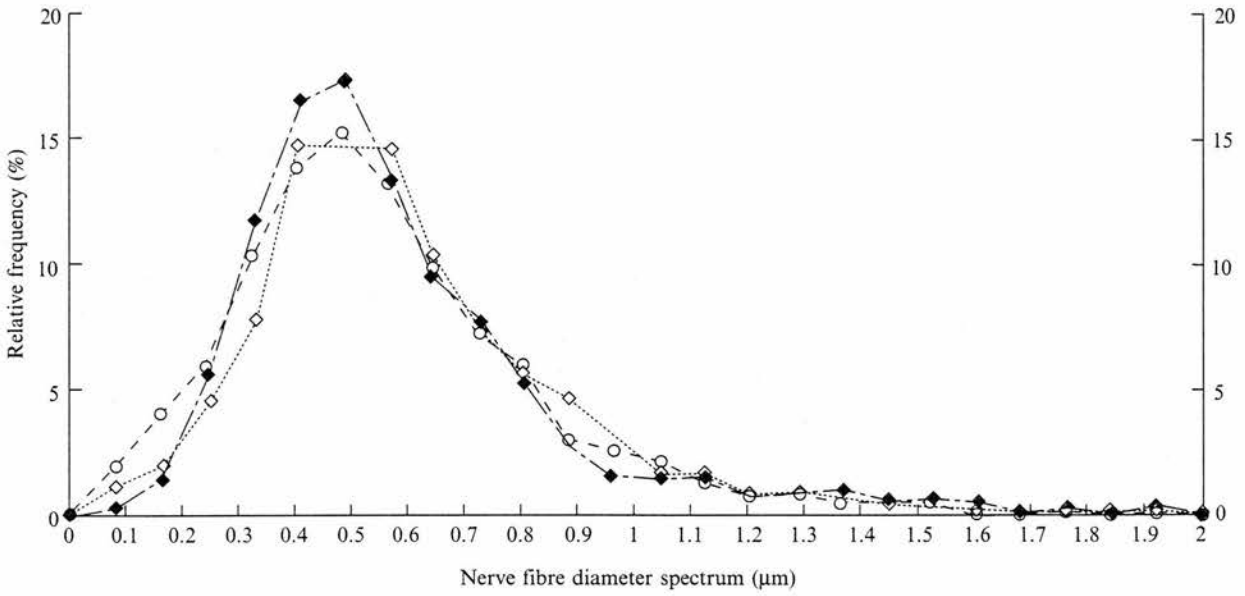

Fig. Nerve fibre size spectrum in the optic nerve of adult C57BL, CBA and (C57BL × CBA) F1 mice: –·–· ◆; ···· ◇; ––– ○.

right optic nerves in each of the strains studied. The pooled values showed a significant difference between the C57BL and both of the other strains ($0.01 < P < 0.05$) (see Table 2). There was no significant difference between the F1 and CBA. The highest mean myelinated nerve fibre density was observed in the CBA (1411 ± 36 (S.E.M.)) and the smallest in the C57BL (1194 ± 51 (S.E.M.)). As for *csa* and total myelinated fibre counts, no evidence of sexual dimorphism was seen in the CBA, so that the individual male and female findings as well as the pooled data have been included in Tables 1 and 2.

Size (diameter) distribution of myelinated nerve fibres

Over 90% of the nerve fibres in each strain of mice were not more than 1.04 μm in diameter. The largest fibres analysed were seen in the C57BL and were 1.92 μm in diameter. These constituted only 0.28% of the total fibre population of that strain. The largest fibres seen in the F1 and CBA were 1.84 μm in diameter. They constituted 0.09% and 0.04% of the total fibre population of the F1 and CBA, respectively (see Figure). The mean nerve fibre diameter was 0.62 ± 0.02 μm (S.E.M.), 0.57 ± 0.03 μm (S.E.M.) and 0.55 ± 0.01 μm (S.E.M.) for the C57BL, F1 and the CBA respectively. In all the strains examined, the distribution of nerve fibre diameter was unimodal, with a modal value of 0.48 μm. Each strain of mice exhibited a slight skewing of the fibres in favour of those with a smaller diameter. The C57BL and the CBA had similar populations of fibres (17.25% and 17.37%, respectively) with this modal diameter. The F1 had 15.2% of its fibres with the modal diameter (see Figure).

DISCUSSION

The findings reported in this study indicate that of the variables analysed, no significant differences were observed in the cross-sectional areas, total number of myelinated nerve fibres present, and nerve fibre density between the left and right optic nerves of male C57BL, CBA and (C57BL × CBA) F1 hybrid mice. In an additional analysis of the optic nerves isolated from a group of CBA females, no significant difference was observed in any of the variables studied between the left and right optic nerves, and between male and female mice. Interstrain differences were, however, seen between the different strains studied. Of the 3 strains of mice involved in this study, the C57BL strain had the largest cross-sectional area, but their optic nerves were the least densely populated with myelinated nerve fibres. Because the CBA strain has a high mean nerve fibre count and a relatively small *csa*, it has the highest nerve fibre density. The relatively small difference in the variables measured between individuals of each of the strains studied, both male and female for the CBA strain mice, indicates a considerable degree of intrastrain uniformity as might be expected in inbred strains of animals. The fact that there was a significant difference in the variables measured between the various strains studied should also not be surprising, and would seem to be reasonable evidence of genetic variation induced as a result of many generations of brother × sister matings

the methodology employed to determine this value. In contrast to the present study where transmission electron micrographs of thin sections of the optic nerve were studied, these authors analysed paraffin sections of mouse optic nerves using phase-contrast microscopy. The error factor using the latter approach, both in estimating the total number of fibres present as well as determining their mean diameters, was found to be considerable. When these authors used photomicrographs obtained following transmission electron microscopy of the optic nerve, a modal diameter of 0.6–0.8 μm was reported, compared with 1.0 μm when paraffin sections were analysed. Furthermore, it is unclear why the distribution of fibre diameter should have been trimodal in Gyllensten & Malmfors (1963) and Gyllensten et al. (1966) compared with a unimodal distribution as reported in this study. Whether any clear species specificity exists between total fibre count and the lifestyle of that species has yet to be fully evaluated. Gyllensten & Malmfors (1963) suggested that this may reflect the fact that the mouse is more dependent on other senses than sight for most of its activities, and that this may be the reason why the majority of the myelinated fibres present are of small diameter.

ACKNOWLEDGEMENTS

We are grateful to the staff of the Microbiology Animal House for animal care and Mr R. McDougall for excellent electron microscopy technical assistance. This work was supported by a grant from the Scottish Home and Health Department (K/MRS/50/C1875); as well as a Studentship for Y. Y. D. from the Kaduna State Government, Nigeria. We wish to thank Dr Baljean Dhillon for valuable advice and discussion.

REFERENCES

CHACKO LW (1948) An analysis of fibre-size in the human optic nerve. *British Journal of Ophthalmology* **32**, 457–461.

DONOVAN A (1967) The nerve fibre composition of the cat optic nerve. *Journal of Anatomy* **101**, 1–11.

FORRESTER JF, PETERS A (1967) Nerve fibres in optic nerve of rat. *Nature* **214**, 245–247.

GYLLENSTEN L, MALMFORS T (1963) Myelinization of the optic nerve and its dependence on visual function—a quantitative investigation in mice. *Journal of Embryology and Experimental Morphology* **11**, 255–266.

GYLLENSTEN L, MALMFORS T, NORRLIN-GRETTVE M-L (1966) Developmental and functional alterations in the fiber composition of the optic nerve in visually deprived mice. *Journal of Comparative Neurology* **128**, 413–418.

HUGHES A (1977) The pigmented-rat optic nerve: fiber count and fiber diameter spectrum. *Journal of Comparative Neurology* **176**, 263–268.

MATHESON DF (1970) Some quantitative aspects of myelination of the optic nerve in rat. *Brain Research* **24**, 257–269.

MAYHEW TM (1988) An efficient sampling scheme for estimating fibre number from nerve cross sections: the fractionator. *Journal of Anatomy* **157**, 127–134.

MAYHEW TM (1990) Efficient and unbiased sampling of nerve fibres for estimating fiber number and size. In *Methods in Neuroscience*, vol. 3. *Quantitative and Qualitative Microscopy* (ed. P. M. Conn), pp. 172–187. New York: Academic Press.

OGDEN TE, MILLER RF (1966) Studies of the optic nerve of the rhesus monkey: nerve fiber spectrum and physiological properties. *Vision Research* **6**, 485–506.

POTTS AM, HODGES D, SHELMAN CB, FRITZ KJ, LEVEY NS, MAGNALL Y (1972*a*) Morphology of the primate optic nerve: I. Method and total fiber count. *Investigative Ophthalmology* **11**, 980–988.

POTTS AM, HODGES D, SHELMAN CB, FRITZ KJ, LEVEY NS, MAGNALL Y (1972*b*) Morphology of the primate optic nerve: II. Total fiber size distribution and fiber density distribution. *Investigative Ophthalmology* **11**, 989–1003.

REYNOLDS ES (1963) The use of lead citrate at high pH as an electron-opaque stain in electron microscopy. *Journal of Cell Biology* **17**, 208–212.

SANCHEZ RM, DUNKELBERGER GR, QUIGLEY HA (1986) The number and diameter distribution of axons in the monkey optic nerve. *Investigative Ophthalmology and Visual Science* **27**, 1342–1350.

VANEY DI, HUGHES A (1976) The rabbit optic nerve: fibre diameter spectrum, fibre count, and comparison with a retinal ganglion cell count. *Journal of Comparative Neurology* **170**, 241–252.

WATAKUWA K, WATANABE M, SUGIMOTO T, WASHIDA A, FUKUDA Y (1987) An electron microscopic analysis of the optic nerve of the eastern chipmunk (Tamias sibiricus asiaticus): total fiber count and retinotopic organisation. *Vision Research* **27**, 1891–1901.

J. Anat. (1994) 185, pp. 627–635, with 2 figures Printed in Great Britain

Morphometric study of the optic nerve of adult normal mice and mice heterozygous for the *Small eye* mutation (*Sey*/+)

Y. Y. DANGATA[1], G. S. FINDLATER[1], B. DHILLON[2] AND M. H. KAUFMAN[1]

[1] *Department of Anatomy, University Medical School, and* [2] *Princess Alexandra Eye Pavilion, Royal Infirmary, Edinburgh, Scotland, UK*

(*Accepted 23 June 1994*)

ABSTRACT

The Small eye (*Sey*) gene, which has been mapped to chromosome 2 in the mouse, is known to cause variable malformations of the eye and nose. The effect of the gene in the heterozygous state is mainly on the eye. A combined electron microscopy and morphometric analysis of the optic nerve in adult littermates with a normal (+/+) and heterozygous mutant (*Sey*/+) genotype was carried out. The optic nerve could be dissected from the posterior pole of the eyeball to the optic chiasma in all the mice examined. The results of morphometric analyses carried out in this study show that the *Sey* gene indirectly affects the normal morphogenesis of the optic nerve in the heterozygous mutant *Sey* male mouse to a significant degree compared with its male normal littermate. The heterozygous mutant *Sey* female mouse is also affected, but not significantly so when compared with its normal female littermate. The mean nerve cross-sectional area and mean nerve fibre counts for the *Sey* strain are lower than those observed in other strains of mice that have been studied. The nerve fibre densities and the spectrum of nerve fibre sizes encountered are, however, similar to those seen in other strains of mice. We believe that the findings indicate that the smaller mean nerve fibre counts observed in the heterozygous mutant (*Sey*/+) mice compared to their normal (+/+) siblings is unlikely to have resulted from primary retinal dysgenesis, but is a consequence of the reduced size of their neural retina, and total retinal ganglion cell population.

Key words: *Sey* gene.

INTRODUCTION

The gene mutation in the mouse causing Small eye (*Sey*) arose spontaneously in Edinburgh in 1967 (Roberts, 1967). Since then the gene, which is allelic to the aniridia gene in the human, has been mapped to chromosome 2 (Hogan et al. 1986, 1988; Jong et al. 1990; Hill et al. 1991; Ton et al. 1992). Other genes known to cause developmental abnormalities of the eye also located on the same chromosome include *Ocular retardation* (*or*^{J}), *Dickie's small eye* (*Dey*) and *coloboma* (*Cm*) (Theiler et al. 1976, 1978, 1980; Theiler & Varnum, 1981). These are semidominant genes except the *Ocular retardation* gene which is recessive. Homozygous *Small eye* (*Sey*/*Sey*) embryos develop to term but do not develop either eyes or nose, and die soon after birth because of the breathing problems associated with the absence of the nose (Hogan et al. 1986). The effect of the *Sey* mutation is believed to be limited to the growth and differentiation of the lens placode and nasal placode, and it is the failure of the former to develop normally that has secondary consequences on the rest of the ocular apparatus in both the homozygous in particular and, but to a considerably lesser degree, the heterozygous state.

It is the eyes that are mainly affected in the heterozygous mutant *Sey* mice (Hogan et al. 1986). Abnormalities of the eyeball associated with the presence of the mutant gene, when in the heterozygous state, include microphthalmos often associated with cataracts, partial or complete absence of the iris,

Correspondence to Professor M. H. Kaufman, Department of Anatomy, University Medical School, Teviot Place, Edinburgh EH8 9AG, Scotland, UK.

absence of the lens and retinal abnormalities (Jong et al. 1990). No evidence is yet available to indicate whether the gene exercises its ocular effect on the eyeball and its contents alone, or influences, either directly or indirectly, the development of the optic nerve and other parts of the visual system; and, if the optic nerve is affected, to what extent. This study has set out to establish whether the presence of the *Sey* gene influences the development of the optic nerve, and attempts to quantify the extent of the influence in relation to the parameters of the optic nerve measured.

MATERIALS AND METHODS

A breeding colony of *Small eye* mice was obtained from Dr Ruth Clayton, formerly of the Department of Genetics, University of Edinburgh, and maintained by brother × sister matings of heterozygous male and female mice. The latter were easily distinguished from their normal siblings due to the fact that their eyes were significantly smaller than those of their genetically normal (i.e. +/+) littermates.

Eleven week old normal (i.e. +/+) and heterozygous mutant *Sey* mice (i.e. *Sey*/+) of both sexes were studied. A total of 5 mice of each sex of normal, and 8 females and 5 males of heterozygous mutant *Sey* mice were used. Each animal was deeply anaesthetised by an intraperitoneal injection of 0.02 ml/g body weight of a 1.2% solution of tribromoethanol (Avertin) in 0.9% saline. The heart was exposed, and using a 21G needle, intracardiac perfusion was carried out by giving 2.0 ml/g body weight of a 2.5% solution of glutaraldehyde in 0.1 M phosphate buffer through the left ventricle while the heart was still beating.

The whole length of the optic nerve was immediately, but carefully, dissected out avoiding traction on the nerve. Each nerve was put into a prelabelled bottle containing 2.5% glutaraldehyde fixative in 0.1 M phosphate buffer and left for a total of 12 h. The nerves were then washed in 0.1 M phosphate buffer and transferred into a secondary fixative consisting of 1% osmium tetroxide in 0.1 M phosphate buffer for a further 2 h. After this they were dehydrated in a graded alcohol series and then embedded in Araldite.

From each nerve, semithin sections (~ 1 μm) were cut perpendicular to the long axis of the nerve using a Reichert-Jung Ultracut E microtome. Sections were stained with 1% toluidine blue in 1% borax for light microscopy. Ultrathin sections (~ 80 nm) thickness were then cut for electron microscopy. These were picked up on copper grids and subsequently stained with 0.2% lead citrate solution and a saturated solution of uranyl acetate. A selection of photomicrographs was taken from the centre to the periphery of each nerve using a Philips EM301 transmission electron microscope. The micrographs were developed and printed to a final magnification of × 3000.

Using the semithin sections, the cross-sectional area (*csa*) of each nerve excluding its epineurium was measured in a Magiscan image analysis system (Applied Imaging). From the measurements of the *csa* of the individual nerves, the mean *csa* of the optic nerves from each group of mice was calculated. Other detailed morphometric measurements of the nerves were also carried out on the photomicrographs of the ultrathin sections using the image analyser. A systematic random sampling method (Mayhew, 1990) was used to determine the number and diameter spectrum of the myelinated nerve fibres present in each nerve. This was done by locating the centre of the nerve from which point sectors of 10° were drawn over different areas of the nerve. A grid of approximately 1 cm × 1 cm squares (equivalent to 7.8 μm^2 of nerve *csa*) was placed over each sector. Using the sampling method indicated above, and starting from the centre of each nerve, every 4th square falling completely within each sector in each direction (i.e. 1 in 16) was sampled for the estimation of nerve fibre counts and fibre size distribution. Also, only myelinated nerve fibres whose centres fell within a sampled square were included in the analysis. Mayhew & Sharma (1984*a*, *b*) have shown that it is only necessary to count in the region of 200 nerve fibres to obtain an estimate of within 95% of the actual number of nerve fibres present in the whole nerve. The Magiscan allowed a histogram of the diameter profile of the sampled nerve fibres of each nerve studied to be plotted. A summary histogram of the nerve fibre diameter profile for each group of mice was then plotted by hand.

The number of myelinated nerve fibres present in the whole nerve was calculated using the ratio technique (Matheson 1970; Mayhew, 1988, 1990), and from the figures obtained the numerical density of fibres per 1000 μm^2 was calculated for each nerve. The mean nerve fibre count and fibre density of the optic nerve for each group of mice was also calculated.

A Student's 2-tailed t test was performed on all results to establish whether there was a significant difference in the parameters measured between the left and the right optic nerve of both males and females, and between males and females in each of the two groups of mice studied. This test was carried out to compare corresponding sexes of the two groups of

Table 1*a*. *Optic nerve cross sectional area for normal (+/+) and heterozygous mutant (Sey/+) adult mice*

Group/sex of mouse		Mean cross-sectional area (μm²)		
			L (Left) or R (Right)	Pooled (L+R)
Normal (+/+)	Male (n = 9)	L	49464±5335	49397±4259
		R	49343±6932	
	Female (n = 10)	L	42154±4867	43996±2571
		R	45838±257	
Heterozygous mutants (Sey/+)	Male (n = 9)	L	34411±4968	33179±2778
		R	31636±1897	
	Female (n = 16)	L	41985±2420	40535±1685
		R	39085±2387	

Table 1*b*. *Level of significance between optic nerve cross sectional areas of normal (+/+) and heterozygous mutant (Sey/+) adult mice*

Normal (+/+) male (n = 9)			
n.s.	Normal (+/+) female (n = 10)		
(0.01 < *P* < 0.05)	xxxxxx	Mutant (Sey/+) male (n = 9)	
xxxxxx	n.s.	(0.01 < *P* < 0.05)	Mutant (Sey/+) female (n = 16)

n.s., not significant.

Table 2*a*. *Mean myelinated nerve fibre counts of normal (+/+) and heterozygous mutant (Sey/+) adult mice*

Group/sex of mouse		Mean myelinated nerve fibre count		
			L (Left) or R (Right)	Pooled (L+R)
Normal (+/+)	Male (n = 9)	L	71392±3394	70021±4886
		R	68924±8836	
	Female (n = 10)	L	61241±8472	62589±4305
		R	63937±3210	
Heterozygous mutants (Sey/+)	Male (n = 9)	L	47584±7204	48605±4062
		R	49881±3352	
	Female (n = 16)	L	54943±4190	54558±2856
		R	54173±4161	

Table 2*b*. *Level of significance between mean nerve fibre count of normal (+/+) and heterozygous mutant (Sey/+) adult mice*

Normal (+/+) male (n = 9)			
n.s.	Normal (+/+) female (n = 10)		
(0.01 < *P* < 0.05)	xxxxxx	Mutant (Sey/+) male (n = 9)	
xxxxxx	n.s.	n.s.	Mutant (Sey/+) female (n = 16)

n.s., not significant.

Table 3*a*. *Mean myelinated nerve fibre densities in the optic nerve of normal (+/+) and heterozygous mutant (Sey/+) adult mice*

Group/sex of mouse		Mean myelinated nerve fibre density (per 1000 μm²)		
		L (Left) or R (Right)		Pooled (L+R)
Normal (+/+)	Male (n = 9)	L	1470±88	1441±75
		R	1417±123	
	Female (n = 10)	L	1437±78	1416±41
		R	1395±34	
Heterozygous mutants (Sey/+)	Male (n = 9)	L	1373±114	1469±83
		R	1590±109	
	Female (n = 16)	L	1309±69	1349±50
		R	1389±74	

Table 3*b*. *Level of significance between mean nerve fibre densities of normal (+/+) and heterozygous mutant (Sey/+) adult mice*

Normal (+/+) male (n = 9)	Normal (+/+) female (n = 10)	Mutant (Sey/+) male (n = 9)	Mutant (Sey/+) female (n = 16)
n.s.			
n.s.	xxxxxxx		
xxxxxx	n.s.	n.s.	

n.s., not significant.

mice to determine whether a significant difference existed between them. Level of significance was taken as $P < 0.05$.

RESULTS

Cross-sectional areas (μm²)

The optic nerve, which had a well defined dural sheath in both the normal and the heterozygous mutant *Sey* mice, could be dissected from the eyeball to the optic chiasma. One nerve from the male series of each group of mice was lost during the course of dissection. No significant difference was observed in *csa* between the left and the right optic nerves of either sexes of each of the two groups of mice. For this reason the sample size for each sex in each of the two groups of mice was pooled for the purpose of the statistical analysis of the mean *csa* for each sex. The female heterozygous mutant *Sey* significantly differed from their male littermates with respect to their *csa* ($P < 0.05$), but in the normal series no significant difference was observed between the two sexes. The inter-group comparison of the *csa* between corresponding series revealed a significant difference between heterozygous mutant *Sey* males and normal *Sey* males ($0.01 < P < 0.05$). No such difference was seen between females of the two groups of mice (see Tables 1*a*, *b*).

Total myelinated nerve fibre counts and nerve fibre density per 1000 μm²

The statistical analysis of the mean myelinated nerve fibre counts showed no significant difference between the left and the right optic nerve of either males or females of the same group of mice. Because of this, all samples for each sex in each of the *Sey* groups studied were pooled together for the purpose of the statistical analysis of the mean myelinated nerve fibre count. There was also no significant difference between males and females in each group of mice with respect to the mean myelinated nerve fibre count. The heterozygous mutant *Sey* series consistently had lower values for the mean myelinated nerve fibre count compared to their normal littermates. The heterozygous mutant

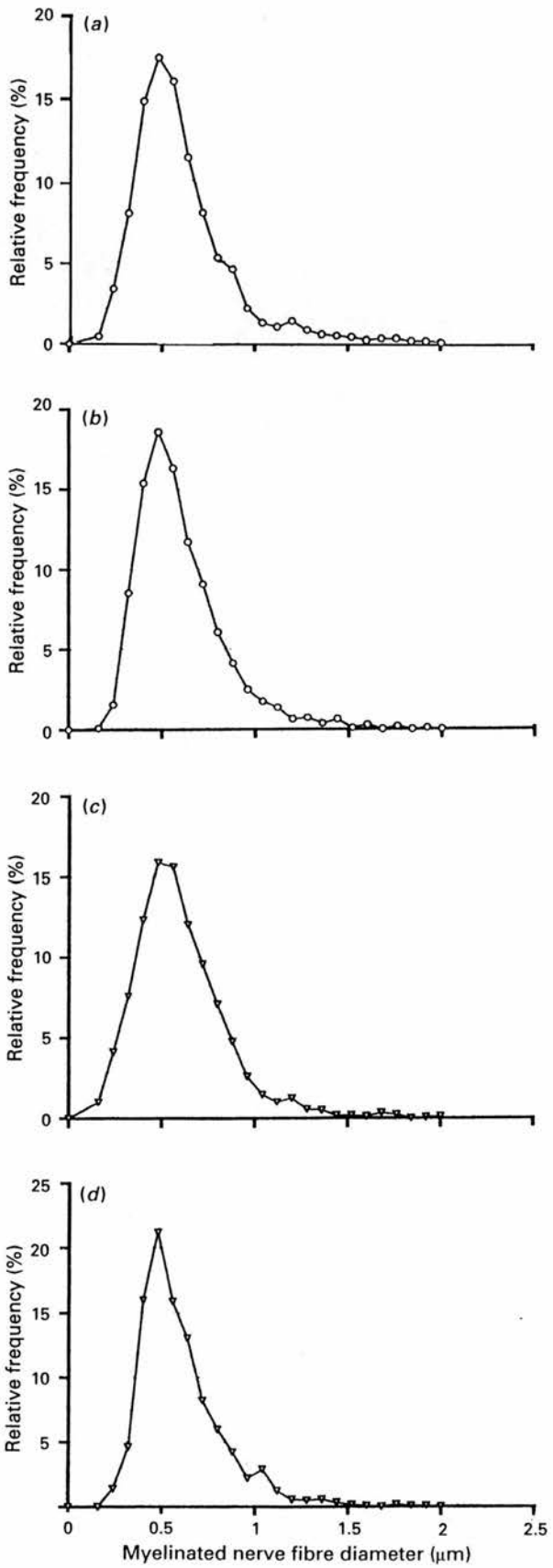

Fig. 1. Graphs showing distribution of myelinated nerves of different fibre diameters within the optic nerve of normal *Sey* (+/+) female (*a*) and male (*b*) mice, and heterozygous mutant *Sey* (*Sey*/+) female (*c*) and male (*d*) mice.

Sey males significantly differed from their normal male littermates ($0.01 < P < 0.05$) though in the case of +/+ and *Sey*/+ females, the difference observed was not significant (see Table 2*a*, *b*). There was no significant difference in the mean myelinated nerve fibre density either within the groups or between them (see Table 3).

Myelinated nerve fibre diameter spectrum

More than 90% of the myelinated nerve fibres analysed in each group of mice were less than 1.0 μm in diameter, with the largest nerve fibres measured in each group being slightly less than 2.0 μm in diameter. The distribution of the fibres in both groups was unimodal, with a modal diameter of 0.48 μm. In each case, there was a positive skewing of the nerve fibres in favour of the small diameter fibres (see Fig. 1*a–d*).

Representative electron micrographs which display the appearance of transverse sections through nerve fibres within the optic nerve of normal *Sey* (+/+) and heterozygous mutant *Sey* (*Sey*/+) mice, are presented in Figure 2*a* and *b*, respectively.

DISCUSSION

The findings from this study suggest that the influence of the *Sey* gene, in the heterozygous mutant mouse, is primarily on the development of the eyeball, but also extends secondarily to the optic nerve. From earlier studies, other mutant genes have been shown to have a primary effect on the development of the optic nerve in the mouse (Theiler et al. 1976; Robb et al. 1978; Franz & Besecke, 1991). The small eyeballs generally observed in the heterozygous mutant *Sey* were always associated with corresponding small-calibre optic nerves. This is highlighted by the significant difference that was observed in the mean *csa* and the mean myelinated nerve fibre counts between the male series of both *Sey* groups of mice involved in the study. Although the difference in these two parameters between the female series of both groups of mice was not significant, values of the parameters for the heterozygous mutant *Sey* females were always considerably lower than those of their normal female littermates. The reason for the greater effect of the gene on the heterozygous mutant *Sey* male mouse compared to their female siblings is, however, not clear.

Earlier reports on the effect of the *Sey* gene on the development of the eye have been mainly concerned with the effect of the gene on the lens and contents of the orbit in the homozygous mutant during the early

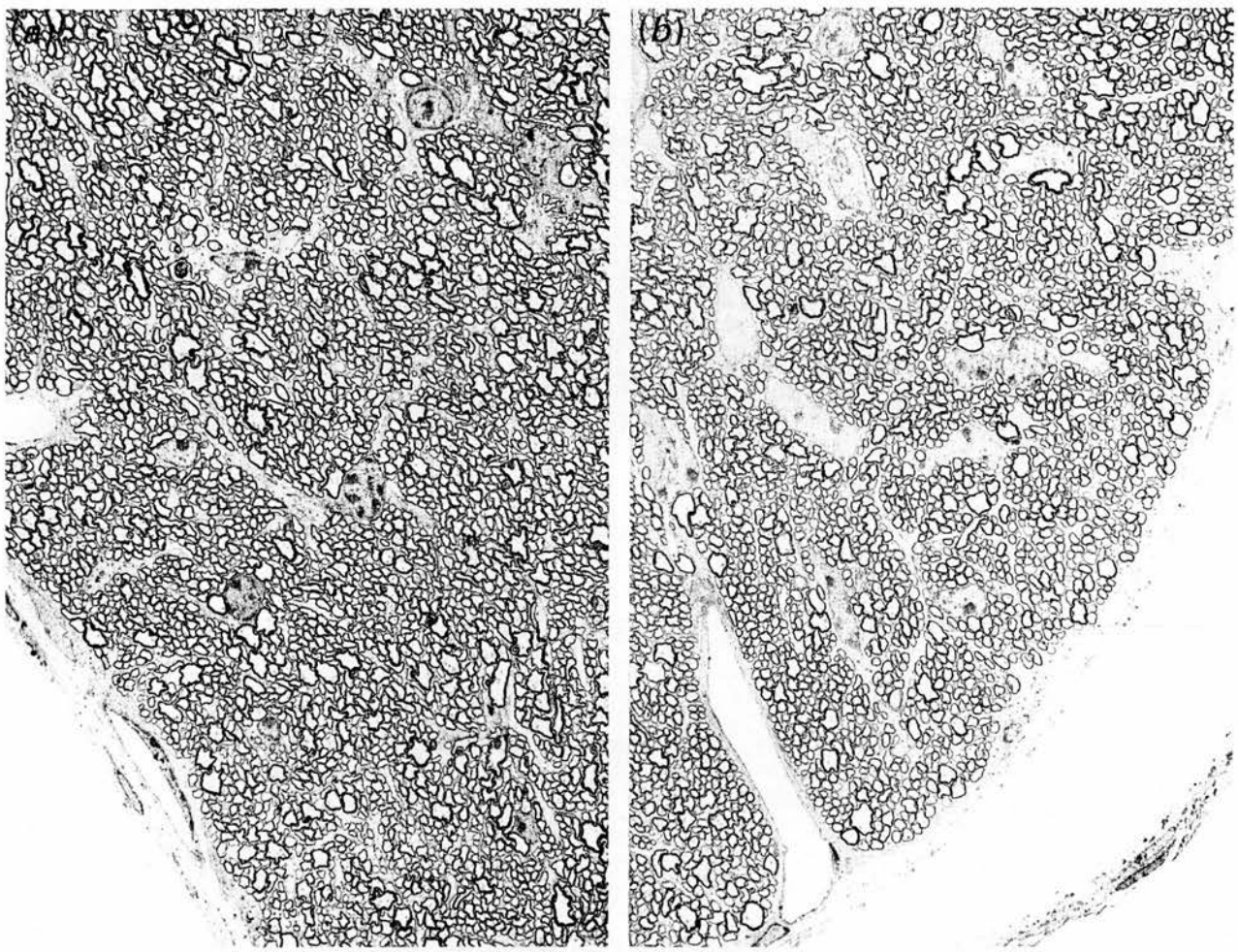

Fig. 2. Representative low-magnification transmission electronmicrographs of transverse sections through the optic nerve of a normal *Sey* (+/+) mouse (*a*), and a heterozygous mutant *Sey* (*Sey*/+) mouse (*b*). ×750.

embryonic period. Little information is available on its effect on the development and contents of the optic nerve in the adult heterozygous mutant mouse. In the homozygous mutant, while an irregularly shaped optic vesicle initially forms, in the absence of an inductive influence from the lens vesicle, it soon degenerates, and no remnant of the optic apparatus beyond the optic chiasma is generally seen (Hogan et al. 1986, 1988). A similar situation is seen in another mutant involving the eye, namely the *Ocular retardation* gene (or^J) when present in the homozygous state (see Truslove, 1962; Robb et al. 1978). Theiler et al. (1976) observed that in the adult (*or*/*or*) mutant, where the *or* gene was believed to be allelic but not identical to the or^J gene, small eyes are present with closed lids. This was associated with abnormalities of the retinal layers and absence of the optic nerve, the latter being replaced by a thin layer of connective tissue.

Robb et al. (1978) observed that in normal (+/+) *Ocular retardation* mice, by d 14.5 postcoitus (p.c.) the eyeball increases in volume and the optic nerve increases in diameter as a result of the differentiation of large numbers of ganglion cells within the neural retina which send axons to the brain. This is in contrast to the situation in homozygous or^J mutant mice of about the same age, where they observed that despite the presence of a substantial retinal neuroblastic layer in which it was difficult to distinguish ganglion cells and nerve fibres, no axons exited from the eye. Furthermore, they suggested that another factor that might have induced regression of the optic stalk was the absence of vascularisation of the optic nerve (Robb et al. 1978).

In the homozygous mouse mutant *extra-toe* (X^t/X^t), Franz & Besecke (1991) observed that the optic nerve was either completely absent or at most only partly developed. No explanation is yet available, however, for the variable phenotype observed in the (X^t/X^t) mice, nor has the developmental mechanism that leads to the ocular pathology seen in these mice yet been established. Theiler et al. (1978, 1980), in their

work on *Dickie's small eye* (*Dey*) found that the morphogenesis of the eye in the heterozygous mutant animals was delayed compared to that observed in controls on d 12 p.c. This apparent lagging in development generally starts between d 10 and 11 p.c. though, in some instances, it was observed as early as d 7 p.c. and was invariably noted by d 12 p.c. The ocular abnormalities noted in adult (*Dey/+*) heterozygotes were small eyes with coloboma, small or absent lens, with cataract if present, abnormal folding of the retina and reduction in the pigment layers, with often absence of the anterior chamber. Homozygotes invariably die during the early post-implantation period, often at the egg cylinder stage.

The normal development of the eye in the mouse begins with the invagination of the central region of the optic placode to form the optic pit and its progressive differentiation, in association with cephalic neurulation, to form the optic vesicle. This forms from the neuroepithelium in the diencephalic region of the forebrain during d 8–9 p.c. By about d 9.5 p.c., an optic stalk is present and the optic cup has begun to indent, while between about 9.5–11 d p.c., the lens placode indents to form the lens pit and subsequently differentiates to form the lens vesicle. This then separates from the surface and progressively indents the optic cup so that it is now seen to have an inner and an outer layer which are destined, respectively, to form the neural and pigment layers of the retina (Kaufman, 1979, 1992; Rugh, 1990).

The normal process of ocular development is believed to be influenced by the process of embryonic induction by which regions of the anterior head ectoderm become progressively specified as the presumptive optic apparatus. Similar mechanisms are believed to be involved with regard to the differentiation of the nasal placode. The mechanism of embryonic induction may itself be affected by gene mutation (Jong et al. 1990). Direct contact between the neuroepithelium of the optic vesicle and the overlying surface ectoderm is believed to be a necessary prerequisite for the induction of the lens placode (Bard, 1990). Other factors that influence normal morphogenesis include programmed cell death (apoptosis) and cell resorption, the appropriate location of component tissues at the time of cell–cell interaction, and the availability of an adequate blood supply (Truslove, 1962; Silver & Hughes, 1974; Silver & Robb, 1979; Perry et al. 1983). In the optic stalk, cell death and cell resorption allow access for the ingrowing nerve fibres that exit from the neural retina with the eventual formation of the optic nerve, while the blood supply that facilitates the nutrition of this process mainly comes from the hyaloid vessels. Truslove (1962) observed that in both normal and homozygous mutant (or^J/or^J) mice the blood supply was adequate up to d 11 p.c., but from d 12 p.c. the choroid fissure in the mutant mice gradually became obliterated. A progressive reduction in the size of the eyeball was then apparent, and this was eventually followed by the resorption of the optic stalk. When an inadequate blood supply was observed in this mutant strain of mice, this was generally associated with the failure of the optic vesicle to form a proper cup. The relationship between these two events, however, is not entirely clear.

The presence of the *Sey* gene in the homozygous state is believed to interfere with the normal mechanism of embryonic induction necessary for the development of the lens vesicle (and nasal apparatus), and results in the formation of a smaller lens vesicle than normal in the heterozygous mice bearing this mutation. Although it is the lens that is primarily affected, there appears to be a consequential effect on other components of the eyeball, as well as secondary effects on the optic nerve. Had the effect of the *Sey* gene (in the heterozygous mutants) been primarily on the development of the optic nerve, through a failure of optic vesicle and stalk formation, then it is likely that a similar effect to that seen in the or^J mutant would have been observed (Truslove, 1962).

It is logical that, since nerve fibres from the neural retina are directed into the optic stalk, the calibre of the optic nerve will necessarily reflect the number of nerve fibres which it contains (Ogden & Miller, 1966; Potts et al. 1972*a*, *b*; Hughes, 1977). Such a direct relationship between the calibre of the nerve and its nerve fibres has been demonstrated in this study by the *csa* and the mean nerve fibre count. Despite the presence of a significant difference in both mean *csa* and mean nerve fibre counts between the normal *Sey* male series and their heterozygous mutant *Sey* littermates, their mean nerve fibre densities, which reflect the actual relationship between calibre and the number of nerve fibres of a nerve, were not significantly different. The distribution of nerve fibres within the nerves was similar in both normal and heterozygous mutant *Sey* series. This was demonstrated by the similarity of the nerve fibre diameter spectrum in both the sexes of both groups of mice, with each having a modal diameter of 0.48 μm. Not surprisingly, if the overall size of the neural retina is reduced, as it is in the heterozygous mutant *Sey* mice, then the diameter of the optic nerve is also likely to be smaller than that of its normal littermates.

The similarity in myelinated nerve fibre diameter

spectrum as well as the mean myelinated nerve fibre densities between the normal and the heterozygous mutant *Sey* mice is an indication of the fact that myelinogenesis is not affected by the *Sey* gene. Myelination itself does not occur in the optic nerve of the mouse before the 5th day of postnatal life (Gyellensten & Malmfors, 1963; Gyellensten et al. 1966), and this is well after the process of embryonic induction. It would seem the primary inhibitory effect of the gene is on the induction of the lens vesicle, and this indirectly affects the size of the eyeball and the calibre of the optic nerve, but does not appear to influence to any degree retinal differentiation or myelination of the nerve fibres within the optic nerve. Mylination in the *Sey* mice does not appear to lag behind that observed in normal strains of mice. This is evident in the density of myelinated nerve fibres in the normal and *Sey*/+ groups of mice which are comparable with that observed in F1, C57BL and CBA strains of mice of the same age (Dangata et al. 1994).

The *Sey* gene is believed to be analogous to the human aniridia gene (Glaser et al. 1990). In the mouse, the effect of the mutant gene in the homozygous state primarily causes inhibition of the inductive mechanism necessary for the formation of the lens vesicle (Harch et al. 1978). In the heterozygous state, it influences the overall size of the eyeball and its component structures such as the iris and retina, while any effect on the optic nerve is likely to be secondary to that on the eye. Optic nerve hypoplasia which is observed in about 75% of aniridic patients is believed to be a consequence of poor macular and/or retinal development. These effects of the gene on the development of the eye in the human manifest themselves in a variety of ways. A reduction in the size of the iris leads to narrow angle glaucoma. The reduced visual acuity and nystagmus observed have been attributed to macular hypoplasia rather than being due to abnormalities of the iris (Hittner, 1989). Histological findings in the human include hypoplasia of the iris, absence of trabecular meshwork and Schlemm's canal (Hittner, 1989). From the results obtained for the myelinated nerve fibre spectrum and density for the *Sey* mouse in this study, it appears that the hypoplasia of the optic nerve observed in heterozygous mutant *Sey* mice is unlikely to have resulted from primary retina dysgenesis. It is likely to be secondary to a smaller total number of ganglion cells present in the neural retinal resulting from an overall reduction in the size of the eyeball, which itself is a consequence of the inhibitory effect of the *Sey* gene on embryonic induction.

ACKNOWLEDGEMENTS

We wish to thank Mrs Lesley Stevenson for meticulous animal husbandry and Mr R. McDougall for excellent technical assistance. The work was supported by a grant from the Scottish Office, Home and Health Department (Ref: K/MRS/50/C1785); as well as a Studentship Grant for Dr Dangata by the Kaduna State Government, Nigeria.

REFERENCES

BARD J (1990) *Morphogenesis: the Cellular and Molecular Processes of Developmental Anatomy*. Cambridge: Cambridge University Press.

DANGATA Y, FINDLATER GS, KAUFMAN MH (1994) Morphometric analysis of myelinated fibre composition in the optic nerve of adult C57BL and CBA strain mice and (C57BL × CBA) F1 hybrids: an analysis of interstrain variation. *Journal of Anatomy* **184**, 202.

FRANZ T, BESECKE A (1991) The development of the eye in homozygotes of the mouse mutant Extra-toes. *Anatomy and Embryology* **184**, 355–361.

GLASER T, LANE J, HOUSMAN D (1990) A mouse model of the Aniridia-Wilms tumor. *Science* **250**, 823–827.

GYELLENSTEN L, MALMFORS T (1963) Myelinization of the optic nerve and its dependence on visual function – a quantitative investigation in mice. *Journal of Embryology and Experimental Morphology* **11**, 255–266.

GYELLENSTEN L, MALMFORS T, NORRLIN-GRETTVE M-L (1966) Developmental and functional alterations in the fibre composition of the optic nerve in visually deprived mice. *Journal of Comparative Neurology* **128**, 413–418.

HARCH C, CHASE HB, GONSALVES NI (1978) Studies on an anophthalmic strain of mice. VI. Lens and cup interaction. *Developmental Biology* **63**, 352–357.

HILL RE, FAVOR J, HOGAN BLM, TON CCT, SAUNDERS GF et al. (1991) Mouse small eye results from mutation in a paired-like homeobox-containing gene. *Nature* **354**, 522–525.

HITTNER HM (1989) Aniridia. *The Glaucomas*, vol. 2, 869–884. Toronto: C. V. Mosby.

HOGAN BLM, HORSBURGH G, COHEN J, HETHERINGTON CM, FISHER G et al. (1986) *Small eyes* (*Sey*): a homozygous lethal mutation on chromosome 2 which affects the differentiation of both lens and nasal placodes in the mouse. *Journal of Embryology and Experimental Morphology* **97**, 95–110.

HOGAN BLM, HIRST EMA, HORSBURGH G, HETHERINGTON CM (1988) *Small eye* (*Sey*): a mouse model for the genetic analysis of craniofacial abnormalities. *Development* **103** (Suppl.), 115–119.

HUGHES A. (1977) The pigmented-rat optic nerve: fiber count and fiber diameter spectrum. *Journal of Comparative Neurology* **176**, 263–268.

JONG RVDM-D, DICKINSON ME, WOYCHIK RP, STUBBS L, HETHERINGTON C et al. (1990) Location of the gene involved in the small eye mutation on mouse chromosome 2 suggests homology with human aniridia 2 (AN2). *Genomics* **7**, 270–275.

KAUFMAN MH (1979) Cephalic neurulation and optic vesicle formation in the early mouse embryo. *American Journal of Anatomy* **155**, 425–444.

KAUFMAN MH (1992) *The Atlas of Mouse Development*. London: Academic Press.

MATHESON DF (1970) Some quantitative aspects of myelination of the optic nerve in rat. *Brain Research* **24**, 257–269.

MAYHEW TM (1988) An efficient sampling scheme for estimating fibre number from nerve cross sections: the fractionator. *Journal of Anatomy* **157**, 127–134.

MAYHEW TM (1990) An efficient and unbiased sampling of nerve fibres for estimating fibre number and size. In *Methods in Neuroscience*, vol. 3, pp. 172–187. New York: Academic Press.

MAYHEW, TM, SHARMA AK (1984*a*) Sampling schemes for estimating nerve fibre size. I. Methods for nerve trunks of mixed fascicularity. *Journal of Anatomy* **139**, 45–58.

MAYHEW, TM, SHARMA AK (1984*b*) Sampling schemes for estimating nerve fibre size. II. Methods for unifascicular nerve trunks. *Journal of Anatomy* **139**, 59–66.

OGDEN TE, MILLER RF (1966) Studies of the optic nerve of the rhesus monkey: nerve fiber spectrum and physiological properties. *Vision Research* **6**, 485–506.

PERRY VH, HENDERSON Z, LINDEN R. (1983) Postnatal changes in retinal ganglion cell and optic axon populations in the pigmented rat. *Journal of Comparative Neurology* **219**, 356–368.

POTTS AM, HODGES D, SHELMAN CB, FRITZ KJ, LEVY NS et al. (1972*a*) Morphology of the primate optic nerve. I. Method and total fiber count. *Investigative Ophthalmology* **11**, 980–988.

POTTS AM, HODGES D, SHELMAN CB, FRITZ KJ, LEVY NS et al. (1972*b*) Morphology of the primate optic nerve. II. Total fiber size distribution and fiber density distribution. *Investigative Ophthalmology* **11**, 989–1003.

ROBB RM, SILVER J, SULLIVAN RT (1978) Ocular retardation (or) in the mouse. *Investigations in Ophthalmology and Visual Science* **17**, 468–473.

ROBERTS RC (1967) *Small eyes* – a new dominant eye mutant in the mouse. *Genetical Research* **9**, 121–122.

RUGH R. (1990) *The Mouse: Its Reproduction and Development*. Oxford: Oxford Science Publications.

SILVER J, HUGHES AFW (1974) The relationship between morphogenetic cell death and the development of congenital anophthalmia. *Journal of Comparative Neurology* **157**, 281–302.

SILVER J, ROBB RM (1979) Studies on the development of the eye cup and optic nerve in normal mice and in mutants with congenital optic nerve aplasia. *Developmental Biology* **68**, 175–190.

THEILER K, VARNUM DS, NADEAU JH, STEVENS LC, CAGIANUT B (1976) A new allele of ocular retardation: early development and morphogenetic cell death. *Anatomy and Embryology* **150**, 85–97.

THEILER K, VARNUM DS, STEVENS LC (1978) Development of Dickie's small eye, a mutation in the house mouse. *Anatomy and Embryology* **155**, 81–86.

THEILER K, VARNUM DS, STEVENS LC (1980) Development of Dickie's small eye: an early lethal mutation in the house mouse. *Anatomy and Embryology* **161**, 115–120.

THEILER K, VARNUM DS (1981) Development of coloboma (Cm/+), a mutation with anterior lens adhesion. *Anatomy and Embryology* **162**, 121–126.

TON CCT, MIWA H, SAUNDERS GF (1992) Small eye (Sey): cloning and characterization of the murine homolog of the human aniridia gene. *Genomics* **13**, 251–256.

TRUSLOVE GM (1962) A gene causing ocular retardation in the mouse. *Journal of Embryology and Experimental Morphology* **10**, 652–660.